2.6 NONCLINICAL SUMMARY

2.6.4—PHARMACOKINETICS WRITTEN SUMMARY

ELVITEGRAVIR/COBICISTAT/EMTRICITABINE/TENOFOVIR DISOPROXIL FUMARATE SINGLE TABLET REGIMEN (EVG/COBI/FTC/TDF; QUAD STR)

NDA 203-100

Gilead Sciences

[redacted] 20[redacted]

TABLE OF CONTENTS

LIST OF IN-TEXT TABLES

LIST OF IN-TEXT FIGURES

GLOSSARY OF ABBREVIATIONS AND DEFINITION OF TERMS

A-B	apical to basal
AAG	α1-acid glycoprotein (AGP, ORM, orosomucoid)
AhR	aryl hydrocarbon receptor (AHR gene product)
APV	amprenavir (Agenerase®, GlaxoSmithKline)
ATV	atazanavir (Reyataz®, Bristol-Myers Squibb)
B-A	basal to apical
BCRP	breast cancer resistance protein (ABCG2)
Caco-2	human colonic adenocarcinoma cell line
cDNA	complementary deoxyribose nucleic acid
CHO	Chinese hamster ovary (cell line)
CNS	central nervous system
COBI	cobicistat (GS-9350)
CYP	cytochrome(s) P450
DF	disoproxil fumarate
DMSO	dimethyl sulfoxide
EFV	efavirenz (Sustiva®, Bristol-Myers Squibb)
EVG	elvitegravir; GS-9137 (also known as JTK-303)
EVG/COBI/FTC/TDF	elvitegravir/cobicistat/emtricitabine/tenofovir DF (coformulated), QUAD
FMO	flavin-containing monooxygenase
FTC	emtricitabine (Emtriva®, Gilead)
FTC/TDF	emtricitabine/tenofovir DF, TVD (Truvada®, Gilead)
f_u	fraction unbound
GI	gastrointestinal
GS-9200	EVG metabolite M4 (JTP-65386 and JTP-71051; glucuronide conjugate of the carboxylic acid)
GS-9202	EVG metabolite M1 (JTP-71081; hydroxylation of the chlorofluorophenyl group)
GS-9137	(see EVG)
HEK293	human embryonic kidney 293 cells
HIV, HIV-1, HIV-2	human immunodeficiency virus, type 1, and type 2
HSA	human serum albumin
$[I]_1$	inhibitor concentration corresponding to steady state C_{max}
$[I]_2$	inhibitor concentration corresponding to theoretical maximum concentration in the intestinal lumen
IC_{50}	concentration required to produce 50% inhibition
IDV	indinavir (Crixivan®, Merck)
INSTI	integrase strand transfer inhibitor
ISR	Incurred Sample Reanalysis

GLOSSARY OF ABBREVIATIONS AND DEFINITION OF TERMS (CONTINUED)

JTK-303	(see EVG)
K_I	affinity constant for enzyme inactivation
k_{inact}	theoretical maximum enzyme inactivation rate
K_M	Michaelis-Menten enzyme affinity constant
LC	(high pressure) liquid chromatography
LC/MS/MS	high performance liquid chromatography coupled to tandem mass spectrometry
LLC-PK1	porcine kidney cell line
LLOQ	lower limit of quantification
LPV	lopinavir (Aluviran®, Abbott)
MATE1	multidrug and toxin extrusion protein 1 (SLC47A1)
MATE2-K	multidrug and toxin extrusion protein 2-K (SLC47A2)
MDCK II	Madin-Darby canine kidney cell line
MDR1	P-glycoprotein (Pgp, ABCB1 gene product)
mRNA	messenger ribonucleic acid
MRP1	multi-drug resistance-associated protein-1 (ABCC1)
MRP2	multi-drug resistance-associated protein-2 (ABCC2, cMOAT)
MRP4	multi-drug resistance-associated protein-4 (ABCC4)
MS	mass spectrometry
NADPH	β-nicotinamide adenine dinucleotide phosphate (reduced form)
NC	Not Calculated
ND	Not Detectable / Not Determined
NDA	new drug application
NFV	nelfinavir (Viracept®, Pfizer)
NRTI	nucleoside/nucleotide reverse transcriptase inhibitor
NVP	nevirapine (Viramune®, Boehringer Ingelheim)
OAT1	organic anion transporter 1 (SLC22A6)
OAT3	organic anion transporter 3 (SLC22A8)
OATP	organic anion transporting polypeptide (SLCO or SLC22A gene products)
OATP1B1	organic anion transporting polypeptide 1B1 (SLCO1B1)
OATP1B3	organic anion transporting polypeptide 1B3 (SLCO1B3)
OCT2	organic cation transporter 2 (SLC22A2)
OCTN1	organic cation transporter novel, type 1 (SLC22A4)
P_{app}	apparent permeability
PAPS	3'-phosphoadenosine 5'-phosphosulfate
PBMC	peripheral blood mononuclear cell
Pgp	(see MDR1)
PI	protease inhibitor
PXR	pregnane X receptor (SXR, NR1I2 gene product)

GLOSSARY OF ABBREVIATIONS AND DEFINITION OF TERMS (CONTINUED)

QWBA	quantitative whole-body autoradiography
RT-PCR	reverse transcriptase – polymerase chain reaction
RTV, r	ritonavir (Norvir®, Abbott)
S9	postmitochondrial (9,000 x g) supernatant
S_2	Schneider 2 cell line
SD	standard deviation
SQV	saquinavir (Invirase®, Roche)
STR	single-tablet regimen
TDF	tenofovir disoproxil fumarate, tenofovir DF (Viread®, Gilead)
TFV	tenofovir
UDPGA	uridine diphospho-glucuronic acid
UGT	uridine diphosphate glucuronosyl transferase
US	United States
ZDV	zidovudine (Retrovir®, GlaxoSmithKline)

PHARMACOKINETIC ABBREVIATIONS

AUC	The area under the plasma concentration versus time curve
$AUC_{0-\infty}$	The area under the plasma concentration versus time curve extrapolated to infinite time, calculated as $AUC_{0-last} + (C_{last}/\lambda_z)$
AUC_{x-xx}	Partial area under the plasma concentration versus time curve from time "x" to time "xx" (default units are hours)
CL	The systemic clearance of the drug after intravenous administration
CL/F	The apparent clearance after oral administration of the drug
C_{last}	The last observed quantifiable concentration of the drug in plasma
C_{max}	The maximum observed concentration of drug in plasma
C_x	The plasma concentration at time "x" (default units are hours)
F	The estimated oral bioavailability of the drug (%)
λ_z	Elimination rate determined from the terminal phase of the plasma concentration versus time curve
MAT	mean absorption time
MRT	mean residence time
$t_{½}$	Half-life
t_{last}	The time (observed time point) of C_{last}
t_{max}	The time (observed time point) of C_{max}
V_{ss}	The apparent steady-state volume of distribution of the drug
V_{ss}/F	The apparent steady-state volume of distribution of the drug after oral administration

NOTE TO REVIEWER

This application is being submitted in support of a new drug application (NDA) for a single tablet regimen (STR) that contains the active substances elvitegravir (EVG), cobicistat (COBI), emtricitabine (FTC), and tenofovir disoproxil fumarate (tenofovir DF, TDF). The STR is referred to as elvitegravir/cobicistat/emtricitabine/tenofovir disoproxil fumarate (EVG/COBI/FTC/TDF) STR throughout this document. As the EVG and COBI components are new chemical entities, [redacted]. Per the agreement reached at the [redacted] 20[redacted] ([redacted]) meeting between Gilead Sciences, Inc. (Gilead) and the Food and Drug Administration (FDA; refer to the Agency's comments, dated [redacted] 20[redacted] in Module 1.6.3), this NDA is supported [redacted].

In order to simplify the review, the order of presentation in each section follows the general format: EVG, followed by COBI, and then EVG/COBI/FTC/TDF combination studies. Results of FTC, TDF, and FTC/TDF studies are incorporated when needed to describe the presence or absence of overlapping pharmacokinetics.

Throughout this module reference is made to EVG, but in the titles and summaries of individual studies the compound numbers GS-9137 or JTK-303 may also be used. Table 1 illustrates the structures of EVG and chemically related compounds for which synthetic standards have been prepared, and lists the alternative names that have been used in individual studies.

The following conversions are also provided to aid the reviewer:

1 μM EVG (GS-9137; JTK-303) = 0.448 μg/mL free acid

1 ng/mL EVG free acid = 2.23 nM

Table 1. Names and Structures of EVG and Related Compounds

Name	Alternative Names	Identity	Structure
EVG	Elvitegravir, GS-328934, GS-9137, JTK-303	Parent Compound	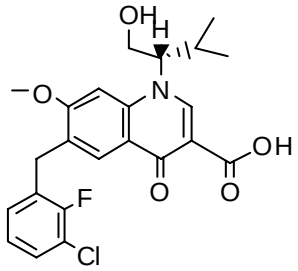
GS-9204	JTP-65384	Internal standard for parent compound [redacted]	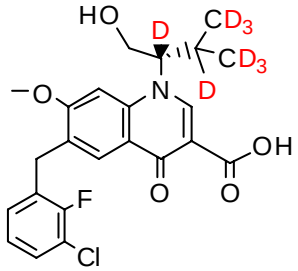
[^{14}C]EVG	[^{14}C]JTK-303	Radiolabeled parent	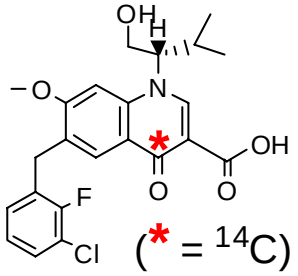
GS-9200	JTP-655386, JTP-71051 (morpholine salt)	M4 metabolite standard (acyl glucuronide)	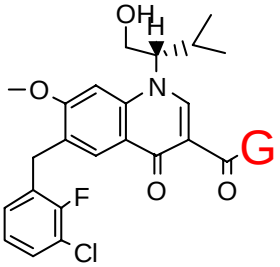
GS-9201	JTP-71052	Internal standard for GS-9200 [redacted]	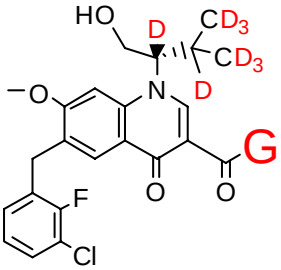

Table 1. Names and Structures of EVG and Related Compounds (Continued)

Name	Alternative Names	Identity	Structure
GS-9202	JTP-71081	M1 metabolite standard (p-hydroxylated)	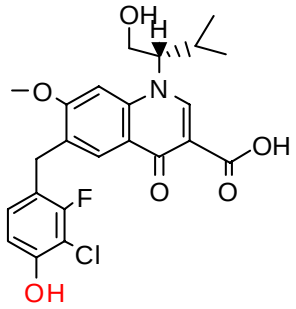
GS-9203	JTP-754458	Internal standard for GS-9202 [redacted]	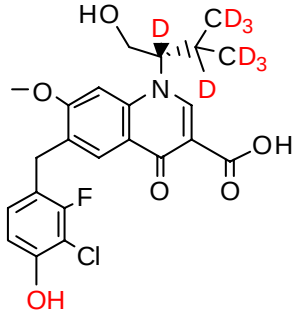
JTP-71007		M3 metabolite standard (ether glucuronide)	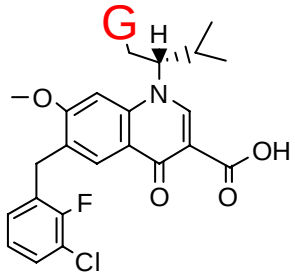
JTP-71040 and JTP-71041 (diastereomers)		M2 metabolite standard (benzylic hydroxylated)	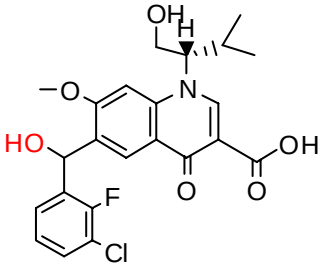

Table 1. Names and Structures of EVG and Related Compounds (Continued)

Name	Alternative Names	Identity	Structure
JTP-71064		Putative metabolite (o-hydroxylated)	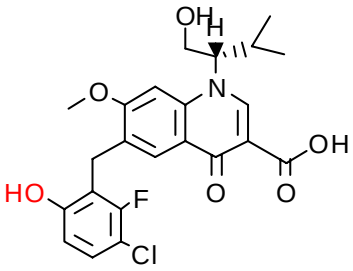
JTP-71100		Putative metabolite (m-hydroxylated)	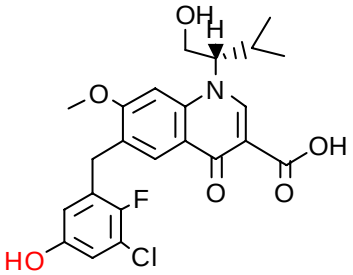
JTP-74488		M7 metabolite standard (M1 glucuronide: p-hydroxylated + glucuronide)	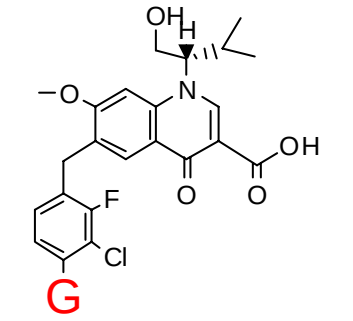
JTP-74492	HM1	Putative metabolite (hydroxylated + sulfated)	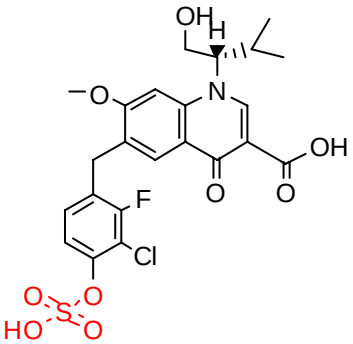

G = Glucuronic acid

Throughout this module reference is made to COBI, but in the titles and summaries of individual studies, its compound number, GS-9350, or its earlier designation, GS-340649, may also be used. Table 2 illustrates the structures of COBI and related compounds for which synthetic standards have been prepared, and lists the alternative names that have been used in individual studies. Similarly, in some studies comparison is made to ritonavir (RTV), a HIV-1 protease inhibitor (HIV-PI) that is also a pharmacokinetic enhancer approved in the EU for use in combination with several HIV-PIs. In the titles of reports and summaries, RTV may be referred to by compound number GS-9233 or GS-017415.

The following conversions are also provided to aid the reviewer:

1 µM COBI (GS-9350) = 0.776 µg/mL free base

1 ng/mL COBI free base = 1.29 nM

Table 2. Names and Structures of COBI and Related Compounds

Name	Alternative Names	Identity	Structure
COBI	Cobicistat, GS-9350, GS-340649	Parent Compound	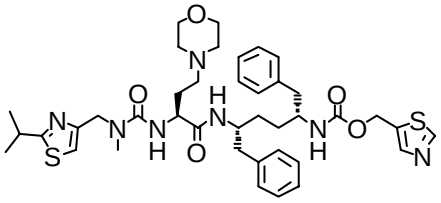
RTV	Ritonavir, GS-9233, GS-017415	HIV-1 Protease Inhibitor Pharmacokinetic Enhancer (EU)	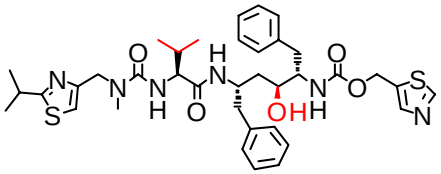
GS-427990		Internal standard for parent compound [redacted]	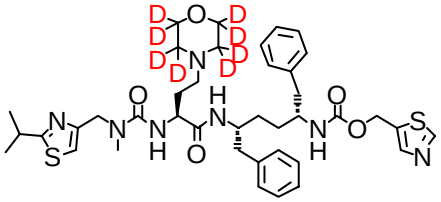
[^{14}C]COBI	[^{14}C]GS-9350	Radiolabeled parent ([^{14}C]Methyl)	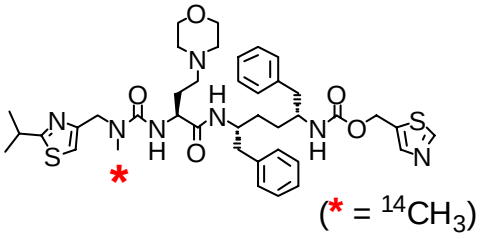

Table 2. Names and Structures of COBI and Related Compounds (Continued)

Name	Alternative Names	Identity	Structure
GS-9454	GS-342006	M21 (E1) metabolite standard (carbamate cleavage)	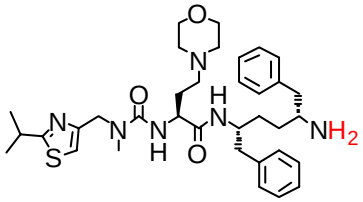
GS-428885		Internal standard for GS-9454 [redacted]	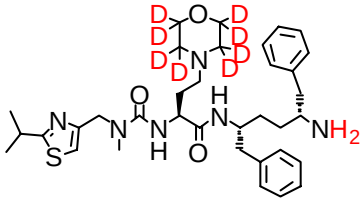
GS-441405		M14 (E2) metabolite standard (isopropyl methine hydroxylated + carbamate cleavage)	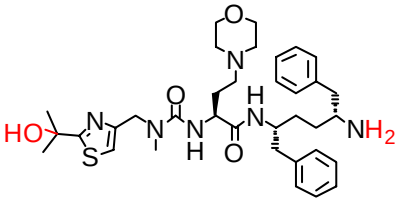
GS-9612	GS-364751	M31 (E3) metabolite standard (isopropyl methine hydroxylated)	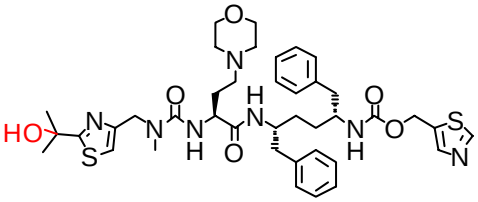
GS-341842		M26 (E5) metabolite standard (dealkylation at methylurea)	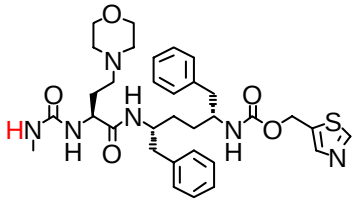
GS-428886		Internal standard for GS-341842 [redacted]	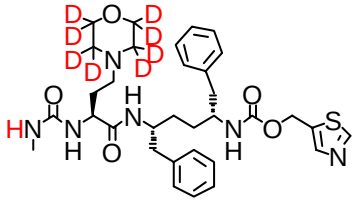

Table 2. Names and Structures of COBI and Related Compounds (Continued)

Name	Alternative Names	Identity	Structure
GS-432605		Putative metabolite (pro-(R) hydroxylated)	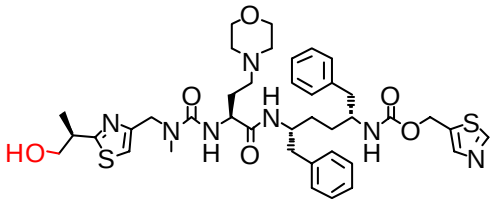
GS-432606		Putative metabolite (pro-(S) hydroxylated)	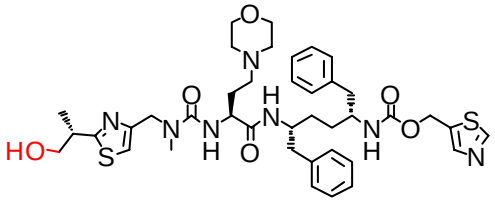

1. BRIEF SUMMARY

This application is being submitted in support of a new drug application (NDA) for a single tablet regimen (STR) that contains a fixed-dose combination of elvitegravir (EVG), cobicistat (COBI), emtricitabine (FTC, Emtriva®), and tenofovir disoproxil fumarate (TDF, Viread®): the EVG/COBI/FTC/TDF (QUAD, 150/150/200/300 mg) tablet. The proposed indication for the EVG/COBI/FTC/TDF (QUAD) tablet is for use once daily as a complete regimen for the treatment of human immunodeficiency virus-1 (HIV-1) infection in adults aged 18 years and over who are antiretroviral-naive or have no known resistance mutations to the individual components.

Elvitegravir is a new chemical entity that belongs to the new class of HIV-1 integrase strand-transfer inhibitors (INSTI) that prevent integration of HIV-1 genetic material into the host-cell genome. Cobicistat is a new chemical entity and structural analogue of ritonavir (RTV, r) with no antiretroviral activity. It is a more specific, mechanism-based cytochrome P450 3A (CYP3A) inhibitor than RTV that enhances or "boosts" the exposure of CYP3A substrates, including EVG. Gilead Sciences (Gilead) has developed EVG and COBI for use within a new 4-drug fixed-dose combination tablet that also contains the current standard-of-care dual nucleoside/nucleotide reverse transcriptase inhibitor (NRTI) backbone emtricitabine/tenofovir disoproxil fumarate (FTC/TDF, TVD).

The EVG/COBI/FTC/TDF (QUAD) tablet contains the same dosages of FTC and TDF that are currently approved within Viread, Emtriva, and Truvada® (FTC/TDF) for use in adults (200 mg of FTC and 300 mg of TDF). The dose of EVG (150 mg) was selected based on results from a Phase 1 pharmacokinetic/pharmacodynamic study (GS-US-183-0101), a Phase 2 study in heavily treatment-experienced HIV-1 infected subjects (GS-US-183-0105), and a Phase 1 biopharmaceutics/formulation study (GS-US-183-0140). The dose of COBI (150 mg) was selected based on the results from 2 studies in healthy volunteers (GS-US-216-0101 and GS-US-236-0101).

Comprehensive programs of nonclinical pharmacokinetic studies with EVG, COBI, FTC, and TFV/TDF have been conducted. Information from all nonclinical studies with EVG, COBI, FTC, and TDF (which includes tenofovir [TFV]) should be considered in the context of the substantial clinical experience with FTC and TDF within antiretroviral combination therapy for the treatment of HIV-1 infection, the Phase 2 clinical experience with EVG administered with RTV, the Phase 2 clinical experience with COBI, and the Phase 2 and 3 experience with the EVG/COBI/FTC/TDF STR.

In order to simplify the review, the order of presentation in each section follows the general format: EVG, followed by COBI, and then EVG/COBI/FTC/TDF combination studies. Results of FTC, TDF, and FTC/TDF studies are incorporated when needed to describe the presence or absence of potential pharmacokinetic interactions between the 4 agents.

The nonclinical data discussed within this document support the proposed use of the EVG/COBI/FTC/TDF STR as a complete regimen for the treatment of HIV-1 infection in

adults who are antiretroviral treatment-naive or who have no known resistance-associated substitutions to the individual components of EVG/COBI/FTC/TDF STR tablet. All information from nonclinical studies that is of relevance to the prescriber and patient has been included in the proposed Product Information and Patient Prescribing Information.

EVG

A comprehensive program of studies has been conducted to characterize the nonclinical drug absorption and disposition profile for EVG. The pharmacokinetic studies for EVG are listed in the overview table (Tabulated Summary 2.6.5.1), and study details are given in the individual study overview tables in Module 2.6.5.

Elvitegravir shows modest bioavailability in rats and dogs, driven by a combination of moderate absorption and first-pass elimination. Elvitegravir is rapidly absorbed and widely distributed, although it is excluded from the central nervous system (CNS) and eye. Binding to human plasma and purified human albumin is high (≥ 99.3%) and this property was confirmed in ex vivo clinical analysis, including plasma samples from subjects with renal and/or hepatic impairment, where average binding was 98%–99%. Elimination from tissues parallels that from plasma and is complete by 96 hours after dosing.

In the absence of a pharmacokinetic enhancer, EVG is extensively metabolized by oxidation, glucuronidation, and combinations of the two. The most abundant metabolites are common between mouse, rat, rabbit, dog, and human. The predominant metabolite is M1 (GS-9202, p-hydroxylated), with lesser amounts of M4 (GS-9200, acyl glucuronide) and M7 (JTP-74488, glucuronide of M1), but parent EVG accounts for the majority of radioactivity in plasma. Recovery of radioactivity after dosing with [^{14}C]EVG is high. Very little (≤ 1%) of EVG and its metabolites are excreted in urine, the majority being recovered in bile and feces. The potential for enterohepatic recirculation is low. Low levels of EVG, but not its metabolites, are detectable in milk.

Elvitegravir has low potential for drug interactions through inhibition of human cytochromes P450 (CYP) or P-glycoprotein (MDR1). Elvitegravir also shows no potential for causing drug interactions through induction of CYP1A2 or other proteins regulated by the aryl hydrocarbon receptor (AhR). Elvitegravir is an inhibitor of human organic anion transporting polypeptide 1B3 (OATP1B3) and shows concentration-dependent induction of CYP3A activity in human hepatocytes. The oxidation of EVG is catalyzed by CYP3A enzymes and glucuronidation is catalyzed by UDP glucuronosyl transferase (UGT) enzymes UGT1A1 and UGT1A3. Metabolism of EVG by human hepatic microsomal fraction is reduced by CYP3A inhibitors, such as COBI and RTV, and by atazanavir (ATV), a known inhibitor of human UGT1A1.

COBI

A comprehensive program of studies has been conducted to characterize the nonclinical drug absorption and disposition profile for COBI. The pharmacokinetic studies for COBI are listed

in the overview table (Tabulated Summary 2.6.5.1), and study details are given in the individual study overview tables in Module 2.6.5.

Cobicistat is a potent mechanism-based inhibitor of human CYP3A enzymes with inactivation kinetics similar to RTV. In contrast, COBI does not inactivate CYP3A enzymes appreciably in other species, but instead shows potent reversible inhibition.

Cobicistat exhibits high permeability across human colonic adenocarcinoma (Caco-2) cell monolayers with little evidence of efflux, although some transport of COBI by human MDR1 and breast cancer resistance protein (BCRP) can be demonstrated in cell systems overexpressing those proteins. After oral administration of [^{14}C]COBI to bile duct-cannulated rats and dogs, ≥ 65% of radioactivity was recovered in bile and urine (the majority in the bile), confirming high absorption in vivo.

Cobicistat shows moderately high plasma protein binding, which is concentration-independent in humans. The fraction unbound, measured in vitro, was 6.3% at 1 μM, but in ex vivo samples from clinical studies the fraction unbound in plasma was slightly lower (2.47%–3.23%), including samples from subjects with hepatic and/or renal impairment. After oral administration of [^{14}C]COBI to rats, radioactivity is widely distributed, although relatively excluded from brain, testes, eye, and the cellular fraction of blood. Cobicistat is metabolized rapidly by hepatic microsomal fractions from nonclinical species, but exhibits self-limiting metabolism with human hepatic microsomal fraction, due to concurrent enzyme inactivation. CYP3A (major) and CYP2D6 (minor) enzymes are responsible for the in vitro human metabolism of COBI and there is no evidence for metabolism by direct conjugation. In vitro metabolism in all species yields 3 predominant primary oxidative metabolites (M21, M26, and M31). The same 3 metabolites, and M39, another common primary metabolite, are the 4 most abundant in vivo (in mouse, rat, dog, and human); several secondary, tertiary, and minor primary metabolites are also detected in vivo. In all species, COBI is the major radioactive component circulating in plasma. Metabolites M21, M26, and M31 are weak or inactive inhibitors of human CYP3A enzymes and are thus unlikely to contribute to the overall pharmacological effect. After oral administration of [^{14}C]COBI to mice, rats, and dogs, recovery of radioactivity was high, and was largely found in feces or bile with very little found in urine.

Cobicistat is a selective inhibitor of human CYP3A enzymes, with modest inhibition of CYP2B6, weak inhibition of CYP2D6 and UGT1A1, and very weak or undetectable inhibition of other enzymes, and so is unlikely to cause clinically significant drug-drug interactions due to inhibition of enzymes other than CYP3A. Cobicistat was found to be a weak inhibitor of CYP2D6 and did not inhibit CYP2B6 in humans in vivo (Module 2.7.2, Section 2.3.2.2.3 [GS-US-216-0112]). Cobicistat shows weak or undetectable inhibition of the efflux transporters MDR1, multi-drug resistance associated proteins 2 and 4 (MRP2 and MRP4, respectively), BCRP, and multidrug and toxin extrusion protein 2-K (MATE2-K), and the renal uptake transporters, organic anion transporters 1 and 3 (OAT1 and OAT3, respectively), so systemic concentrations of COBI would be insufficient to inhibit their activity. However, high concentrations of COBI present relatively briefly in the intestinal lumen during drug absorption can inhibit intestinal efflux transporters, such as MDR1 and

BCRP; COBI was found to inhibit intestinal MDR1 only transiently in humans in vivo (Module 2.7.2, Section 2.3.2.2.3 [GS-US-216-0112]). Cobicistat is a moderate inhibitor of uptake transporters, OATP1B1 and OATP1B3 (IC_{50} values 3.5 μM and 1.88 μM, respectively), and organic cation transporter 2 (OCT2; IC_{50} 8.24 μM). It also inhibits the renal efflux transporters, novel organic cation transporter 1 (OCTN1; IC_{50} 2.49 μM) and multidrug and toxin extrusion protein 1 (MATE1; IC_{50} 1.87 μM). Cobicistat does not activate human AhR, and shows no evidence of induction of CYP1A2 (activity or mRNA) in human hepatocytes. Cobicistat is a very weak activator of human pregnane X receptor (PXR) and induces CYP3A mRNA and immunodetectable protein in human hepatocytes only at high (not clinically relevant) concentrations. There is no detectable induction of CYP3A activity in human hepatocytes in vitro. This lack of PXR activation is not conserved between species, as COBI activates rat PXR, and multiple oral dose treatment of mice and rats with COBI leads to increases in hepatic microsomal CYP3A activity.

FTC

A comprehensive nonclinical pharmacokinetics program was undertaken in support of the registration of FTC. The results of this evaluation were presented in detail in the original NDA and subsequent submissions for Emtriva.

In mice, rats, and cynomolgus monkeys, FTC was rapidly and extensively absorbed with oral bioavailability ranging from 58% to 97%. In general, there were no differences in pharmacokinetics following single and multiple dosing. Systemic exposure to FTC (C_{max} and AUC) increased approximately proportionally with dose and was similar between males and females. With chronic dosing, somewhat higher exposures were observed in the mouse and rat studies when compared to short term dosing; however, there was no evidence of accumulation in the monkey studies.

Emtricitabine is widely distributed throughout the body, with a volume of distribution similar to that of total body water. After oral administration, the highest concentrations of FTC were found in the kidneys, intestine, and liver and exceeded those in plasma, while concentrations in CNS tissues were less than 10% of those in plasma. Emtricitabine was also readily transferred across the placenta. Emtricitabine is almost completely eliminated within 72 hours following dosing, with no evidence of tissue accumulation. Emtricitabine does not undergo extensive first-pass or systemic metabolism, and is eliminated primarily by renal excretion of unchanged drug. The total body clearance of FTC exceeds the glomerular filtration rate, suggesting the drug is actively secreted by the kidney. Metabolism is a minor route of elimination and is similar in humans and monkeys. It includes oxidation of the thiol moiety (Phase 1 metabolism) to form the 3'-sulfoxide diastereomers (M1 and M2) and conjugation with glucuronic acid (Phase 2 metabolism) to form the 2'-O-glucuronide (M3). The most abundant metabolite was one of the 3'-sulfoxides (M1 or M2). Several minor metabolites account for $< 2\%$ of the dose and are eliminated primarily in the urine. Importantly, FTC is not converted to 5-fluorouracil. Oxidation of FTC is largely catalyzed by CYP3A, but flavin-containing monooxygenase (FMO) enzymes may also play a role. Emtricitabine does not inhibit human cytochromes P450 and demonstrates no liability to be an inducer.

TDF and TFV

A comprehensive nonclinical pharmacokinetics program was undertaken in support of the registration of TDF. The results of this evaluation were presented in detail in the original NDA and subsequent submissions for Viread.

No circulating metabolites of TDF or TFV, other than the monoester (TFV soproxil), observed at early time points in rats, were detected. This is consistent with the lack of metabolism of TFV in intestinal and liver preparations. Little or no inhibition of CYP enzymes was observed in human hepatic microsomes. Little or no induction of CYP activities was observed in livers from rats treated with a high dose of TDF. Extensive tissue distribution, suggested by the plasma pharmacokinetics of TFV, was confirmed in studies with [^{14}C]TFV in dogs. Major sites of tissue uptake included the liver and kidney. Placental transfer of TFV appeared to be significant in monkeys. TFV was excreted, but not concentrated in rat and monkey breast milk.

Renal excretion was identified as the primary route of elimination of TFV in all species tested, and is achieved by a combination of glomerular filtration and tubular secretion. In vitro transport studies indicate that the active tubular secretion of TFV in humans is mediated by OAT1 and MRP4 acting in series, as the major uptake and efflux transporters in proximal tubules, respectively. Human OAT3 may play a secondary role in the tubular uptake of TFV. Neither MDR1 nor MRP1 or MRP2 appear to be involved in the tubular efflux of TFV. As the primary transporter for the tubular uptake of TFV, OAT1 has been assessed for its potential as a target for drug interactions between TFV and other renally secreted therapeutics including antibiotics, anti-inflammatory agents, and other antivirals (including COBI and protease inhibitors [PIs]). Under physiologically relevant conditions, a number of renally excreted drugs showed no effect in vitro on the OAT1-mediated transport of TFV. Similarly, PIs and COBI did not exhibit any effect on the in vitro active cellular elimination of TFV mediated by the MRP4 efflux pump, indicating that PIs and COBI are unlikely to exert any substantial effect on the accumulation of TFV in renal proximal tubules or renal elimination of TFV. Tenofovir did not inhibit the activity of the renal uptake transporter, OCT2, or the renal efflux transporter, MATE1.

In vitro studies have shown that the intestinal absorption of TDF, the oral prodrug of TFV, can be modestly affected by other drugs through a combination of effects on MDR1-mediated efflux transport and esterase degradation in intestinal tissue. Further studies in human intestinal S9 fractions, the human colon carcinoma cell line Caco-2, and Madin-Darby canine kidney II (MDCK II) cells stably transfected with the human gene that encodes MDR1 have suggested that the relative ability of PIs to inhibit esterase activity and inhibit or induce intestinal MDR1 may account for the modest changes in plasma TFV levels when TDF is coadministered in humans with some PIs.

EVG/COBI/FTC/TDF

The intended, positive pharmacokinetic interaction within the 4-drug combination is an increase in the bioavailability and a decrease in the rate of elimination of EVG due to inhibition of CYP3A activity by COBI, and a consequent profound reduction in the formation of M1 (GS-9202), the major oxidative metabolite of EVG. This interaction has been well characterized in vitro. Animal models are inappropriate to investigate this interaction due to the lack of mechanism-based inhibition by COBI in nonhuman species.

Based upon the differences in routes of elimination, EVG and COBI are unlikely to affect the pharmacokinetics of FTC or TFV adversely. The only interaction, predicted in vitro and observed in the clinic, is a modest increase in TFV exposure due to inhibition of intestinal efflux of TDF by COBI. This effect has already been noted with other MDR1 inhibitors, such as HIV PIs, commonly co-administered with TDF. Cobicistat does not significantly inhibit OAT1 or MRP4, the transporters responsible for the renal excretion of TFV. Single-dose pharmacokinetic studies in dogs demonstrate that generally comparable exposures for each of the 4 components can be achieved through coformulation, relative to coadministration of the individual clinical formulations. This has been confirmed in comprehensive clinical pharmacokinetic data for the STR (Module 2.7.2).

2. METHODS OF ANALYSIS

2.1. EVG

The in vivo pharmacokinetics, toxicokinetics, distribution, and excretion of EVG were assessed in the mouse, rat, rabbit, and dog. The in vitro absorption, metabolism, and drug interaction characteristics of EVG were studied in appropriate model systems.

2.1.1. Bioanalytical Methods Supporting Pharmacokinetic Studies

Analysis of EVG in plasma from mouse, rat, and dog (Tabulated Summary 2.6.5.2.1, BA-183-2003, JTK303-AD-003, BA-183-2011, and JTK303-AD-004) utilized validated methods based upon high performance liquid chromatography coupled to tandem mass spectrometry (LC/MS/MS). Validation parameters included selectivity, sensitivity, linearity, carry-over, intra- and inter-assay precision and accuracy, stock solution stability, injection medium integrity, short-term matrix stability, freeze-thaw matrix stability, long-term matrix stability, and dilution integrity. Lower limits of quantification (LLOQs) were 100 ng/mL for mouse plasma, 1.00 or 100 ng/mL for rat plasma, and 1.00 ng/mL for dog plasma.

GS-9204 ([redacted]) was used as the internal standard for EVG analyses. Samples were processed by solid phase extraction and EVG was quantified by LC/MS/MS. Analyses were also performed with samples spiked with EVG acyl glucuronide (GS-9200), to assess the potential for interference due to degradation of the metabolite (M4) in plasma, but this was found to be insignificant. The methods for mouse plasma (BA-183-2003) and rat plasma (BA-183-2011) (Tabulated Summary 2.6.5.2.1) also included validation of methods for analysis of GS-9200 ([redacted] as internal standard) and GS-9202 (for metabolite M1, [redacted] as internal standard) with LLOQs of 100 ng/mL for both analytes.

A validated method was utilized for the simultaneous analysis of EVG and COBI in rat plasma (Tabulated Summary 2.6.5.2.2, BA-216-2007). [redacted] was used as the internal standard for both analytes. Lower limits of quantification were 10.0 ng/mL for EVG and 5.00 ng/mL for COBI.

Analysis of EVG, GS-9200, and GS-9202 in rat breast milk (Tabulated Summary 2.6.5.2.1, BA-183-2008) utilized a validated method similar to that described above for plasma. Lower limits of quantification were 100 ng/mL for all 3 analytes.

Analysis of RTV in rat plasma (Tabulated Summary 2.6.5.2.1, BA-183-2012) also utilized a validated method and the LLOQ was 5.00 ng/mL.

2.1.2. Other In Vivo Bioanalytical Methods

After administration of [^{14}C]EVG to rats (Tabulated Summary 2.6.5.3.3, JTK303-AD-005) and dogs (Tabulated Summary 2.6.5.3.5, JTK303-AD-006), radioactivity in plasma, urine, feces, bile, and liver homogenates was quantified by liquid scintillation counting, and radioprofiling was performed by LC with flow radiodetection (Tabulated Summary 2.6.5.9.1,

JTK303-AD-019 and Tabulated Summary 2.6.5.9.2, JTK303-AD-020). Mass spectrometry was also used to identify peaks in radiochromatograms. Tissue distribution in rats (Tabulated Summary 2.6.5.5.1, JTK303-AD-005) and dogs was determined by scintillation counting after homogenization and combustion (Tabulated Summary 2.6.5.5.4, JTK303-AD-006). Quantitative distribution of radioactivity in rats was also assessed by quantitative whole body autoradiography (QWBA) (Tabulated Summary 2.6.5.5.2, 60N-0518).

2.1.3. In Vitro Methods

The bidirectional permeability and level of polarized transport of [^{14}C]EVG were determined using monolayers of the porcine kidney cell line, LLC-PK1, transfected with an expression vector for human MDR1 or with empty vector (Tabulated Summary 2.6.5.3.1, JTK303-AD-026).

The extent of [^{14}C]EVG binding to plasma from rat, dog, cynomolgus monkey, and human was assessed by equilibrium dialysis at 37°C (Tabulated Summary 2.6.5.6.2, JTK303-AD-014). Binding was also determined to solutions of physiological concentrations of human serum albumin (HSA) and α1-acid glycoprotein (AAG). Binding of [^{14}C]EVG to plasma from mice pretreated in vivo with EVG or EVG+RTV was also assessed (Tabulated Summary 2.6.5.6.1, AD-183-2024).

The relative distribution of [^{14}C]EVG between the soluble and cellular fractions of blood from rat, dog, cynomolgus monkey, and human was determined by scintillation counting (Tabulated Summary 2.6.5.8.1, JTK303-AD-013).

The hepatic microsomal stability of [^{14}C]EVG was determined with microsomal fractions from mouse (Tabulated Summary 2.6.5.10.1, AD-183-2019), rat, dog, cynomolgus monkey, and human (Tabulated Summary 2.6.5.10.2, JTK303-AD-015) using reduced β-nicotinamide adenine dinucleotide phosphate (NADPH) as the cofactor for oxidative metabolism. Similar studies were also performed with UDP-glucuronic acid (UDPGA) as the cofactor for glucuronidation (Tabulated Summary 2.6.5.10.1, AD-183-2019 and Tabulated Summary 2.6.5.10.3, JTK303-AD-016). The rates of oxidative metabolism of [^{14}C]EVG by 11 recombinant baculovirus-expressed human cytochromes P450 were also determined (Tabulated Summary 2.6.5.10.4, JTK303-AD-017). The Michaelis-Menten enzyme affinity constant (K_M) for generation of M1, the major oxidative metabolite of EVG, from [^{14}C]EVG by human hepatic microsomal fraction was determined (Tabulated Summary 2.6.5.10.5, JTK303-AD-024), as was the K_M for generation of M4, the acyl glucuronide metabolite (Tabulated Summary 2.6.5.10.5, AD-183-2028) using an LC/MS/MS assay for GS-9200.

The stability of [^{14}C]EVG in plasma from rat, dog, cynomolgus monkey, and human was determined by radiochromatography following incubation at 37°C (Tabulated Summary 2.6.5.6.2, JTK303-AD-014). The stability in whole blood from the same species was also determined (Tabulated Summary 2.6.5.8.1, JTK303-AD-013).

Metabolites of [^{14}C]EVG generated in vitro and in vivo were identified by radiochromatography-guided ion trap mass spectrometry and by comparison with synthetic

standards. Initial analyses with in vivo samples were performed with dog urine, dog feces, and rat bile. In vitro samples were from hepatic microsomal fractions from rat, dog, cynomolgus monkey, and human with NADPH as the cofactor, and with rat hepatic microsomal fraction with UDPGA as the cofactor (Tabulated Summary 2.6.5.11.2, JTK303-AD-021). Results from this study were applied during radioprofiling of samples from in vivo studies in rat (Tabulated Summary 2.6.5.9.1, JTK303-AD-019) and dog (Tabulated Summary 2.6.5.9.2, JTK303-AD-020). Independent metabolite identification was performed with samples from [^{14}C]EVG incubated with mouse and rabbit hepatic microsomal fractions with NADPH and UDPGA as cofactors. Mouse hepatic microsomal fractions were prepared from untreated animals and from those treated with prototypical inducers (Tabulated Summary 2.6.5.11.1, AD-183-2020). Rabbit hepatic microsomal fraction was from untreated animals and was additionally fortified with phosphoadenosine phosphosulfate (the cofactor for sulfation) during the incubation (Tabulated Summary 2.6.5.11.3, 60N-0508).

The potential for EVG to inhibit the major human drug metabolizing cytochrome P450 enzymes was assessed using human hepatic microsomal fractions and enzyme-selective activities, namely ethoxyresorufin O-deethylase, coumarin 7-hydroxylase, tolbutamide 4-hydroxylase, (S) mephenytoin 4'-hydroxylase, bufuralol 1'-hydroxylase, chlorzoxazone 6-hydroxylase, testosterone 6β-hydroxylase, and midazolam 1'-hydroxylase (Tabulated Summary 2.6.5.12.1, JTK303-AD-027). Positive control inhibitors were tested in parallel.

To better understand the enzymology of the metabolism of EVG and to assess the potential for the metabolism of EVG to be inhibited by other agents, the effects of selective inhibitors of CYP2C9, CYP2D6, and CYP3A activity on the human hepatic microsomal oxidative metabolism of [^{14}C]EVG were determined (Tabulated Summary 2.6.5.15.1, JTK303-AD-018). The effects of representative potential co-medications were tested in a similar manner (Tabulated Summary 2.6.5.15.2, JTK303-AD-025). The abilities of 12 recombinant human UGTs to metabolize EVG to its acyl glucuronide metabolite (M4) were tested using an LC/MS/MS assay for GS-9200 (Tabulated Summary 2.6.5.10.6, AD-183-2034). The effects of ketoconazole and ATV on the generation of M4 by human hepatic microsomal fraction were determined (Tabulated Summary 2.6.5.15.3, AD-183-2028).

To assess the potential for EVG to cause drug interactions through induction, a study was performed with fresh primary human hepatocytes. The effects of treatment with EVG for three days on phenacetin O-deethylase, tolbutamide 4-hydroxylase, and midazolam 1'-hydroxylase activities were determined (Tabulated Summary 2.6.5.12.2, JTK303-AD-023). Positive control inducers were tested in parallel.

The effect of EVG on human MDR1 activity was determined in LLC-PK1 cells transfected with an expression vector for human MDR1 and with [^{3}H]digoxin as the probe substrate and verapamil as the positive control inhibitor (Tabulated Summary 2.6.5.15.4, JTK303-AD-026). The effects of EVG on human OATP1 and OATP3 activities were determined in Chinese hamster ovary (CHO) cells expressing the recombinant human

proteins and with Fluo 3 as the substrate and rifampicin as the positive control inhibitor (Tabulated Summary 2.6.5.15.5, AD-183-2030).

2.2. COBI

The in vivo pharmacokinetics, toxicokinetics, distribution, and excretion of COBI were assessed in mouse, rat, rabbit, dog, and monkey. The in vitro absorption, metabolism, and drug interaction characteristics of COBI were studied in appropriate model systems.

2.2.1. Bioanalytical Methods Supporting Non-GLP Pharmacokinetic and Toxicokinetic Studies

Analysis of COBI in plasma from rats (Tabulated Summary 2.6.5.3.9, AD-216-2020 and Tabulated Summary 2.6.7.6.2, TX-216-2001), dogs (Tabulated Summary 2.6.5.3.10, AD-216-2021 and Tabulated Summary 2.6.7.6.2, TX-216-2002), and cynomolgus monkeys (Tabulated Summary 2.6.5.3.12, AD-216-2022) employed methods based LC/MS/MS. These methods were evaluated for selectivity, sensitivity, linearity, intra-assay accuracy, and precision.

2.2.2. Bioanalytical Methods Supporting GLP Toxicokinetic Studies

Analysis of COBI in plasma from mice (Tabulated Summary 2.6.5.2.2, BA-216-2005), rats (Tabulated Summary 2.6.5.2.2, BA-216-2202), rabbits (Tabulated Summary 2.6.5.2.2, BA-216-2004), and dogs (Tabulated Summary 2.6.5.2.2, BA-216-2003) utilized fully validated methods based upon LC/MS/MS. Validation parameters included selectivity, sensitivity, linearity, carry-over, intra- and inter-assay precision, and accuracy, stock solution stability, injection medium integrity, short-term matrix stability, freeze-thaw matrix stability, long-term matrix stability, and dilution integrity. Results of Incurred Sample Reanalysis (ISR) assessments that were conducted during the toxicology studies confirmed the repeatability of the methods. The LLOQ was 5.00 ng/mL for all matrices.

Similar methods were used for the analysis of the COBI metabolite, GS-9612, in plasma from mice (Tabulated Summary 2.6.5.2.2, BA-216-2010), rats (Tabulated Summary 2.6.5.2.2, BA-216-2008), and dogs (Tabulated Summary 2.6.5.2.2, BA-216-2009) (LLOQ 1.00 ng/mL for all matrices). Other fully validated methods were used for the analysis of both COBI and EVG in rat plasma (LLOQs 5.00 and 10.0 ng/mL, respectively; Tabulated Summary 2.6.5.2.2, BA-216-2007), ATV in rat plasma (LLOQ 10.0 ng/mL; Tabulated Summary 2.6.5.2.2, BA-216-2006), and COBI in rat milk (LLOQ 2.00 ng/mL; Tabulated Summary 2.6.5.2.2, BA-216-2013).

2.2.3. Other In Vivo Bioanalytical Methods

After administration of [^{14}C]COBI to mice (Tabulated Summary 2.6.5.13.4, AD-216-2073), rats (Tabulated Summary 2.6.5.13.5, AD-216-2034), and dogs (Tabulated Summary 2.6.5.13.6, AD-216-2067 and AD-216-2068), radioactivity in plasma, urine, and feces was quantified by liquid scintillation counting and radioprofiling was performed by LC with flow radiodetection (Tabulated Summaries 2.6.5.9.3, AD-216-2073; 2.6.5.9.4, AD-216-2082; and

2.6.5.9.5, AD-216-2101). In studies in bile duct-cannulated rats (Tabulated Summary 2.6.5.13.5, AD-216-2034) and dogs (Tabulated Summary 2.6.5.13.6, AD-216-2068), the radioactivity in bile was also quantified and profiled. Mass spectrometry was also performed to identify the COBI-derived peaks in radiochromatograms. Tissue distribution in albino rats (Tabulated Summary 2.6.5.5.5, AD-216-2034) and pigmented rats (Tabulated Summary 2.6.5.5.6, AD-216-2060) was assessed by QWBA.

2.2.4. In Vitro Methods

The bidirectional permeability of COBI and the extent of polarized transport were assessed using monolayers of human Caco-2 cells (Tabulated Summary 2.6.5.3.7, AD-216-2023).

The extent of COBI binding to plasma from mouse (Tabulated Summary 2.6.5.6.3, AD-216-2076), rat, dog, monkey, and human (Tabulated Summary 2.6.5.6.3, AD-216-2026) was assessed by equilibrium dialysis.

The rates of hepatic metabolism of COBI were assessed in vitro in human cryopreserved hepatocytes and in hepatic microsomal fractions from mouse, rat, dog, monkey, and human (Tabulated Summary 2.6.5.10.7, AD-216-2074 and AD-216-2024). Major in vitro metabolites generated from COBI were initially identified tentatively by LC with ion trap mass spectrometry (MS) and by comparison with synthetic standards (Tabulated Summary 2.6.5.11.4, AD-216-2074 and AD-216-2038). More comprehensive metabolite identification was performed using samples generated in vivo.

Cytochrome P450 reaction phenotyping was determined by incubating COBI with complementary deoxyribose nucleic acid (cDNA) expressed human CYP enzyme preparations co-expressed with human NADPH CYP reductase (Tabulated Summary 2.6.5.10.8, AD-216-2025). The panel of CYP450 enzymes consisted of CYP1A2, CYP2C9, CYP2C19, CYP2D6, and CYP3A4, which are the major drug metabolizing enzymes in human. Compounds known to be metabolized by each CYP enzyme were used as controls.

The potential for COBI to inhibit the major human drug metabolizing CYP enzymes was assessed using pooled human hepatic microsomal fraction and specific probe activities (Tabulated Summary 2.6.5.12.6, AD-216-2029 and AD-216-2070), namely ethoxyresorufin O-deethylase (CYP1A2), bupropion 4-hydroxylase (CYP2B6), paclitaxel 6α-hydroxylase (CYP2C8), tolbutamide 4-hydroxylase (CYP2C9), (S) mephenytoin 4'-hydroxylase (CYP2C19), dextromethorphan O-demethylase (CYP2D6), testosterone 6β-hydroxylase (CYP3A), and midazolam 1'-hydroxylase (CYP3A). Assays were performed individually in the presence and absence of positive control inhibitors or COBI at different concentrations. The rates of production of the relevant metabolites were calculated and, where possible, 50% inhibitory concentration (IC_{50}) values were determined. Similarly, the potential for metabolites of COBI to inhibit human CYPs was determined by testing their effects against selective activities catalyzed by human hepatic microsomal fraction (Tabulated Summary 2.6.5.12.7, AD-216-2041).

The intended pharmacodynamic effect of COBI is inhibition of human CYP3A enzymes. This was studied further in vitro with human hepatic microsomal fraction as the enzyme source and using a panel of four other substrates (terfenadine, EVG, ATV, and telaprevir) (Tabulated Summary 2.6.5.12.4, AD-216-2028). Preincubation and cofactor dependence of inhibition were tested and the kinetics for inactivation of CYP3A by COBI were determined. To test species dependence in CYP3A inhibition, analogous studies were also performed with rat, dog, and monkey hepatic microsomal fractions with midazolam 1'-hydroxylase as the probe activity (Tabulated Summary 2.6.5.12.5, AD-216-2040).

The potential for COBI to inhibit the UGT enzyme, UGT1A1, was tested with human hepatic microsomal fraction and estradiol 3-glucuronide formation as the probe activity (Tabulated Summary 2.6.5.12.8, AD-216-2075). Atazanavir was tested in parallel as a positive control.

The potential for COBI to induce metabolizing enzymes and drug transporters through the activation of the AhR or human PXR was initially assessed by transactivation analysis in reporter cell lines (Tabulated Summary 2.6.5.12.9, AD-216-2027). Firefly luciferase was the reporter gene and positive control inducers were tested in parallel. Similarly, the potential for metabolites of COBI to cause drug interactions through induction was tested in the same manner (Tabulated Summary 2.6.5.12.7, AD-216-2041). Also, to aid in the understanding of time-dependent pharmacokinetics in nonclinical species, an analogous study was performed to assay rat PXR activation (Tabulated Summary 2.6.5.12.11, AD-216-2039). The potential for COBI to be an inducer was further tested in primary cultures of human hepatocytes (3 donors), with enzyme activity, mRNA expression (by reverse transcription-polymerase chain reaction [RT-PCR]), and western immunoblotting of target proteins as endpoints (Tabulated Summary 2.6.5.12.10, AD-216-2071).

Transfected MDCK II cells were used to test the dose dependent inhibition of efflux of model substrates of human MDR1, MRP1, MRP2 (Tabulated Summary 2.6.5.15.9, AD-216-2030), and BCRP (Tabulated Summary 2.6.5.15.10, AD-216-2099). Positive control inhibitors were tested in parallel. Similar studies were performed with human OAT1 (Tabulated Summary 2.6.5.15.15, AD-216-2105), OCT2 (Tabulated Summary 2.6.5.15.12, AD-216-2093), and OATP1B1 and OATP1B3 (Tabulated Summary 2.6.5.15.11, AD-216-2100) expressed in CHO cells. Other studies were performed with novel OCTN1 expressed in Drosophila melanogaster Schneider 2 (S_2) cells (Tabulated Summary 2.6.5.15.14, AD-216-2098), and with OAT3 (Tabulated Summary 2.6.5.15.15, AD-216-2105) and MATE1 and MATE2-K (Tabulated Summary 2.6.5.15.13, AD-216-2094) expressed in human embryonic kidney (HEK293) cells. Vesicles derived from porcine kidney LLC-PK1 cells transfected with human MRP4 were used to assess the sensitivity of this transporter to inhibition (Tabulated Summary 2.6.5.15.16, AD-216-2105).

Using Caco-2 cell monolayers, the effects of COBI on the polarized efflux of the MDR1 substrate, digoxin (Tabulated Summary 2.6.5.15.6, AD-216-2072), and the BCRP substrate, prazosin (Tabulated Summary 2.6.5.15.7, AD-216-2104) were determined.

The potential for COBI to be a substrate for MDR1 or BCRP was assessed by examining polarized transport in transfected MDCK II cells (Tabulated Summary 2.6.5.15.8,

AD-216-2103). Positive control substrates and inhibitors were tested in parallel. An attempt was made to assess the potential for COBI to be a substrate for human OCT2 by determining uptake of [^{14}C]COBI by CHO cells expressing recombinant OCT2 (Tabulated Summary 2.6.5.13.7, AD-216-2095).

3. ABSORPTION

3.1. In Vitro Absorption Studies for EVG

The in vitro bidirectional permeability of [^{14}C]EVG was studied using monolayers of LLC-PK1 porcine kidney cells transfected with an expression vector for human MDR1 or with the empty control expression vector (Tabulated Summary 2.6.5.3.1, JTK303-AD-026). [^{14}C]Mannitol (low permeability control) and [^{3}H]digoxin (MDR1 substrate) were assessed in parallel. All compounds were tested at an initial concentration of 1 µM in the donor compartment. Transferred amounts in the apical to basal (A-B) and basal to apical (B-A) directions were quantified as cleared volumes (µL/mg cellular protein), determined after 1, 2, and 4 hours of incubation, and the propensity for efflux was quantified as the ratio of B-A to A-B cleared volumes. The results are summarized in Table 3.

Rates of transfer of all compounds were approximately linear with incubation time over the duration tested. The permeability of EVG in control cells was relatively independent of direction (B-A/A-B ratio < 2) and was 6 to 12-fold higher than that of mannitol, the low permeability control. There was significant efflux of the positive control MDR1 substrate, digoxin, in MDR1-expressing cells (ratios ≥ 9.1) confirming competence of the cells for polarized transport. Elvitegravir also underwent significant efflux across these cells (ratio ≥ 13.6), suggesting that it is a substrate for human MDR1. However, in dose escalation studies in rats to 2000 mg/kg (Tabulated Summary 2.6.7.7.1.2, JTK303-TX-003), and dogs to 100 mg/kg (Tabulated Summary 2.6.7.7.1.6, JTK303-TX-004), there was no evidence for a greater than dose-proportional increase in exposure at high doses (which would have been consistent with saturation of intestinal efflux).

Table 3. Transport of EVG and Control Compounds Across Monolayers of LLC-PK1 Cells Transfected with Control Vector or Expression Vector for Human MDR1

Compound	Time (h)	Cleared Volume (µL/mg Cellular Protein)					
		Control Cells			MDR1-Expressing Cells		
		A-B	B-A	Ratio	A-B	B-A	Ratio
EVG	1	179.2 ± 16.7	207.8 ± 11.2	1.2	64.1 ± 17.3	961.9 ± 75.8	15.0
	2	412.7 ± 20.0	512.8 ± 34.4	1.2	139.4 ± 25.2	1891.6 ± 126.1	13.6
	4	606.4 ± 18.7	912.6 ± 62.9	1.5	212.1 ± 34.7	3085.4 ± 65.7	14.5
Digoxin	1	21.6 ± 1.1	44.6 ± 10.3	2.1	25.3 ± 9.0	245.8 ± 27.0	9.7
	2	48.6 ± 9.5	96.7 ± 16.1	2	54.9 ± 5.1	498.1 ± 69.8	9.1
	4	103.0 ± 20.1	229.8 ± 27.4	2.2	97.4 ± 12.3	1000.2 ± 125.8	10.3
Mannitol	1	24.1 ± 12.8	16.2 ± 1.2	0.7	53.9 ± 36.4	42.9 ± 18.2	0.8
	2	36.6 ± 10.4	35.7 ± 4.0	1	97.0 ± 63.6	83.6 ± 27.4	0.9
	4	89.9 ± 14.4	73.5 ± 6.3	0.8	176.9 ± 100.2	131.7 ± 33.8	0.7

A-B = apical to basal; B-A = basal to apical; EVG = elvitegravir; MDR1 = P-glycoprotein
Source: Report JTK303-AD-026

3.2. In Vitro Absorption Studies for COBI

The cellular permeability of COBI was assessed in vitro using Caco-2 monolayers, at an initial COBI concentration of 1 μM (Tabulated Summary 2.6.5.3.7, AD-216-2023). Transfer rates in both the A-B (forward) and B-A (reverse) directions were assessed (Table 4).

At a target concentration of 1 μM, COBI had high forward permeability (7.61×10^{-6} cm/s), with little evidence for significant efflux (ratio = 1.1).

Table 4. Bidirectional Permeability of COBI Through Caco-2 Cell Monolayers

Direction	Target Conc. (μM)	Initial Conc. (μM)	Recovery (%)	P_{app} (10^{-6} cm/s)	Efflux Ratio
Cell-Free	1	1.2	ND	9.45	
Forward		1.4	73.8	7.61	1.1
Reverse		1.3	55.0	8.51	

COBI = cobicistat; P_{app} = apparent permeability; ND = not determined due to missing donor well concentration at 120 minutes

Source: Report AD-216-2023

3.3. Single-Dose Studies

3.3.1. EVG: Single-Dose In Vivo Studies

The in vivo disposition of EVG was assessed in rats and dogs following intravenous and oral administration. For intravenous bolus administration, the dose was 1 mg/kg and the vehicle was 80% (v/v) aqueous polyethylene glycol 400. For oral administration, the doses were 1, 3, and 10 mg/kg and the vehicle was 0.5% (w/v) aqueous methylcellulose. Animals in these groups were nonfasted. A further group (dosed at 3 mg/kg) was dosed in the fasted state to explore the influence of feeding on pharmacokinetics.

Similar studies were also performed with [^{14}C]EVG administered intravenously at 1 mg/kg and orally at a dose of 3 mg/kg to nonfasted animals. Pharmacokinetic parameters were derived using the concentrations of total radioactivity in plasma.

3.3.1.1. EVG: Single-Dose Studies in Rats

After administration of [^{14}C]EVG to nonfasted male Sprague-Dawley rats, the bioavailability of total radioactivity was 41.1% ± 5.0% (Tabulated Summary 2.6.5.3.3, JTK303-AD-005 and JTK303-AD-007).

The mean plasma concentration-time profiles of EVG following intravenous and oral administration of EVG to nonfasted male Sprague-Dawley rats are illustrated in Figure 1 and

the pharmacokinetic parameters are provided in Table 5 and Table 6 (Tabulated Summary 2.6.5.3.2, JTK303-AD-009 and JTK303-AD-011).

Clearance of EVG in rats was low relative to hepatic blood flow, and the volume of distribution was moderate, with a value between that of extracellular fluid and total body water. Oral pharmacokinetics were linear over the range tested with relatively rapid absorption ($t_{max} \leq 0.83$ h) and moderate bioavailability 30% to 35%. At a dose of 3 mg/kg to nonfasted rats, the oral bioavailability of parent compound (34.1%) was similar to that for radioactivity (41.1%), indicating low (< 30%) first pass elimination. Fasting the animals increased the C_{max} of EVG by ~2-fold, but had little effect on the area under the curve.

Figure 1. Pharmacokinetics of EVG in Rats after Oral (Nonfasted) or Intravenous Administration (Mean ± SD, n = 3)

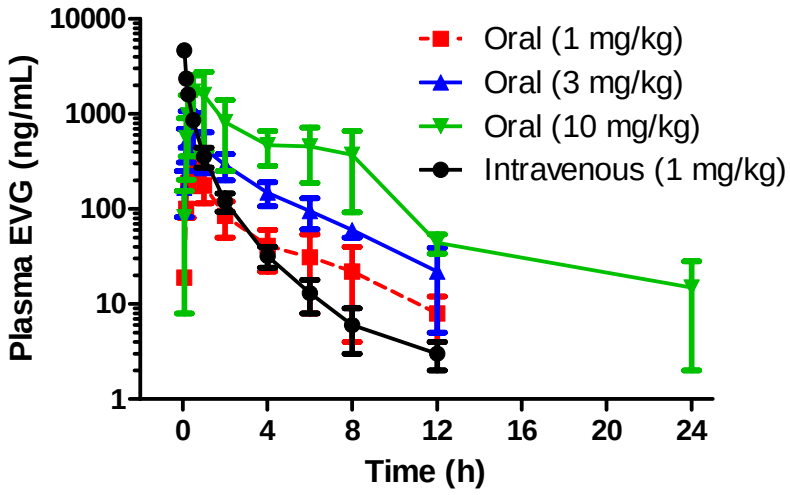

EVG = elvitegravir; SD = standard deviation
Source: Reports JTK303-AD-009 and JTK303-AD-011

Table 5. Mean Pharmacokinetic Parameters Following Intravenous Administration of 1 mg/kg EVG to Male Rats (Mean ± SD, n = 3)

Parameter	MRT (h)	V_{ss} (L/kg)	CL (L/h/kg)	$AUC_{0-\infty}$ (ng•h/mL)
Value	0.8 ± 0.1	0.4 ± 0.1	0.5 ± 0.1	1955 ± 224

SD = standard deviation
Source: Reports JTK303-AD-009 and JTK303-AD-011

Table 6. Mean Pharmacokinetic Parameters Following Oral Administration of EVG to Male Rats (Mean ± SD, n = 3)

Dose	1 mg/kg	3 mg/kg	3 mg/kg	10 mg/kg
Feeding Status	Nonfasted	Nonfasted	Fasted	Nonfasted
t_{max} (h)	0.42 ± 0.14	0.25 ± 0.0	0.5 ± 0.0	0.83 ± 0.29
C_{max} (ng/mL)	251 ± 51	755 ± 311	1536 ± 240	1947 ± 971
MRT (h)	3.4 ± 0.7	3.4 ± 0.4	1.6 ± 0.3	4.9 ± 1.6
$AUC_{0-\infty}$ (ng•h/mL)	643 ± 285	1999 ± 675	1762 ± 215	6825 ± 2455
F (%)	32.9 ± 14.6	34.1 ± 11.5	30.0 ± 3.7	34.9 ± 12.5

SD = standard deviation
Source: Reports JTK303-AD-009 and JTK303-AD-011

3.3.1.2. EVG: Single-Dose Studies in Dogs

After administration of [^{14}C]EVG to nonfasted male beagle dogs, the bioavailability of total radioactivity was 41.4% ± 15.1% (Tabulated Summary 2.6.5.3.5, JTK303-AD-006 and JTK303-AD-008).

The mean plasma concentration-time profiles of EVG following intravenous and oral administration to male beagle dogs are illustrated in Figure 2 and the pharmacokinetic parameters are provided in Table 7 and Table 8 (Tabulated Summary 2.6.5.3.4, JTK303-AD-010 and JTK303-AD-012).

Results were generally similar to those seen in rats. Clearance was intermediate relative to hepatic blood flow and the volume of distribution exceeded that of total body water. Absorption was rapid ($t_{max} \leq 0.83$ hour), bioavailability was ≥ 26%, and exposure was dose-linear. At a dose of 3 mg/kg to nonfasted dogs, the oral bioavailability of parent compound (29.6%) was similar to that for radioactivity (41.4%), indicating low first pass metabolism. Fed animals again showed a ~2-fold higher C_{max} for EVG, but little change in the area under the curve.

Figure 2. **Pharmacokinetics of EVG in Dogs after Oral (Nonfasted) or Intravenous Administration (Mean ± SD, n = 3)**

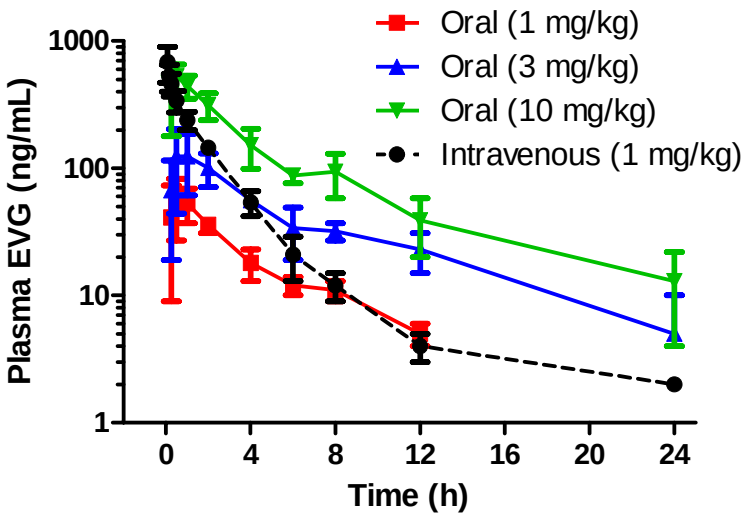

EVG = elvitegravir; SD = standard deviation
Source: Reports JTK303-AD-010 and JTK303-AD-012

Table 7. **Mean Pharmacokinetic Parameters Following Intravenous Administration of 1 mg/kg EVG to Male Dogs (Mean ± SD, n = 3)**

Parameter	MRT (h)	V_{ss} (L/kg)	CL (L/h/kg)	$AUC_{0-\infty}$ (ng•h/mL)
Value	2.5 ± 0.2	2.6 ± 0.4	1.0 ± 0.2	954 ± 130

SD = standard deviation
Source: Reports JTK303-AD-010 and JTK303-AD-012

Table 8. **Mean Pharmacokinetic Parameters Following Oral Administration of EVG to Male Dogs (Mean ± SD, n = 3)**

Dose	1 mg/kg	3 mg/kg	3 mg/kg	10 mg/kg
Feeding Status	Non-fasted	Non-fasted	Fasted	Non-fasted
t_{max} (h)	0.67 ± 0.29	1.00 ± 0.87	0.83 ± 0.29	0.67 ± 0.29
C_{max} (ng/mL)	58 ± 24	136 ± 61	312 ± 158	529 ± 126
MRT (h)	5.1 ± 1.1	7.6 ± 3.8	2.8 ± 0.7	7.6 ± 5.3
$AUC_{0-\infty}$ (ng•h/mL)	255 ± 40	843 ± 73	923 ± 320	2495 ± 682
F (%)	26.7 ± 2.4	29.6 ± 1.7	33.0 ± 13.7	26.0 ± 4.3

SD = standard deviation
Source: Reports JTK303-AD-010 and JTK303-AD-012

3.3.2. COBI: Single-Dose Pharmacokinetic Profile Following Intravenous Administration in the Rat, Dog, and Monkey

The mean plasma pharmacokinetic parameters for COBI following intravenous administration to Sprague-Dawley rats (Tabulated Summary 2.6.5.3.9, AD-216-2020), beagle dogs (Tabulated Summary 2.6.5.3.10, AD-216-2021), and cynomolgus monkeys (Tabulated Summary 2.6.5.3.12, AD-216-2022) are summarized in Table 9. Rat studies were performed with both sexes, while males were used for the studies in dogs and monkeys. The mean plasma concentration-time profiles for male animals are illustrated in Figure 3.

The systemic clearance (CL) of COBI was high in males of all species and was close to hepatic blood flow in each case. Female rats showed lower CL than males. The volume of distribution (V_{ss}) was equal to (rat), or somewhat larger (other species) than the volume of total body water.

Figure 3. Mean Plasma Concentration vs. Time Profile Following 30-Minute Intravenous Infusion of COBI at 1 mg/kg to Male Sprague–Dawley Rats, Beagle Dogs, and Cynomolgus Monkeys (mean ± SD, N = 3)

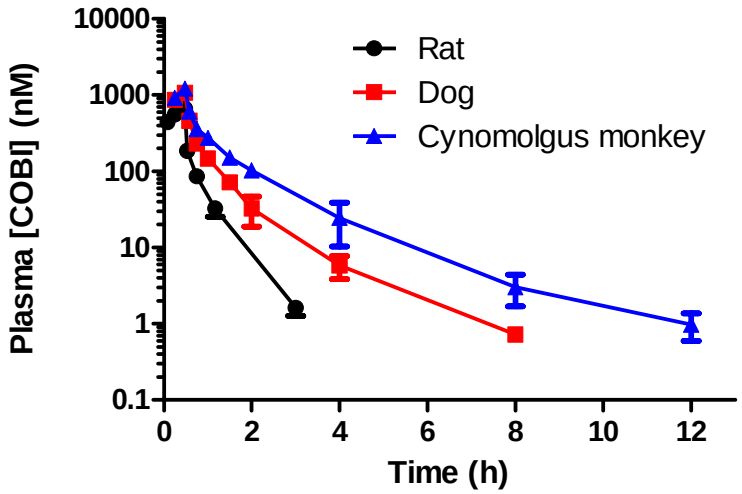

COBI = cobicistat; SD = standard deviation
Source: Reports AD-216-2020 (rat), AD-216-2021 (dog), and AD-216-2022 (monkey)

Table 9. Mean Plasma Pharmacokinetic Parameters for COBI Following 30-Minute Intravenous Infusion at 1 mg/kg to Sprague-Dawley Rats, Beagle Dogs, and Cynomolgus Monkeys (mean ± SD, N = 3)

Species	Sex	C_{max} (nM)	$AUC_{0-\infty}$ (nM•h)	CL (L/h/kg)	V_{ss} (L/kg)	$t_{½}$ (h)
Rat	Male	664 ± 31.4	351 ± 12.6	3.59 ± 0.14	0.76 ± 0.14	0.40 ± 0.02
	Female	890 ± 74.3	566 ± 50.1	2.37 ± 0.18	0.70 ± 0.09	0.35 ± 0.01
Dog	Male	924 ± 267	565 ± 155	2.18 ± 0.69	1.33 ± 0.69	1.02 ± 0.04
Monkey	Male	1222 ± 41.1	977 ± 83.7	1.36 ± 0.14	1.31 ± 0.12	1.42 ± 0.07

COBI = cobicistat; SD = standard deviation

Source: Reports AD-216-2020 (rat), AD-216-2021 (dog), and AD-216-2022 (monkey)

3.3.3. COBI: Single-Dose Oral Pharmacokinetic Profiles in Rats, Dogs, and Monkeys

The mean plasma concentration profiles of COBI following oral administration in solution to male Sprague-Dawley rats, beagle dogs, and cynomolgus monkeys are presented in Figure 4 (Tabulated Summaries 2.6.5.3.9, 2.6.5.3.10, and 2.6.5.3.12; AD-216-2020, AD-216-2021, and AD-216-2022, respectively). The mean plasma pharmacokinetic parameters are summarized in Table 10.

At doses of 5 or 6 mg/kg, oral bioavailability of COBI was moderate in the rat (33%) and low in the dog and monkey (11% and 7%, respectively). The high clearance values in these species indicate the potential for high hepatic metabolic first-pass extraction following oral absorption in these species. Comparing bioavailability and predicted hepatic extraction values, it is likely that a substantial proportion (> 50%) of the dose was absorbed from the gastrointestinal (GI) tract.

Figure 4. **Mean Plasma Concentration vs. Time Profile Following Oral Administration of COBI in Solution to Male Sprague-Dawley Rats, Beagle Dogs, and Cynomolgus Monkeys (mean ± SD, N = 3)**

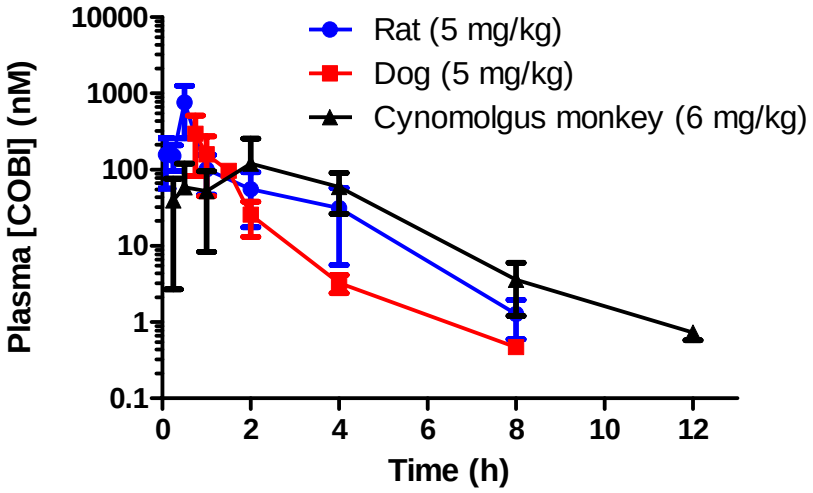

COBI = cobicistat; SD = standard deviation
Source: Reports AD-216-2020 (rat), AD-216-2021 (dog), and AD-216-2022 (monkey)

Table 10. **Mean Plasma Pharmacokinetic Parameters Following Oral Administration of COBI in Solution to Male Sprague-Dawley Rats, Beagle Dogs, and Cynomolgus Monkeys (mean ± SD, N = 3)**

Species	Dose (mg/kg)	t_{max} (h)	C_{max} (nM)	$t_{½}$ (h)	$AUC_{0-\infty}$ (nM•h)	%F
Rat	5	0.50 ± 0.00	764 ± 506	0.92 ± 0.22	594 ± 42.6	33 ± 3
Dog	5	1.00 ± 0.43	313 ± 186	1.12 ± 0.14	331 ± 130	11 ± 4
Monkey	6	2.17 ± 1.76	161 ± 102	1.36 ± 0.21	445 ± 280	7.3 ± 4.6

COBI = cobicistat; SD = standard deviation
Source: Reports AD-216-2020 (rat), AD-216-2021 (dog) and AD-216-2022 (monkey)

Exploratory single-dose escalation studies were also performed in male and female Balb/cBy x C57BL/6 F1-Tg(HRAS)2Jic hybrid mice (Model 001178-W; wild type for rasH2 transgenic mice), male and female rats, and male dogs (Tabulated Summaries 2.6.5.3.8, 2.6.5.3.10, and 2.6.5.3.9; PC-216-2013-PK, AD-216-2021, and AD-216-2020, respectively). The results are summarized in Table 11, Table 12, and Table 13. In the mice, the animals dosed at 300 mg/kg were moribund and euthanized 4 hours after dosing. There were no remarkable sex differences in exposure, and exposure increased in a roughly dose-proportional manner from 30 to 100 mg/kg. In the male rat and the male dog, there was a greater than proportional increase in AUC_{0-t} as the dose was increased from 5 to 25 mg/kg

and 10 to 30 mg/kg, respectively, likely reflecting saturation of first-pass metabolism. Following saturation, the change in AUC_{0-t} was near proportional as the dose was increased further, from 25 to 100 mg/kg in the male rat and 30 to 100 mg/kg in the male dog. In the female rat, as seen after intravenous administration, exposures were higher than in the males at both doses consistent with the known gender difference in CYP3A expression in this species. The increase in AUC_{0-t} in female rats, when the dose was increased from 25 to 110 mg/kg, was greater than dose proportional.

Table 11. Mean Plasma Pharmacokinetic Parameters Following Oral Administration of Increasing Doses of COBI in Solution to CByB6F1-Tg(HRAS)2Jic Mice (mean, N = 4 animals per time point)

Dose (mg/kg)	Sex	t_{max} (h)	C_{max} (ng/mL)	t_{last} (h)	C_{24h} (ng/mL)	AUC_{0-t} (ng•h/mL)
30	M	2.0	5940	24	1.67	35535
	F	1.0	10158	24	1.28	46306
100	M	2.0	11130	24	1418	108796
	F	1.0	16205	24	1532	128930
300	M	4.0	29392	4[a]	NC[a]	NC[a]
	F	2.0	23464	4[a]	NC[a]	NC[a]

COBI = cobicistat; NC = not calculated
a Animals moribund and euthanized after 4 hours, so parameters were not calculated
Source: Report PC-216-2013-PK

Table 12. Mean Plasma Pharmacokinetic Parameters Following Oral Administration of Increasing Doses of COBI in Solution to Sprague-Dawley Rats (mean ± SD, N = 3)

Dose (mg/kg)	Sex	t_{max} (h)	C_{max} (nM)	t_{last} (h)	C_{last} (nM)	AUC_{0-t} (nM•h)
5	M	0.50 ± 0.00	764 ± 506	--	1.58 ± 0.70	594 ± 42.6
25		1.08 ± 0.88	4000 ± 684	8	6.58 ± 2.02	13,233 ± 1942
100		1.42 ± 1.01	6895 ± 933	24	14.0 ± 8.70	65,185 ± 21,658
25	F	0.83 ± 1.01	4506 ± 237	24	1.24 ± 0.16	26,087 ± 6923
110		6.67 ± 2.31	12,784 ± 956	24	2708 ± 1510	170,525 ± 20,189

COBI = cobicistat; SD = standard deviation
Source: Report AD-216-2020

Table 13. Mean Plasma Pharmacokinetic Parameters Following Oral Administration of Increasing Doses of COBI in Solution to Male Beagle Dogs (mean ± SD, N = 3)

Dose (mg/kg)	t_{max} (h)	C_{max} (nM)	t_{last} (h)	C_{last} (nM)	AUC_{0-t} (nM•h)
10	1.50 ± 2.17	118 ± 57.6	9.33 ± 2.31	2.90 ± 2.73	355 ± 435
30	2.33 ± 1.53	4373 ± 2307	24.0 ± 0.0	13.6 ± 14.3	34,538 ± 13,033
100	1.67 ± 2.02	9640 ± 572	24.0 ± 0.0	872 ± 752	102,223 ± 23,511

COBI = cobicistat; SD = standard deviation
Source: Report AD-216-2021

3.4. Repeat-Dose Studies

3.4.1. EVG: Multiple-Dose In Vivo Studies

3.4.1.1. Pharmacokinetics in Rats after Repeated Oral Administration of [^{14}C]EVG

[^{14}C]EVG was administered orally to nonfasted male Sprague-Dawley rats daily for 7 days at a dose of 3 mg/kg. The vehicle was 0.5% (w/v) methylcellulose. Plasma concentrations of total radioactivity were determined on dosing Days 1 and 7. The ratio of values for $AUC_{0-\tau}$ for Day 7 compared to Day 1 was 1.16 ± 0.24 (Tabulated Summary 2.6.5.4.1, JTK303-AD-022 and JTK303-AD-028), indicating that multiple dosing with EVG did not appreciably affect the fraction of total radioactivity absorbed.

3.4.1.2. EVG: Other Multiple-Dose In Vivo Studies

During nonclinical safety studies, toxicokinetic parameters after multiple doses were determined in mice, rats, and dogs. The data are presented in that context in Module 2.6.6, Section 3.1 and salient points are described below.

In mice (Tabulated Summary 2.6.7.7.1.1, TX-183-2004 and Tabulated Summary 2.6.7.10.1, TX-183-2011) and rats (Tabulated Summary 2.6.7.7.1.2, JTK303-TX-003; Tabulated Summary 2.6.7.7.1.3, JTK303-TX-021; Tabulated Summary 2.6.7.7.1.4, JTK303-TX-022; and Tabulated Summary 2.6.7.10.2, TX-183-2012), exposure of EVG was higher in females than males. In humans, EVG oxidative metabolism is primarily catalyzed by CYP3A4 (Tabulated Summary 2.6.5.10.4, JTK303-AD-017). In mice, there is also evidence for CYP3A enzymes being involved, as pretreatment with dexamethasone, a prototypical CYP3A inducer, yielded hepatic microsomal fractions with a high rate of EVG metabolism (Tabulated Summary 2.6.5.10.1, AD-183-2019). CYP3A enzymes are known to display sex differences in rodents, with higher expression in males, and this may contribute to the differences seen in EVG exposure, and the more rapid rate of metabolism seen in vitro (Tabulated Summary 2.6.5.10.1, AD-183-2019). In contrast, in the dog, there was no clear

sex difference in exposure to EVG (Tabulated Summary 2.6.7.7.1.6, JTK303-TX-004 and Tabulated Summary 2.6.7.7.1.7, JTK303-TX-023), consistent with a lack of gender difference in CYP3A expression in this species.

Treatment of mice with EVG for up to 26 weeks led to no notable decreases in exposure (Tabulated Summary 2.6.7.10.1, TX-183-2011), suggesting low potential for autoinduction of EVG clearance in this species. This was confirmed in vitro, as microsomal fractions prepared from EVG-treated mice (200 or 2000 mg/kg/day) showed similar rates of metabolism of [^{14}C]EVG as vehicle-treated animals (Tabulated Summary 2.6.5.10.1, AD-183-2019). Similarly, in rats there was no evidence for autoinduction in either sex after 1 month (Tabulated Summary 2.6.7.7.1.2, JTK303-TX-003), 3 months (Tabulated Summary 2.6.7.7.1.3, JTK303-TX-021), 6 months (Tabulated Summary 2.6.7.7.1.4, JTK303-TX-022), or 360 days (Tabulated Summary 2.6.7.10.2, TX-183-2012) of treatment. Analysis of hepatic microsomal fractions from rats treated with EVG for 90 days (Tabulated Summary 2.6.7.7.3.1, TX-236-2001) revealed no notable changes in CYP3A activity, confirming a lack of autoinduction in this species. In dogs there was also no evidence for autoinduction in either sex after treatment for 1 month (Tabulated Summary 2.6.7.7.1.6, JTK303-TX-004) or 9 months (Tabulated Summary 2.6.7.7.1.7, JTK303-TX-023).

Multiple dose in vivo toxicokinetic studies were also performed with EVG in combination with other agents. These studies were performed in support of safety evaluation and were not intended as pharmacokinetic drug interaction studies. In mice treated for 26 weeks (Tabulated Summary 2.6.7.10.1, TX-183-2011), exposure to EVG was increased 4- to 7-fold by co-treatment with RTV (25 mg/kg), likely due to reversible inhibition of CYP3A-mediated metabolism. In rats treated for 90 days (Tabulated Summary 2.6.7.7.1.5, TX-183-2007), EVG exposures were also higher when co-dosed with RTV (10 mg/kg) than when dosed alone. In the animals treated with RTV, the levels of the oxidative metabolite, M1 (GS-9202), were reduced to levels below quantification, while the levels of the glucuronide metabolite, M4 (GS-9200), were largely unaffected. Similarly, in rats treated for 90 days (Tabulated Summary 2.6.7.7.3.1, TX-236-2001), EVG levels were increased when co-dosed with COBI (30 mg/kg) compared to EVG alone.

3.4.2. COBI: Multiple-Dose In Vivo Studies

Multiple dose in vivo toxicokinetic studies were performed in mouse, rat, and dog in support of safety evaluation. The results are presented in detail in Module 2.6.6, Section 3.2 and general conclusions from representative studies are noted below.

Similar to the single-dose study in CByB6F1-Tg(HRAS)2Jic mice described above (Table 11), in CD-1 mice treated daily with COBI for 13 weeks (Tabulated Summary 2.6.7.7.2.1, TX-216-2026) there were no notable sex differences in exposure. Exposure was greater than dose-proportional when the dose was increased from 5 to 15 mg/kg, likely due to saturation of first-pass metabolism, and then roughly dose-proportional from 15 to 50 mg/kg. After treatment for 13 weeks, there were modest increases in hepatic microsomal CYP2B and CYP3A activities, but these were only manifest at the highest dose. This is consistent with COBI activating rodent PXR (Tabulated Summary 2.6.5.12.11, AD-216-2039), which

regulates these enzymes. Despite the increase in enzyme activity, exposure did not change appreciably in these animals after 13 weeks of dosing, likely due to continued saturation of metabolism. Similar toxicokinetic results were found in a 4-week dose range-finding study in CByB6F1-Tg(HRAS)2Jic mice (Tabulated Summary 2.6.7.6.2, TX-216-2041).

Similar to the results seen in the single-dose study described above (Table 12), in rats treated with COBI for up to 26 weeks (Tabulated Summary 2.6.7.7.2.3, TX-216-2017) there was an approximate 2-fold sex difference in exposure (females > males). After daily oral dosing with COBI for 26 weeks, there were modest increases in hepatic microsomal CYP3A activity in both males (at 100 mg/kg) and females (at 30 and 100 mg/kg). This is consistent with the ability of COBI to activate rat PXR (Tabulated Summary 2.6.5.12.11, AD-216-2039) which regulates CYP3A enzymes. Increases in hepatic microsomal CYP1A activity (up to 3.5-fold compared to vehicle treated animals) were also seen, but the magnitude of the changes is very small compared to the typical response to a potent CYP1A inducer. Increasing rat CYP1A activity through AhR activation by COBI would be a species-specific phenomenon as there were no notable increases in CYP1A activity after multiple dosing studies in mice or dogs, and COBI does not activate human AhR (Tabulated Summary 2.6.5.12.9, AD-216-2027) or increase CYP1A2 activity in human hepatocytes (Tabulated Summary 2.6.5.12.10, AD-216-2071; see Section 7.2.3 below).

In dogs treated daily with COBI at doses of 5, 15, or 45 mg/kg/day for 4 weeks (Tabulated Summary 2.6.7.7.2.5, TX-216-2005) or 5, 10, or 20 mg/kg/day for 39 weeks (Tabulated Summary 2.6.7.7.2.6, TX-216-2016), there were no notable sex differences in exposure. As seen in the single-dose studies described above (Table 13), exposure increased in a greater than dose-proportional manner from 5 to 15 mg/kg/day (4-week study) or to 20 mg/kg/day (39-week study), likely due to saturation of metabolism, and then was roughly proportional from 15 to 45 mg/kg (4-week study). Dosing for 4 weeks led to an apparent decrease in hepatic microsomal CYP3A activity. As discussed in detail in Section 7.2.1.1 below, unlike its effects in humans, COBI is not an effective mechanism-based CYP3A enzyme inhibitor in nonclinical species, but it is a potent reversible CYP3A inhibitor. In vitro studies (Tabulated Summary 2.6.5.12.5, AD-216-2040) showed that dog hepatic microsomal CYP3A activity is very sensitive to inhibition by COBI (IC_{50} 0.12 μM). The apparent reduction in CYP3A activity may be due to the presence of low levels of residual COBI in the microsomal fraction.

Multiple-dose in vivo toxicokinetic studies were also performed with COBI in combination with other agents. These studies were performed in support of safety evaluation and were not intended as pharmacokinetic drug interaction studies as, due to the species differences in CYP3A inhibition noted above, the results would not be representative of those expected in humans. In rats treated for 90 days (Tabulated Summary 2.6.7.7.3.1, TX-236-2001), EVG exposures were higher when co-dosed with COBI than when dosed alone, consistent with inhibition of CYP3A-dependent metabolism of EVG. Similarly, in rats treated for 90 days (Tabulated Summary 2.6.7.7.2.4, TX-216-2024), ATV exposures were higher when co-dosed with COBI than when dosed alone, again consistent with inhibition of CYP3A-dependent metabolism of ATV.

3.5. EVG/COBI/FTC/TDF: Absorption

With respect to potential drug interactions within the combination that could affect absorption, FTC shows high passive permeability and so is unlikely to be affected when administered with EVG, COBI or TDF. In vitro mechanistic studies on the potential for COBI to affect the absorption of TDF are described in Section 7.2.4.2. Although formal studies of the absorption kinetics of the EVG/COBI/FTC/TDF STR have not been conducted, a single dose comparison of the exposure of an EVG/COBI/FTC/TDF STR after oral administration of a prototype combination tablet and coadministration of the individual compounds in dogs has demonstrated comparable systemic exposure to all agents (Tabulated Summary 2.6.5.3.13, AD-216-2061). Comprehensive clinical studies on the combination have also been performed (Module 2.7.2).

4. DISTRIBUTION

4.1. Plasma Protein Binding

4.1.1. EVG: Plasma Protein Binding

The binding of [^{14}C]EVG to plasma from rats, dogs, cynomolgus monkeys, and humans was determined by equilibrium dialysis at 37°C against isotonic phosphate-buffered saline (Tabulated Summary 2.6.5.6.2, JTK303-AD-014). Initial EVG concentrations in plasma were 0.1, 1, and 10 µg/mL. Pilot experiments with human plasma demonstrated that equilibrium was achieved by 6 hours. Stability of [^{14}C]EVG in plasma was determined with an incubation time of 8 hours and concentrations of EVG of 0.1 and 10 µg/mL.

To understand the relative binding to human plasma, proteins studies were also performed with purified HSA and AAG dissolved in water. Representative physiological concentrations of the individual proteins were tested (5% w/v HSA and 0.07% w/v AAG). Since in vivo plasma concentrations of AAG can vary, mixtures of 5% (w/v) HSA with varying concentrations of AAG (0.05, 0.1, and 0.2% w/v) were also tested. A pilot study was performed with 0.07% (w/v) AAG and found that equilibrium was achieved by 6 hours.

The results of the studies are summarized in Table 14. There was no evidence of instability of [^{14}C]EVG (0.1 or 10 µg/mL) when incubated with rat, dog, monkey, or human plasma for 8 hours at 37°C. Binding to all matrices was independent of the concentration of EVG over the range 0.1 to 10 µg/mL. Binding was highest in the rat and lowest in the monkey, with dog and human showing similar, intermediate values. There was little binding of EVG to 0.07% (w/v) AAG, but the extent of binding to 5% (w/v) HSA was very similar to that in human plasma, suggesting that albumin is the major plasma binding protein. Addition of 0.05% to 0.2% (w/v) AAG had no appreciable effect on the binding to HSA.

Approximately the same extent of binding of EVG was found in human plasma samples from clinical studies in which subjects were coadministered 150 mg EVG plus 150 mg COBI once daily for 7 to 10 days. Mean fraction unbound values, determined ex vivo, were between 1.15% and 1.16% in normal human subjects, 1.22% in subjects with moderate hepatic impairment, and 1.42% in subjects with severe renal impairment (Module 2.7.2, Sections 2.4.1.1 and 2.4.1.2 [Studies GS-US-183-0133 and GS-US-216-0124, respectively]).

Table 14. Extent of Protein Binding of [^{14}C]EVG in Rats, Dogs, Monkeys, and Humans and to Purified Human Proteins (Mean ± SD, n = 3)

Species	Sample	Concentration (µg/mL)	Fraction Bound (%)	Mean Fraction Unbound (%)
Rat	Plasma	0.1	99.9 ± 0.01	0.1
		1	99.9 ± 0.01	0.1
		10	99.9 ± 0.00	0.1
Dog	Plasma	0.1	99.2 ± 0.17	0.8
		1	99.2 ± 0.15	0.8
		10	99.2 ± 0.16	0.8
Monkey	Plasma	0.1	98.8 ± 0.11	1.2
		1	98.8 ± 0.09	1.2
		10	98.8 ± 0.09	1.2
Human	Plasma	0.1	99.4 ± 0.05	0.6
		1	99.3 ± 0.07	0.7
		10	99.3 ± 0.04	0.7
	5% HSA	0.1	99.4 ± 0.02	0.6
		1	99.4 ± 0.01	0.6
		10	99.4 ± 0.01	0.6
	0.07% AAG	0.1	39.3 ± 1.04	60.7
		1	39.1 ± 0.93	60.9
		10	40.7 ± 1.99	59.3
	0.05% AAG / 5% HSA	0.1	99.5 ± 0.01	0.5
		1	99.4 ± 0.01	0.6
		10	99.4 ± 0.03	0.6
	0.1% AAG / HSA	0.1	99.1 ± 0.63	0.9
		1	99.3[a]	0.7
		10	99.4 ± 0.01	0.6
	0.2% AAG / 5% HSA	0.1	99.4 ± 0.02	0.6
		1	99.4 ± 0.01	0.6
		10	99.4 ± 0.01	0.6

AAG = α1-acid glycoprotein; EVG = elvitegravir; HSA = human serum albumin; SD = standard deviation
a The mean of 2 values.
Source: Report JTK303-AD-014

The ex vivo binding of [^{14}C]EVG (0.5 µg/mL) to plasma from male and female CD-1 mice was also determined by equilibrium dialysis (Tabulated Summary 2.6.5.6.1, AD-183-2024). Plasma samples were obtained from a study in which the animals were dosed with EVG, EVG+RTV or vehicle daily for 1 or 7 days. When [^{14}C]EVG was added to these samples, the fraction unbound varied from 0.22% to 0.41%, with females showing higher binding than males. The fraction of [^{14}C]EVG bound in plasma from mice treated with vehicle for 7 days

was 99.6% in males and 99.7% in females. The extent of binding of EVG in mice thus lies between that in rats (99.9%) and dogs (99.2%) or humans (99.3% to 99.4%).

4.1.2. EVG: Distribution of EVG within Blood In Vitro

The relative distribution of [^{14}C]EVG into the cellular and soluble fractions of blood was determined with blood from rats, dogs, cynomolgus monkeys, and humans (Tabulated Summary 2.6.5.8.1, JTK303-AD-013). Initial EVG concentrations were 0.1, 1, and 10 µg/mL. After equilibration at 37°C, the concentration of radioactivity in whole blood was compared to that in plasma prepared by centrifugation. A pilot experiment with human blood demonstrated that equilibrium was achieved by 30 minutes. The stability of [^{14}C]EVG (0.1 and 10 µg/mL) in blood from rats, dogs, monkeys, and humans was determined with an incubation time of 2 hours at 37°C.

There was no evidence for instability of [^{14}C]EVG when incubated with blood for 2 hours. The distribution data are summarized in Table 15. The distribution was relatively independent of EVG concentration. Elvitegravir was largely excluded from the cellular fraction of rat blood, yielding a whole blood/plasma concentration ratio of 0.6. In blood from dog, monkey, and human, there was greater distribution into blood cells. The results with human blood are consistent with findings in vivo (Module 2.7.2, Section 2.2.1.3 [GS-US-183-0126]) in which the mean C_{max} values for radioactivity, for subjects dosed with 50 mg [^{14}C]EVG plus 100 mg RTV, were 378 and 543 ng equivalents/mL in blood and plasma, respectively (blood/plasma ratio 0.7).

Table 15. Distribution of [^{14}C]EVG within Rat, Dog, Monkey, and Human Blood

Species	Concentration (µg/mL)	Distribution to Blood Cells (%)	Estimated Blood/Plasma Ratio
		Mean ± SD (n = 3)	Mean
Rat	0.1	2.2 ± 1.9	0.6
	1	3.0 ± 2.0	0.6
	10	3.2 ± 2.8	0.6
Dog	0.1	32.4 ± 1.9	0.8
	1	30.8 ± 3.0	0.8
	10	25.6 ± 3.4	0.7
Monkey	0.1	26.4 ± 4.9	0.8
	1	28.6 ± 3.4	0.8
	10	26.1 ± 8.0	0.8
Human	0.1	24.0 ± 5.4	0.7
	1	21.9 ± 6.4	0.7
	10	20.8 ± 2.0	0.6

SD = standard deviation
Source: Report JTK303-AD-013

4.1.3. COBI: Plasma Protein Binding

The binding of COBI in plasma from CD-1 mouse, Sprague-Dawley rat, beagle dog, cynomolgus monkey, and human (Tabulated Summary 2.6.5.6.3, AD-216-2076 and AD-216-2026) was assessed by equilibrium dialysis against isotonic phosphate buffer at 37°C for 3 hours (the time determined to achieve equilibration). The data are summarized in Table 16.

The plasma protein binding of COBI was determined to be moderately high in all species, ranging from 90.9% to 97.7% over the concentration range 1 to 30 µM. Binding to mouse, rat, and monkey plasma showed modest concentration dependence.

Table 16. Protein Binding for COBI in Mouse, Rat, Dog, Monkey, and Human Plasma Determined by Equilibrium Dialysis (mean ± SD, n = 3)

Plasma source	Fraction Unbound (%)			
	1 µM COBI	10 µM COBI	30 µM COBI	Mean
Mouse	3.31 ± 0.14	4.78 ± 0.27	6.15 ± 0.48	4.75
Rat	2.33 ± 0.06	5.34 ± 0.24	8.51 ± 0.48	5.40
Dog	5.68 ± 0.60	6.46 ± 0.60	6.33 ± 0.40	6.16
Monkey	4.31 ± 0.50	6.17 ± 0.50	9.13 ± 0.30	6.54
Human	6.33 ± 0.80	8.92 ± 0.90	7.54 ± 0.60	7.60

COBI = cobicistat; SD = standard deviation
Source: Reports AD-216-2076 (mouse) and AD-216-2026 (other species)

Moderately high binding of COBI in human plasma was also found in samples from clinical studies in which subjects were coadministered 150 mg EVG plus 150 mg COBI once daily for 7 to 10 days. Plasma samples were spiked with a trace amount of [^{14}C]COBI and subject to equilibrium dialysis. The absolute values for the free fraction in these studies were slightly lower than that found in vitro (Table 16). Mean fraction unbound values were between 2.49% and 2.71% in normal subjects, 3.23% in subjects with moderate hepatic impairment, and 2.47% in subjects with severe renal impairment (Module 2.7.2, Sections 2.4.1.1 and 2.4.1.2 [Studies GS-US-183-0133 and GS-US-216-0124, respectively]).

4.2. Tissue Distribution Studies

4.2.1. EVG: Tissue Distribution Studies

The distribution of radioactivity after treatment of rats with [^{14}C]EVG was studied by whole body autoradiography and by extraction and scintillation counting. The effect of pretreatment with RTV on the distribution of radioactivity was also explored. Residual radioactivity in tissues collected from dogs 7 days after a single dose of [^{14}C]EVG was also quantified.

4.2.1.1. EVG: Tissue Distribution in Rats

The tissue distribution of radioactivity was initially visualized in male rats by whole body autoradiography after oral administration of [^{14}C]EVG (3 mg/kg) in aqueous methylcellulose (0.5% w/v). Time points were 0.25, 24, and 96 hours postdose. The distribution of radioactivity, to selected tissues of male rats, after intravenous (1 mg/kg) or oral (3 mg/kg) dosing of [^{14}C]EVG was then determined by analysis of tissue homogenates (Tabulated Summary 2.6.5.5.1, JTK303-AD-005). Time points after oral dosing were 0.5, 4, 24, and 96 hours postdose. Animals treated intravenously were sacrificed 96 hours postdose. In a later study, the tissue distribution was determined by QWBA after oral administration of [^{14}C]EVG (10 mg/kg) to male and female rats in aqueous methylcellulose (1% w/v). Time points were 1 and 8 hours after dosing. The influence of oral pretreatment with RTV (20 mg/kg, 12 and 2 hours prior to EVG dosing) was also assessed (Tabulated Summary 2.6.5.5.2, 60N-0518).

Whole body autoradiography performed 0.25 hour after administration of 3 mg/kg [^{14}C]EVG revealed rapid distribution of radioactivity to highly perfused organs (liver, adrenal gland, kidney, heart, lung, and pancreas), with relative exclusion from the eye and brain (Figure 5). By 24 hours after dosing, the remaining low level of radioactivity was largely confined to the intestinal contents, with traces detectable in the liver. Radioactivity was almost completely cleared by 96 hours postdose, with traces only remaining in the intestinal contents and the liver.

Quantitative analysis of radioactivity in selected tissues was determined by excision of the tissues, homogenization, combustion, and scintillation counting. The results confirm the findings in the autoradiography study and are summarized in Table 17. The plasma radioactivity t_{max} was 0.5 hour and this was true of all other tissues apart from epididymis and testis (t_{max} 4 hours). Tissue concentrations of radioactivity declined largely in parallel with those in plasma, reaching undetectable or trace levels by 96 hours postdose. Tissue/plasma concentration ratios were generally < 1 apart from liver and GI tract.

Quantitative whole body autoradiography was performed in male and female rats following an oral dose of [^{14}C]EVG (10 mg/kg). The results for distribution of radioactivity to tissues of male rats were largely similar to those described above. For female rats, the distribution pattern was similar to that in males (similar tissue/blood concentration ratios), but absolute blood and tissue concentrations were ~3-fold higher than in males. Distribution to female mammary gland and primary female sexual organs was similar to that for most other tissues (other than the high levels seen in liver or GI tract). The effect of oral pretreatment with RTV (20 mg/kg in the Norvir® pediatric solution vehicle of ethanol, propylene glycol, and Cremophor EL) was also assessed (RTV dosed 12 and 2 hours prior to administration of [^{14}C]EVG). Following RTV pretreatment and 1 hour after dosing with [^{14}C]EVG, the tissue concentrations of radioactivity were largely reduced by 40% to 60%. However, by 8 hours postdose, some tissue concentrations were 1.5-fold higher than in animals without RTV pretreatment and this is largely attributable to higher blood concentrations of radioactivity in the RTV-pretreated animals at this time point. It is noteworthy that RTV pretreatment did not allow access of radioactivity to the CNS, so the blood brain barrier was unaffected.

Figure 5 Annotated Whole Body Autoradiograph of a Male Rat Obtained 0.25 Hour After Administration of [^{14}C]EVG (3 mg/kg)

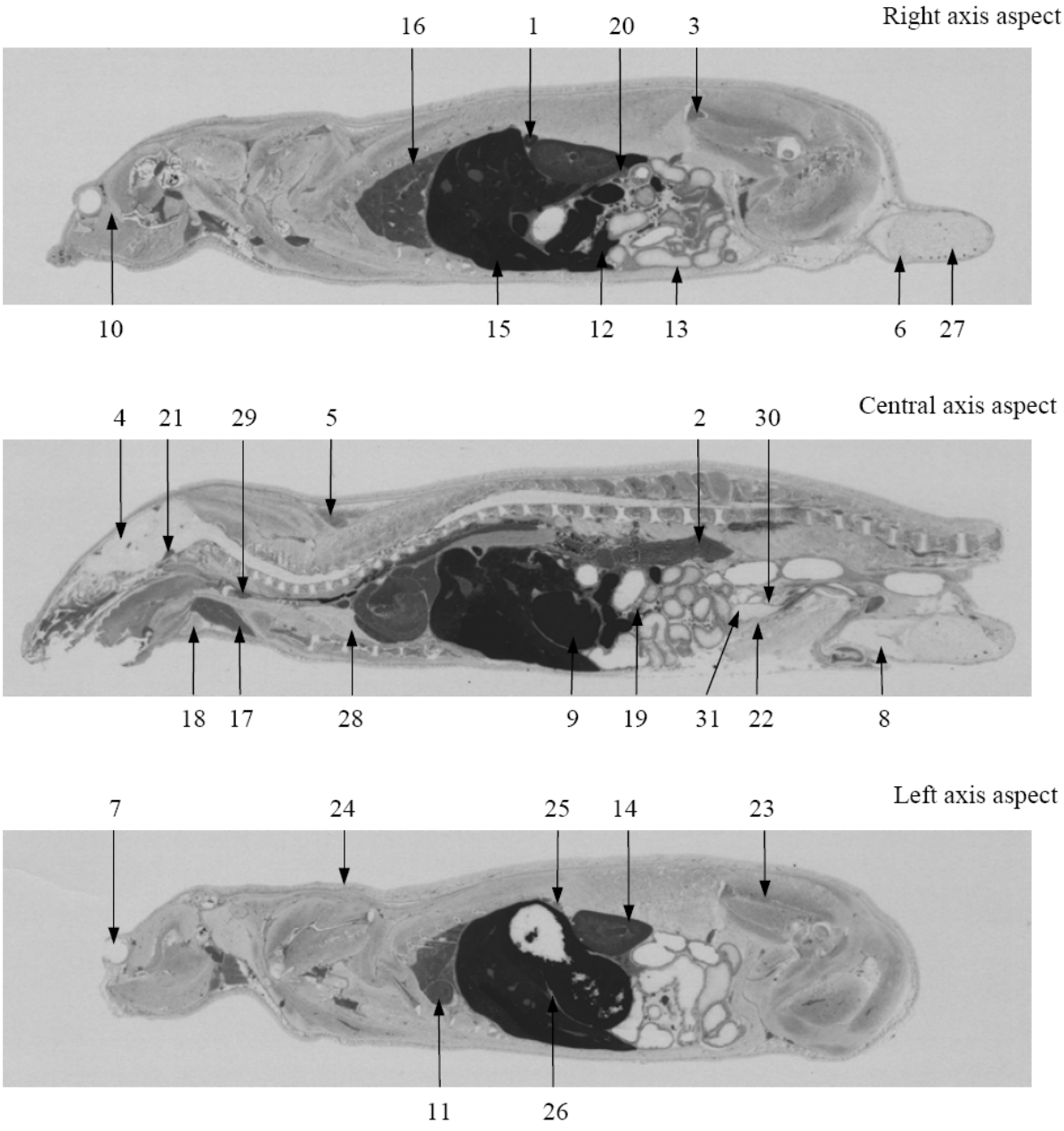

1. Adrenal gland
2. Blood
3. Bone marrow
4. Brain
5. Brown fat
6. Epididymis
7. Eyeball
8. Fat
9. Gastric contents
10. Harderian gland
11. Heart
12. Intestinal contents
13. Intestine
14. Kidney
15. Liver
16. Lung
17. Mandibular gland
18. Mandibular lymph node
19. Mesenteric lymph node
20. Pancreas
21. Pituitary gland
22. Prostate gland
23. Skeletal muscle
24. Skin
25. Spleen
26. Stomach
27. Testis
28. Thymus
29. Thyroid gland
30. Urinary bladder
31. Urine in bladder

Table 17. Tissue Radioactivity Levels in Rats After Oral Dosing with [^{14}C]EVG (3 mg/kg) Determined by Homogenization and Scintillation Counting (Mean ± SD, n = 3)

Tissue	Radioactivity Concentration (ng EVG eq./g or mL)			
	0.5 h	4 h	24 h	96 h
Plasma	1181 ± 238 (1.00)	332 ± 5 (1.00)	9 ± 3 (1.00)	1 ± 0 (1.00)
Blood	703 ± 138 (0.60)	194 ± 6 (0.58)	5 ± 2 (0.56)	1 ± 0 (1.00)
Cerebrum	15 ± 6 (0.01)	4 ± 1 (0.01)	< 1 (0.00)	ND
Cerebellum	21 ± 9 (0.02)	6 ± 1 (0.02)	< 1 (0.00)	ND
Pituitary Gland	360 ± 111 (0.30)	95 ± 22 (0.29)	ND	ND
Eyeball	35 ± 10 (0.03)	18 ± 1 (0.05)	1 ± 1 (0.11)	ND
Harderian Gland	149 ± 48 (0.13)	92 ± 11 (0.28)	1 ± 1 (0.11)	< 1 (0.00)
Thyroid Gland	308 ± 91 (0.26)	80 ± 33 (0.24)	ND	ND
Trachea	211 ± 97 (0.18)	81 ± 11 (0.24)	3 ± 1 (0.33)	ND
Mandibular Gland	393 ± 89 (0.33)	97 ± 17 (0.29)	2 ± 1 (0.22)	< 1 (0.00)
Thymus	71 ± 15 (0.06)	40 ± 4 (0.12)	1 ± 0 (0.11)	< 1 (0.00)
Heart	403 ± 100 (0.34)	108 ± 16 (0.33)	2 ± 1 (0.22)	< 1 (0.00)
Lung	330 ± 91 (0.28)	106 ± 12 (0.32)	2 ± 1 (0.22)	< 1 (0.00)
Liver	1488 ± 89 (1.26)	374 ± 59 (1.13)	27 ± 3 (3.00)	8 ± 2 (8.00)
Kidney	593 ± 75 (0.50)	176 ± 5 (0.53)	6 ± 1 (0.67)	1 ± 1 (1.00)
Adrenal Gland	746 ± 68 (0.63)	140 ± 26 (0.42)	2 ± 2 (0.22)	ND
Spleen	206 ± 29 (0.17)	49 ± 4 (0.15)	1 ± 1 (0.11)	< 1 (0.00)
Pancreas	330 ± 82 (0.28)	92 ± 9 (0.28)	1 ± 1 (0.11)	< 1 (0.00)
Fat	45 ± 12 (0.04)	23 ± 4 (0.07)	1 ± 1 (0.11)	ND

Tissue	Radioactivity Concentration (ng EVG eq./g or mL)			
	0.5 h	4 h	24 h	96 h
Brown Fat	205 ± 14 (0.17)	82 ± 9 (0.25)	3 ± 1 (0.33)	< 1 (0.00)
Skeletal Muscle	117 ± 7 (0.10)	43 ± 4 (0.13)	1 ± 0 (0.11)	ND
Skin	97 ± 25 (0.08)	73 ± 4 (0.22)	3 ± 1 (0.33)	1 ± 0 (1.00)
Bone Marrow	248 ± 35 (0.21)	56 ± 7 (0.17)	ND	ND
Aorta	248 ± 175 (0.21)	69 ± 8 (0.21)	2 ± 1 (0.22)	ND
Mesenteric Lymph node	597 ± 126 (0.51)	138 ± 25 (0.42)	3 ± 1 (0.33)	1±1 (1.00)
Testis	46 ± 13 (0.04)	64 ± 8 (0.19)	1 ± 1 (0.11)	< 1 (0.00)
Epididymis	68 ± 15 (0.06)	70 ± 4 (0.21)	2 ± 0 (0.22)	< 1 (0.00)
Prostate Gland	101 ± 14 (0.09)	47 ± 14 (0.14)	1 ± 0 (0.11)	ND
Seminal Vesicle	70 ± 9 (0.06)	42 ± 4 (0.13)	1 ± 0 (0.11)	ND
Stomach	1589 ± 345 (1.35)	1227 ± 167 (3.70)	9 ± 9 (1.00)	< 1 (0.00)
Small Intestine	2545 ± 792 (2.15)	2139 ± 383 (6.44)	12 ± 5 (1.33)	ND
Cecum	176 ± 31 (0.15)	419 ± 276 (1.26)	207 ± 144 (23.00)	< 1 (0.00)
Large Intestine	152 ± 24 (0.13)	207 ± 115 (0.62)	48 ± 21 (5.33)	< 1 (0.00)
Urinary Bladder	128 ± 17 (0.11)	85 ± 8 (0.26)	2 ± 1 (0.22)	ND

EVG = elvitegravir; ND: Not detected; SD = standard deviation
Values in parentheses show the ratio to plasma concentration (mean value of concentration in each tissue/mean value of plasma concentration).
Source: Report JTK303-AD-005

4.2.1.2. EVG: Tissue Distribution in Dogs

The concentrations of radioactivity in selected tissues of dogs were determined 168 hours following administration of [^{14}C]EVG intravenously (1 mg/kg in aqueous polyethylene glycol) or orally (3 mg/kg in aqueous 0.5% w/v methylcellulose; Tabulated Summary 2.6.5.5.4, JTK303-AD-006). Tissues were excised, homogenized, and combusted prior to scintillation counting.

Plasma concentrations of radioactivity were low (2 ± 1 ng EVG equivalent/mL) and levels in most organs were 1 ng eq/mL or below the limit of detection. The only exceptions were liver (8 ± 1 and 15 ± 6 ng eq/mL after intravenous and oral dosing, respectively) and kidney (2 ng eq/mL).

4.2.2. COBI: Tissue Distribution Studies

[^{14}C]COBI was administered orally as a solution to male albino Sprague-Dawley rats (Tabulated Summary 2.6.5.5.5, AD-216-2034) and pigmented Long Evans rats (Tabulated Summary 2.6.5.5.6, AD-216-2060) at a target dose of 10 mg/kg and 200–250 μCi/kg. Animals were sacrificed at various times postdose, frozen, embedded, and sectioned. The distribution of radioactivity was then determined by QWBA. Representative autoradiographic images from animals terminated at 4 hours postdose are provided in Figure 6 (albino) and Figure 7 (pigmented). Comparative quantification data for selected tissues and time points are provided in Table 18. A full listing of tissue concentrations of radioactivity is provided in tabular form in Module 2.6.5 (Tabulated Summaries 2.6.5.5.5 for albino animals and 2.6.5.5.6 for pigmented animals).

After oral administration of [^{14}C]COBI to rats, radioactivity was widely distributed to most tissues by 0.25 hour postdose. Almost all of the tissues reached maximum radioactive concentration by 1 hour postdose. Generally, the radioactivity was preferentially distributed into glandular tissues and organs of elimination. The tissues showing the highest concentrations of radioactivity, excluding the GI tract, included liver, adrenal, kidney, and pituitary. The tissues with the lowest C_{max} values were eye, spinal cord, and brain, bone, seminal vesicles, epididymis, and testes (with concentrations all < 400 ng COBI equivalent/g tissue). Low levels of radioactivity in the brain, spinal cord, and testes suggest minimal transport across the blood:brain and blood:testes barriers. Compared to albino rats, the pigmented rats showed very similar patterns of distribution of radioactivity, but with higher concentrations in the uveal tract of the eye. There were also higher concentrations of radioactivity in pigmented skin compared to nonpigmented skin, suggesting that COBI was associated with melanin.

In the Sprague-Dawley rats, clearance from most tissues was not complete by 24 hours postdose; however, radioactivity showed a time-dependent decrease in all tissues examined over the sampling period. Also, in an excretion study an average total of 6.9% of dosed radiolabel was recovered in excreta between 24 and 168 hours postdose (see Section 6.1.2.2). In the Long Evans rats, there was detectable radioactivity in pigmented tissues and some other tissues at 72 hours postdose, but dosimetry analysis showed that concentrations were declining, indicating association with the tissues was reversible.

Table 18. Comparative Tissue Concentrations of Radioactivity in Male Sprague Dawley and Long Evans Rats After Oral Administration of [^{14}C]COBI (n = 1 per time point)

Organ	Radioactivity (ng COBI equivalent/g tissue)									
Time point	0.25 h		1 h		4 h		12 h		24 h	
Rat Strain	SD	LE	SD	LE	SD	LE	SD	LE	SD	LE
Blood (LSC)	653	1200	1060	1840	261	202	167	131	101	95.1
Blood	347	960	723	1700	200	192	117	132	77.7	127
Plasma (LSC)	1100	1890	1830	3060	454	283	272	183	147	118
Adipose (brown)	1320	1430	2870	7610	1330	1180	1480	1080	1280	1270
Adipose (white)	205	297	748	2380	142	BLQ	117	82.5	87.8	113
Adrenal gland	5090	8530	28800	35400	4290	3280	1480	1850	1740	2600
Bile	353000	175000	214000	94100	89300	30000	11500	ND	11000	8170
Bone	74	51.8	142	255	54.6	128	52.7	65.6	BLQ	52.7
Bone marrow	1020	1070	3710	5000	1170	902	1260	817	650	735
Brain	BLQ	BLQ	47.7	BLQ	49	53.4	49.1	BLQ	BLQ	BLQ
Eye	87	63.7	144	587	85	480	98.3	709	62	678
Eye (lens)	BLQ	BLQ	BLQ	BLQ	BLQ	BLQ	BLQ	BLQ	BLQ	BLQ
Eye (uveal tract)	349	1030	979	5820	545	4400	318	6620	197	6530
Heart	1070	2010	2260	4440	707	815	763	643	634	669
Kidney	3630	5290	6350	11500	1810	1530	1550	1260	1030	1230
Large intestinal contents	NR	BLQ	51.2	4520	BLQ	9030	330000	145000	11600	11000
Large intestine	582	594	2350	3250	1620	2060	2540	947	1900	709
Liver	49800	77400	33900	48000	16500	12700	5570	6350	2620	3850
Lung	865	2160	2230	6090	579	642	540	523	486	522
Lymph nodes	279	496	2860	3880	708	726	650	664	477	397
Muscle (skeletal)	424	465	1150	2190	231	246	349	260	149	249

Organ	Radioactivity (ng COBI equivalent/g tissue)									
Time point	0.25 h		1 h		4 h		12 h		24 h	
Rat Strain	SD	LE	SD	LE	SD	LE	SD	LE	SD	LE
Pancreas	1280	2150	2960	5010	1370	1510	1010	1280	725	820
Pituitary gland	1550	2600	6720	14200	2820	3130	3500	3520	1550	4570
Prostate	242	279	1100	2030	751	605	720	552	342	537
Salivary gland	1430	2410	5190	7660	1950	1410	1170	895	691	564
Skin (nonpigmented)	191	244	521	1280	232	233	236	238	186	224
Skin (pigmented)	--	292	--	1440	--	396	--	502	--	315
Small intestinal contents	318000	205000	608000	310000	803000	316000	3910	2870	1910	613
Small intestine	1440	1150	4110	10600	2670	2440	961	1730	623	961
Spinal cord	BLQ	BLQ	BLQ	46.6	BLQ	51.1	BLQ	BLQ	BLQ	BLQ
Spleen	1990	2330	6060	8220	1470	1620	1630	1060	785	726
Stomach	1340	1220	2550	3150	1550	1070	1470	1040	1230	829
Stomach contents	198000	291000	147000	74300	3610	1400	BLQ	BLQ	5840	BLQ
Testis	BLQ	BLQ	128	174	120	125	282	122	136	122
Thymus	247	274	1360	2340	602	524	462	305	366	297
Thyroid	2520	3510	6140	6350	536	1120	1200	756	748	1110
Urinary bladder	630	2240	1830	8350	1660	10200	NR	281	NR	477

COBI = cobicistat; BLQ = below the limit of quantification; LE = Long Evans rat, NR = not represented on images, SD = Sprague-Dawley rat, LSC = concentrations quantified by Liquid Scintillation Counting, rather than autoradiography, and provided for comparison

Source: Reports AD-216-2034 (SD) and AD-216-2060 (LE)

Figure 6. Annotated Whole-body Autoradiogram 4 Hours Following Oral Administration of [^{14}C]COBI to a Sprague-Dawley Rat (10 mg/kg, 200 µCi/kg) (Animal B07116)

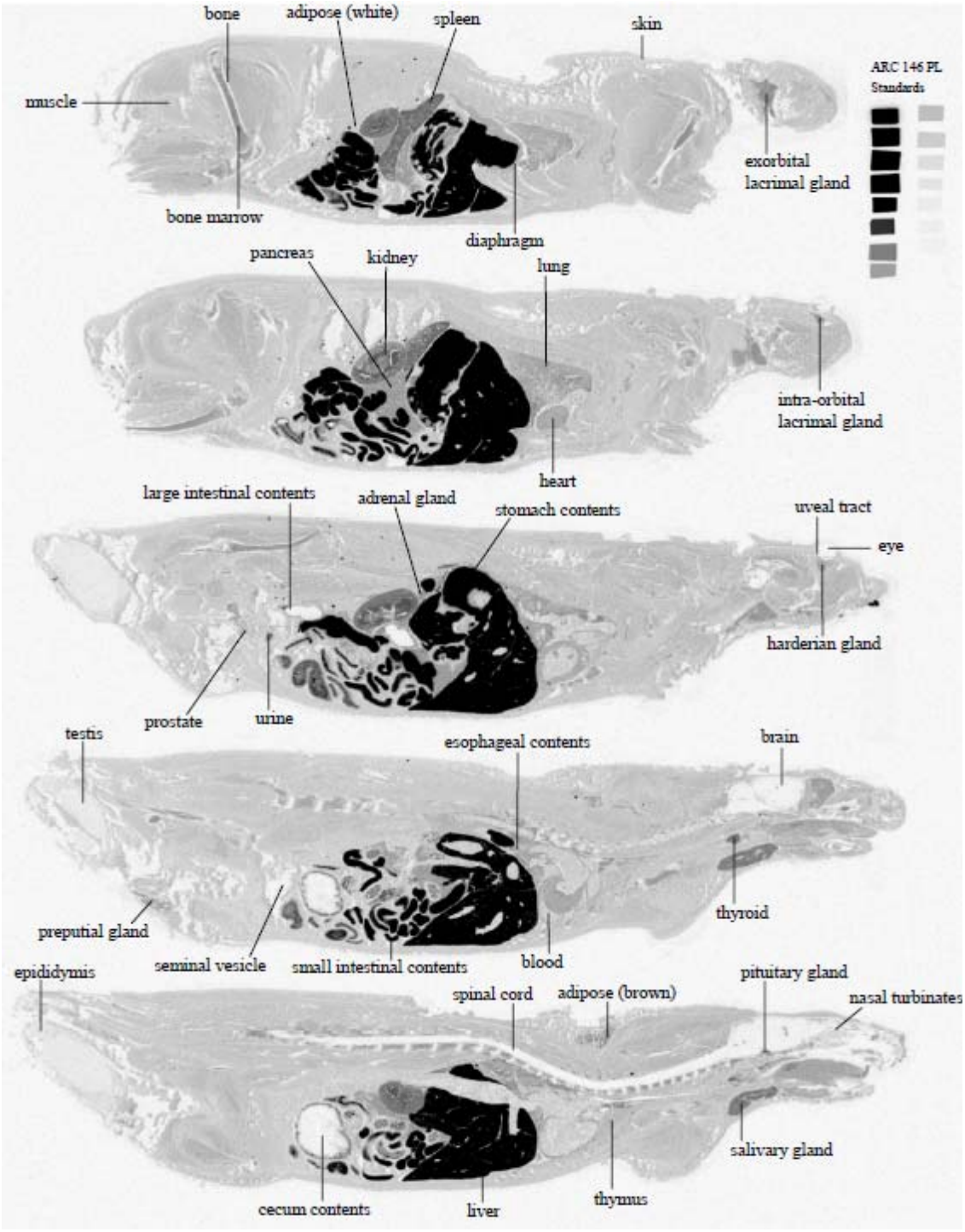

Source: Report AD-216-2034

Figure 7. Annotated Whole-body Autoradiogram 4 Hours Following Oral Administration of [^{14}C]COBI to a Long Evans Rat (10 mg/kg, 250 µCi/kg) (Animal B10529)

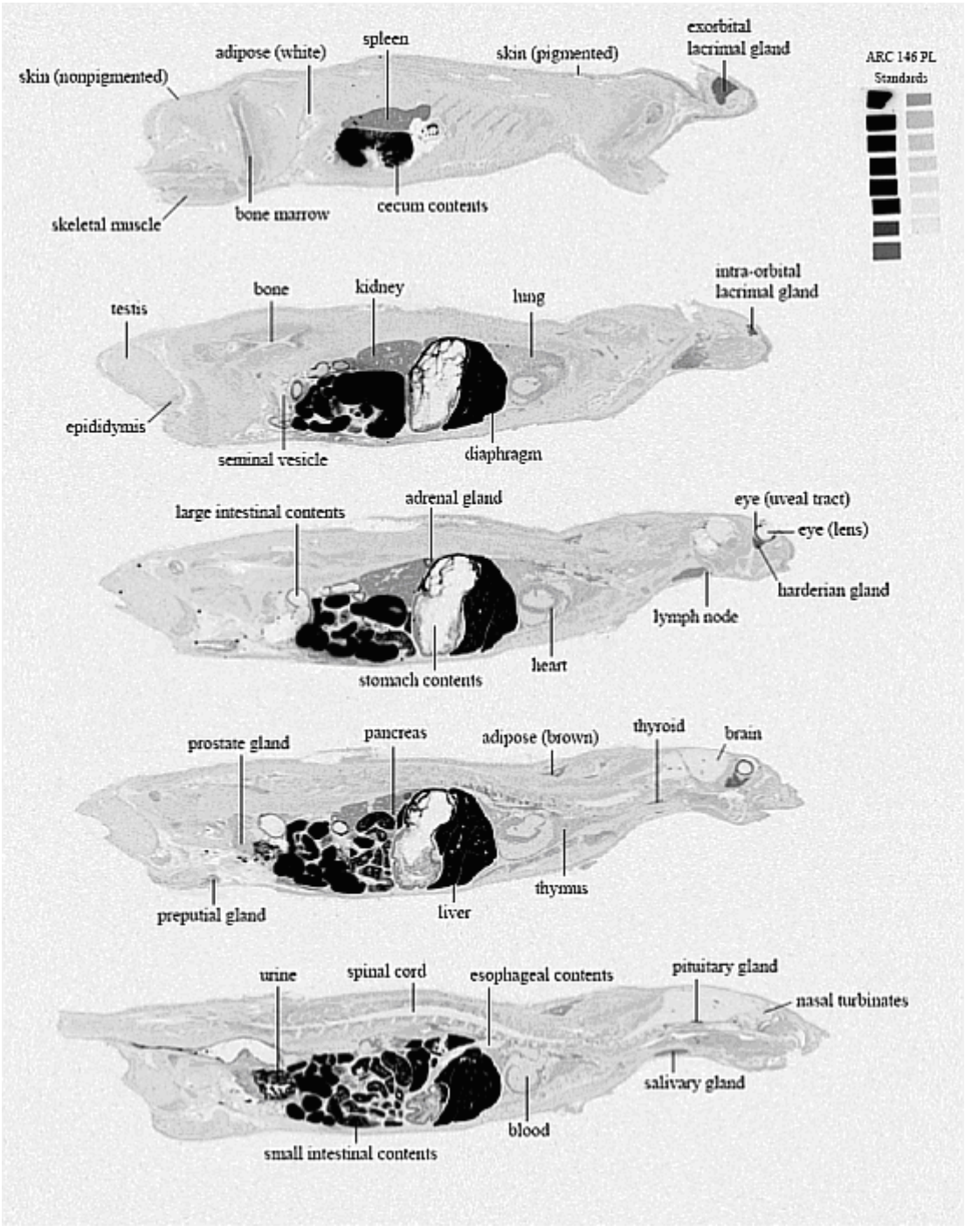

Source: Report AD-216-2060

4.2.3. COBI: Blood-Plasma Ratio

Whole blood to plasma concentration ratios for COBI can be estimated from the distribution of radioactivity within blood obtained from in vivo studies with [^{14}C]COBI. Representative results are summarized in Table 19.

Blood to plasma ratios are all low, indicating that COBI does not distribute well into the cellular fraction of blood.

Table 19. Whole Blood to Plasma Concentration Ratios of Radioactivity after Oral Administration of [^{14}C]COBI

Species	Value	Tabulated Summary (Report)
CD-1 mouse	0.562 at 1 h (n = 3)	2.6.5.9.3 (AD-216-2073)
Sprague-Dawley rat	0.605 at 1 h (n = 3)	2.6.5.5.5 (AD-216-2034)
Long Evans rat	0.600 at 1 h (n = 1)	2.6.5.5.6 (AD-216-2060)
Beagle dog	0.508 at 1 h (n = 3)	2.6.5.9.5 (AD-216-2067)
Human	0.589 at 1.5 h (n = 8)	Module 2.7.2, Section 2.2.2.3 (GS-US-216-0111)

COBI = cobicistat

4.3. Studies in Pregnant or Nursing Animals

Toxicokinetic studies of EVG and COBI in pregnant animals are described in detail in Module 2.6.6, Sections 6.1 and 6.2, respectively. In general, exposures in pregnant rats were comparable to those in nonpregnant animals.

4.3.1. EVG and COBI in Milk

During postnatal toxicology studies, the excretion of EVG and COBI in rat milk were studied. The results are summarized in Section 6.3.1 and Section 6.3.2, respectively.

4.4. EVG/COBI/FTC/TDF

Drug interactions, within the 4-drug combination, that affect distribution would not be expected from the data available. Although plasma protein binding of EVG is high, the binding is very low for FTC and TFV, and moderate for COBI, so interactions through binding displacement would not be anticipated. An in vivo study with [^{14}C]EVG and co-dosed RTV (Section 4.2.1.1) revealed no change in the tissue distribution of EVG, and notably no increase in CNS penetration of EVG. Because COBI displays transporter inhibition potencies similar to, or weaker than, RTV (Section 7.2.4), COBI would not be expected to affect the tissue distribution of the other agents.

5. METABOLISM

Summaries of the metabolic pathways for EVG are provided in Figure 8 and Figure 9, and for COBI in Figure 10 and Figure 11.

5.1. Proposed Metabolic Pathways

5.1.1. EVG: Metabolic Pathways

Metabolite identification was performed by LC radiochromatography-guided ion trap MS and through the use of synthetic standards of putative metabolites. The structures of the available synthetic standards are illustrated in Table 1. The initial analysis was performed with dog urine, dog feces, rat bile, and with samples from in vitro incubations with hepatic microsomal fractions from rat, dog, cynomolgus monkey, and human (Tabulated Summary 2.6.5.11.2, JTK303-AD-021). Subsequent independent studies were performed with in vitro incubations with hepatic microsomal fractions from mouse (Tabulated Summary 2.6.5.11.1, AD-183-2020) and rabbit (Tabulated Summary 2.6.5.11.3, 60N-0508).

Elvitegravir is subject to phase I metabolism (aromatic and aliphatic hydroxylation) and phase II metabolism (glucuronidation). Sequential pathways generate dihydroxylated metabolites and glucuronide conjugates of hydroxylated metabolites. Metabolites designated as M1 to M8 account for the majority of those detected. One other oxidative metabolite was identified with rabbit hepatic microsomal fraction. Synthetic standards allowed structural assignments of metabolites M1, M2, M3, M4, and M7. Structures for M5 (dihydrodiol), M6 (aromatic or benzylic oxidation + glucuronidation), and M8 (aromatic hydroxylation + benzylic hydroxylation) have been proposed from MS fragmentation. A summary of the proposed routes of metabolism (covering the majority of the nonclinical samples analyzed) is provided in Figure 8. The tentative structures proposed for M5 and M6 are in Figure 9. Potential hydroxylated metabolites JTP-71064 and JTP-71100 (Table 1) were not detected in any samples. Trace amounts of metabolite HM1 (JTP-74492) were found in samples generated by rabbit hepatic microsomal fractions when fortified with NADPH, UDPGA, and 3'-phosphoadenosine 5'-phosphosulfate (PAPS).

Figure 8. Proposed Metabolic Pathway of EVG

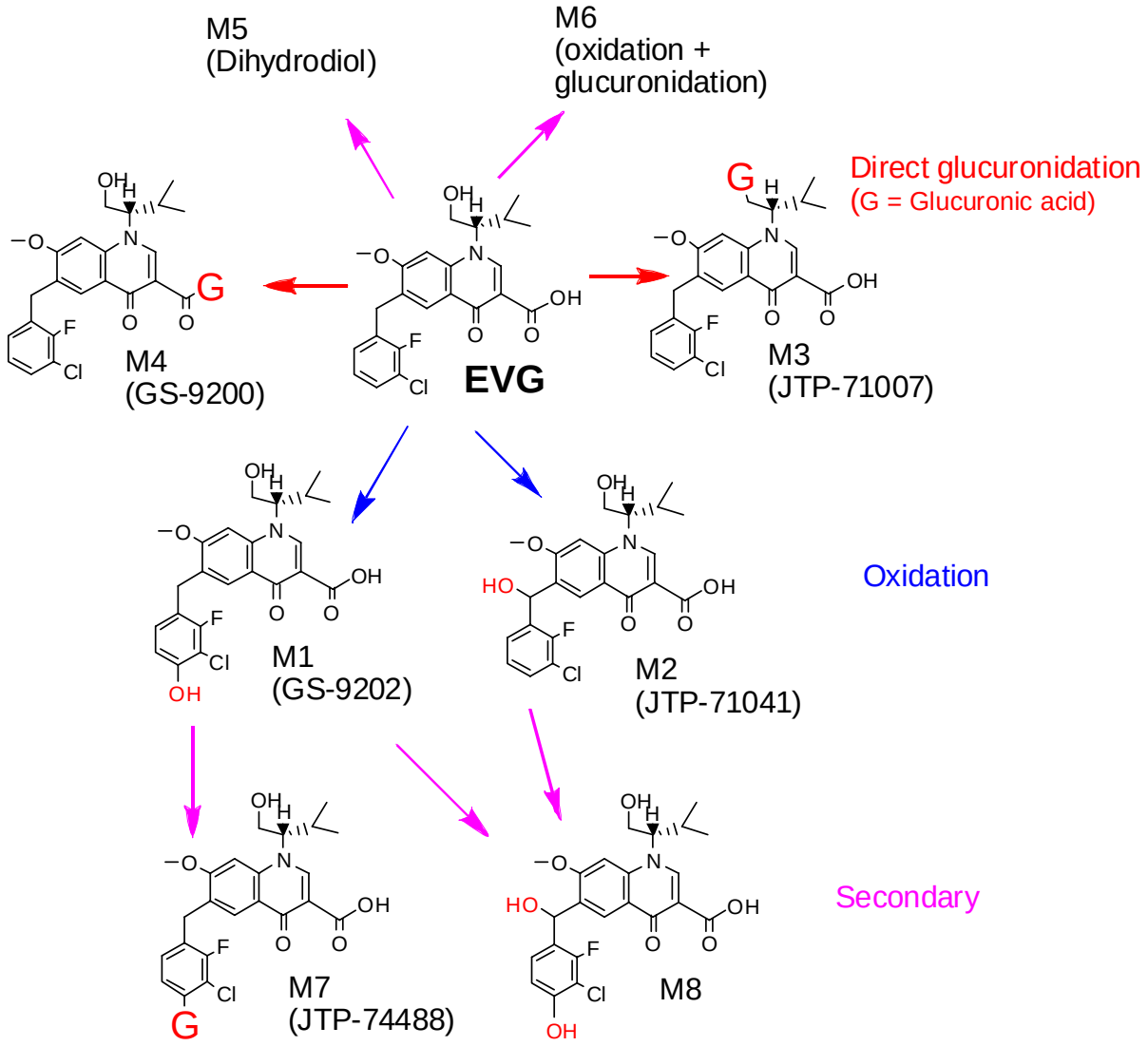

Source: Reports JTK303-AD-021, AD-183-2020, and 60N-0508

Figure 9. Proposed Structures for EVG Metabolites, M5 and M6

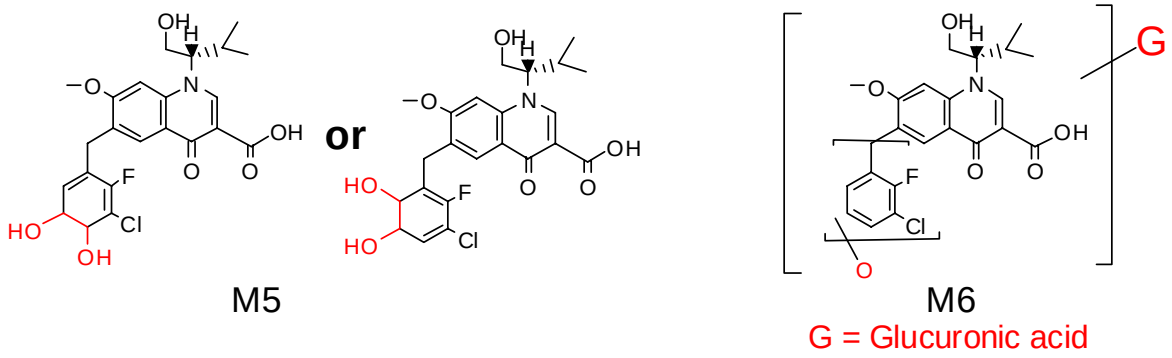

Source: Reports JTK303-AD-021, AD-183-2020, and 60N-0508

A summary of the samples in which the metabolites have been identified is in Table 20.

Table 20. Metabolites of [^{14}C]EVG Detected in Samples from Hepatic Microsomal Fractions In Vitro and Rat and Dog Samples In Vivo

Metabolite	In Vitro (Microsomes)	In Vivo
M1 (GS-9202)	Mouse[a], Rat, Rabbit, Dog, Monkey, **Human**	Rat liver, Rat feces, Rat bile Dog plasma, Dog feces, Dog urine
M2	Mouse	Rat liver, Rat feces, Rat bile Dog plasma, Dog feces
M3	Rat, Dog	Rat liver
M4 (GS-9200)	Rat, Dog, Monkey, **Human**	Rat plasma, Rat liver, Rat urine, Rat bile Dog plasma, Dog urine
M5	Rabbit, Dog, Monkey, **Human**	Dog urine, Dog feces
M6	Rabbit	Dog plasma, Dog urine
M7	Mouse	Rat plasma, Rat urine, Rat bile Dog urine, Dog feces
M8	Rat, Monkey, **Human**	

a Implied by presence of the glucuronide conjugate of M1

Source: Reports JTK303-AD-021, AD-183-2020, and 60N-0508

Metabolite identification has also been performed with samples from humans treated with an oral dose of 50 mg EVG/subject (containing [^{14}C]EVG) with RTV (100 mg/subject) (Module 2.7.2, Section 2.2.1.3 [GS-US-183-0126]). Plasma, urine, and feces were subjected to radiochromatography and MS analysis. Elvitegravir, GS-9200 (M4), and GS-9202 (M1) were identified from their MS fragmentation patterns and retention times. Metabolites potentially similar to M2 (M464), M3 (M624), M5 (M482), M6 (M640), M7 (M7), and M8 (M480) were also identified by their molecular weights.

5.1.2. COBI: Metabolic Pathways

5.1.2.1. Identification of Major Metabolites of COBI In Vitro

Preliminary identification of COBI metabolites was performed using samples generated in vitro by human hepatocytes, and mouse, rat, dog, and human hepatic microsomal fractions. Analysis was performed by LC-ion trap MS (Tabulated Summary 2.6.5.10.7, AD-216-2074; Tabulated Summary 2.6.5.11.4, AD-216-2038). In all species, apart from dog, metabolism of COBI could be accounted for by the generation of 3 metabolites. These metabolites were initially denoted E1, E3, and E5, but during comprehensive cross-species radioprofiling of samples generated in vivo, the metabolites were named M21, M31, and M26, respectively. In dog microsomal samples, the pattern was more complex, but M21, M31, and M26 were still the most abundant metabolites. Standards of M21, M31, and M26 were synthesized chemically. The structures of M21 (cleavage of carbamate) and M26 (dealkylation at N-methyl urea) could be assigned by diagnostic MS fragmentation. The structure of M31 (hydroxylation of isopropyl) was assigned by comparison of the LC retention time and MS fragmentation with those of synthetic standards of the potential hydroxyisopropyl metabolites (GS-9612, GS-432605, and GS-432606; see Table 2). The assigned structures of M21, M31, and M26 are illustrated in Figure 10. Further metabolite identification studies using samples generated in vivo (see below) also found these 3 metabolites to be the most abundant.

Figure 10. Common Primary Pathways for Metabolism of COBI by Mouse, Rat, Dog, and Human In Vitro

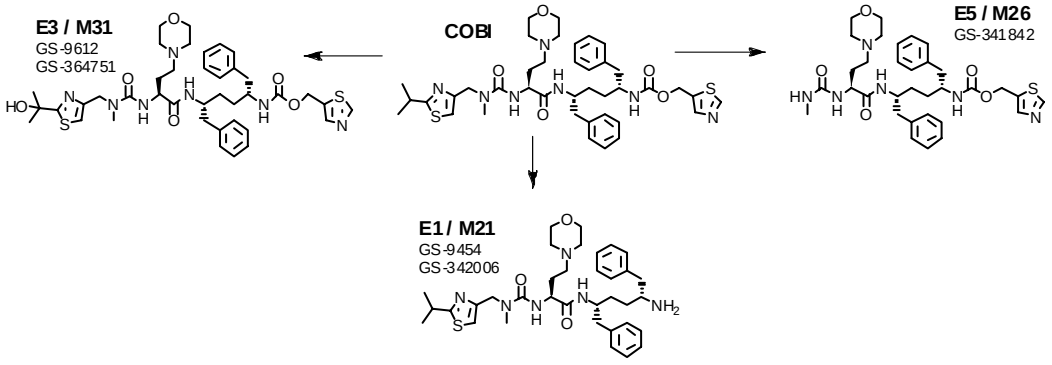

COBI = cobicistat
Source: Reports AD-216-2074 and AD-216-2038

5.1.2.2. Identification of Major Metabolites of COBI In Vivo

Metabolite identification was performed with samples from in vivo studies with [^{14}C]COBI in mice (Tabulated Summary 2.6.5.9.3, AD-216-2073), rats (Tabulated Summary 2.6.5.9.4, AD-216-2082), dogs (Tabulated Summary 2.6.5.9.5, AD-216-2101), and humans (Module 2.7.2, Section 2.2.2.3 [GS-US-216-0111]). Samples were profiled by LC-radiochromatography and, where possible, metabolite structures were assigned by LC-MS. Speculative LC-MS/MS profiling was also performed to detect the presence, but not

the quantity, of potential metabolites. Radiochromatographic and MS-chromatographic peaks were assigned arbitrary names (M1–M86). Where achievable, when MS identification was possible, the names were conserved between samples from different matrices and different species. For minor peaks with unknown or ambiguous structures, there may be redundancy in naming.

No direct conjugates of COBI were detected. Three primary metabolites (M21, M26, and M31) were common to all species in vivo and in vitro and are illustrated in Figure 11. Metabolite M39, found in all species, is formed by de-ethylation of the morpholine moiety and may involve a 2-step reaction, but no intermediate metabolite was detected and thus this is included here as a primary metabolite. The most common secondary metabolites were formed by combinations of these primary reactions and all possible pairwise combinations of the common primary reactions, M21, M26, M31, and M39 were detected. Common metabolites are illustrated in Figure 11.

Figure 11. Common Primary and Secondary Pathways for Metabolism of COBI by Mouse, Rat, Dog, and Human In Vivo

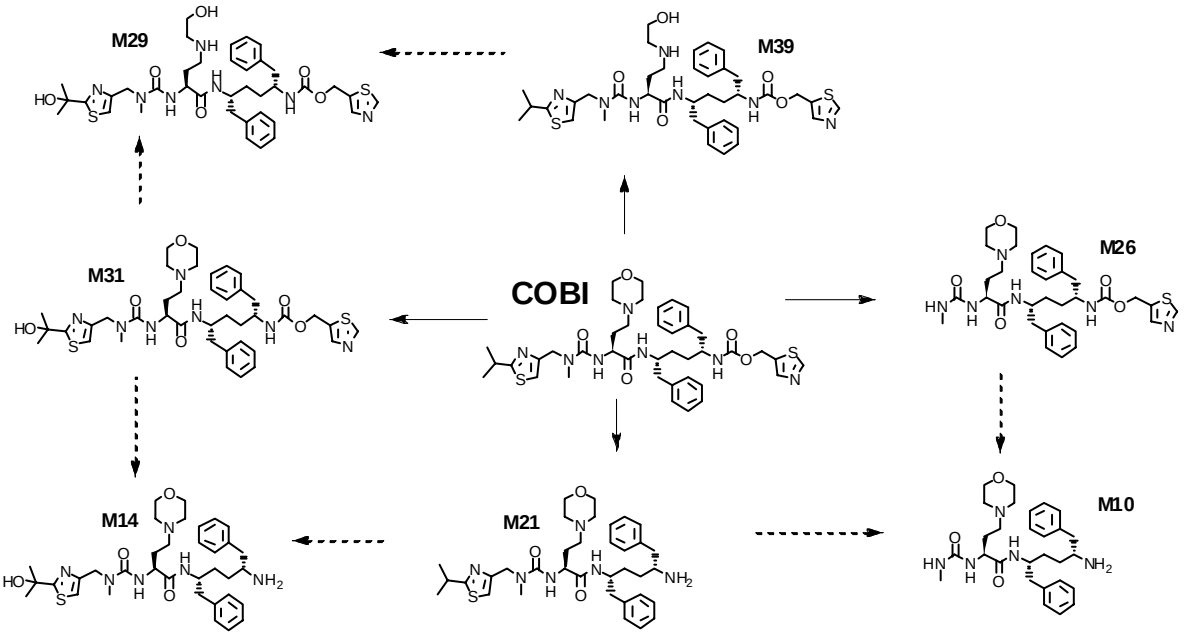

COBI and all metabolites were detected in samples from mouse, rat, dog and human, except M29 (not in human).
Dashed arrows indicate combinations of primary metabolic pathways, not proven routes of metabolism.
Source: Reports AD-216-2073 (mouse), AD-216-2082 (rat), AD-216-2101 (dog), and GS-US-216-0111 (human)

Other routes of metabolism are illustrated in figures in Module 2.6.5 (Tabulated Summaries 2.6.5.11.4, 2.6.5.11.5, and 2.6.5.11.6) and include further oxidation of the isopropyl moiety (M28) and oxidation of the diphenyldiamine core (M48, M50, and M65). For metabolites for which some structural information was proposed, Table 21 provides a comparison of their presence in plasma and/or excreta of mouse, rat, dog, and human. Cobicistat was detected in all samples apart from rat bile. Urine and plasma generally had similar profiles, with COBI,

M21, and M31 being the most significant analytes. The common primary metabolites, M21 and M31, were found in all urine, feces, and bile samples, while M26 and M39 were limited to feces and bile. M14 was the most common secondary metabolite.

Table 21. Cross-Species Comparison of Metabolites

Analyte	Class	Route(s)	Mouse	Rat	Dog	Human
COBI	Parent	Unmodified	PUF	PUF	PUFB	PUF
M10	Secondary	Carbamate cleavage + Dealkylation at N-methylurea	U			
M14	Secondary	Carbamate cleavage + Isopropyl oxidation	F	FB	FB	F
M21	Primary	Carbamate cleavage	PUF	PUFB	PUFB	UF
M26	Primary	Dealkylation at N-methylurea		FB		
M28	Secondary	Dioxidation of isopropyl	F	F	FB	
M29	Secondary	Isopropyl oxidation + Deethylation of morpholine	PUF	UFB	PUFB	UF
M31	Primary	Isopropyl methine oxidation	F	FB	FB	F
M39	Primary	Deethylation of morpholine			F	
M48 (M49 in rat)	Secondary	Isopropyl oxidation + Core oxidation	F	FB	FB	F
M50	Secondary	Isopropyl oxidation + Core oxidation		FB		
M65	Primary	Core oxidation (aromatic)			FB	

B: detected in bile; F: detected in feces; P: detected in plasma; U: detected in urine

5.2. Metabolism In Vitro

5.2.1. EVG: Metabolism In Vitro

5.2.1.1. Metabolic Stability of [^{14}C]EVG In Mouse Hepatic Microsomal Fractions

The stability of [^{14}C]EVG (2 μM) with male or female CD-1 mouse hepatic microsomal fractions was investigated (Tabulated Summary 2.6.5.10.1, AD-183-2019). Commercially obtained mouse hepatic microsomal fractions were from male CD-1 mice treated with corn oil or with prototypic inducers (β-naphthoflavone, dexamethasone, or clofibric acid). Microsomal fractions from female mice were from untreated animals. Incubations were performed with NADPH in the absence and presence of UDPGA. Positive control substrates for oxidation (7-ethoxycoumarin) and conjugation (7-hydroxycoumarin) were tested in parallel.

Key data are summarized in Table 22. Addition of UDPGA cofactor did not result in a large increase in the rate of metabolism of EVG by microsomal fractions from male animals

suggesting that oxidative metabolism, supported by NADPH, was the major route. Metabolism by microsomal fractions from female mice was slower than that catalyzed by microsomal fractions from corn oil treated males. There was a modest increase in the rate of metabolism when UDPGA was added, suggesting that glucuronidation may play a proportionally greater role in females than in males. Of the 3 prototypical inducers tested, dexamethasone, an activator of mouse PXR and inducer of mouse CYP3A enzymes, such as CYP3A11, had the greatest effect suggesting that CYP3A enzymes may be the major catalysts of the oxidation of EVG in mice. This is consistent with the finding that human CYP3A enzymes are efficient catalysts of EVG oxidation (see Section 7.1.2.1 and Table 58 below).

Table 22. Metabolism of [^{14}C]EVG (2 µM) by Hepatic Microsomal Fractions from Mice

Sex	Pretreatment	EVG Remaining at 30 min (%)	
		NADPH	NADPH+UDPGA
Male	Corn oil	53.4	49.3
	Dexamethasone	11.8	7.3
	β-Naphthoflavone	45.9	46.4
	Clofibric acid	59.3	46.6
Female	Untreated	69.9	61.8

EVG = elvitegravir; NADPH = β-nicotinamide adenine dinucleotide phosphate; UDPGA = uridine diphospho-glucuronic acid
Source: Report AD-183-2019

5.2.1.2. Oxidative Metabolism of [^{14}C]EVG by Hepatic Microsomal Fractions from Rat, Dog, Monkey, and Human

The rates of metabolism of [^{14}C]EVG (1 µg/mL) by hepatic microsomal fractions (1.0 mg/mL) from Sprague-Dawley rat, beagle dog, cynomolgus monkey, and human were investigated. Reduced β-nicotinamide adenine dinucleotide phosphate was the cofactor and incubations were for 10 minutes at 37°C (Tabulated Summary 2.6.5.10.2, JTK303-AD-015). The formation of the p-hydroxylated metabolite (M1) and di-hydroxylated metabolites (M5 and M8) was monitored.

The data are presented in Table 23. The rank order for rates of metabolism of EVG was monkey > rat ≥ human > dog. In all 4 species, the p-hydroxylated metabolite, M1, was the major metabolite, with lesser amounts of the dihydroxylated metabolites, M5 and M8. Rat microsomal fraction did not generate detectable M5 and dog microsomal fraction did not generate detectable M8.

Table 23. Oxidative Metabolism of [^{14}C]EVG by Hepatic Microsomal Fractions (Mean, n = 2)

Species	Rate of Metabolism of EVG and Formation Rate of Metabolites (pmol/min/mg protein)				
	EVG	M1 (GS-9202)	M5	M8	Others
Rat	130.8 (40.0)	99.2 (45.1)	ND	2.6 (1.2)	29.0 (13.7)
Dog	15.4 (92.1)	16.2 (7.4)	1.1 (0.5)	ND	ND
Monkey	193.8 (10.3)	155.0 (71.4)	8.4 (3.8)	10.0 (4.6)	20.3 (10.0)
Human	129.4 (40.9)	113.3 (51.5)	9.9 (4.5)	2.6 (1.2)	3.7 (2.0)

EVG = elvitegravir; ND: Not Detected
Values in parentheses: percentage of the radioactivity in the sample.
Source: Report JTK303-AD-015

5.2.1.3. Conjugative Metabolism of [^{14}C]EVG by Hepatic Microsomal Fractions from Rat, Dog Monkey and Human

The rates of metabolism of [^{14}C]EVG (1 µg/mL) by hepatic microsomal fractions (1.0 mg/mL) from Sprague-Dawley rat, beagle dog, cynomolgus monkey, and human were investigated. Uridine diphospho-glucuronic acid (UDPGA) was the cofactor and incubations were for 10 minutes at 37°C (Tabulated Summary 2.6.5.10.3, JTK303-AD-016). The formation of the ether glucuronide (M3) and acyl glucuronide (M4) metabolites was monitored.

The data are presented in Table 24. The rank order for rates of metabolism of EVG was rat > monkey > dog > human. In all 4 species the acyl glucuronide metabolite, M4, was generated most abundantly. No M3 formation was detected with human or monkey microsomal fractions.

Table 24. Glucuronidation of [^{14}C]EVG by Hepatic Microsomal Fractions (Mean, n = 2)

Species	Rate of Metabolism of EVG and Formation Rate of Metabolites (pmol/min/mg protein)			
	EVG	M3	M4 (GS-9200)	Others
Rat	17.9 (51.1)	0.8 (2.1)	17.2 (46.8)	ND
Dog	3.7 (90.0)	0.3 (0.7)	3.4 (9.3)	ND
Monkey	7.1 (79.9)	ND	7.4 (20.1)	ND
Human	0.9 (96.8)	ND	1.2 (3.2)	ND

EVG = elvitegravir; ND: Not Detected

Values in parentheses: percentage of the radioactivity in the sample.

Source: Report JTK303-AD-016

5.2.1.4. Metabolic Profiling of [^{14}C]EVG in Mice In Vitro

When [^{14}C]EVG (50 μM) was incubated for 60 minutes with CD-1 mouse hepatic microsomal fractions (from male mice treated with corn oil and from untreated females), with NADPH and UDPGA as cofactors, 4 major metabolites were identified (Tabulated Summary 2.6.5.11.1, AD-183-2020). "M1c" appears to be the same as the M2 (benzylic hydroxylated) metabolite identified earlier (JTP-71041 as standard). One or 2 direct glucuronide metabolites were identified ("M3 or M4"), but fragmentation patterns did not allow distinction between an ether glucuronide (M3, JTP-71007) or an acyl glucuronide (M4, GS-9200). The other 2 metabolites ("M7a" and "M7b") were formed by glucuronidation of p-hydroxylated EVG (GS-9202; M1) and are thus likely equivalent to metabolites M6 and M7 identified previously. GS-9202 itself was not detected, likely due to loss through efficient glucuronidation. The results from quantitative radioprofiling are in Table 25.

Incubations were also performed with microsomal fractions prepared from male and female mice pretreated daily for 7 days with EVG orally (200 or 2000 mg/kg/day), some of which were also treated with RTV (25 mg/kg/day). Treatment with EVG alone had little effect on the resulting chromatographic radioprofiles. Treatment with EVG+RTV eliminated the formation of the metabolites "M1c," "M7a," and "M7b," all of which involve oxidation of EVG.

Table 25. Nomenclature and Chromatographic Abundance of Major Metabolites Detected after Incubation of [^{14}C]EVG (50 µM) with Mouse Hepatic Microsomal Fraction for 60 Minutes

Designation in Study	Abundance in Chromatogram (%)		Equivalent Name
	Male	Female	
EVG	60.93	78.36	EVG
"M1c"	8.87	(Trace)	M2 (JTP-71041)
"M3 or M4"	11.17	7.51	M3 or M4
"M7a"	10.49	9.38	M6 or M7
"M7b"	8.53	4.76	M6 or M7

Source: Report AD-183-2020

5.2.1.5. Metabolite Profiling of [^{14}C]EVG In Rats, Dogs and Monkeys In Vitro

When [^{14}C]EVG (1 µg/mL) was incubated with hepatic microsomal fractions from male Sprague-Dawley rats, beagle dogs, cynomolgus monkeys and humans, with NADPH and UDPGA as cofactors, M1, M3, M4, M5, and M8 were the most abundant metabolites (Tabulated Summaries 2.6.5.10.2 and 2.6.5.10.3; JTK303-AD-015 and JTK303-AD-016, respectively). The chromatographic profiling results are summarized in Table 21 and Table 22 and are discussed in Sections 5.3.1.1 and 5.3.1.2.

5.2.1.6. Metabolite Profiling of [^{14}C]EVG in Rabbits In Vitro

When [^{14}C]EVG (10 or 50 µM) was incubated with hepatic microsomal fraction from female New Zealand white rabbits, with NADPH, UDPGA and PAPS as cofactors, 3 major metabolites and several minor metabolites were identified (Tabulated Summary 2.6.5.11.3, 60N-0508). The major metabolites were denoted M1, M5 and M6. "M1" appears to be the same as the M1 (p-hydroxylated) metabolite identified previously (and was found to co-elute with the M1 metabolite standard, GS-9202). "M5" was tentatively identified as a dihydrodiol metabolite of the fluorophenyl moiety and is thus likely equivalent to M5. "M6" appears to be the equivalent of M7 in other species (JTP-74488 as standard). Small amounts of 1 or 2 direct glucuronide metabolites ("M3 or M4") were detected and are likely equivalent to either the ether glucuronide or the acyl glucuronide (M3 and M4), identified in other matrices. Small amounts of the sulfated hydroxylated metabolite, HM1 (JTP-74492 as standard) were also detected. Quantitative profiling was performed with samples incubated with 50 µM [^{14}C]EVG for 60 minutes. The results are summarized in Table 38. The abundance of each of the minor peaks was ≤ 2.5%.

Table 26. Nomenclature and Chromatographic Abundance of Major Metabolites Detected after Incubation of [^{14}C]EVG (50 µM) with Rabbit Hepatic Microsomal Fraction for 60 Minutes

Designation in Study	Abundance in Chromatogram (%)	Equivalent Name
EVG	41.0	EVG
"M1"	13.3	M1 (GS-9202)
"M5"	16.3	M5
"M6"	11.7	M7 (JTP-74488)

Source: Report 60N-0508

5.2.2. COBI: Metabolism In Vitro

The rates of hepatic metabolism of COBI were assessed in vitro in cryopreserved human hepatocytes and hepatic microsomes from mouse, rat, dog, monkey, and human (Tabulated Summary 2.6.5.10.7, AD-216-2024 and AD-216-2074). Table 27 summarizes the results for in vitro half life, predicted hepatic metabolic clearance, and percent hepatic extraction obtained from hepatic microsomal fractions.

The in vitro half-life for COBI when incubated with human hepatocytes was 12.7 hours, yielding a predicted human hepatic clearance of 0.19 L/h/kg. With microsomal fractions, the rank order for species (by increasing predicted hepatic extraction) was CD-1 mouse < human < Sprague Dawley rat < beagle dog < cynomolgus monkey. Prediction of human clearance of COBI is rendered complex by enzyme inactivation occurring during the incubations (see Section 7.2.1.1).

Table 27. In Vitro Rates of Metabolism of COBI by Hepatic Microsomal Fractions

Species	In Vitro $t_{½}$ (min)	Predicted Hepatic Clearance (L/h/kg)	Predicted Hepatic Extraction (%)
Mouse	137.0	0.99	19.1
Rat	82.1	1.50	35.6
Dog	43.7	0.88	48.8
Cynomolgus monkey	8.9	1.35	84.7
Human	154.9	0.37	28.3

COBI = cobicistat

Source: Reports AD-216-274 (mouse) and AD-216-2074 (others)

5.3. Metabolism In Vivo

5.3.1. EVG: Metabolism In Vivo

5.3.1.1. Metabolite Profiling of Samples from Rats after Administration of [^{14}C]EVG

Radio-LC and metabolite profiling of representative plasma, urine, feces, bile and liver homogenate samples from rats dosed with [^{14}C]EVG were performed (Tabulated Summary 2.6.5.9.1, JTK303-AD-019). The effect of treating bile samples with β-glucuronidase was also determined. Since JTP-71041 (metabolite M2 standard) and JTP-71007 (metabolite M3 standard) were not resolved by LC, the combined radiochromatogram peak area was quantified and qualitative LC/MS/MS was used to determine the absence or presence of each of the components.

Data from plasma from rats treated orally with 3 mg/kg [^{14}C]EVG are presented in Table 28. Data from livers from the same animals are in Table 29. Data from excreta collected after oral dosing (3 mg/kg) are in Table 30 and after intravenous dosing (1 mg/kg) are in Table 31.

After oral administration of [^{14}C]EVG, parent EVG was the most abundant radiolabeled component in plasma. The acyl glucuronide (M4) was also detectable, as were small amounts of M7, the glucuronide of hydroxylated EVG. In liver homogenates, parent EVG, the acyl glucuronide (M4), and the p-hydroxylated metabolite (M1) were present in significant proportions.

There were no significant differences in the metabolite profiles, in urine and feces, between animals dosed orally and intravenously. Small amounts of the glucuronides, M4 and M7, were detected in urine but these metabolites were much more abundant in bile. In feces samples, parent compound and the oxidative metabolites, M1 and M2, were the most abundant with no detectable glucuronides. This suggests that biliary glucuronide metabolites are cleaved within the intestine before being excreted with the feces. In support of this, β-glucuronidase treatment of bile resulted in almost complete loss of the glucuronide peaks and increases in the signals for parent EVG and M1 metabolite. However, enterohepatic recirculation is unlikely to be significant in rats as intraduodenal administration of bile to naive bile duct-cannulated animals resulted in the majority of radioactivity being passed out in the feces with only a small proportion reentering the bile (see Section 6.2.1 and Table 53 below).

Table 28. Composition of Radioactivity in Rat Plasma After an Oral Dose of [^{14}C]EVG (3 mg/kg)

Time (h)	Plasma Concentration (ng EVG eq./mL)				
	Radioactivity	EVG	M4 (GS-9200)	M7	Others
0.5	1181 (100.0)	993 (84.1)	91 (7.7)	ND	96 (8.1)
4	332 (100.0)	264 (79.8)	35 (10.5)	5 (1.6)	27 (8.1)
24	9 (100.0)	ND	ND	ND	6 (69.7)

EVG = elvitegravir; ND: Not Detected
Pooled samples from 3 animals.
The values in parentheses are the percentages of sample radioactivity associated with each component.
Source: Report JTK303-AD-019

Table 29. Composition of Radioactivity in Rat Liver After an Oral Dose of [^{14}C]EVG (3 mg/kg)

Time (h)	Liver Concentration (ng EVG eq./g)						
	Radioactivity	EVG	M1 (GS-9202)	M2	M3	M4 (GS-9200)	Others
0.5	1488 (100.0)	997 (67.0)	107 (7.2)	30[a] (2.0)		302 (20.3)	52 (3.5)
4	374 (100.0)	231 (61.9)	46 (12.3)	ND	ND	66 (17.8)	30 (8.0)
24	27 (100.0)	ND	ND	ND	ND	ND	19 (72.0)

EVG = elvitegravir; ND: Not Detected
Pooled samples from 3 animals.
The values in parentheses are the percentages of sample radioactivity associated with each component.
a M2 and M3 not resolved chromatographically but both detected by LC/MS/MS
Source: Report JTK303-AD-019

Table 30. Composition of Radioactivity in Rat Urine, Feces, and Bile After an Oral Dose of [^{14}C]EVG (3 mg/kg)

Sample	Time (h)	Excretion of Radioactivity (% of dose)							
		Radio-activity	EVG	M1 GS-9202	M2	M3	M4 GS-9200	M7	Others
Urine	0–48	0.1 (100.0)	ND	ND	ND	ND	0.0 (41.7)	0.1 (58.3)	ND
Feces	0–48	96.5 (100.0)	65.8 (68.2)	17.5 (18.1)	1.4 (1.5)	ND	ND	ND	11.7 (12.2)
Bile	0–24	23.0 (100.0)	0.8 (3.7)	0.2 (0.9)	0.1[a] (0.6)		9.5 (41.4)	6.5 (28.2)	5.8 (25.4)
β-glucuronidase-treated bile	0–24	23.0 (100.0)	9.6 (41.8)	7.5 (32.6)	0.5[a] (2.2)		0.4 (1.9)	0.2 (1.0)	4.7 (20.5)

EVG = elvitegravir; ND: Not Detected
Pooled samples from 3 animals.
The values in parentheses are the percentages of sample radioactivity associated with each component.
a M2 and M3 not resolved chromatographically but both detected by LC/MS/MS

Source: Report JTK303-AD-019

Table 31. Composition of Radioactivity in Rat Urine and Feces After an Intravenous Dose of [^{14}C]EVG (1 mg/kg)

Sample	Time (h)	Excretion of Radioactivity (% of dose)							
		Radio-activity	EVG	M1 GS-9202	M2	M3	M4 GS-9200	M7	Others
Urine	0–48	0.4 (100.0)	ND	ND	ND	ND	0.4 (100.0)	ND	ND
Feces	0–48	97.5 (100.0)	38.9 (39.9)	34.9 (35.9)	3.6 (3.7)	ND	ND	ND	20.1 (20.6)

EVG = elvitegravir; ND: Not Detected
Pooled samples from 3 animals.
The values in parentheses are the percentages of sample radioactivity associated with each component.

Source: Report JTK303-AD-019

5.3.1.2. Metabolite Profiling of Samples from Dogs after Administration of [^{14}C]EVG

Radio-LC and metabolite profiling of representative plasma, urine and feces samples from dogs dosed with [^{14}C]EVG were performed (Tabulated Summary 2.6.5.9.2, JTK303-AD-020). Results from plasma profiling are summarized in Table 32 and results from excreta are summarized in Table 33.

After intravenous or oral administration of [^{14}C]EVG, parent EVG was the most abundant radioactive component circulating in plasma, with M4 being the most abundant metabolite. Additional glucuronide metabolites (M6 and M7) were detected in urine, and low amounts of EVG and oxidized metabolites were also present. As seen with rats (Section 5.3.1.1 above), parent compound and oxidized metabolites were the most abundant components in feces, with glucuronide metabolites almost completely absent.

Table 32. Composition of Radioactivity in Dog Plasma After Oral and Intravenous Dose of [^{14}C]EVG

Administration Route and Dose	Time (h)	Plasma Concentration (ng eq./mL)							
		Radio-activity	EVG	M1 GS-9202	M2	M4 GS-9200	M6	M7	Others
Oral 3 mg/kg	2	122 (100.0)	108 (88.4)	ND	ND	ND	9 (7.4)	ND	5 (4.2)
	6	80 (100.0)	52 (65.4)	ND	ND	24 (29.8)	ND	ND	4 (4.8)
Intravenous 1 mg/kg	0.083	691 (100.0)	624 (90.2)	ND	11 (1.6)	39 (5.7)	ND	ND	17 (2.5)
	0.5	375 (100.0)	326 (86.8)	7 (1.9)	ND	22 (5.9)	ND	ND	20 (5.4)
	6	38 (100.0)	33 (86.6)	ND	ND	ND	ND	ND	5 (13.4)

EVG = elvitegravir; ND: Not Detected
Pooled samples from 3 animals.
The values in parentheses are the percentages of sample radioactivity associated with each component.
Source: Report JTK303-AD-020

Table 33. Composition of Radioactivity in Dog Urine and Feces After Oral and Intravenous Administration of [^{14}C]EVG

Route and Dose	Sample	Time (h)	Excretion of Radioactivity (% of dose)								
			Radio-activity	EVG	M1 GS-9202	M2	M4 GS-9200	M5	M6	M7	Others
Oral 3mg/kg	Urine	0–48	0.5 (100.0)	ND	ND	ND	ND	0.2 (32.3)	0.1 (26.0)	0.2 (41.8)	ND
	Feces	0–48	95.0 (100.0)	70.9 (74.6)	11.7 (12.3)	3.1 (3.2)	ND	3.1 (3.3)	ND	ND	6.2 (6.6)
Intra-venous 1 mg/kg	Urine	0–48	1.0 (100.0)	0.2 (15.6)	0.1 (10.0)	ND	0.1 (11.3)	0.0 (4.5)	0.1 (12.2)	0.3 (26.4)	0.2 (19.9)
	Feces	0–48	98.0 (100.0)	62.2 (63.5)	16.3 (16.6)	4.9 (5.0)	ND	2.1 (2.1)	ND	1.6 (1.6)	11.0 (11.2)

EVG = elvitegravir; ND: Not Detected
Pooled samples from 3 animals.
The values in parentheses are the percentages of sample radioactivity associated with each component.
Source: Report JTK303-AD-020

5.3.2. COBI: Metabolism In Vivo

5.3.2.1. Summary of Human Metabolites of COBI Found In Vivo

Following administration of [^{14}C]COBI to humans (see Module 2.7.2, Section 2.2.2.3 [GS-US-216-0111]), radioprofiling of pooled (n = 8 subjects) plasma collected revealed COBI as the predominant analyte. Comparing AUC_{0-24} of COBI with that for total radioactivity suggests that COBI accounted for 98.6% of the radioactivity over 24 hours. No other peak exceeded 10% of sample radioactivity at any time point (1–24 hours). The majority of the radiolabel was recovered in feces; an average of 85.34% of the dose by 240 hours. Radioanalysis of fecal samples (0–240 hours) revealed that COBI was the most abundant component (26.9% of the dose) with M31, M21, M39, M14, and M26 also being detected (14.0%, 5.47%, 2.41%, 2.40%, and 2.37% of the dose, respectively). All other analytes accounted for < 2% of dosed radioactivity. An average of 7.37% of dosed radioactivity was recovered in urine by 24 hours postdose. The majority (5.45% of the dose) was COBI, with M31 and M21 being the most abundant metabolites (0.7% and 0.09% of the dose, respectively).

5.3.2.2. Metabolite Profiling and Identification of Mouse Plasma, Urine, and Feces Following Oral Administration of [^{14}C]COBI

The metabolic profiles of COBI were determined after administration of a single oral dose (target 30 mg/kg) of [^{14}C]COBI to Hsd:ICR(CD-1) mice (Tabulated Summary 2.6.5.9.3,

AD-216-2073). In plasma (Table 34), parent drug contributed a large majority (approximately 86% to 91%) of the circulating radioactivity, and M21 and M31 were the most abundant circulating metabolites. In urine collected 0–24 hours postdose (Table 35), the predominant radioactive peak was M21 and accounted for 0.66% of dosed radioactivity. Unchanged parent and all other observed metabolites were each present at ≤ 0.13% of the dose. In feces collected 0–48 hours postdose (Table 36), unchanged parent drug accounted for 14.5% of the dose. M21 and M31 were the most abundant metabolites and accounted for 13.4% and 5.21% of the dose, respectively. All other metabolites were each < 5% of the dose. For full profiles see the tabulated data in Tabulated Summary 2.6.5.9.3.

Table 34. Metabolite Profiling of Plasma Following Oral Administration of [^{14}C]COBI to Mice

Analyte	Concentration (ng equivalent [^{14}C]COBI/g)				
	1 hour	**2 hours**	**4 hours**	**8 hours**	**24 hours**
M21	158	154	165	54.4	ND
M31	141	146	146	35.6	ND
COBI	5900	3530	3440	1340	ND
Total[a]	6670 ± 1690	4270 ± 2270	4310 ± 320	1890 ± 1210	344 ± 79

COBI = cobicistat; ND: Not detectable in sample
a Total concentration of radioactivity by scintillation counting
Analytes listed in **bold** have assigned structures
Source: Report AD-216-2073

Table 35. Metabolite Profiling of Urine Collected 0–24 Hours Following Oral Administration of [^{14}C]COBI to Mice

Analyte	% Chromatogram	% Dose
M55	6.19	0.11
M10	7.30	0.13
M21	38.21	0.66
M31	6.35	0.11
COBI	3.02	0.05
Total[a]	--	1.79

COBI = cobicistat
a Total recovery of radioactivity by scintillation counting
Minor analytes each accounted for < 0.1% of dosed radioactivity. Analytes listed in **bold** have assigned structures.
Source: Report AD-216-2073

Table 36. Metabolite Profiling of Feces Following Oral Administration of [^{14}C]COBI to Mice

Analyte	% Chromatogram		% Dose		
	0 – 24 hours	24 – 48 hours	0 – 24 hours	24 – 48 hours	0 – 48 hours
M14	4.54	7.48	3.29	0.39	3.68
M21	16.43	28.14	11.9	1.48	13.4
M26	2.75	1.34	1.99	0.07	2.06
M29	3.24	2.82	2.35	0.15	2.50
M31	6.96	3.08	5.04	0.16	5.21
M65	3.27	1.41	2.37	0.07	2.44
M69	5.49	3.30	3.98	0.17	4.15
M39	0.75	1.15	0.54	0.06	0.60
COBI	19.74	4.23	14.3	0.22	14.5
Total[a]	--	--	79.1	5.37	84.5

COBI = cobicistat; ND: Not detectable in sample
a Total recovery of radioactivity by scintillation counting
Minor analytes each accounted for < 2.0% of dosed radioactivity. Analytes listed in **bold** have assigned structures.
Source: Report AD-216-2073

5.3.2.3. Metabolite Profiling and Identification of Rat Plasma, Bile, Urine, and Feces Following Oral Administration of [^{14}C]COBI

The metabolic profiles of radioactivity derived from [^{14}C]COBI in plasma, bile, urine, and feces following administration of an oral dose to rats were evaluated (Tabulated Summary 2.6.5.9.4, AD-216-2082). After oral administration, most of the circulating radioactivity was associated with COBI (Table 37). In addition to unchanged parent drug, M21 was the major circulating metabolite in plasma. In urine, low levels of unchanged parent drug were detected (0.05% of the dose in urine collected 0–24 hours postdose; Table 38), while M21 and M31 were the most abundant metabolites, and accounted for 0.43% and 0.21%, respectively, of the dose administered to intact rats. M21 and M31 were the major metabolites in feces from intact rats, accounting for 11.4% and 7.22% of the dose, respectively (Table 39). Unchanged parent drug accounted for 5.67% of the dose. No unchanged COBI was detected in bile. M21, M26, M14, M28, and M39 were the major metabolites in this matrix (Table 40).

Table 37. Metabolite Profiling of Plasma Following Oral Administration of [^{14}C]COBI to Rats

Analyte	Concentration (ng equivalent [^{14}C]COBI/g)					
	0.083 hour	**0.25 hours**	**1 hour**	**2 hours**	**4 hours**	**24 hours**
M21	9.78	73.2	116	35.2	38.3	ND
COBI	111	815	1490	526	201	ND
Total[a]	160 ± 89	1170 ± 580	2170 ± 210	844 ± 480	567 ± 194	150 ± 22

COBI = cobicistat; ND: Not detectable in sample
a Total concentration of radioactivity by scintillation counting
Analytes listed in **bold** have assigned structures
Source: Reports AD-216-2034 (total radioactivity) and AD-216-2082 (metabolite profiling)

Table 38. Metabolite Profiling of Urine Following Oral Administration of [^{14}C]COBI to Bile Duct-Intact Rats

Analyte	% Chromatogram		% Dose		
	0 – 12 hours	**12 – 24 hours**	**0 – 12 hours**	**12 – 24 hours**	**0 – 24 hours**
M1	10.48	23.55	0.16	0.05	0.21
M6	4.77	12.11	0.07	0.02	0.10
M21	25.16	16.65	0.40	0.03	0.43
M26	1.16	ND	0.02	ND	0.02
M31	13.46	ND	0.21	ND	0.21
COBI	3.10	ND	0.05	ND	0.05
Total[a]	--	--	1.57 ± 0.22	0.20 ± 0.05	1.77 ± 0.24

COBI = cobicistat; ND: Not detectable in sample
a Total recovery of radioactivity by scintillation counting (mean ± SD, n=3)
Minor analytes each accounted for < 0.1% dosed radioactivity. Analytes listed in **bold** have assigned structures.
Source: Reports AD-216-2034 (total radioactivity) and AD-216-2082 (metabolite profiling)

Table 39. Metabolite Profiling of Feces Following Oral Administration of [^{14}C]COBI to Bile Duct-Intact Rats

Analyte	% Chromatogram		% Dose		
	0 – 24 hours	**24 – 48 hours**	**0 – 24 hours**	**24 – 48 hours**	**0 – 96 hours**
M14	2.84	4.08	1.84	0.36	2.25
M21	14.97	16.53	9.69	1.48	11.4
M25	2.97	2.46	1.92	0.22	2.16
M26	3.91	3.17	2.53	0.28	2.83
M28	4.56	3.75	2.95	0.34	3.31
M29	3.30	2.11	2.14	0.19	2.35
M31	10.20	6.39	6.60	0.57	7.22
M39	5.01	4.98	3.24	0.44	3.72
COBI	8.24	3.62	5.33	0.32	5.67
Total[a]	--	--	77.8 ± 15.2	11.7 ± 13.2	90.8 ± 1.7

COBI = cobicistat
a Total recovery of radioactivity by scintillation counting
Minor analytes each accounted for < 2.0% dosed radioactivity. Analytes listed in **bold** have assigned structures.
Source: Reports AD-216-2034 (total radioactivity) and AD-216-2082 (metabolite profiling)

Table 40. Metabolite Profiling of Bile Following Oral Administration of [^{14}C]COBI to Bile Duct-Cannulated Rats

Analyte	% Dose				
	0 – 2 hours	**2 – 4 hours**	**4 – 6 hours**	**6 – 8 hours**	**0 – 96 hours**
M14	0.65	0.85	0.71	0.33	3.44
M21	0.59	0.95	0.57	0.34	3.50
M26	0.66	0.85	0.48	0.16	2.35
M28	0.65	1.23	0.90	0.19	2.97
M31	0.80	0.72	ND	0.20	1.92
M34	0.74	0.85	0.53	ND	2.12
M39	0.63	0.76	0.53	0.22	2.34
COBI	ND	ND	ND	ND	ND
Total[a]	17.6 ± 4.8	19.9 ± 4.8	14.7 ± 1.3	5.27 ± 2.87	68.3 ± 5.5

COBI = cobicistat; ND: Not detectable in sample
a Total recovery of radioactivity by scintillation counting
Minor analytes each accounted for < 2.0% dosed radioactivity. Analytes listed in **bold** have assigned structures.
Source: Reports AD-216-2034 (total radioactivity) and AD-216-2082 (metabolite profiling)

5.3.2.4. Metabolite Profiling and Identification of Dog Plasma, Urine, Bile, and Feces Following Oral Administration of [^{14}C]COBI

The metabolic profiles of plasma, urine, feces, and bile were determined after administration of a single oral dose (target 5 mg/kg) of [^{14}C]COBI to beagle dogs (Tabulated Summary 2.6.5.9.5, AD-216-2101). Cobicistat was the major component circulating in plasma (Table 41), with M21, M31, and M37 also being detected. Cobicistat was also detected in urine (Table 42), but the most abundant analytes in that matrix were M56 (a structurally unassigned highly polar peak), M21, and M31 (all < 0.2% of the dose). In feces (Table 43), the most abundant analytes were M21, M31, M39, and COBI, accounting for 12.4%, 8.76%, 8.63%, and 7.15% of the dose recovered within 48 hours, respectively. In bile (Table 44), the profile was more complex, with only M21 exceeding 5% of the dose. Unchanged COBI accounted for 1.65% of the dose in this matrix.

Table 41. Metabolite Profiling of Plasma Following Oral Administration of [^{14}C]COBI to Bile Duct-Intact Dogs

Analyte	Concentration (ng equivalent [^{14}C]COBI/g)				
	0.5 hour	**1 hour**	**2 hours**	**4 hours**	**8 hours**
M21	64.0	59.0	53.8	19.6	ND
M31	47.9	25.7	41.2	23.6	ND
M37	64.0	36.8	70.9	31.6	ND
COBI	419	423	473	226	ND
Total[a]	519 ± 472	821 ± 447	796 ± 191	456 ± 151	BQL

BQL: Radioactivity below quantification limit; COBI = cobicistat; ND: Not detectable in sample
a Total concentration of radioactivity by scintillation counting
Analytes listed in **bold** have assigned structures
Source: Reports AD-216-2067 (total radioactivity) and AD-216-2101 (metabolite profiling)

Table 42. Metabolite Profiling of Urine Following Oral Administration of [^{14}C]COBI to Bile Duct-Intact Dogs

Analyte	% Chromatogram		% Dose		
	0 – 24 hours	**24 – 48 hours**	**0 – 24 hours**	**24 – 48 hours**	**0 – 48 hours**
M56	9.06	34.92	0.11	0.06	0.17
M21	12.56	14.47	0.15	0.03	0.18
M31	28.92	5.86	0.35	0.01	0.37
COBI	2.56	3.47	0.03	0.01	0.04
Total[a]	--	--	1.60 ± 0.56	0.21 ± 0.06	1.81 ± 0.59

COBI = cobicistat
a Total recovery of radioactivity by scintillation counting
Minor analytes each accounted for < 0.1% dosed radioactivity. Analytes listed in **bold** have assigned structures.
Source: Reports AD-216-2067 (total radioactivity) and AD-216-2101 (metabolite profiling)

Table 43. Metabolite Profiling of Feces Following Oral Administration of [^{14}C]COBI to Bile Duct-Intact Dog

Analyte	% Chromatogram		% Dose		
	0 – 24 hours	24 – 48 hours	0 – 24 hours	24 – 48 hours	0 – 72 hours
M14	2.81	4.58	0.71	2.07	2.86
M21	16.17	17.41	4.10	7.86	12.4
M48	1.47	4.57	0.37	2.06	2.47
M26	2.97	3.23	0.75	1.46	2.25
M50	1.47	3.55	0.37	1.60	2.00
M29	4.91	7.48	1.25	3.38	4.72
M31	10.16	13.49	2.58	6.09	8.76
M63	2.42	3.15	0.61	1.42	2.08
M65	3.96	7.00	1.00	3.16	4.22
M39	11.31	12.49	2.87	5.64	8.63
COBI	20.24	4.35	5.13	1.96	7.15
Total[a]	--	--	33.54 ± 30.77	43.29 ± 34.87	78.95 ± 4.27

COBI = cobicistat

a Total recovery of radioactivity by scintillation counting

Minor analytes each accounted for < 2.0% dosed radioactivity. Analytes listed in **bold** have assigned structures.

Source: Reports AD-216-2067 (total radioactivity) and AD-216-2101 (metabolite profiling)

Table 44. Metabolite Profiling of Bile Following Oral Administration of [^{14}C]COBI to Bile Duct-Cannulated Dogs

Analyte	% Dose				
	0 – 4 hours	4– 12 hours	12 – 24 hours	24 – 48 hours	0 – 48 hours
M14	1.95	0.84	ND	ND	2.79
M21	4.75	0.38	0.14	ND	5.27
M48	1.32	0.86	ND	0.03	2.21
M26	1.69	0.45	0.14	0.04	2.31
M80	2.12	0.68	0.11	0.56	3.47
M29	1.41	0.96	0.11	0.12	2.60
M31	3.64	ND	0.07	0.03	3.74
M30	1.22	2.24	ND	ND	3.46
M65	1.34	0.48	0.27	0.16	2.25
M39	2.93	1.13	0.28	0.04	4.38
COBI	1.01	0.44	0.09	0.12	1.65
Total[a]	39.3 ± 0.33	17.8 ± 2.93	4.53 ± 0.13	2.28 ± 0.32	63.9 ± 3.70

COBI = cobicistat; ND: Not detectable in sample

a Total recovery of radioactivity by scintillation counting

Minor analytes each accounted for < 2.0% dosed radioactivity. Analytes listed in **bold** have assigned structures.

Source: Reports AD-216-2068 (total radioactivity) and AD-216-2101 (metabolite profiling)

5.4. Metabolism of EVG/COBI/FTC/TDF

Neither FTC nor TDF interact with drug metabolizing enzymes as substrates, inhibitors, or inducers so metabolic drug interactions between these agents and EVG or COBI are very unlikely. The intended pharmacokinetic drug interaction of inhibition of the CYP3A-dependent metabolism of EVG by COBI has been studied extensively in vitro (see Section 7.2.1.1) and in humans in vivo (Module 2.7.2).

Emtricitabine and TDF are analogs of 2 different nucleosides, adenosine and cytidine, respectively, and do not share a common intracellular metabolism pathway for pharmacological activation through phosphorylation. In experiments where both drugs were incubated together at concentrations higher than achieved in the plasma, the intracellular activation of TFV to its active diphosphate was not negatively influenced by the presence of FTC, and the activation of FTC to FTC-triphosphate, was not negatively affected by the presence of TFV (Module 1.4.4, PC-164-2002). Also, because the 2 drugs are derived from different nucleosides, there should be no competition for incorporation by HIV-1 RT and subsequent chain termination. This was confirmed in vitro in antiviral assays where strong synergy between the 2 compounds was observed (Module 2.7.2, Section 4.1 [PC-183-2004]). Similarly, because of the highly restricted substrate specificity of the enzymes catalyzing the phosphorylation of FTC and TFV, inhibition of pharmacological activation by EVG or COBI is unlikely and, again, there is no evidence for antagonism in antiviral assays in vitro. Three-drug (EVG+FTC+TFV) and 4-drug (EVG+COBI+FTC+TFV) combinations showed identical synergy in anti-HIV activity studies with MT-2 cells (Module 2.7.2, Section 4.1.3.5).

6. EXCRETION

6.1. Route and Extent of Excretion

6.1.1. EVG

6.1.1.1. Excretion of Radioactivity by Rats after Single Administration of [^{14}C]Elvitegravir

The routes and rates of excretion of radioactivity after administration of [^{14}C]EVG as an intravenous (1 mg/kg) or oral (3 mg/kg) dose to male Sprague-Dawley rats were explored (Tabulated Summary 2.6.5.13.1, JTK303-AD-005). The results are summarized in Table 45 and Table 46.

The amounts and time courses for recovery of radioactivity were very similar after intravenous and oral administration. Recovery of radioactivity was high (≥ 97.7%) and was largely complete by 48 hours after dosing. Almost all radioactivity was recovered in feces, with ≤ 0.4% recovered in urine.

Table 45. Cumulative Excretion of Radioactivity After an Intravenous Dose of [^{14}C]EVG (1 mg/kg) to Intact Rats (Mean ± SD, n = 3)

	Excretion of radioactivity (% of dose)			
Time (h)	Urine	Feces	Cage washing	Total
0–24	0.4 ± 0.1	80.5 ± 14.1	0.0 ± 0.0	80.9 ± 14.1
0–48	0.4 ± 0.1	97.5 ± 0.2	0.0 ± 0.0	97.9 ± 0.2
0–72	0.4 ± 0.1	98.2 ± 0.7	0.0 ± 0.0	98.6 ± 0.7
0–96	0.4 ± 0.1	98.2 ± 0.8	0.0 ± 0.0	98.6 ± 0.7

SD = standard deviation
Source: Report JTK303-AD-005

Table 46. Cumulative Excretion of Radioactivity After an Oral Dose of [^{14}C]EVG (3 mg/kg) to Intact Rats (Mean ± SD, n = 3)

Time (h)	Excretion of Radioactivity (% of dose)			
	Urine	Feces	Cage Washing	Total
0–24	0.1 ± 0.1	79.6 ± 14.2	0.0 ± 0.0	79.7 ± 14.2
0–48	0.1 ± 0.1	96.5 ± 2.0	0.0 ± 0.0	96.7 ± 1.9
0–72	0.2 ± 0.1	97.5 ± 0.9	0.0 ± 0.0	97.7 ± 0.9
0–96	0.2 ± 0.1	97.6 ± 0.9	0.0 ± 0.0	97.7 ± 0.8

SD = standard deviation

Source: Report JTK303-AD-005

6.1.1.2. Excretion of Radioactivity by Dogs after Single Administration of [^{14}C]EVG

The routes and rates of excretion of radioactivity after administration of [^{14}C]EVG as an intravenous (1 mg/kg) or oral (3 mg/kg) dose to male beagle dogs were explored (Tabulated Summary 2.6.5.13.3, JTK303-AD-006). The results are summarized in Table 47 and Table 48.

Results were very similar to those seen with intact rats. The amounts and time courses for recovery of radioactivity were very similar after intravenous and oral administration. Recovery of radioactivity was high (≥ 98.0%) and was largely complete by 48 hours after dosing. The majority of radioactivity was recovered in feces, with ≤ 1.0% recovered in urine.

Table 47. Cumulative Excretion of Radioactivity After an Intravenous Dose of [^{14}C]EVG (1 mg/kg) to Intact Dogs (Mean ± SD, n = 3)

	Excretion of radioactivity (% of dose)			
Time (h)	Urine	Feces	Cage Washing	Total
0–4	0.6 ± 0.4	--	--	--
0–8	0.8 ± 0.5	--	--	--
0-12	0.9 ± 0.5	--	--	--
0–24	0.9 ± 0.5	89.6 ± 5.4	0.1 ± 0.1	90.7 ± 5.8
0–48	1.0 ± 0.5	98.0 ± 0.6	0.2 ± 0.0	99.2 ± 0.2
0–72	1.0 ± 0.5	98.5 ± 0.7	0.2 ± 0.0	99.7 ± 0.3
0–96	1.0 ± 0.5	98.7 ± 0.7	0.2 ± 0.0	99.8 ± 0.4
0-120	1.0 ± 0.5	98.7 ± 0.7	0.2 ± 0.0	99.9 ± 0.4
0-144	1.0 ± 0.5	98.8 ± 0.7	0.2 ± 0.0	100.0 ± 0.4
0-168	1.0 ± 0.5	98.8 ± 0.8	0.2 ± 0.0	100.0 ± 0.5

SD = standard deviation

Source: Report JTK303-AD-006

Table 48. Cumulative Excretion of Radioactivity After an Oral Dose of [^{14}C]EVG (3 mg/kg) to Intact Dogs (Mean ± SD, n = 3)

	Excretion of radioactivity (% of dose)			
Time (h)	Urine	Feces	Cage Washing	Total
0–4	0.1 ± 0.1	--	--	--
0–8	0.2 ± 0.1	--	--	--
0-12	0.2 ± 0.1	--	--	--
0–24	0.4 ± 0.1	79.9 ± 4.6	0.0 ± 0.1	80.4 ± 4.7
0–48	0.5 ± 0.1	95.0 ± 0.9	0.0 ± 0.1	95.5 ± 0.9
0–72	0.5 ± 0.1	96.8 ± 1.7	0.0 ± 0.1	97.4 ± 1.7
0–96	0.5 ± 0.1	97.2 ± 1.9	0.1 ± 0.1	97.7 ± 1.9
0-120	0.5 ± 0.1	97.3 ± 2.0	0.1 ± 0.1	97.9 ± 2.1
0-144	0.5 ± 0.1	97.3 ± 2.0	0.1 ± 0.1	97.9 ± 2.1
0-168	0.5 ± 0.1	97.4 ± 2.0	0.1 ± 0.1	98.0 ± 2.1

SD = standard deviation

Source: Report JTK303-AD-006

6.1.2. COBI

6.1.2.1. Excretion of Radioactivity after Administration of [^{14}C]COBI to Mice

The excretion of radioactivity was determined after administration of a single oral dose (target 30 mg/kg) of [^{14}C]COBI to Hsd:ICR(CD-1) mice (Tabulated Summary 2.6.5.13.4, AD-216-2073). Excretion of radioactivity in urine and feces was determined through 168 hours postdose. The highest mean concentrations of radioactivity in blood and plasma were 3740 and 6670 ng equivalents [^{14}C]COBI/g, respectively, at 1 hour postdose. Concentrations of radioactivity in blood and plasma then declined through 24 hours postdose.

Radioactivity derived from [^{14}C]COBI was rapidly excreted, primarily within the first 24 hours after dosing. An average of 85.9% of the administered radioactivity was excreted in feces and 2.00% was excreted in urine by 168 hours postdose. Average overall recovery of radioactivity was 88.7%. Data are summarized in Table 49.

Table 49. Mean Cumulative Percent Total Radioactive Dose Recovered in Urine and Feces Following Oral Administration of [^{14}C]COBI at 30 mg/kg to Male CD-1 Mice

Collection Period (h)	Urine	Feces	Other[a]	Total
0 - 6	1.00	--	--	1.0
0 - 12	1.49			1.5
0 - 24	1.79	79.1	0.06	81.0
0 - 48	1.89	84.5	0.07	86.5
0 - 72	1.93	85.5	0.08	87.5
0 - 96	1.96	85.7	0.09	87.8
0 - 120	1.98	85.8	0.09	87.9
0 - 144	1.99	85.9	0.09	88.0
0 - 168	2.00	85.9	0.79	88.7

a Daily cage washings (cumulative 0.19% dose over 168 h) and carcass radioactivity at 168 h (0.6% dose)
Source: Report AD-216-2073

6.1.2.2. Excretion of Radioactivity after Administration of [^{14}C]COBI to Rats

Radiolabeled COBI ([^{14}C]COBI) was dosed orally to male Sprague-Dawley rats at 10 mg/kg (Tabulated Summary 2.6.5.13.5, AD-216-2034). Recovery in excreta, collected up to 7 days after dosing, and the concentration of radioactivity in blood and plasma up to 72 hours after dosing were assessed. Recovery in bile, urine, and feces from bile duct-cannulated animals was also assessed and is described below in Section 6.2.2.1.

In animals in which blood samples were taken sequentially, the t_{max} was 0.83 ± 0.29 hour and C_{max} values were 1310 ± 130 and 2170 ± 210 ng equivalents [^{14}C]COBI/mL in blood and plasma, respectively (mean ± SD, n = 3). The blood to plasma concentration ratio averaged 0.61 over the first 4 hours, indicating exclusion from the cellular components of blood.

In unmodified animals, recovery in excreta collected up to 168 hours postdose was high (mean ± SD = 93.5% ± 1.6% of dose, n = 3). The majority of the radioactivity (> 90%) was recovered in the first 48 hours, with 89.6% in the feces and 1.9% in the urine. Data are summarized in Table 50.

Table 50. Cumulative Percent Total Radioactive Dose Recovered in Urine, and Feces Following Oral Administration of [^{14}C]COBI at 10 mg/kg to Male Sprague-Dawley Rats (mean ± SD, N = 3)

Collection Period (h)	Urine	Feces	Cage Wash	Mean Total
0 - 12	1.57 ± 0.22	--	--	1.6
0 - 24	1.77 ± 0.24	77.8 ± 15.2	0.05 ± 0.02	79.6
0 - 48	1.88 ± 0.27	89.6 ± 2.4	0.06 ± 0.03	91.5
0 - 72	1.94 ± 0.28	90.5 ± 1.8	0.08 ± 0.03	92.5
0 - 96	1.98 ± 0.28	90.8 ± 1.7	0.08 ± 0.03	92.9
0 - 120	2.01 ± 0.29	91.1 ± 1.8	0.09 ± 0.04	93.2
0 - 144	2.04 ± 0.29	91.3 ± 1.8	0.09 ± 0.04	93.4
0 - 168	2.06 ± 0.29	91.4 ± 1.8	--	93.5

COBI = cobicistat
Source: Report AD-216-2034

6.1.2.3. Excretion of Radioactivity after Administration of [^{14}C]COBI to Dogs

Radiolabeled COBI ([^{14}C]COBI) was dosed orally to male beagle dogs at 5 mg/kg (Tabulated Summary 2.6.5.13.6, AD-216-2067). Recovery in excreta, collected up to 7 days after dosing, and the concentration of radioactivity in blood and plasma were determined. Recovery in bile, urine, and feces from bile duct-cannulated animals was also assessed and is described below in Section 6.2.2.2.

Radioactivity was quantifiable in blood samples collected 0.25–4 hours postdose. C_{max} values were 460 ± 87 and 821 ± 447 ng equivalents [^{14}C]COBI/mL in blood and plasma, respectively (mean ± SD, n = 3).

In unmodified animals, recovery in excreta collected up to 168 hours postdose was high (mean ± SD = 86.12% ± 0.96% of dose, n = 3). The majority of the radioactivity (> 80%) was recovered in the first 48 hours, with 76.8% in the feces and 1.8% in the urine. Data are summarized in Table 51.

Table 51. Cumulative Percent Total Radioactive Dose Recovered in Urine and Feces Following Oral Administration of [^{14}C]COBI at 5 mg/kg to Male Beagle Dogs (mean ± SD, N = 3)

Collection Period (h)	Urine	Feces	Cage Debris	Mean Total
0 - 12	1.37 ± 0.56	0.04 ± 0.08	0.07 ± 0.04	1.5
0 - 24	1.60 ± 0.56	33.5 ± 30.8	1.78 ± 2.20	36.9
0 - 48	1.81 ± 0.59	76.8 ± 4.27	2.05 ± 2.27	80.7
0 - 72	1.89 ± 0.59	79.0 ± 4.27	2.30 ± 2.54	83.1
0 - 96	1.96 ± 0.59	79.6 ± 4.14	2.46 ± 2.75	84.0
0 - 120	1.99 ± 0.59	80.0 ± 4.11	2.51 ± 2.84	84.5
0 - 144	2.04 ± 0.58	80.3 ± 4.17	2.56 ± 2.93	84.9
0 - 168	2.06 ± 0.58	80.5 ± 4.13	3.5[a]	86.1

COBI = cobicistat
a Includes hair, cage wash and cage wipe at 168 h post-dose
Source: Report AD-216-2067

6.2. Excretion into Bile

6.2.1. EVG

6.2.1.1. Study of [^{14}C]EVG in Bile Duct-Cannulated Rats

[^{14}C]EVG (3 mg/kg) was administered orally to male bile duct-cannulated Sprague-Dawley rats and the routes and rates of recovery of radioactivity were determined (Tabulated Summary 2.6.5.14.1, JTK303-AD-005). The data are summarized in Table 52.

Mean total cumulative recovery of dosed radioactivity was high (97.6%). The proportion of the dose recovered in bile was 25.0% indicating that at least this proportion was absorbed. As with the intact animals there was little excretion in urine (0.1%).

Table 52. Cumulative Excretion of Radioactivity After an Oral Dose of [^{14}C]EVG (3 mg/kg) to Bile Duct-Cannulated Rats (Mean ± SD, n = 3)

Time (h)	Excretion of Radioactivity (% of dose)		
	Bile	Urine	Feces
0–0.5	0.1 ± 0.1	--	--
0–1	0.9 ± 0.3	--	--
0–2	3.2 ± 0.6	--	--
0–4	7.4 ± 1.5	--	--
0–8	13.5 ± 4.2	--	--
0–24	23.0 ± 2.9	0.1 ± 0.0	42.4 ± 2.4
0–48	25.0 ± 3.7	0.1 ± 0.0	69.2 ± 6.1
Gastrointestinal contents (48 hours)			3.3 ± 0.9
Carcass (48 hours)			0.0 ± 0.1
Mean Total Cumulative Recovery (48 hours)			97.6

EVG = elvitegravir; SD = standard deviation

Source: Report JTK303-AD-005

The potential for recirculation of material excreted in bile was assessed by intraduodenal administration of bile (collected over 24 hours postdose) to a second group of 3 male bile duct-cannulated animals and the routes and rates of excretion were monitored (Tabulated Summary 2.6.5.14.1, JTK303-AD-005). The equivalent dose to the second group was 12.51 µg equivalents of EVG per rat. The results are summarized in Table 53.

Mean total recovery of radioactivity from the second group of rats was high (98.4%). The majority was found in the feces, with only 6.0% found in urine and bile, indicating low potential for reabsorption of metabolites excreted in bile.

Table 53. Cumulative Excretion of Radioactivity After Intraduodenal Administration of [^{14}C]EVG-Derived Bile Sample[a] to Bile Duct-Cannulated Rats (Mean ± SD, n = 3)

Time (h)	Excretion of Radioactivity (% of radioactivity injected)		
	Bile	Urine	Feces
0–2	1.6 ± 0.5	--	--
0–4	3.2 ± 1.2	--	--
0–8	4.4 ± 1.8	--	--
0–24	5.7 ± 1.7	0.1 ± 0.0	65.0 ± 22.5
0–48	5.9 ± 1.6	0.1 ± 0.0	91.5 ± 2.5
Gastrointestinal contents (48 hours)			0.9 ± 0.8
Carcass (48 hours)			0.0 ± 0.0
Mean Total Cumulative Recovery (0-48 h)			98.4

EVG = elvitegravir; SD = standard deviation

a Obtained from non-fasting male rats (0–24 hours) after single oral administration of [14C]EVG (dose: 3 mg/5 mL/kg, vehicle; 0.5 w/v% methylcellulose)

Source: Report JTK303-AD-005

6.2.2. COBI

6.2.2.1. Study of [^{14}C]COBI in Bile Duct-Cannulated Rats

[^{14}C]Cobicistat was dosed orally to male bile duct-cannulated Sprague-Dawley rats at 10 mg/kg (Tabulated Summary 2.6.5.14.2, AD-216-2034). Recovery in bile, urine, and feces was assessed up to 7 days postdose.

Recovery of radioactivity in the excreta of bile duct-cannulated animals (93.2% ± 2.84%) was almost identical to that of unmodified animals (see Section 6.1.2.2), with an average of 69.3% in the bile and 4.2% in the urine; indicating that at least 73.5% of dosed radioactivity was absorbed and that biliary excretion was the major route of elimination of radioactivity (Table 54). Excretion of radioactivity in bile was relatively rapid with an average of 37.6% of the dose recovered in the first 4 hours postdose and 57.6% by 8 hours postdose. Only 2.5% of dosed radioactivity was recovered in excreta 48 to 168 hours after dosing.

Table 54. Cumulative Percent Total Radioactive Dose Recovered in Bile, Urine, and Feces Following Oral Administration of [^{14}C]COBI at 10 mg/kg to Bile-duct Cannulated Rats (mean ± SD, N = 3)

Collection Period (h)	Bile	Urine	Feces	Total[a]
0 - 2	17.6 ± 4.8	--	--	17.6 ± 4.8
0 - 4	37.6 ± 9.5			37.6 ± 9.5
0 - 6	52.3 ± 9.7			52.3 ± 9.7
0 - 8	57.6 ± 7.1			57.6 ± 7.1
0 - 12	61.8 ± 5.4	3.6 ± 0.9		65.3 ± 5.0
0 - 24	65.3 ± 5.3	3.8 ± 1.0	17.2 ± 3.9	86.2 ± 2.5
0 - 48	66.8 ± 5.4	4.0 ± 1.1	19.2 ± 4.7	90.0 ± 3.3
0 - 72	67.7 ± 5.4	4.1 ± 1.1	19.5 ± 4.8	91.2 ± 3.1
0 - 96	68.3 ± 5.5	4.1 ± 1.1	19.6 ± 4.7	91.9 ± 3.0
0 - 120	68.7 ± 5.5	4.2 ± 1.1	19.6 ± 4.8	92.5 ± 3.0
0 - 144	69.0 ± 5.5	4.2 ± 1.1	19.6 ± 4.8	92.8 ± 3.0
0 - 168	69.3 ± 5.5	4.2 ± 1.1	19.6 ± 4.8	93.1 ± 2.9

COBI = cobicistat; SD = standard deviation
a Recovery of radioactivity from cage washes, cage wipes, cannulae and collection jackets totaled < 0.15% of total dose.
Source: Report AD-216-2034

6.2.2.2. Study of [^{14}C]COBI in Bile Duct-Cannulated Dogs

[^{14}C]COBI was dosed orally to male bile duct-cannulated beagle dogs at 10 mg/kg (Tabulated Summary 2.6.5.14.3, AD-216-2068). Recovery in bile, urine, and feces, collected up to 7 days after dosing, was assessed. Of the 3 dogs dosed, 1 was an outlier in which no radioactivity was detected in plasma or blood at any time point, and 90.19% of dosed radioactivity was found in the first urine sample, collected 0–12 hours postdose. The data for the other 2 dogs were very comparable and are summarized in Table 55. In those 2 dogs, mean total recovery was high (90.3%), with 63.9% in bile and 1.88% in urine, suggesting at least 65.8% of dosed radioactivity was absorbed. More than half of dosed radioactivity was recovered by 8 hours postdose and the majority was recovered by 72 hours postdose (only 3.2% recovered in excreta after 72 hours).

Table 55. Cumulative Percent Total Radioactive Dose Recovered in Bile, Urine, and Feces Following Oral Administration of [^{14}C]COBI at 5 mg/kg to Bile-duct Cannulated Dogs (mean ± SD, N = 2)

Collection Period (h)	Bile	Urine	Feces	Mean Total[a]
0 - 2	22.3 ± 0.01	--	--	22.3
0 - 4	39.3 ± 0.33			39.3
0 - 6	48.7 ± 1.51			48.7
0 - 8	53.5 ± 2.97			53.5
0 - 12	57.1 ± 3.25	1.07 ± 0.34	0.24 ± 0.33	58.5
0 - 24	61.6 ± 3.38	1.40 ± 0.12	1.26 ± 1.12	64.3
0 - 48	63.9 ± 3.70	1.56 ± 0.01	16.1 ± 1.43	81.7
0 - 72	(63.9 ± 3.70)[b]	1.72 ± 0.02	21.3 ± 3.41	87.1
0 - 96	(63.9 ± 3.70)[b]	1.78 ± 0.04	22.4 ± 3.07	88.3
0 - 120	(63.9 ± 3.70)[b]	1.82 ± 0.04	23.4 ± 2.78	89.4
0 - 144	(63.9 ± 3.70)[b]	1.85 ± 0.04	23.9 ± 2.68	89.9
0 - 168	(63.9 ± 3.70)[b]	1.88 ± 0.04	24.3 ± 2.73	90.3

COBI = cobicistat; SD = standard deviation

a Additional radioactivity in cage debris (collected daily 0–168 hours) and cage wash and wipe performed at 168 hours averaged 0.26% of the dose

b Bile collection was only performed 0–48 hours postdose

Source: Report AD-216-2068

6.3. Excretion into Milk

6.3.1. EVG

The excretion of EVG, GS-9200 (M4) and GS-9202 (M1) in the milk of Sprague-Dawley rats was assessed, on Day 14 of lactation, as part of a postnatal toxicology study (Tabulated Summary 2.6.5.7.1, TX-183-2006). Milk was collected before dosing and 30 minutes after dosing orally with 0 (vehicle control), 300, 1000, and 2000 mg EVG/kg/day. Plasma concentrations in the dams were also determined. None of the 3 analytes was detectable in plasma or milk from vehicle-treated animals. In the predose samples, none of the analytes was detectable in milk, and low concentrations of EVG and GS-9200 were detected in individual animals. The results from samples from EVG-treated animals collected at the 30-minute time point are summarized in Table 56.

EVG was excreted in milk and concentrations were 9- to 13-fold lower than those in plasma. The oxidative metabolite, GS-9202, was only detectable in the plasma of a single animal dosed at 2000 mg/kg/day, at a level (120 ng/mL) close to the limit of quantification (100 ng/mL). GS-9202 was not detectable in any milk sample. The acyl glucuronide

metabolite, GS-9200, was detectable in plasma at levels 15% to 19% of those of the parent, but was not detectable in any of the milk samples.

Table 56. Concentrations (ng/mL) of EVG, GS-9200 and GS-9202 in Milk and Plasma from Rats 30 min after Oral Dosing with EVG (Mean ± SD, n = 3 or 4)

Analyte	Matrix	Dose (mg/kg)		
		300	1000	2000
EVG	Milk	1360 ± 514	2780 ± 755	4160 ± 1980
	Plasma	17500 ± 5600	34700 ± 8120	36000 ± 6380
	(Milk/Plasma)	(0.08)	(0.08)	(0.12)
GS-9200 (M4)	Milk	< 100	< 100	< 100
	Plasma	3100 ± 998	5260 ± 1710	6640 ± 3390
GS-9202 (M1)	Milk	< 100	< 100	< 100
	Plasma	< 100	< 100	30 ± 60

EVG = elvitegravir; SD = standard deviation
Source: Report TX-183-2006

6.3.2. COBI: Excretion in Milk

The excretion of COBI in rat milk was examined as part of a postnatal development study. The data are reported in this context in Module 2.6.6, Section 6.2.3. Two hours after treatment of lactating females (postnatal Day 10) with COBI, mean milk/plasma concentration ratios were 1.3, 1.9, and 1.7 after doses of 10, 30, and 75 mg/kg/day, respectively (Tabulated Summary 2.6.7.14.2, TX-216-2033), indicating that COBI is distributed into milk in this species.

6.4. Excretion of EVG/COBI/FTC/TFV

Since FTC and TFV are almost exclusively eliminated by renal excretion, while very little EVG or COBI is excreted in the urine, interactions between the compounds during excretion are unlikely. Cobicistat has also been shown to have no inhibitory effect on OAT1 and only weak inhibition of MRP4 (Section 7.2.4.1), the transporters responsible for renal excretion of TFV. The potential for the 2 renally excreted compounds (FTC and TDF) to interact was tested in two 14-day rat toxicity studies and in a 28-day dog study; the combination did not exacerbate the renal toxicity of TDF (Module 1.4.4, TX-164-2001, TX-164-2005, and TX-164-2004, respectively).

7. PHARMACOKINETIC DRUG INTERACTIONS

Discussions of drug interaction liability are made by reference to current industry and US and European regulatory guidelines {11006}, {15555}, {18022}, {18670}.

7.1. EVG: Pharmacokinetic Drug Interactions

The effects of EVG on the activities of human hepatic microsomal drug metabolizing cytochromes P450 were assessed. The potential for inhibition of efflux and uptake transporters was assessed in cell lines. Induction potential was determined in primary human hepatocytes. The potential for EVG to be a substrate of human cytochromes P450 and UGTs was determined with recombinant enzymes, and with microsomal fractions and selective inhibitors. The potential for EVG to be a substrate for human MDR1 was assessed with cell monolayers expressing the protein.

To allow quantitative calculation of drug interaction liability, human pharmacokinetics of EVG summarized from multiple clinical studies (Module 2.7.2, Appendix 5.5, Table 1 and Table 2.1) are considered representative. In that analysis, a steady-state C_{max} value (also known as $[I]_1$) of 1.7 µg/mL (3.8 µM) was found. The representative unbound plasma concentration at C_{max} is thus 1.7 µg/mL × 0.7% = 12 ng/mL or 0.03 µM. The value of $[I]_2$, the theoretical maximal concentration in the intestinal lumen (calculated as 150 mg/250 mL) is 1.34 mM.

7.1.1. EVG: Cytochrome P450 Inhibition

The potential for EVG to inhibit major human drug metabolizing cytochrome P450 enzymes was evaluated using pooled human hepatic microsomal fractions and enzyme-specific activities (Tabulated Summary 2.6.5.12.1, JTK303-AD-027). The results are summarized in Table 57.

All enzyme-selective positive control inhibitors reduced their respective activities by > 50% confirming appropriate sensitivity to inhibition. Elvitegravir did not inhibit any of the activities tested (IC_{50} > 30 µg/mL) apart from testosterone 6β-hydroxylase, where an IC_{50} of 28.3 µg/mL (63 µM) was determined. Elvitegravir is thus unlikely to cause drug interactions through inhibition of the metabolism of other drugs.

Table 57. Effect of EVG on the Activities of Human Hepatic Microsomal Cytochromes P450

Enzyme	Activity	EVG	Control Inhibitor[a]
		Calculated IC_{50} (µg/mL)	Activity remaining (%)
CYP1A2	Ethoxyresorufin O-deethylase	> 30	5.6%
CYP2A6	Coumarin 7-hydroxylase	> 30	< 10.2%
CYP2C9	Tolbutamide 4-hydroxylase	> 30	42.5%
CYP2C19	(S) Mephenytoin 4'-hydroxylase	> 30	29.6%
CYP2D6	Bufuralol 1'-hydroxylase	> 30	< 17.5%
CYP2E1	Chlorzoxazone 6-hydroxylase	> 30	48.3%
CYP3A	Midazolam 1'-hydroxylase	> 30	< 9.6%
	Testosterone 6β-hydroxylase	28.32	5.6%

a Control Inhibitors: CYP1A2, α Naphthoflavone (1 µM); CYP2A6, Methoxsalen (5 µM); CYP2C9, Sulfaphenazole (3 µM); CYP2C19, Tranylcypromine (20 µM); CYP2D6, Quinidine (4 µM); CYP2E1 Diethyldithiocarbamate (100 µM); CYP3A, Ketoconazole (1 µM).

Source: Report JTK303-AD-027

7.1.2. EVG: Enzymology of Metabolism

The enzymes responsible for oxidation and glucuronidation of EVG were studied using recombinant enzymes and using microsomal fractions with enzyme-selective inhibitors.

7.1.2.1. Metabolism of EVG by Recombinant Human Cytochromes P450

The rates of metabolism of [^{14}C]EVG (10 µg/mL) by recombinant baculovirus-expressed human cytochromes P450 were determined by quantifying the loss of parent and the formation of mono- and di-hydroxylated metabolites after incubation for 30 minutes (Tabulated Summary 2.6.5.10.4, JTK303-AD-017). In the reaction the concentration of each enzyme was 50 pmol cytochrome P450/mL and the total insect cell microsomal fraction concentration was 1 mg/mL. All preparations included recombinant co-expressed human cytochrome P450 reductase. CYP2A6 and CYP2E1 were also co-expressed with recombinant human cytochrome b5. Exogenous recombinant human cytochrome b5 was added to CYP2B6, CYP2C8, CYP2C9, CYP2C19, CYP2E1, and CYP3A4. Incubations with human hepatic microsomal fraction were run in parallel. All incubations were performed in duplicate. The mean results are summarized in Table 58.

The benzylic oxidation product (M2) (minimum 0.2% of the radiochromatogram) and other minor peaks (minimum 1.4% of the radiochromatogram) were detected at low levels in all incubations and, for most enzyme preparations, were considered to be generated nonspecifically. Elvitegravir was metabolized by CYP1A1 (yielding metabolites M1 and M2), CYP3A4 (yielding M1, M2, M5, M8 and other metabolites), and CYP3A5 (yielding

M1). Metabolism by CYP3A4 was the most rapid and the resulting pattern of metabolites most closely resembled that generated by human hepatic microsomal fraction.

Table 58. Metabolism of [^{14}C]EVG by Recombinant Human Cytochrome P450 Enzymes

Enzyme	Proportion (%) of Radiochromatogram After 30 min Incubation					
	EVG	M1	M2	M5	M8	Other
CYP1A1	92.2	0.3	6.1	ND	ND	1.4
CYP1A2	97.9	ND	0.5	ND	ND	1.6
CYP2A6	98.2	ND	0.4	ND	ND	1.4
CYP2B6	98.3	ND	0.2	ND	ND	1.5
CYP2C8	98.1	ND	0.4	ND	ND	1.5
CYP2C9	98.0	ND	0.5	ND	ND	1.5
CYP2C19	98.1	ND	0.4	ND	ND	1.5
CYP2D6	98.2	ND	0.4	ND	ND	1.4
CYP2E1	98.3	ND	0.3	ND	ND	1.4
CYP3A4	34.8	50.3	0.5	0.9	3.1	10.4
CYP3A5	95.6	2.5	0.4	ND	ND	1.5
HLM[a]	28.9	51.0	0.9	6.5	4.6	8.0

ND = not detected
a Human hepatic microsomal fraction
Source: Report JTK303-AD-017

7.1.2.2. Effects of Enzyme-Selective Cytochrome P450 Inhibitors on the Metabolism of [^{14}C]EVG by Human Hepatic Microsomal Fraction

The effects of enzyme-selective inhibitors on the oxidative metabolism of [^{14}C]EVG by human hepatic microsomal fraction was determined (Tabulated Summary 2.6.5.15.1, JTK303-AD-018). The rate of metabolism of EVG was quantified by loss of parent and by the formation of metabolites M1, M5, and M8. The results are summarized in Table 59.

The rate of loss of EVG in the absence of inhibitor was 144.6 pmol/min/mg protein. The rates of formation of metabolites M1, M5, M8, and others were 123.7, 12.3, 3.0, and 5.6 pmol/min/mg. At the highest concentrations tested the CYP2C9-selective inhibitor, sulfaphenazole, and the CYP2D6-selective inhibitor, quinidine, had relatively little effect upon the rate of loss of EVG or the rate of formation of the major metabolite, M1. In contrast, the CYP3A-selective inhibitor, ketoconazole, showed potent, concentration-dependent inhibition of the loss of EVG and of the formation of all metabolites.

From these results, as well as the results obtained using recombinant human cytochromes P450, it is apparent the CYP3A enzymes are the major catalysts of the oxidative metabolism of EVG by human hepatic microsomal fraction.

Table 59. Metabolism of [^{14}C]EVG by Human Hepatic Microsomal Fraction in the Presence of Enzyme-Selective Inhibitors (Mean, n = 2)

Inhibitor (Target Enzyme)	Concentration (µM)	Reduction in Rate (%)				
		EVG	M1 (GS-9202)	M5	M8	Other Metabolites
Sulfaphenazole	2	8.0	6.9	4.1	NC	66.1
(CYP2C9)	20	14.6	10.0	8.1	70.0	98.2
Quinidine	0.2	5.1	3.7	9.8	NC	32.1
(CYP2D6)	2	4.1	0.4	4.9	16.7	78.6
Ketoconazole	0.2	69.8	68.0	69.1	100.0	91.1
(CYP3A)	2	97.5	96.8	100.0	100.0	100.0

NC: Not Calculated
Source: Report JTK303-AD-018

7.1.2.3. Metabolism of EVG by Recombinant Human UDP Glucuronosyl Transferases

Elvitegravir (20 µM) was incubated with insect cell microsomal fractions (2 mg/mL) containing 12 individual recombinant baculovirus-expressed human UGTs. The rates of formation of the acyl glucuronide metabolite, M4 (GS-9200), were then determined (Tabulated Summary 2.6.5.10.6, AD-183-2034). Positive control UGT substrates (3 µM raloxifene, 3 µM trifluoperazine, 10 µM 7-hydroxycoumarin, 10 µM 4-hydroxyestradiol, or 10 µM scopoletin) were tested in parallel and metabolism was quantified as the in vitro half-life for loss of substrate. The results are summarized in Table 60.

All enzymes showed activity with the positive control substrates. Of the enzymes tested, UGT1A1 and UGT1A3 generated appreciable amounts of GS-9200, suggesting that these would be the major catalysts for the glucuronidation of EVG in humans. Very slow (19- to 31-fold slower than UGT1A1) generation of GS-9200 by UGT1A9 and UGT2B15 was also detected.

Table 60. Metabolism of EVG to GS-9200 (M4) by Human UGT Enzymes (Mean, n = 2)

Enzyme	Positive Control	Positive control T½ (min)	GS-9200 formation (pmol/mg protein/min)
None	(None)	--	< 0.1
UGT1A1	Raloxifene	31.5	3.75
UGT1A3	Raloxifene	89.1	16.6
UGT1A4	Trifluoperazine	176	< 0.1
UGT1A6	7-Hydroxycoumarin	< 10	< 0.1
UGT1A7	7-Hydroxycoumarin	18.0	< 0.1
UGT1A8	7-Hydroxycoumarin	193	< 0.1
UGT1A9	7-Hydroxycoumarin	< 10	0.2
UGT1A10	Raloxifene	122	< 0.1
UGT2B4	4-Hydroxyestradiol	51.1	< 0.1
UGT2B7	4-Hydroxyestradiol	< 10	< 0.1
UGT2B15	Scopoletin	< 10	0.12
UGT2B17	4-Hydroxyestradiol	58.3	< 0.1

Source: Report AD-183-2034

7.1.2.4. Effects of Ketoconazole and ATV on Glucuronidation of EVG by Human Hepatic Microsomal Fraction

The effects of ketoconazole and the UGT1A1-selective inhibitor, ATV, on the formation of M4, the acyl glucuronide metabolite of EVG were determined using human hepatic microsomal fractions (Tabulated Summary 2.6.5.15.3, AD-183-2028). Using an LC/MS/MS assay for GS-9200, the kinetics for acyl glucuronide formation were first assessed and a K_M of 21 µM was determined (Tabulated Summary 2.6.5.10.5, AD-183-2028). The effects of ketoconazole and ATV were then determined at an EVG substrate concentration of 10 µM.

Atazanavir was a potent inhibitor of EVG glucuronidation with an IC_{50} value of 0.4 µM. Maximum inhibition by ATV with human hepatic microsomal fraction was 83% at 100 µM, consistent with a minor role for other UGT enzymes in this activity. In contrast, with recombinant human UGT1A1 an average of 99.3% inhibition was achieved with 100 µM ATV confirming full efficacy of this inhibitor against the target enzyme. Ketoconazole also inhibited EVG glucuronidation with an IC_{50} of 9.6 µM, consistent with previous reports on inhibition of UGT1A1 by this compound. In combination with the results above (Section 7.1.2.3), it is likely that both UGT1A1 and UGT1A3 are responsible for the human hepatic microsomal metabolism of EVG, with UGT1A1 playing a quantitatively more important role.

7.1.2.5. Interaction Study of EVG with Co-administered Drugs

To further explore the potential for pharmacokinetic drug interactions with EVG the effects of a variety of potential comedications on the oxidative metabolism of [^{14}C]EVG by human hepatic microsomal fractions were determined (Tabulated Summary 2.6.5.15.2, JTK303-AD-025). The metabolism of EVG was quantified by the loss of parent (initial concentration 2 μM) and by the formation of the major oxidative metabolite, M1. Medications were tested at concentrations up to 50 μM, except for zidovudine (ZDV, 100 μM). All reactions were performed in duplicate. The results are summarized in Table 61.

Inhibition of the loss of EVG substrate largely paralleled inhibition of the loss of formation of M1. The potent CYP3A-selective inhibitors, ketoconazole and RTV, were the strongest inhibitors of EVG metabolism and M1 formation. Efavirenz, nevirapine (NVP), and ZDV inhibited by < 50%, even at the highest concentrations tested. The other compounds showed intermediate potencies with IC_{50} values from 0.51 to 4.5 μM.

Table 61. Metabolism of [^{14}C]EVG by Human Hepatic Microsomal Fraction in the Presence of Potential Comedications (Mean, n = 2)

Compound	IC_{50} (μM)	Maximum Inhibition (%)	
		Loss of EVG	M1 formation
APV	1.1	96.6	96.6
EFV	> 50	41.4	46.4
IDV	0.51	98.2	100.0
Ketoconazole	0.099	93.8	94.6
LPV	3.1	96.1	96.5
NFV	1.1	98.5	100.0
NVP	> 50	5.3	8.0
RTV	0.079	100.0	100.0
SQV	4.5	99.6	97.6
ZDV	> 100	5.3	5.2

APV = amprenavir; EFV = efavirenz; EVG = elvitegravir; IC_{50} = concentration required to produce 50% inhibition; IDV = indinavir; LPV = lopinavir; NFV = nelfinavir; NVP = nevirapine; RTV = ritonavir; SQV = saquinavir; ZDV = zidovudine

Source: Report JTK303-AD-025

7.1.3. EVG: Assessment of Induction Liability

The potential for EVG to cause drug interactions through induction was assessed in primary cultures of human hepatocytes (Tabulated Summary 2.6.5.12.2, JTK303-AD-023). After plating and recovery, duplicate wells were exposed to EVG (0.1, 1, or 10 µg/mL) or positive control inducers or 0.1% (v/v) dimethyl sulfoxide (DMSO) vehicle control for 3 days. The activities of CYP1A2 (phenacetin O-deethylase), CYP2C9 (tolbutamide 4-hydroxylase), CYP2C19 ((S)-mephenytoin 4'-hydroxylase), and CYP3A (midazolam 1'-hydroxylase) were then determined using enzyme-selective assays with quantification of the metabolites by LC/MS/MS. The results are summarized in Table 62.

Treatment with the positive control inducer β-naphthoflavone increased the activity of CYP1A2 in hepatocytes from the 2 donors by an average of 30.6- and 48.4-fold. Treatment of the same cells with EVG at concentrations up to 10 µg/mL resulted in ≤ 1.58-fold increase of CYP1A2 activity, indicating that EVG is very unlikely to cause drug interactions through activation of AhR. Treatment with the positive control, rifampicin, resulted in 34.1- and 25.7-fold increases in CYP3A activity, a sensitive marker for PXR activation. The secondary, less-sensitive markers, CYP2C9 and CYP2C19 responded more weakly (CYP2C19 activity was only detectable in 1 donor, and only after rifampicin treatment). Treatment with EVG resulted in concentration-dependent increases of CYP3A activity in both donors. At 1 µg/mL the calculated increase was 16.3% and 21.5% (mean 18.9%) of the positive control, and this increased to 54.7% and 38.9% (mean 46.8%) at 10 µg/mL.

Table 62. Effects of EVG and Positive Control Inducers on Enzyme Activities of Primary Cultures of Fresh Human Hepatocytes (Mean, n = 2)

Test Article	Donor Lot	Fold Increase Compared to Vehicle Control			
		CYP1A2	CYP2C9	CYP2C19	CYP3A
EVG 0.1 µg/mL	66	1.18	0.96	ND	1.74
	68	1.08	0.92	ND	1.48
EVG 1 µg/mL	66	1.24	1.19	ND	6.41
	68	1.58	1.64	ND	6.32
EVG 10 µg/mL	66	0.63	1.49	ND	19.1
	68	1.16	2.72	ND	10.6
Positive Control[a]	66	30.6	3.14	ND	34.1
	68	48.4	4.29	NC	25.7

EVG = elvitegravir; NC: Cannot be calculated due to lack of activity in vehicle control; ND: Activity not detectable

Fractional increase = (Fold Increase of test compound – 1) / (Fold Increase of positive control – 1) x 100%

a Positive controls: 20 µM β-naphthoflavone (CYP1A2), 20 µM rifampicin (CYP2C9, CYP2C19), 10 µM rifampicin (CYP3A)

Source: Report JTK303-AD-023

7.1.4. EVG: Interactions with Transporters

Evidence that EVG is a substrate for human MDR1 is presented above (Section 3.1), but there are no nonclinical or clinical data to suggest that MDR1 plays a role in limiting intestinal absorption of EVG. In this section the potential for EVG to be an inhibitor of human MDR1, OATP1B1, or OATP1B3 was explored using cell lines expressing these transporters.

7.1.4.1. Effect of EVG on the MDR1-Dependent Transport of Digoxin

The effects of EVG (0.3 to 30 µM) on the bidirectional permeability of [^{3}H]digoxin (1 µM) across monolayers of LLC-PK1 porcine kidney cells, transfected with an expression vector for human MDR1 or with the empty control expression vector, were determined (Tabulated Summary 2.6.5.15.4, JTK303-AD-026). Results were compared with the positive control MDR1 inhibitor, verapamil (10 µM). Data are summarized in Table 63.

In the absence of inhibitor digoxin showed clear polarized transport in MDR1-expressing cells (mean efflux ratio 9.9). In the presence of the positive control MDR1 inhibitor, verapamil, the A-B flux of digoxin was increased 1.9-fold and the B-A flux reduced by 0.6-fold resulting in a reduction of the efflux ratio to 3.2. Elvitegravir had no clear effect on digoxin transport at concentrations up to 10 µM. At 30 µM EVG the A-B flux was increased modestly (1.5-fold) and the B-A flux decreased slightly (0.9-fold) resulting in an efflux ratio of 6.0. The efflux ratio at an EVG concentration of 30 µM is thus ~56% of that with the vehicle control giving an IC_{50} of > 30 µM for inhibition of MDR1.

Table 63. Effects of EVG and Positive Control Inhibitor on the Transport of Digoxin by LLC-PK1 Cells (Mean ± SD, n = 2)

Inhibitor	Transcellular Flux (µL/mg protein/h)					
	Control Cells			MDR1-Expressing Cells		
	A-B	B-A	Ratio	A-B	B-A	Ratio
None	20.6 ± 2.9	44.8 ± 6.7	2.2	18.5 ± 5.8	183.6 ± 10.6	9.9
EVG 0.3 µM	53.4 ± 3.5	73.5 ± 8.6	1.4	19.6 ± 7.1	204.6 ± 19.2	10.4
EVG 1 µM	47.7 ± 4.4	75.7 ± 4.7	1.6	27.0 ± 4.6	213.8 ± 21.1	7.9
EVG 3 µM	28.1 ± 2.8	46.6 ± 3.2	1.7	19.2 ± 1.7	205.9 ± 13.5	10.7
EVG 10 µM	29.1 ± 1.8	33.9 ± 3.3	1.2	18.0 ± 1.0	176.1 ± 9.3	9.8
EVG 30 µM	24.6 ± 2.8	29.9 ± 2.3	1.2	27.5 ± 6.8	164.6 ± 11.4	6.0
Verapamil 10 µM	24.9 ± 1.1	25.4 ± 2.9	1.0	34.6 ± 14.6	110.0 ± 6.8	3.2

A-B = apical to basal; B-A = basal to apical; EVG = elvitegravir; MDR1 = P-glycoprotein
Source: Report JTK303-AD-026

7.1.4.2. Effects of EVG on the Activities of OATP1B1 and OATP1B3

The effects of EVG on the human solute carrier uptake transporters, OATP1B1 and OATP1B3, was assessed in CHO cells expressing the transporters at concentrations of EVG up to 2 µM (Tabulated Summary 2.6.5.15.5, AD-183-2030). For each cell line the transport substrate, Fluo 3, was used at its measured K_M value.

The positive control, rifampicin (50 µM) reduced OATP1B1 activity by 98.6% and OATP1B3 by 98.4%, confirming the sensitivity of the cells to inhibition. Elvitegravir was a weak inhibitor of OATP1B1, with < 40% reduction in activity at the highest concentration tested (IC_{50} > 2 µM). Elvitegravir was a more potent inhibitor of OATP1B3 with an IC_{50} of 0.44 µM. Inhibition of OATP transporters is consistent with a clinical drug interaction study (Module 2.7.2, Section 2.5.2.2.3 [GS-US-216-0123]) in which, after dosing with 150 mg EVG and 150 mg COBI, there was a modest increase in exposure of co-dosed rosuvastatin ($AUC_{0-\infty}$ increased 38% compared to the reference treatment), that was not considered clinically relevant.

7.2. COBI: Pharmacokinetic Drug Interactions

The potential for COBI to be the perpetrator (precipitant) or victim (object) of drug interactions was tested through in vitro assays. These included: inhibition of cytochromes P450 and other drug metabolizing enzymes, inhibition of drug transporters, induction liability, and assessing the possibility that COBI is a substrate for cytochromes P450 or transporters. Since inhibition of CYP3A enzymes is the intended pharmacological effect of COBI, this property was studied in particular detail. To allow quantitative calculation of drug interaction liability, human pharmacokinetics of COBI summarized from multiple clinical studies (Module 2.7.2, Appendix 5.5, Table 2.2) are considered representative. The key parameters from this analysis are provided in Table 64 below and include the total and unbound plasma concentrations of COBI and the theoretical maximal concentration of COBI in the intestinal lumen ($[I]_2$).

Table 64. Clinical Concentrations for Drug Interaction Liability Assessment

Parameter	Value	Rationale
Total C_{max} ($[I]_1$)	1.4 µM	Representative C_{max} 1.1 µg/mL
$C_{average}$	0.4 µM	Representative AUC_{0-24} 8.3 µg.h/mL, dose interval 24 h
$C_{max,u}$	0.1 µM	AD-216-2026 f_u 6.33% at 1 µM
$C_{average,\ u}$	0.03 µM	AD-216-2026 f_u 6.33% at 1 µM
$[I]_2$	770 µM	150 mg/250 mL

f_u = fraction unbound; $[I]_1$ = inhibitor concentration corresponding to steady state C_{max}; $[I]_2$ = inhibitor concentration corresponding to theoretical maximum concentration in the intestinal lumen

7.2.1. COBI: Cytochrome P450 Inhibition

7.2.1.1. Inhibition of CYP3A Activity by COBI

The intended pharmacological effect of COBI is inhibition of human CYP3A enzyme activity. CYP3A inhibition studies in human hepatic microsomal fractions, using an established clinical CYP3A inhibitor, RTV, as a comparator, were performed to test the generality of CYP3A inhibition, mechanism of inhibition, and enzyme inactivation parameters (Tabulated Summary 2.6.5.12.4, AD-216-2028).

Cobicistat was a potent inhibitor of all human hepatic microsomal CYP3A activities tested (Table 65), including established CYP3A probe activities (midazolam 1'-hydroxylase, testosterone 6β-hydroxylase, and terfenadine t-butyl hydroxylase), and clinically relevant interactions (elvitegravir hydroxylase, atazanavir oxidase, telepravir oxidase). Studies with midazolam 1'-hydroxylase and testosterone 6β-hydroxylase showed that the apparent inhibitory potency could be increased in a preincubation time-dependent and NADPH cofactor-dependent manner, suggesting that COBI is a mechanism-based inhibitor of human CYP3A enzymes.

Detailed enzyme inactivation kinetic studies were performed with COBI and RTV. Cobicistat was found to be an efficient inactivator of human hepatic microsomal CYP3A activity, with kinetic parameters (k_{inact} = 0.47 min^{-1}, K_I = 1.1 μM) similar to those of RTV (k_{inact} = 0.23 min^{-1}, K_I = 0.26 μM), but with a higher theoretical maximal inactivation rate and a lower affinity.

To allow an understanding of the non-dose-linear pharmacokinetics seen in nonclinical species, and the pharmacokinetic drug interactions in the EVG/COBI and ATV/COBI combination toxicology studies, the effect of COBI on rat, dog, and monkey hepatic microsomal CYP3A activity was assessed (Tabulated Summary 2.6.5.12.5, AD-216-2040). Midazolam 1'-hydroxylase was used as the probe activity and RTV was tested in parallel. Both RTV and COBI were potent inhibitors of midazolam 1'-hydroxylase activity in all 3 species. In dog and monkey, there was no evidence for preincubation time-dependence, indicating that these compounds were potent reversible inhibitors, but not mechanism-based inhibitors in these species. Inactivation of hepatic microsomal activity of the rat was much less efficient than human (k_{inact} values 10-fold lower), suggesting that reversible inhibition would predominate in the rat.

Table 65. Effect of COBI and RTV on Various Activities Catalyzed by Human Hepatic Microsomal CYP3A Enzymes

Activity	Calculated IC_{50} (μM)	
	COBI	RTV
Midazolam 1'-hydroxylase	0.15	0.11
Testosterone 6β-hydroxylase	0.15	0.12
Terfenadine *t*-butyl-hydroxylase	0.29	0.28
Elvitegravir hydroxylase (to metabolite M1)	0.03	0.03
Atazanavir oxidation	0.04	0.04
Telaprevir oxidation	0.03	0.02

COBI = cobicistat; RTV = ritonavir
Source: Report AD-216-2028

7.2.1.2. Inhibition of Other Human Cytochromes P450

Having demonstrated that COBI is a potent mechanism-based inhibitor of human CYP3A activities, the specificity of inhibition was assessed using pooled human hepatic microsomal fractions and enzyme-specific activities (Tabulated Summary 2.6.5.12.6, AD-216-2029 and AD-216-2070). Ritonavir was tested in parallel as a relevant comparator. The IC_{50} values for in vitro CYP inhibition by COBI, RTV, and positive control inhibitors are presented in Table 66.

As reported above (Section 7.2.1.1), both COBI and RTV were potent inhibitors of CYP3A activities in vitro, with IC_{50} values less than 0.2 μM. At concentrations up to 25 μM, neither COBI nor RTV inhibited CYP1A2 or CYP2C19 activity. In contrast to RTV, COBI did not inhibit CYP2C9, and COBI was a weaker inhibitor of CYP2D6. Cobicistat is a potent inhibitor of human CYP3A activity and a weak inhibitor of CYP2D6 activity. Cobicistat was a weak inhibitor of CYP2C8 activity in vitro, with potency lower than RTV. Although COBI was a stronger inhibitor of CYP2B6 activity, with a potency very similar to RTV, the IC_{50} is above the human plasma C_{max} value. At clinically relevant plasma concentrations, COBI is unlikely to cause drug interactions by inhibition of CYP2C8 and interactions with CYP2D6 (C_{max}/IC_{50} = 0.15) and CYP2B6 (C_{max}/IC_{50} = 0.50) are likely to be modest and brief. These later conclusions are supported by the clinical probe drug interaction study (Module 2.7.2, Section 2.3.2.2.3 [GS-US-216-0112]) in which COBI was found to be a weak inhibitor of CYP2D6 (assessed with desipramine as the probe substrate) and did not inhibit CYP2B6 (assessed with efavirenz [EFV] as the probe substrate).

Table 66. IC_{50} Values for Inhibition of Major Human Cytochrome P450 Enzymes by COBI, RTV, and Positive Control Inhibitors (mean, N = 6)

Enzyme	Activity	Calculated IC_{50} (μM)		
		Control Inhibitor[a]	COBI	RTV
CYP1A2	Ethoxyresorufin O-deethylase	0.03	> 25	> 25
CYP2B6	Bupropion 4-hydroxylase	2.8	2.8	2.9
CYP2C8	Paclitaxel 6α-hydroxylase	0.06	30.1	5.5
CYP2C9	Tolbutamide hydroxylase	1.6	> 25	3.9
CYP2C19	(S) Mephenytoin 4'-hydroxylase	10.8	> 25	> 25
CYP2D6	Dextromethorphan O-demethylase	0.04	9.2	3.4
CYP3A	Midazolam 1'-hydroxylase	0.07	0.15	0.10
	Testosterone 6β-hydroxylase	0.09	0.15	0.11

COBI = cobicistat; CYP = cytochrome P450 enzyme; RTV = ritonavir

a Control Inhibitors: CYP1A2, α-Napthoflavone (0–100 μM); CYP2B6, Triethylenethiophosphoramide (0–30 μM); CYP2C8 Montelukast (0–30 μM); CYP2C9, Sulfaphenazole (0–10 μM); CYP2C19, Tranylcypromine (0–100 μM); CYP2D6, Quinidine (0–10 μM); CYP3A, Ketoconazole (0–10 μM).

Source: Reports AD-216-2029 and AD-216-2070

7.2.1.3. Inhibition of Human Cytochromes P450 by Human Metabolites of COBI

Three metabolites of COBI were initially identified during incubations with both human hepatocytes and human hepatic microsomal fractions. These metabolites are also the most abundant in human feces and urine (Module 2.7.2, Section 2.2.2.3 [GS-US-216-0111]). The effects of these metabolites on the activities of 5 major human drug metabolizing cytochrome P450 enzymes were assessed and the results are presented in Table 67 (Tabulated Summary 2.6.5.12.7, AD-216-2041). Data reported for COBI are provided for comparison (Tabulated Summaries 2.6.5.12.4 and 2.6.5.12.6; AD-216-2028 and AD-216-2029, respectively). Multiple CYP3A activities were tested because of the known substrate-dependent inhibition potency of this enzyme.

Metabolites M21 (E1, GS-342006; cleavage at carbamate) and M26 (E5, GS-341842; dealkylation at urea) showed substantially less inhibition of human CYP3A activity compared to COBI and are thus unlikely to contribute to the pharmacologic effect. These metabolites also show no ability to inhibit other drug metabolizing cytochromes P450. Metabolite M31 (E3, GS-364751; oxidation of isopropylthiazole) is an inhibitor of human CYP3A activity, but somewhat weaker than COBI. M31 is also a more potent inhibitor of CYP2C19 and CYP2D6 activities. The contribution of M31 to the pharmacologic effect of COBI and the potential to cause drug interactions through inhibition of CYP2D6 activity is unlikely to be significant as circulating concentrations of this metabolite are very low.

Table 67. Inhibition of Human Cytochromes P450 by COBI and Human Metabolites

Enzyme	Activity	Calculated IC_{50} (μM)			
		COBI	GS-342006 (M21)	GS-364751 (M31)	GS-341842 (M26)
CYP1A2	Ethoxyresorufin O-deethylase	> 25	> 25	> 25	> 25
CYP2C9	Tolbutamide hydroxylase	> 25	> 25	> 25	> 25
CYP2C19	(S) Mephenytoin 4'-hydroxylase	> 25	> 25	2.95	> 25
CYP2D6	Dextromethorphan O-demethylase	9.17	> 5	0.21	> 5
CYP3A	Midazolam 1'-hydroxylase	0.154	2.41	0.179	0.23
	Testosterone 6β-hydroxylase	0.151	> 5	0.287	0.71
	Terfenadine oxidase	0.25	> 25	1.85	> 25

COBI = cobicistat; CYP = cytochrome P450 enzyme; IC_{50} = concentration at which 50% maximum inhibition is achieved
Source: Report AD-216-2041

7.2.1.4. In Vitro Assessment of Human UGT1A1 Inhibition Potential of COBI

The potential for COBI to inhibit the catalytic activity of human UGT1A1 was evaluated (Tabulated Summary 2.6.5.12.8, AD-216-2075). The rates of formation of β-estradiol-3-glucuronide from β-estradiol substrate by hepatic microsomal fractions were determined in the presence and absence of COBI and IC_{50} values were determined where possible. Ritonavir and ATV were used as comparators. Cobicistat was a weak inhibitor of human UGT1A1 activity, being 19.6-fold less potent than the positive control, ATV, and 3.4-fold less potent than RTV.

Table 68. IC_{50} Values for Human Hepatic Microsomal UGT1A1 Activity for COBI, RTV, and ATV (mean, n = 3)

Enzyme	Activity	Calculated IC_{50} (μM)		
		ATV	COBI	RTV
UGT1A1	β-Estradiol-3-glucuronidation	0.83	16.3	4.73

ATV = atazanavir; COBI = cobicistat; RTV = ritonavir; UGT = uridine diphosphate glucuronosyl transferase
Source: Report No. AD-216-2075

7.2.2. COBI: Enzymology of Metabolism

The rates of metabolism of COBI and RTV were determined by incubating the compounds with cDNA expressed human CYP enzyme preparations coexpressed with human NADPH cytochrome P450 reductase (Tabulated Summary 2.6.5.10.8, AD-216-2025). Cobicistat was a substrate for CYP2D6 and CYP3A4, but there was no significant

metabolism by the other 3 enzymes tested. Ritonavir was also metabolized by CYP2D6 and CYP3A4 and there was also detectable metabolism by CYP2C19 (Table 69). The apparent slow rates of metabolism of COBI and RTV by CYP3A4 are likely due to self-limiting inhibition during the incubation.

Table 69. Rates of Metabolism of COBI and RTV Catalyzed by Major Human Cytochrome P450 Enzymes (min^{-1} pmol $P450^{-1}$)

Compound	CYP1A2	CYP2C9	CYP2C19	CYP2D6	CYP3A4
COBI (% Positive Control)	0.0 (0.0%)	0.0 (0.0%)	0.0 (0.0%)	0.105 (22.5%)	0.003 (4.5%)
RTV (% Positive Control)	0.001 (0.2%)	0.001 (0.2%)	0.003 (8.6%)	0.139 (29.8%)	0.004 (6.0%)
Ethoxycoumarin	0.407	—	—	—	—
Diclofenac	—	0.467	—	—	—
Diazepam	—	—	0.035[a]	—	—
Dextromethorphan	—	—	—	0.467	—
Testosterone	—	—	—	—	0.066

COBI = cobicistat; CYP = cytochrome P450 enzyme; RTV = ritonavir

a Diazepam is a selective substrate for CYP2C19 but is metabolized relatively slowly

Source: Report AD-216-2025

7.2.3. COBI: Assessment of Induction Liability

7.2.3.1. Xenobiotic Receptor Activation by COBI

The potential for COBI to induce human drug metabolizing enzymes and transporters through activation of the human AhR or the human PXR was initially evaluated by receptor transactivation analysis (Tabulated Summary 2.6.5.12.9, AD-216-2027). The studies were performed using human hepatoma cell lines transfected with expression vectors for the receptors and containing the promoter of an appropriate responsive gene linked to firefly luciferase as a reporter gene. The cell lines were DRE, expressing AhR and with the human CYP1A2 promoter and DPX2 (PXR with CYP3A4 promoter).

At concentrations up to 10 μM, neither COBI nor RTV showed significant activation of AhR (Table 70). In contrast, RTV showed significant activation of PXR (10-fold at 10 μM), while COBI was much weaker (2.2-fold at 10 μM; Table 71). Cobicistat is therefore expected to have little liability to cause clinically relevant drug-drug interactions through PXR activation and is very unlikely to activate AhR at clinically used doses. The lack of efficacy at human PXR was species specific as COBI, like RTV, was found to activate rat PXR in a cell-based system (Section 7.2.3.3).

Table 70. Activation of Human Aryl Hydrocarbon Receptor (AhR) by COBI, RTV, or Positive Control Compounds

Concentration	Fold Induction over 0.1% DMSO Control[a]			
	Test Compounds		Positive controls	
	COBI	RTV	β-Naphthoflavone	Omeprazole
0.1 μM	—	—	2.17	—
1 μM	1.12	0.80	5.91	—
3 μM	1.28	0.69	—	—
5 μM	—	—	17.72	—
10 μM	1.60	0.80	27.31	—
25 μM	—	—	—	8.16
50 μM	—	—	—	13.46
100 μM	—	—	—	27.34
200 μM	—	—	—	67.33

COBI = cobicistat; RTV = ritonavir

a Fold activation of human CYP1A2 promoter after 24 hours incubation at the indicated extracellular concentration

Source: Report AD-216-2027

Table 71. Activation of the Human Pregnane X Receptor (PXR) by COBI, RTV, and Positive Control Compounds

Concentration	Fold Induction Over 0.1% DMSO Control[a]				
	COBI	RTV	Rifampin	Mifepristone	Androstanol
0.3 μM	—	—	3.15	—	—
1 μM	1.57	3.64	6.09	—	—
3 μM	1.61	7.62	9.90	—	—
10 μM	2.24	10.14	14.30	8.58	3.38

COBI = cobicistat; PXR = pregnane X receptor; RTV = ritonavir

a Fold activation of CYP3A4 promoter after 24 hours incubation at the indicated extracellular concentration.

Source: Report AD-216-2027

7.2.3.2. In Vitro Assessment of the Induction Potential of COBI in Primary Cultures of Human Hepatocytes

The potential of COBI to induce drug metabolizing enzymes and transporters was further evaluated in primary cultures of human hepatocytes (Tabulated Summary 2.6.5.12.10, AD-216-2071). Cobicistat (1, 3, 10, and 30 μM) and known inducers (3-methylcholanthrene, phenobarbital, and rifampicin) were incubated in cultures of human hepatocytes from 3 separate donors for 3 consecutive days. The activities of CYP1A2, CYP2B6, and CYP3A were determined using selective metabolite markers (CYP1A2-catalyzed acetaminophen

formation from phenacetin; CYP2B6-catalyzed hydroxybupropion formation from bupropion; and CYP3A-catalyzed 6β-hydroxytestosterone from testosterone; summarized in Table 72). Other endpoints assessed were mRNA expression levels for CYP1A2, CYP2B6, CYP3A4, UGT1A1, and MDR1 (summarized in Table 73) and immunodetectable CYP3A protein (illustrated in Figure 12). Full results for this study are provided in the Tabulated Summary 2.6.5.12.10.

Cobicistat was not cytotoxic to hepatocytes at concentrations up to 30 μM. No clear concentration-related increases of CYP1A2, CYP2B6, or CYP3A enzyme activity were observed with any of the concentrations of COBI examined in any of the human donor preparations. Maximal increases in enzyme activity in individual donors were 4.2%, 20.5%, and 8.2% of the positive controls for CYP1A2, CYP2B6, and CYP3A, respectively (Tabulated Summary 2.6.5.12.10). For CYP3A activity, most activities were below those of the vehicle control, likely due to enzyme inactivation. The lack of response of CYP1A2, a sensitive marker for AhR activation, and CYP2B6, a sensitive marker for CAR activation, was confirmed at the mRNA level. The mRNA expression for CYP3A4, a sensitive marker for PXR activation, was increased weakly in a concentration-dependent manner, reaching an average of 27.4% of the positive control at 10 μM COBI. Immunodetectable CYP3A protein was also increased in a concentration-dependent manner. Secondary markers for PXR activation, UGT1A1 and MDR1 mRNA expression, were increased only at high concentrations of COBI (MDR1) in a hepatocyte donor-dependent manner (UGT1A1).

Collectively these data corroborate the analyses performed by xenobiotic receptor transactivation analysis (Section 7.2.3.1): COBI does not activate human AhR and is a very weak activator of human PXR. At plasma concentrations found in humans, COBI would be expected to have no effect on the expression of secondary targets of PXR, such as CYP2C9, CYP2C19, UGT1A1, and MDR1, and would have very little effect on the expression of CYP3A4 mRNA. Any effect on CYP3A enzyme activity would be masked by mechanism-based inhibition.

Table 72. Summary of Changes in Enzyme Activity After Treatment of Primary Human Hepatocytes with COBI or Positive Controls (Mean ± SD, N = 3)

Treatment	Conc. (µM)	CYP1A2 Phenacetin O-deethylase		CYP2B6 Bupropion 4-hydroxylase		CYP3A Testosterone 6β-hydroxylase	
		Fold change[a]	%Max[b]	Fold change[a]	%Max[b]	Fold change[a]	%Max[b]
3-Methylcholanthrene	2	53.5 ± 44.6[c]	100%	1.3 ± 0.4	3.2%	1.3 ± 0.8	0.2%
Phenobarbital	1000	2.8 ± 1.9	2.2%	10.6 ± 6.1[c]	100%	14.1 ± 6.1	69.6%
Rifampicin	10	2.2 ± 1.5	0.9%	5.7 ± 1.4	57.6%	19.6 ± 8[c]	100%
COBI	1	0.8 ± 0.7	-1.9%	1.4 ± 0.4	4.9%	0.7 ± 0.3	-2.8%
	3	0.8 ± 0.5	-1.7%	1.5 ± 0.9	3.6%	0.7 ± 0.3	-2.7%
	10	1.7 ± 1	0.5%	1.9 ± 1	7%	0.7 ± 0.3	-2.5%
	30	1.7 ± 1	1.1%	1.6 ± 0.4	8.9%	1.3 ± 1.3	0.2%

COBI = cobicistat; CYP = cytochrome P450 enzyme

a Fold increase in enzyme activity compared to cells treated with 0.1% (v/v) DMSO vehicle control

b Change in enzyme activity as a fraction of that achieved by the positive control

c Positive control for this activity

Table 73. Summary of Changes in mRNA Content After Treatment of Primary Human Hepatocytes with COBI or Positive Controls (Mean ± SD, N = 3)

Treatment		CYP1A2		CYP2B6		CYP3A4		UGT1A1		MDR1	
	Conc. (µM)	Fold change[a]	%Max[b]	Fold change[a]	%Max[b]	Fold change[a]	%Max[b]	Fold change[a]	%Max[b]	Fold change[a]	%Max[b]
3MC	2	457 ± 93.6[c]	100%	1.7 ± 1.2	1.1%	0.3 ± 0.2	–1.7%	8.5 ± 4.1	101.6%	0.7 ± 0.1	–29.9%
Phenobarbital	1000	1.9 ± 0.5	0.2%	41.3 ± 27[c]	100%	29.8 ± 16.6	62.8%	10 ± 4.9	119.3%	2.1 ± 0.2	98.2%
Rifampicin	10	1.4 ± 0.4	0.1%	17 ± 6.4	50.4%	45.9 ± 25[c]	100%	8.3 ± 3.6[c]	100%	2.1 ± 0.2[c]	100%
COBI	1	1.1 ± 0.2	0%	1.3 ± 0.5	2.1%	5.3 ± 1.8	10.5%	1.4 ± 0.4	6.5%	0.8 ± 0.2	–16.9%
	3	1.1 ± 0.6	0%	1.7 ± 0.7	4.6%	11 ± 2.7	24.9%	1.7 ± 0.5	10.5%	0.9 ± 0.2	–6%
	10	3 ± 1.7	0.4%	1.4 ± 0.5	3%	12.6 ± 4.7	27.4%	1.6 ± 0.6	9.7%	1 ± 0.1	3.4%
	30	10.1 ± 3.3	2%	0.4 ± 0.1	-2.9%	4.4 ± 3.5	8.6%	1.1 ± 0.6	0%	1.3 ± 0.2	28.7%

3MC = 3-methylcholanthrene; COBI = cobicistat; CYP = cytochrome P450 enzyme

a Fold increase in mRNA expression compared to cells treated with 0.1% (v/v) DMSO vehicle control

b Change in mRNA expression as a fraction of that achieved by the positive control

c Positive control for this activity

Figure 12. CYP3A Western Immunoblotting of Primary Human Hepatocytes after Treatment with COBI or Positive Control Inducers

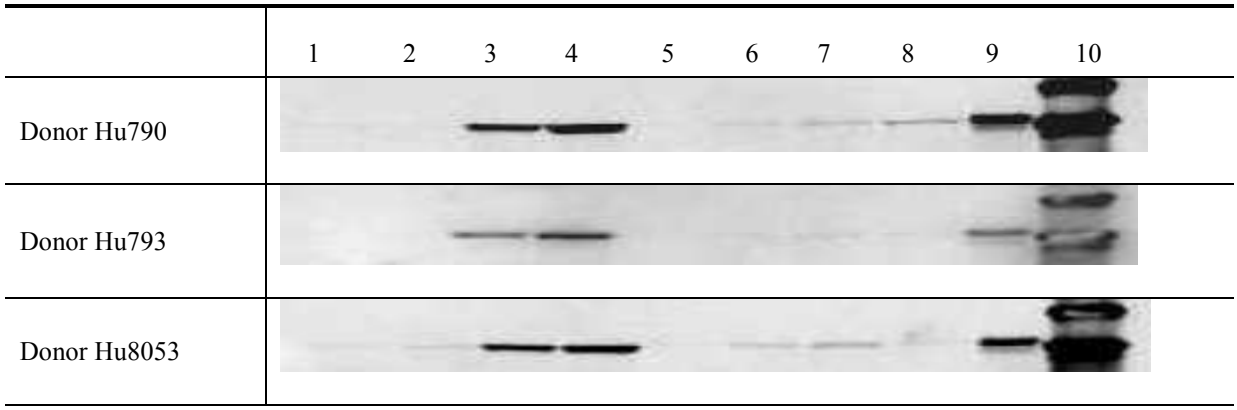

Treatments

1. Dimethylsulfoxide vehicle (0.1%)
2. 3-Methylcholanthrene (2 µM)
3 Phenobarbital (1000 µM)
4. Rifampicin (10 µM)
5. COBI (1 µM)
6. COBI (3 µM)
7. COBI (10 µM)
8. COBI (30 µM)
9. CYP3A4 standard
10. Electrophoresis molecular weight standards

7.2.3.3. Induction of Metabolizing Enzymes of Rat by COBI In Vitro

To better understand the changes in microsomal cytochrome P450 levels seen in multiple-dose rodent toxicology studies, the potential for induction of rat drug metabolizing enzymes and transporters through the activation of PXR by COBI was assessed in vitro using a reporter cell line (Tabulated Summary 2.6.5.12.11, AD-216-2039). Table 74 shows the results for the activation of rat PXR by COBI, RTV, and positive control compounds.

Both COBI and RTV activated rat PXR in a concentration-dependent manner, with potencies similar to that of the moderately potent inducer, miconazole. Concentrations of COBI and RTV up to 30 µM had no significant effect on cell viability. At a COBI concentration of 100 µM, the relative viability was reduced to 77% of the 1% (v/v) DMSO vehicle control.

The results suggest that, in contrast to its lack of effect on human PXR (Section 7.2.3.1), COBI has the potential to activate rat PXR and increase the expression of proteins regulated by this receptor, such as rat CYP3A, UGT1A1, and OATP2, in repeat dose toxicology studies (see Section 3.4.2).

Table 74. Rat PXR Activation by COBI, RTV, and Positive Control Inducers

Concentration	Fold Induction Over DMSO Control			
	COBI	RTV	Dexamethasone	Miconazole
1 μM	1.25	1.36	—	—
3 μM	1.5	1.62	—	—
5 μM	—	—	6.54	—
10 μM	5.87	4.94	8.75	5.68
30 μM	5.14	6.53	—	—
100 μM	0.88	1.17	—	—

COBI = cobicistat; RTV = ritonavir
Source: Report AD-216-2039

7.2.3.4. Human AhR and PXR Activation by Metabolites of COBI

The potential for 3 metabolites of COBI to activate human xenobiotic receptors (AhR and PXR) was assessed. None of the compounds activated the receptors at concentrations up to 10 μM (Table 75, Table 76, and Tabulated Summary 2.6.5.12.7, AD-216-2041), suggesting no liability for causing drug-drug interactions through induction of drug metabolizing enzymes or drug transporters.

Table 75. Human PXR Activation by COBI, Metabolites, and Positive Control Inducers

Conc. (μM)	Fold Activation Over 0.1% DMSO Control						
	COBI[a]	GS-342006 (M21)	GS-364751 (M31)	GS-341842 (M26)	Rifampicin	Mifepristone	Androstanol
1	1.57	0.85	0.84	1.38	—	—	—
3	1.61	1.50	0.92	1.17	—	—	—
10	2.24	1.62	1.24	1.42	12.49	7.10	3.67

COBI = cobicistat; PXR = pregnane X receptor
a Data for COBI from Report AD-216-2027 are provided for comparison.
Source: Report AD-216-2041

Table 76. Human AhR Activation by COBI, Metabolites, and Positive Control Inducers

Concentration (µM)	Fold Activation Over 0.1% DMSO Control				
	COBI[a]	GS-342006 (M21)	GS-364751 (M31)	GS-341842 (M26)	Omeprazole
1	1.12	0.86	0.93	0.81	-
3	1.28	0.83	0.84	0.75	-
10	1.60	0.83	0.76	0.68	-
25	-	-	-	-	5.94
50	-	-	-	-	13.83
100	-	-	-	-	32.74
200	-	-	-	-	52.45

AhR = aryl hydrocarbon receptor; COBI = cobicistat

a Data for COBI from Report AD-216-2027 are provided for comparison.

Source: Report AD-216-2041

7.2.4. COBI: Interactions with Transporters

7.2.4.1. Inhibition of Individual Recombinant Expressed Human Drug Transporters

The potential for COBI to inhibit human drug transporters was assessed in cell lines or vesicles expressing individual recombinant proteins. Transporters tested, and their respective positive control inhibitors, were MDR1 (20 µM verapamil), MRP1 (100 µM caffeic acid phenethyl ester), MRP2 (100 µM MK571), MRP4 (150 µM MK571), BCRP (2 µM fumitremorgin C), OAT1 (200 µM benzbromarone), OAT3 (200 µM probenecid), OCT2 (100 µM verapamil), OCTN1 (100 µM verapamil), MATE1 (10 µM cimetidine), MATE2-K (100 µM cimetidine), OATP1B1 (50 µM rifampicin), and OATP1B3 (50 µM rifampicin). The data are summarized in Table 77.

All positive control inhibitors reduced transport of their respective substrates, confirming the sensitivities of the cell lines to inhibition. Cobicistat showed negligible or weak inhibition of the efflux transporters MDR1, MRP1, MRP2, MRP4, BCRP, and MATE2-K, and the renal uptake transporters OAT1 and OAT3. Cobicistat is a weak inhibitor of the renal uptake transporter, OCT2 (unbound $C_{max}/IC_{50} = 0.01$), and a more potent inhibitor of the hepatic uptake transporters OATP1B1 and OATP1B3 ($[I]_1/IC_{50}$ 0.4 and 0.7, respectively), and the renal efflux transporters OCTN1 and MATE1 (unbound C_{max}/IC_{50} 0.04 and 0.05, respectively). Inhibition of OATP transporters is consistent with a clinical drug interaction study (Module 2.7.2, Section 2.5.2.2.3 [GS-US-216-0123]) in which, after dosing with 150 mg COBI and 150 mg EVG, there was a modest increase in exposure of co-dosed rosuvastatin ($AUC_{0-\infty}$ increased 38% compared to the reference treatment). Inhibition of MDR1 and BCRP activity is discussed in more detail in Section 7.2.4.2.

Table 77. Effects of COBI and RTV on the Activities of Human Transporters

Transporter	Cell line	Substrate (concentration)	IC_{50} (µM)		Tabulated Summary (Report)
			COBI	RTV	
MDR1	MDCK II	calcein AM (10 µM)	22.5 – 45.0[a]	10.0 – 20.0[a]	2.6.5.15.9 (AD-216-2030)
MRP1	MDCK II	calcein AM (10 µM)	45.0 – 90.0[a]	10.0 – 20.0[a]	
MRP2	MDCK II	calcein[b]	45.0 – 90.0[a]	> 20[d]	
MRP4	LLC-PK1[c]	DHEAS (0.02 µM)	20.7	> 20[d]	2.6.5.15.16 (AD-216-2105)
BCRP	MDCK II	Hoechst 33342 (10 µM)	59.0	> 20[d]	2.6.5.15.10 (AD-216-2099)
OAT1	CHO	p-aminohippurate (5 µM)	> 100[d]	> 20[d]	2.6.5.15.15 (AD-216-2105)
OAT3	HEK293	estrone 3-sulfate (0.2 µM)	> 100[d]	8.46	
OCT2	CHO	metformin (2 µM)	8.24	22.6	2.6.5.15.12 (AD-216-2093)
OCTN1	S_2	tetraethylammonium (5 µM)	2.49	2.08	2.6.5.15.14 (AD-216-2098)
MATE1	HEK293	tetraethylammonium (5 µM)	1.87	1.34	2.6.5.15.13 (AD-216-2094)
MATE2-K	HEK293	tetraethylammonium (5 µM)	33.5	100	
OATP1B1	CHO	Fluo 3 (2 µM)	3.50	2.05	2.6.5.15.11 (AD-216-2100)
OATP1B3	CHO	Fluo 3 (2 µM)	1.88	1.83	

AM = acetomethoxy ester; BCRP = breast cancer resistance protein; COBI = cobicistat; DHEAS = 5-dehydroepiandrosterone sulfate; MATE1 = multidrug and toxin extrusion protein 1 (SLC47A1); MATE2-K = multidrug and toxin extrusion protein 2-K (SLC47A2); MDR1 = P-glycoprotein (multidrug resistance protein 1); MRP = multi-drug resistance-associated protein; OAT = organic anion transporter; OATP = organic anion transporting polypeptide; OCT2 = organic cation transporter 2; OCTN1 = organic cation transporter N1; RTV = ritonavir

a Range of tested concentrations bracketing 50% inhibition (IC_{50} not calculated)

b Generated from 10 µM calcein AM

c Study performed with vesicles derived from the cell line

d Maximum concentration tested

7.2.4.2. Inhibition of Bidirectional Transport of MDR1 and BCRP Substrates Through Caco-2 Cell Monolayers

The potential for inhibition of intestinal MDR1 or BCRP by COBI was assessed by determining its effects on the bidirectional transport of the selective substrates, digoxin and prazosin, respectively (Tabulated Summaries 2.6.5.15.6 and 2.6.5.15.7, AD-216-2072 and AD-216-2104, respectively). As summarized in Table 78, a high concentration (90 µM) of COBI reduced the efflux of digoxin to the same extent as the selective MDR1 inhibitor, cyclosporine A, and another known inhibitor, RTV. Similarly, as summarized in Table 79,

the high concentration (90 μM) of COBI reduced the polarized transport of the BCRP substrate, prazosin, through Caco-2 cells. This suggests that high concentrations of COBI, such as those present in the intestinal lumen during drug absorption, could inhibit intestinal MDR1 and BCRP ($[I]_2/IC_{50} > 10$). However, as demonstrated above (Section 7.2.4.1), COBI is a weak inhibitor of both of these transporters and so would have not be expected to have any effect systemically at concentrations achievable in plasma ($[I]_1/IC_{50} < 0.1$). The result with MDR1 is consistent with a clinical drug interaction study (Module 2.7.2, Section 2.3.2.2.3 [GS-US-216-0112]) in which COBI was found to increase the C_{max} of co-dosed digoxin (41% increase compared to the reference), but to have less effect on the area under the curve (7.7% increase in $AUC_{0-\infty}$ compared to the reference), suggesting the effect was limited to transient inhibition of intestinal MDR1 activity.

Table 78. Bidirectional Permeability of Digoxin Through Caco-2 Cells In the Presence of Known MDR1 Inhibitors and COBI

Inhibitor (Concentration)	Direction	Digoxin P_{app} (10^{-6} cm/s)	Efflux Ratio
None	Cell-Free	38.5	7.72
	Forward	1.30	
	Reverse	10.0	
Cyclosporin A (10 μM)	Cell-Free	47.0	1.68
	Forward	2.25	
	Reverse	3.78	
RTV (20 μM)	Cell-Free	45.6	1.84
	Forward	3.17	
	Reverse	5.81	
COBI (90 μM)	Cell-Free	51.1	1.69
	Forward	2.24	
	Reverse	3.80	

COBI = cobicistat; RTV = ritonavir
Source: Report AD-216-2072

Table 79. Bidirectional Permeability of Prazosin Through Caco-2 Cells In the Presence of RTV or COBI

Inhibitor (Concentration)	Direction	Prazosin P_{app} (10^{-6} cm/s)	Efflux Ratio
None	Cell-Free	36.94	5.1
	Forward	2.50	
	Reverse	12.78	
Fumitremorgin C (2 μM)	Cell-Free	46.75	2.6
	Forward	4.44	
	Reverse	11.58	
RTV (20 μM)	Cell-Free	39.87	2.8
	Forward	4.00	
	Reverse	11.26	
COBI (90 μM)	Cell-Free	38.33	2.4
	Forward	4.74	
	Reverse	11.20	

COBI = cobicistat; RTV = ritonavir
Source: Report AD-216-2104

7.2.4.3. Potential for COBI to be a Substrate for Human OCT2

An attempt was made to determine if COBI and RTV are substrates for the human renal uptake transporter, OCT2 (Tabulated Summary 2.6.5.13.7, AD-216-2095). [^{14}C]COBI or [^{3}H]RTV were incubated with either wild type CHO-K1 cells or CHO-OCT2 cells expressing human OCT2 and the concentration-dependence and time-dependence of accumulation determined. The effects of an OCT2 inhibitor (100 μM verapamil) were also assessed.

The positive control OCT2 substrate, metformin (2 μM), showed 36-fold higher relative accumulation in OCT2-expressing cells compared to wild type cells, and this was almost completely inhibited by verapamil. In contrast to metformin, both COBI and RTV showed high accumulation in wild type cells. Maximum relative accumulation of COBI and RTV was 1.4-fold and 2.0-fold, respectively, and this was relatively insensitive to inhibition by verapamil. Thus, since both COBI and RTV showed rapid OCT2-independent uptake, it was not possible to determine a role for OCT2 in their cellular uptake using this system.

7.2.4.4. Potential for COBI to be a Substrate for Human MDR1 or BCRP

The potential for COBI to be a substrate for human MDR1 or human BCRP was assessed in MDCK II cells expressing those transporters (Tabulated Summary 2.6.5.15.8, AD-216-2103). The efflux ratio for COBI in MDR1-transfected cells (Table 80) and BCRP-transfected cells (Table 81) was higher (16-fold and 1.9-fold, respectively) than in the corresponding wild type cells, suggesting that COBI can act as a substrate for these

transporters. As further confirmation, the efflux in transfected cells could be reduced by selective inhibitors of each transporter. The actual role of these transporters in the disposition of COBI is difficult to determine because, as shown above (Section 3.2), COBI shows high cellular permeability in Caco-2 cells, resulting in relatively little polarized transport.

Table 80. Bidirectional Permeability of COBI Through Wild Type and MDR1-Transfected MDCK II Cells

Cell type (Inhibitor)	Direction	Initial Conc. (µM)	Recovery (%)	P_{app} (x 10^{-6} cm/s)	Efflux Ratio
MDCK II-WT (No inhibitor)	Cell-Free	9.85	110.12	28.88	3.7
	Forward	10.18	81.81	3.26	
	Reverse	10.06	97.65	12.19	
MDCK II-MDR1 (No inhibitor)	Cell-Free	10.19	103.94	33.68	60.9
	Forward	10.34	85.84	0.32	
	Reverse	9.72	102.22	19.38	
MDCKII-MDR1 (10 µM Cyclosporin A)	Cell-Free	11.2	102.90	26.84	3.8
	Forward	11.2	91.24	3.53	
	Reverse	10.1	94.85	13.21	

COBI = cobicistat; MDR1 = P-glycoprotein (multidrug resistance protein 1); WT = wild-type
Source: Report AD-216-2103

Table 81. Bidirectional Permeability of COBI Through Wild Type and BCRP-Transfected MDCK II Cells

Cell type (Inhibitor)	Direction	Initial Conc. (µM)	Recovery (%)	P_{app} (x 10^{-6} cm/s)	Efflux Ratio
MDCKII-WT (No inhibitor)	Cell-Free	9.49	100.66	30.35	7.0
	Forward	9.35	78.66	1.99	
	Reverse	8.60	102.55	14.03	
MDCKII-BCRP (No inhibitor)	Cell-Free	9.15	96.97	26.81	13.4
	Forward	9.29	79.49	1.52	
	Reverse	8.43	110.12	20.33	
MDCKII-BCRP (10 µM Ko134)	Cell-Free	8.90	102.29	31.72	3.2
	Forward	9.12	76.97	3.79	
	Reverse	9.14	87.59	11.94	

BCRP = breast cancer resistance protein; COBI = cobicistat; WT = wild-type
Source: Report AD-216-2103

7.3. EVG/COBI/FTC/TDF: Pharmacokinetic Drug Interactions

For the EVG/COBI/FTC/TDF STR, the clinical pharmacokinetic interaction studies with the components should be given the greatest consideration. Full details are described in Modules 2.5 and 2.7.2.

Neither FTC, TDF, nor TFV interact with drug metabolizing enzymes as substrates, inhibitors, or inducers (oxidative metabolism of FTC plays only a minor role in the elimination of the compound) and so will not take part in metabolic drug interactions with EVG or COBI. As described above (Section 5.4), TFV and FTC do not inhibit each other's pharmacological activation through phosphorylation. Cobicistat does not inhibit OAT1 or OAT3, and is a very weak inhibitor of MRP4, and so should not affect the renal elimination of TFV. While COBI is a weak inhibitor of OCT2 and a more potent inhibitor of MATE1, TFV is not an inhibitor of either transporter (Module 1.4.4, AD-104-2012) so there should be no further decrease in activity of the transporters when the 2 drugs are combined. Cobicistat is a weak inhibitor of intestinal efflux transporters, but high concentrations of COBI in the intestinal lumen, achievable briefly during absorption, may inhibit MDR1 and result in a modest increase in TFV exposure (as seen with HIV-PIs {11255}). While both EVG and COBI are inhibitors of OATP transporters in vitro, only a modest increase in exposure (not considered clinically relevant) of the OATP substrate, rosuvastatin, was observed when it was co-dosed with both EVG and COBI (Module 2.7.2, Section 2.5.2.2.3 [GS-US-216-0123]). Thus, the intended positive drug interaction within the 4-drug combination is the pharmacokinetic enhancement of EVG by COBI, due to inhibition of the oxidative metabolism of EVG.

8. OTHER PHARMACOKINETIC STUDIES

There are no additional studies to report.

9. DISCUSSION AND CONCLUSIONS

Elvitegravir, COBI, FTC, and TDF have been assessed individually in comprehensive nonclinical pharmacokinetic studies.

Results from pharmacokinetic studies of EVG, COBI, and the EVG/COBI/FTC/TDF STR are summarized below.

9.1. EVG

EVG shows moderate oral bioavailability in rats and dogs with values similar in fasted and non-fasted animals. From studies with [^{14}C]EVG this likely reflects moderate absorption of EVG and modest first-pass elimination. Studies in vitro also showed EVG to have modest permeability in LLC-PK1 cell monolayers. Elvitegravir was subject to polarized efflux in MDR1-expressing cells but in clinical studies, with co-administration of EVG with known inhibitors or inducers of MDR1, there were no clinically meaningful interactions attributable to effects on MDR1.

The volume of distribution of EVG in rats and dogs was 0.4 and 2.6 L/kg, respectively, with respect to plasma. The lower volume in the rat likely reflects a lower free fraction in plasma and a lower whole blood/plasma ratio. Plasma protein binding was high in all species and showed no clear concentration dependence. In humans the unbound fraction in plasma was 0.6% to 0.7%. The same fraction was found for binding to a physiological concentration of purified HSA and this was unaffected by AAG suggesting that albumin is the major binding protein for EVG in human plasma. Similar binding was found in ex vivo clinical plasma samples. For humans, the whole blood/plasma ratio for EVG was 0.7, reflecting modest distribution into the cellular components of human blood.

Following oral administration of [^{14}C]EVG to rats, radioactivity was rapidly and widely distributed. Tissue/plasma concentration ratios were > 1 for the liver and GI tract, but were in the range 0.2 to 0.5 in most other tissues. Radioactivity was largely excluded from the CNS and eye. Tissue concentrations of radioactivity declined largely in parallel with those in plasma, with almost complete elimination by 96 hours postdose (trace amounts remained in the intestinal contents). Treatment of rats with RTV had no effect on the exclusion of [^{14}C]EVG-derived radioactivity from the CNS.

Elvitegravir is metabolized extensively in rats and dogs by oxidation and glucuronidation. In samples from rats and dogs in vivo, and in samples from hepatic microsomal fractions from a variety of species, the majority of the biotransformation can be accounted for by 8 metabolites (M1 – M8). The most abundant metabolite is M1 (GS-9202, p-hydroxylated-EVG), with lesser amounts of M4 (GS-9200, EVG acyl glucuronide) and M7 (JTP-74488, M1 glucuronide), but parent EVG is the most abundant component circulating in plasma. In bile from rats dosed with [^{14}C]EVG, the majority of the radiolabel was associated with glucuronide metabolites. However, in rat and dog feces from animals dosed with [^{14}C]EVG, the majority of the radioactivity was accounted for by EVG and oxidative metabolites, suggesting that biliary conjugates were cleaved in the intestine.

The excretion of radioactivity, following intravenous or oral administration of [^{14}C]EVG, was studied in rats and dogs. Recoveries of dosed radioactivity in excreta were high (97.6% to 100.0% collected 2 to 7 days postdose). Excretion in bile and feces were the major routes with ≤ 1% excreted in the urine. In all cases, excretion of radioactivity was largely complete by 48 hours postdose. There was low potential for enterohepatic recirculation of radioactivity following biliary excretion in rats, as intraduodenal administration of pooled bile to naïve bile duct-cannulated rats resulted in only 5.9% of the radioactivity being recovered in freshly excreted bile.

Low levels of EVG were excreted in rat milk, in proportion to plasma concentrations. The major oxidative metabolite (M1, GS-9202) and the acyl glucuronide metabolite (M4, GS-9200) were not detected in milk, despite being detected in the plasma of the lactating rats.

The liability for EVG being involved in pharmacokinetic drug-drug interactions was assessed in vitro. There was no detectable inhibition of human hepatic microsomal CYP1A2, CYP2A6, CYP2C9, CYP2C19, CYP2D6, or CYP2E1 activity by EVG (IC_{50} > 30 μg/mL). There was weak inhibition of the CYP3A-catalyzed activity, testosterone 6β-hydroxylase (IC_{50} 28.32 μg/mL or 63 μM). Elvitegravir was a weak inhibitor (IC_{50} > 30 μM) of the polarized transport of digoxin across cells expressing human MDR1. Elvitegravir was a weak inhibitor of the activity of the human uptake transporter, OATP1B1 (IC_{50} > 2 μM), but was a more potent inhibitor of human OATP1B3 (IC_{50} 0.44 μM). From these data, EVG is predicted to have very low liability to cause drug interactions through inhibition of human cytochromes P450 or MDR1. Inhibition of OATP transporters is consistent with a clinical drug interaction study (see Module 2.7.2, Section 2.5.2.2.3) in which, after dosing with 150 mg EVG and 150 mg COBI, there was a modest increase (38%) in exposure of co-dosed rosuvastatin that was not considered clinically relevant.

In primary human hepatocytes, EVG did not induce CYP1A2 at concentrations up to 10 μg/mL (22 μM). At a concentration of 1 μg/mL (2.2 μM), EVG induced CYP3A activity by an average of 18.9% relative to the positive control. This increased to an average of 46.8% at 10 μg/mL EVG. This suggests that, at expected clinical exposures, EVG would not cause drug interactions through induction of CYP1A2, but would be a weak inducer of CYP3A activity. Since EVG is intended to be coadministered with CYP3A-inhibiting pharmacokinetic enhancers, such as COBI or RTV, any increases in CYP3A expression by EVG would likely be masked and hence not clinically significant.

Studies with recombinant human cytochromes P450 and enzyme-selective inhibitors revealed that CYP3A enzymes (primarily CYP3A4) are responsible for the oxidative metabolism of EVG and yield a metabolite profile similar to that generated by human hepatic microsomal fraction. When selected potential comedications were assessed for their effects on the oxidation of EVG by human hepatic microsomal fraction, those known to interact with human CYP3A enzymes had the greatest inhibitory effects. No effect was seen by EFV (IC_{50} > 50 μM), NVP (IC_{50} > 50 μM), or ZDV (IC_{50} > 100 μM) which do not interact strongly with human CYP3A enzymes. Inhibitors of CYP3A enzymes would be expected to cause drug interactions with EVG when dosed alone. However, since EVG is intended to be

coadministered with pharmacokinetic enhancers that are potent CYP3A inhibitors, any further incremental increase in CYP3A inhibition is likely to be low.

The rates of formation of GS-9200 (the acyl glucuronide metabolite, M4) from EVG, were determined with 12 recombinant human UGTs. Only UGT1A1 and UGT1A3 showed appreciable rates of metabolism. The formation of GS-9200 catalyzed by human hepatic microsomal fraction, was potently and extensively inhibited by ATV, a selective UGT1A1 inhibitor. Thus other clinical UGT1A1 inhibitors may affect the glucuronidation of EVG in vivo.

9.2. COBI

Estimates of fraction absorbed in vivo, derived from bioavailability corrected for predicted first-pass metabolism, or from recovery of radiolabel in bile or urine, are all > 50%. After moderate doses, oral bioavailability in nonclinical species is low due to metabolic instability and resulting high first-pass elimination. Cobicistat can act as a substrate for MDR1 and BCRP intestinal efflux transporters, but this likely does not play a significant role during its absorption as COBI has high passive permeability, as demonstrated in Caco-2 cells.

Cobicistat shows moderately high plasma binding. After oral dosing with [^{14}C]COBI, radioactivity is widely distributed, and volumes of distribution of COBI are close to those for body water. Cobicistat is relatively excluded from the cellular fraction of blood (whole blood to plasma ratios are ~0.6) and from brain, testes, and the eye. Exclusion from the brain may be due to the action of MDR1 and/or BCRP at the blood:brain barrier. Cobicistat shows preferential binding in melanin-containing tissues, but this is reversible.

Interpreting the metabolism of COBI is complicated by concurrent mechanism-based inhibition of human CYP3A enzymes. This attribute is species-specific, as COBI shows high clearance in nonclinical species due to a lack of self-inhibition of metabolism. The primary routes of metabolism of COBI are oxidation by CYP3A (major) and CYP2D6 (minor) enzymes. Metabolites M21, M26, and M31 were identified in mouse, rat, dog, and human samples in vitro, and were later identified in excreta from these species. One other primary metabolite, M39, was also identified in all species in vivo. Other metabolites arise from secondary metabolism, due to combinations of these primary pathways, and from other minor primary metabolites. Parent COBI is the major component circulating in plasma in all species.

After oral dosing of mice, rats, dogs, and humans with [^{14}C]COBI, the majority of radiolabel is recovered in the feces or bile with little in the urine. Total recovery of radiolabel is high for all species. Excretion of COBI into milk was detected in rats.

The intended pharmacologic action of COBI is inhibition of human CYP3A enzymes. In that regard, COBI is a potent mechanism-based inhibitor of human CYP3A and shows activity against a wide range of CYP3A activities. All 3 of the metabolites initially identified (M21, M26, and M31) are weaker inhibitors than COBI and are very unlikely to contribute to the pharmacologic effect, especially considering their low plasma concentrations. Inhibition of human cytochrome P450 enzymes shows high selectivity, with insignificant or very weak inhibition of CYP1A2, CYP2C8, CYP2C9, and CYP2C19, weak inhibition of CYP2D6

(C_{max}/IC_{50} = 0.15), and modest inhibition of CYP2B6 (C_{max}/IC_{50} 0.50). Cobicistat is also a weak inhibitor of human UGT1A1 (C_{max}/IC_{50} = 0.09). In this regard, COBI shows greater selectivity than RTV, which inhibits CYP2C8 and CYP2C9 and is a more potent inhibitor of CYP2D6 and UGT1A1.

At systemic concentrations achieved in plasma, COBI does not inhibit the drug transporters MDR1, MRP1, MRP2, BCRP, OAT1, or OAT3 ($[I]_1/IC_{50} < 0.1$). With respect to renal transporters, COBI is a weak inhibitor of MRP4, MATE2-K and OCT2, and a more potent inhibitor of MATE1 and OCTN1, with similar potencies to RTV.

With respect to hepatic uptake transporters, COBI is a moderate inhibitor of OATP1B1 and OATP1B3 ($[I]_1/IC_{50}$ 0.4 and 0.7, respectively). At high concentrations, achievable briefly in the intestinal lumen during drug absorption, COBI can inhibit intestinal efflux transporters, such as MDR1 and BCRP ($[I]_2/IC_{50} > 10$).

Cobicistat does not activate human AhR and does not induce human CYP1A2 activity or mRNA. Cobicistat is a very weak activator of human PXR, and affects CYP3A4 mRNA and CYP3A immunodetectable protein only at high concentrations. Cobicistat thus has lower liability for drug interactions than RTV, which is a more potent PXR activator. Interestingly, COBI and RTV show similar, moderately potent ability to activate rat PXR, and this is manifest as increased CYP3A activity in hepatic microsomal fraction from rats and mice after repeat dose treatment. Such species differences in PXR activation, caused by differences in the ligand binding domain of the receptor, are well understood {18669}.

In conclusion, COBI is a potent, selective mechanism-based inhibitor of human CYP3A enzymes with low potential for other drug-drug interactions (inhibition of other cytochromes P450, UGT1A1, or drug transporters, and induction of enzymes and transporters).

9.3. EVG/COBI/FTC/TDF

Based on the data supporting the individual components, the extensive clinical data with the FTC/TDF combination within HIV-1 therapy, and the clinical data with EVG and COBI administered with FTC/TDF in Phase 2 and 3 studies, adverse pharmacokinetic interactions that would negatively affect safety or pharmacological efficacy are not anticipated. This is based on the well-characterized routes of elimination demonstrated for each compound and the differences in physicochemical properties between the compounds which influence drug distribution. Pharmacokinetic enhancement of EVG exposure by COBI has been studied in vitro and in humans in vivo. A modest increase in TFV exposure, due to inhibition of intestinal MDR1 by COBI, is predicted in vitro and observed in vivo, and the magnitude is similar to that observed when TDF is co-dosed with RTV-boosted HIV PIs. The combination of co-dosed EVG and COBI has only a modest effect on the exposure of the OATP substrate, rosuvastatin. Cobicistat does not inhibit OAT1 or MRP4, the transporters responsible for the renal excretion of TFV and so will not interfere with the elimination of TFV. Single-dose pharmacokinetic studies in dogs demonstrate that comparable exposures for each component can be achieved through coformulation relative to coadministration of the clinical formulations. Pharmacological activation of FTC and TFV is by phosphorylation by enzymes with highly restricted substrate specificities, so inhibition by EVG or COBI is very unlikely. This is supported in antiviral assays where no evidence for antagonistic interactions was observed.

10. SUMMARY TABLES

Tables and figures have been integrated within the textual summary.

11. REFERENCES

References are available upon request.

11006 Bjornsson TD, Callaghan JT, Einolf HJ, Fischer V, Gan L, Grimm S, et al. The conduct of in vitro and in vivo drug-drug interaction studies: a Pharmaceutical Research and Manufacturers of America (PhRMA) perspective. Drug Metab Dispos 2003;31 (7):815-32.

11255 Tong L, Phan TK, Robinson KL, Babusis D, Strab R, Bhoopathy S, et al. Effects of human immunodeficiency virus protease inhibitors on the intestinal absorption of tenofovir disoproxil fumarate in vitro. Antimicrob Agents Chemother 2007;51 (10):3498-504.

15555 Giacomini KM, Huang SM, Tweedie DJ, Benet LZ, Brouwer KL, Chu X, et al. Membrane transporters in drug development. Nat Rev Drug Discov 2010;9 (3):215-36.

18022 Industry GF. Drug interaction studies - study design, data analysis, and implications for dosing and labeling. US department of health and human services 2006:1-55.

18669 LeCluyse EL. Pregnane X receptor: molecular basis for species differences in CYP3A induction by xenobiotics. Chem Biol Interact 2001;134 (3):283-9.

18670 European Medicines Agency (EMEA). Committee for for Human Medicinal Products (CHMP). Guideline on the investigation of drug interactions [EMA/CHMP/EWP/125211/2010]. April 22, 2010.

2.6 NONCLINICAL SUMMARY

2.6.5—PHARMACOKINETICS TABULATED SUMMARY

ELVITEGRAVIR/COBICISTAT/EMTRICITABINE/TENOFOVIR DISOPROXIL FUMARATE SINGLE TABLET REGIMEN (EVG/COBI/FTC/TDF; QUAD STR)

NDA 203-100

Gilead Sciences

[redacted] 20[redacted]

TABLE OF CONTENTS

NOTE TO REVIEWER

This application is being submitted in support of a New drug Application (NDA) for a film-coated single tablet regimen (STR) that contains the active substances elvitegravir (EVG), cobicistat (COBI), emtricitabine (FTC), and tenofovir disoproxil fumarate (tenofovir DF, TDF). The STR is referred to as elvitegravir/cobicistat/emtricitabine/ tenofovir disoproxil fumarate (EVG/COBI/FTC/TDF) STR throughout this document. As the EVG and COBI components are new chemical entities, [redacted]. Per the agreement reached at the [redacted] 20[redacted] ([redacted]) meeting between Gilead Sciences, Inc. (GSI) and the Food and Drug Administration (FDA; refer to the Agency's comments, dated [redacted] 20[redacted] in Module 1.6.3), [redacted].

2.6.5.1. Pharmacokinetics: Overview

Test Article: EVG and COBI

Type of Study/Description	GLP[a]	Test System	Method of Administration	Testing Facility	Gilead Study No. (CRO Study No.)
Analytical Methods and Validation (EVG)					
Mouse plasma (EVG, GS-9200, GS-9202)	No	NA	In Vitro	[redacted], USA	BA-183-2003 ([redacted]05-197)
Rat plasma (EVG)	No	NA	In Vitro	[redacted], Japan	JTK303-AD-003
Rat plasma (EVG, GS-9200, GS-9202)	No	NA	In Vitro	[redacted], USA	BA-183-2011 ([redacted]06-071)
Rat plasma (EVG, Cobicistat)	No	NA	In Vitro	[redacted], USA	BA-216-2007 ([redacted]08-353)
Rat plasma (RTV)	No	NA	In Vitro	[redacted], USA	BA-183-2012 ([redacted]07-003)
Rat milk (EVG, GS-9200, GS-9202)	No	NA	In Vitro	[redacted], USA	BA-183-2008 ([redacted]06-124)
Dog plasma (EVG)	No	NA	In Vitro	[redacted], Japan	JTK303-AD-004
Analytical Methods and Validation (COBI)					
Mouse plasma (COBI)	No	NA	In Vitro	[redacted], USA	BA-216-2005 (6511-433)

Test Article: EVG and COBI

Type of Study/Description	GLP[a]	Test System	Method of Administration	Testing Facility	Gilead Study No. (CRO Study No.)
Mouse plasma (GS-9612)	No	NA	In Vitro	[redacted], USA	BA-216-2010 (8200-119)
Rat plasma (COBI)	No	NA	In Vitro	[redacted], USA	BA-216-2202 (6511-313)
Rat plasma (COBI, EVG)	No	NA	In Vitro	[redacted], USA	BA-216-2007 ([redacted]08-252)
Rat plasma (GS-9612)	No	NA	In Vitro	[redacted], USA	BA-216-2008 (8200-131)
Rat plasma (ATV)	No	NA	In Vitro	[redacted], USA	BA-216-2006 (6511-447)
Rat milk (COBI)	No	NA	In Vitro	[redacted], USA	BA-216-2013 (8234519)
Rabbit plasma (COBI)	No	NA	In Vitro	[redacted], USA	BA-216-2004 (6511-364)
Dog plasma (COBI)	No	NA	In Vitro	[redacted], USA	BA-216-2003 (6511-314)
Dog plasma (GS-9612)	No	NA	In Vitro	[redacted], USA	BA-216-2009 (8200-115)

Test Article: EVG and COBI

Type of Study/Description	GLP[a]	Test System	Method of Administration	Testing Facility	Gilead Study No. (CRO Study No.)
Absorption (EVG)					
Membrane Permeability and Efflux Potential	No	In Vitro	In Vitro	[redacted], Japan	JTK303-AD-026
Single Dose Pharmacokinetics (Sample Collection and Bioanalysis)	No	Rat	IV, Oral	[redacted], Japan	JTK303-AD-009
Single Dose Pharmacokinetics (Determination of Pharmacokinetic Parameters)				Drug Metabolism & Pharmacokinetics Research Laboratories, Central Pharmaceutical Research Institute, Japan Tobacco Inc., Osaka, Japan	JTK303-AD-011
Single Dose Pharmacokinetics of [^{14}C]EVG (Sample Collection and Bioanalysis)	No	Rat	IV, Oral	[redacted], Japan	JTK303-AD-005
Single Dose Pharmacokinetics of [^{14}C]EVG (Determination of Pharmacokinetic Parameters)				Drug Metabolism & Pharmacokinetics Research Laboratories, Central Pharmaceutical Research Institute, Japan Tobacco Inc., Osaka, Japan	JTK303-AD-007

Test Article: EVG and COBI

Type of Study/Description	GLP[a]	Test System	Method of Administration	Testing Facility	Gilead Study No. (CRO Study No.)
Single Dose Pharmacokinetics (Sample Collection and Bioanalysis)	No	Dog	IV, Oral	[redacted], Japan	JTK303-AD-010
Single Dose Pharmacokinetics (Determination of Pharmacokinetic Parameters)				Drug Metabolism & Pharmacokinetics Research Laboratories, Central Pharmaceutical Research Institute, Japan Tobacco Inc., Osaka, Japan	JTK303-AD-012
Single Dose Pharmacokinetics of [^{14}C]EVG (Sample Collection and Bioanalysis)	No	Dog	IV, Oral	[redacted], Japan	JTK303-AD-006
Single Dose Pharmacokinetics of [^{14}C]EVG (Determination of Pharmacokinetic Parameters)				Drug Metabolism & Pharmacokinetics Research Laboratories, Central Pharmaceutical Research Institute, Japan Tobacco Inc., Osaka, Japan	JTK303-AD-008
Formulation Comparison (Dissolution and Oral Absorption)	No	Dog	Oral	[redacted], Japan	JTK303-P2-102

Test Article: EVG and COBI

Type of Study/Description	GLP[a]	Test System	Method of Administration	Testing Facility	Gilead Study No. (CRO Study No.)
Repeat Dose Pharmacokinetics of [^{14}C]EVG (Sample Collection and Bioanalysis)	No	Rat	Oral	[redacted], Japan	JTK303-AD-022
Repeat Dose Pharmacokinetics of [^{14}C]EVG (Determination of Pharmacokinetic Parameters)				Drug Metabolism & Pharmacokinetics Research Laboratories, Central Pharmaceutical Research Institute, Japan Tobacco Inc., Osaka, Japan	JTK303-AD-028
Absorption (COBI)					
Permeability Across Caco-2 Cell Monolayer	No	In Vitro	In Vitro	[redacted], USA	AD-216-2023
Single Dose Pharmacokinetics	No	Mouse	Oral	[redacted], USA	PC-216-2013-PK (8221867)
Single Dose Pharmacokinetics	No	Rat	IV, Oral	[redacted], USA	AD-216-2020
Single Dose Pharmacokinetics	No	Dog	IV, Oral	[redacted], USA	AD-216-2021
Formulation Comparison	No	Dog	Oral	[redacted], USA	AD-216-2042
Single Dose Pharmacokinetics	No	Cynomolgus Monkey	IV, Oral	[redacted], USA	AD-216-2022 ([redacted] 00302)

Test Article: EVG and COBI

Type of Study/Description	GLP[a]	Test System	Method of Administration	Testing Facility	Gilead Study No. (CRO Study No.)
Absorption After a Single Dose (EVG, COBI, FTC, TDF)					
Formulation Comparison (EVG, COBI, FTC and TDF)	No	Dog	Oral	[redacted], USA	AD-216-2061
Distribution (EVG)					
Plasma Protein Binding	No	In Vitro	In Vitro	Drug Metabolism & Pharmacokinetics Research Laboratories, Central Pharmaceutical Research Institute, Japan Tobacco Inc., Osaka, Japan	JTK303-AD-014
Plasma Protein Binding (Ex Vivo)	No	Mouse	Oral, In Vitro	[redacted], USA	AD-183-2024 (60N-0626)
Distribution into Blood Cells	No	In Vitro	In Vitro	Drug Metabolism & Pharmacokinetics Research Laboratories, Central Pharmaceutical Research Institute, Japan Tobacco Inc., Osaka, Japan	JTK303-AD-013
Tissue Distribution of Radioactivity	No	Rat	IV, Oral	[redacted], Japan	JTK303-AD-005
Tissue Distribution of Radioactivity and Effect of Ritonavir	No	Rat	Oral	[redacted], USA	60N-0518
Tissue Distribution of Radioactivity	No	Dog	IV, Oral	[redacted], Japan	JTK303-AD-006

Test Article: EVG and COBI

Type of Study/Description	GLP[a]	Test System	Method of Administration	Testing Facility	Gilead Study No. (CRO Study No.)
Distribution (COBI)					
Plasma Protein Binding (Mouse)	No	In Vitro	In Vitro	[redacted], USA	AD-216-2076 (60N-0841, 60N-0842)
Plasma Protein Binding (Other Species)	No	In Vitro	In Vitro	[redacted], USA	AD-216-2026 (60D-0708, 60D-0712)
Absorption and Disposition of Radioactivity (Albino Rat)	No	Rat	Oral	[redacted], USA	AD-216-2034 (6511-362A)
Tissue Distribution of Radioactivity (Pigmented Rat)	No	Rat	Oral	[redacted], USA	AD-216-2060 (6511-448)
Metabolism (EVG)					
Hepatic Metabolism (Mouse Microsomal Fraction)	No	In Vitro	In Vitro	[redacted], USA	AD-183-2019 (60N-0629)
Hepatic Metabolism (ex vivo Mouse Microsomal Fraction)	No	In Vitro, Mouse	Oral and In vitro	[redacted], USA	AD-183-2021 (60N-0628)
Hepatic Metabolism (Oxidation by Microsomal Fractions)	No	In Vitro	In Vitro	Drug Metabolism & Pharmacokinetics Research Laboratories, Central Pharmaceutical Research Institute, Japan Tobacco Inc., Osaka, Japan	JTK303-AD-015

Test Article: EVG and COBI

Type of Study/Description	GLP[a]	Test System	Method of Administration	Testing Facility	Gilead Study No. (CRO Study No.)
Hepatic Metabolism (Glucuronidation by Microsomal Fractions)	No	In Vitro	In Vitro	Drug Metabolism & Pharmacokinetics Research Laboratories, Central Pharmaceutical Research Institute, Japan Tobacco Inc., Osaka, Japan	JTK303-AD-016
Hepatic Metabolism (Human Microsomal Fraction Oxidation Kinetics)	No	In Vitro	In Vitro	[redacted], Japan	JTK303-AD-024
Metabolite Identification	No	In Vitro, Rat, Dog	In Vitro, Oral	Drug Metabolism & Pharmacokinetics Research Laboratories, Central Pharmaceutical Research Institute, Japan Tobacco Inc., Osaka, Japan	JTK303-AD-021
Metabolite Identification (Mouse Microsomal Fraction)	No	In Vitro	In Vitro	[redacted], USA	AD-183-2020 (60N-0627)
Metabolite Identification	No	Rat	IV, Oral	Drug Metabolism & Pharmacokinetics Research Laboratories, Central Pharmaceutical Research Institute, Japan Tobacco Inc., Osaka, Japan	JTK303-AD-019
Metabolite Identification (Rabbit Microsomal Fraction)	No	In Vitro	In Vitro	[redacted], USA	60N-0508

Test Article: EVG and COBI

Type of Study/Description	GLP[a]	Test System	Method of Administration	Testing Facility	Gilead Study No. (CRO Study No.)
Metabolite Identification	No	Dog	IV, Oral	Drug Metabolism & Pharmacokinetics Research Laboratories, Central Pharmaceutical Research Institute, Japan Tobacco Inc., Osaka, Japan	JTK303-AD-020
Metabolism (COBI)					
Pharmacokinetics, metabolism, and excretion of radioactivity	No	Mouse	Oral	[redacted], USA	AD-216-2073 (8201467)
Radioprofiling and Metabolite Identification	No	Rat	Oral	[redacted], USA	AD-216-2082 (6511-362B)
Radioprofiling and Metabolite Identification	No	Dog	Oral	[redacted], USA	AD-216-2101 (8233206)
Metabolite identification in vitro (Mouse)	No	In Vitro	In Vitro	[redacted], USA	AD-216-2074
Cytochrome P450 phenotyping	No	In Vitro	In Vitro	[redacted], UK	AD-216-2025 (174-R16)
Metabolite identification in vitro (rat, dog, human)	No	In Vitro	In Vitro	[redacted], USA	AD-216-2038
In Vitro Metabolism in Hepatocytes and Hepatic Subcellular Fractions from Rat, Dog, Monkey, and Human	No	In Vitro	In Vitro	[redacted], USA	AD-216-2024
Excretion (EVG)					
Single Dose Pharmacokinetics	No	Rat	Oral	[redacted], Japan	JTK303-AD-005

Test Article: EVG and COBI

Type of Study/Description	GLP[a]	Test System	Method of Administration	Testing Facility	Gilead Study No. (CRO Study No.)
Repeat Dose Pharmacokinetics	No	Rat	Oral	[redacted], Japan	JTK303-AD-022
Single Dose Pharmacokinetics	No	Dog	IV, Oral	[redacted], Japan	JTK303-AD-006
Excretion (COBI)					
Pharmacokinetics, metabolism, and excretion of radioactivity	No	Mouse	Oral	[redacted], USA	AD-216-2073 (8201467)
Pharmacokinetics, distribution, metabolism, and excretion of radioactivity	No	Rat	Oral	[redacted], USA	AD-216-2034 (6511-362A)
Mass balance of radioactivity (intact dogs)	No	Dog	Oral	[redacted], USA	AD-216-2067 ([redacted]00540)
Mass balance of radioactivity (bile duct-cannulated dogs)	No	Dog	Oral	[redacted], USA	AD-216-2068 ([redacted]00539)
Potential to be a substrate for human OCT2	No	In Vitro	In Vitro	[redacted], USA/ Hungary	AD-216-2095 ([redacted]149, [redacted]108005)
Pharmacokinetic Drug Interactions (EVG)					
Induction Potential	No	In Vitro, Mouse	Oral	[redacted], USA	AD-183-2021 (60N-0628)

Test Article: EVG and COBI

Type of Study/Description	GLP[a]	Test System	Method of Administration	Testing Facility	Gilead Study No. (CRO Study No.)
Human Cytochrome P450 phenotyping	No	In Vitro	In Vitro	Drug Metabolism & Pharmacokinetics Research Laboratories, Central Pharmaceutical Research Institute, Japan Tobacco Inc., Osaka, Japan	JTK303-AD-017
Effects of CYP Inhibitors on the Human Metabolism of EVG	No	In Vitro	In Vitro	Drug Metabolism & Pharmacokinetics Research Laboratories, Central Pharmaceutical Research Institute, Japan Tobacco Inc., Osaka, Japan	JTK303-AD-018
Human UGT Phenotyping for EVG Glucuronidation	No	In Vitro	In Vitro	[redacted], USA	AD-183-2034
Inhibition of EVG Glucuronidation by Ketoconazole	No	In Vitro	In Vitro	[redacted], USA	AD-183-2028
Human Cytochrome P450 Inhibition Potential	No	In Vitro	In Vitro	[redacted], Japan	JTK303-AD-027
Inhibition Human Microsomal Metabolism of [^{14}C]EVG by Other Drugs	No	In Vitro	In Vitro	[redacted], Japan	JTK303-AD-025
Interaction with MDR1	No	In Vitro	In Vitro	[redacted], Japan	JTK303-AD-026
Inhibition of Human OATP1B1 and OATP1B3	No	In Vitro	In Vitro	[redacted], USA	AD-183-2030

Test Article: EVG and COBI

Type of Study/Description	GLP[a]	Test System	Method of Administration	Testing Facility	Gilead Study No. (CRO Study No.)
Induction Potential (Human Hepatocytes)	No	In Vitro	In Vitro	[redacted], Japan	JTK303-AD-023
Pharmacokinetic Drug Interactions (COBI)					
Inhibition of Pgp-dependent bidirectional transport of digoxin through Caco-2 monolayers	No	In Vitro	In Vitro	[redacted], USA	AD-216-2072
Inhibition of BCRP-Dependent Bidirectional Transport	No	In Vitro	In Vitro	[redacted], USA	AD-216-2104
Interaction with MRP1, MRP2, and Pgp	No	In Vitro	In Vitro	[redacted], USA	AD-216-2030
Inhibition of BCRP	No	In Vitro	In Vitro	[redacted], USA	AD-216-2099
Inhibition of OATP1B1 and OATP1B3	No	In Vitro	In Vitro	[redacted], USA	AD-216-2100
Interaction with human OCT2 uptake transporter	No	In Vitro	In Vitro	[redacted], USA/ Hungary	AD-216-2093 ([redacted]136, [redacted]098048)
Interaction with human MATE1 and MATE2-K transporters	No	In Vitro	In Vitro	[redacted], USA/ Japan	AD-216-2094 ([redacted]-011)
Effects on uptake into OCTN1 expressing cells	No	In Vitro	In Vitro	[redacted], USA/ Japan	AD-216-2098 ([redacted]-0032)

Test Article: EVG and COBI

Type of Study/Description	GLP[a]	Test System	Method of Administration	Testing Facility	Gilead Study No. (CRO Study No.)
Human CYP3A inhibition potential	No	In Vitro	In Vitro	[redacted], UK/ [redacted], USA	AD-216-2028 (174-R5, 174-R16, 174-R19)
Human OAT1, OAT3 and MRP4 transporter inhibition potential	No	In Vitro	In Vitro	[redacted], USA/ Hungary	AD-216-2105
Nonhuman CYP3A Inhibition Potential	No	In Vitro	In Vitro	[redacted], USA	AD-216-2040
Cytochrome P450 Inhibition Potential	No	In Vitro	In Vitro	[redacted], UK	AD-216-2029 (174-R16)
Human CYP2B6 and CYP2C8 Inhibition Potential	No	In Vitro	In Vitro	[redacted], USA	AD-216-2070
Drug Interaction Properties of COBI Metabolites	No	In Vitro	In Vitro	[redacted], UK/ [redacted], USA/ [redacted], USA	AD-216-2041 (174-R35, GIL-2007-107, GIL-2007-108)
Human UGT1A1 inhibition potential	No	In Vitro	In Vitro	[redacted], USA	AD-216-2075
Induction of metabolizing enzymes (Xenobiotic Receptors)	No	In Vitro	In Vitro	[redacted], USA	AD-216-2027 (GIL-2006-113, GIL-2007-105)
Induction potential in primary cultures of human hepatocytes	No	In Vitro	In Vitro	[redacted], USA	AD-216-2071 (3210-0913-1800)

Test Article: EVG and COBI

Type of Study/Description	GLP[a]	Test System	Method of Administration	Testing Facility	Gilead Study No. (CRO Study No.)
Induction of Rat Metabolizing Enzymes in vitro (Rat PXR)	No	In Vitro	In Vitro	[redacted], USA	AD-216-2039 (GIL-2007-104)
Permeability in MDR1 and BCRP Overexpressing Cells	No	In Vitro	In Vitro	[redacted], USA	AD-216-2103
Other Pharmacokinetic Studies					
None					

COBI = cobicistat; EVG = elvitegravir; FTC = emtricitabine; TDF = tenofovir disoproxil fumarate; TFV = tenofovir

a An entry of "Yes" indicates that the study includes a GLP compliance statement.

b Study included tenofovir as the test article

2.6.5.2. Pharmacokinetics: Analytical Methods and Validation Reports

2.6.5.2.1. EVG: Analytical Methods and Validation Reports

Test Article: EVG, GS-9200, GS-9202, RTV, COBI

Type of Study:	**Analytical Method Validation**		
Study No.	**Matrix**	**Analyte(s)**	**Analytical Method**
BA-183-2003	Mouse Plasma	EVG, GS-9200, GS-9202	LC/MS/MS
JTK303-AD-003	Rat Plasma	EVG	LC/MS/MS
BA-183-2011	Rat Plasma	EVG, GS-9200, GS-9202	LC/MS/MS
BA-216-2007	Rat Plasma	EVG, COBI	LC/MS/MS
BA-183-2012	Rat Plasma	RTV	LC/MS/MS
JTD303-AD-004	Dog Plasma	EVG	LC/MS/MS
BA-183-2008	Rat Milk	EVG, GS-9200, GS-9202	LC/MS/MS

COBI = cobicistat; EVG = elvitegravir, GS-9200 = EVG metabolite M4 (JTP-65386 and JTP-71051 as standards; glucuronide conjugate of the carboxylic acid); GS-9202 = EVG metabolite M1 (JTP-71081 as standard; hydroxylation of the chlorofluorophenyl group); RTV = ritonavir

2.6.5.2.2. COBI: Analytical Methods and Validation Reports

Test Article: ATV, COBI, EVG, or GS-9612

Type of Study:	**Analytical Method Validation**		
Study No.	**Matrix**	**Analyte(s)**	**Analytical Method**
BA-216-2005	Mouse plasma	COBI	LC/MS/MS
BA-216-2010	Mouse plasma	GS-9612	LC/MS/MS
BA-216-2007	Rat plasma	COBI, EVG	LC/MS/MS
BA-216-2202	Rat plasma	COBI	LC/MS/MS
BA-216-2008	Rat plasma	GS-9612	LC/MS/MS
BA-216-2006	Rat plasma	ATV	LC/MS/MS
BA-216-2013	Rat milk	COBI	LC/MS/MS
BA-216-2004	Rabbit plasma	COBI	LC/MS/MS
BA-216-2003	Dog plasma	COBI	LC/MS/MS
BA-216-2009	Dog plasma	GS-9612	LC/MS/MS

ATV = atazanavir; COBI = cobicistat; EVG = elvitegravir; GS-9612 = cobicistat hydroxylated metabolite

2.6.5.3. Pharmacokinetics: Absorption after a Single Dose

2.6.5.3.1. JTK303-AD-026: Membrane Permeability and Efflux Potential of EVG (In Vitro)

Report Title	Study Type	Test Article	Report Number
Involvement of MDR1 in Membrane Permeation of JTK-303 and Inhibitory Effect of JTK-303 on Digoxin Transport	Absorption study (in vitro)	EVG	JTK303-AD-026

Compound	Time (h)	Cleared Volume (µL/mg Cellular Protein)					
		Control LLC-PK1Cells			MDR1-Expressing LLC-PK1Cells		
		A-B	B-A	Ratio	A-B	B-A	Ratio
EVG	1	179.2 ± 16.7	207.8 ± 11.2	1.2	64.1 ± 17.3	961.9 ± 75.8	15.0
	2	412.7 ± 20.0	512.8 ± 34.4	1.2	139.4 ± 25.2	1891.6 ± 126.1	13.6
	4	606.4 ± 18.7	912.6 ± 62.9	1.5	212.1 ± 34.7	3085.4 ± 65.7	14.5
Digoxin	1	21.6 ± 1.1	44.6 ± 10.3	2.1	25.3 ± 9.0	245.8 ± 27.0	9.7
	2	48.6 ± 9.5	96.7 ± 16.1	2.0	54.9 ± 5.1	498.1 ± 69.8	9.1
	4	103.0 ± 20.1	229.8 ± 27.4	2.2	97.4 ± 12.3	1000.2 ± 125.8	10.3
Mannitol	1	24.1 ± 12.8	16.2 ± 1.2	0.7	53.9 ± 36.4	42.9 ± 18.2	0.8
	2	36.6 ± 10.4	35.7 ± 4.0	1.0	97.0 ± 63.6	83.6 ± 27.4	0.9
	4	89.9 ± 14.4	73.5 ± 6.3	0.8	176.9 ± 100.2	131.7 ± 33.8	0.7

A = apical; B = basal; EVG = elvitegravir; MDR1 = human P-glycoprotein

2.6.5.3.2. JTK303-AD-009 and JTK303-AD-011: Pharmacokinetics of EVG in Rats After Oral or Intravenous Administration

Report Title	Study Type	Test Article	Report Number
Collection of Plasma from Rats and Determination of Concentration of JTK-303 in Plasma	Single Dose Pharmacokinetics	EVG	JTK303-AD-009
Pharmacokinetic Analysis of the Plasma Parent Drug Concentration in Rats after Oral or Intravenous Administration of JTK-303			JTK303-AD-011

Species/Strain Number of Animals/Group Sex	Administration Route	Dose Level (mg/kg)	Dose Volume (mL/kg)	Feeding Condition	t_{max} (h)	C_{max} (ng/mL)	$t½_{\alpha}$ (h)	$MRT_{0-\infty}$ (h)	$AUC_{0-\infty}$ (ng•h/mL)	F (%)	Effect of Diet	Linearity
Rat/SD (Crj:CD[SD]IGS) 3 animals/group male	Oral (MC)	1	5	Non-fasting	0.42 ± 0.14	251 ± 51	2.3 ± 0.4	3.4 ± 0.7	643 ± 285	32.9 ± 14.6	C_{max}: Significant difference $AUC_{0-\infty}$: No significant difference	C_{max}: 1 to 10 mg/kg $AUC_{0-\infty}$: 1 to 10 mg/kg
		3			0.25 ± 0.00	755 ± 311	2.3 ± 0.3	3.4 ± 0.4	1999 ± 675	34.1 ± 11.5		
		3		Fasting	0.50 ± 0.00	1536 ± 240	0.5 ± 0.0	1.6 ± 0.3	1762 ± 215	30.0 ± 3.7		
		10		Non-fasting	0.83 ± 0.29	1947 ± 971	3.8 ± 1.4	4.9 ± 1.6	6825 ± 2455	34.9 ± 12.5		

2.6.5.3.2. JTK303-AD-009 and JTK303-AD-011: Pharmacokinetics of EVG in Rats After Oral or Intravenous Administration (Continued)

Species/Strain Number of Animals/Group Sex	Adminis-tration Route	Dose Level (mg/kg)	Dose Volume (mL/kg)	Feeding Condition	C_{5min} (ng/ mL)	$t_{½\alpha}$ (h)	$MRT_{0-\infty}$ (h)	CL (L/h/kg)	$AUC_{0-\infty}$ (ng•h/mL)	V_{ss} (L/kg)
Rat/SD (Crj:CD[SD]IGS) 3 animals/group male	IV (PEG400)	1	1	Non-fasting	4655 ± 383	0.2 ± 0.0	0.8 ± 0.1	0.5 ± 0.1	1955 ± 224	0.4 ± 0.1

AUC = area under the plasma concentration-time curve; C_{5min} = plasma concentration at 5 minutes after administration; C_{max} = maximum plasma concentration; CL = total body clearance; EVG = elvitegravir; F = bioavailability; IV = intravenous; MC = 0.5% (w/v) aqueous methylcellulose; PEG400 = 80% (v/v) aqueous polyethylene glycol 400; t_{max} = time to reach the maximum plasma concentration; t½ = elimination half-life; MRT = mean residence time; V_{ss} = volume of distribution at steady-state

2.6.5.3.3. JTK303-AD-005 and JTK303-AD-007: Pharmacokinetics of Plasma Radioactivity in Rats after Oral or Intravenous Administration of [^{14}C]EVG

Report Title	Study Type	Test Article	Report Number
Pharmacokinetics in Rats After Single Administration of [^{14}C]JTK-303	Single Dose Pharmacokinetics	[^{14}C]EVG	JTK303-AD-005
Calculation of Pharmacokinetic Parameters of Plasma Radioactivity Concentration in Rats After Oral or IV Administration of [^{14}C]JTK-303			JTK303-AD-007

Species/Strain Number of Animals/Group Sex	Administration Route	Dose Level (mg/kg)	Dose Volume (mL/kg)	Feeding Condition	C_{5min} (ng eq./mL)	$t_{½\alpha}$ (h)	$t_{½\beta}$ (h)	$t_{½\gamma}$ (h)	$AUC_{0-\infty}$ (ng eq.·h/mL)	CL (L/h/kg)	V_{ss} (L/kg)
Rat/SD (Crj:CD(SD)IGS) 3 animals/group male	IV	1 (PEG400)	1	Non-fasting	4824±780	0.2±0.1	1.3±0.1	15.6±3.7	2001±135	0.5±0.0	1.5±0.4

Species/Strain Number of Animals/Group Sex	Administration Route	Dose Level (mg/kg)	Dose Volume (mL/kg)	Feeding Condition	t_{max} (h)	C_{max} (ng·eq./mL)	$t_{½\alpha}$ (h)	$t_{½\beta}$ (h)	$AUC_{0-\infty}$ (ng eq.·h/mL)	F (%)
Rat/SD (Crj:CD(SD)IGS) 3 animals/group male	Oral	3 (MC)	5	Non-fasting	0.42 ± 0.14	780 ± 70	2.0 ± 0.5	12.6 ± 1.3	2468 ± 297	41.1 ± 5.0

AUC = area under the plasma concentration-time curve; F = bioavailability; C_{5min} = plasma concentration at 5 minutes after administration; C_{max} = maximum plasma concentration; CL = total body clearance; EVG = elvitegravir; IV = intravenous; MC = 0.5% (w/v) aqueous methylcellulose; PEG400 = 80% (v/v) aqueous polyethylene glycol 400; t_{max} = time to reach the maximum plasma concentration; $t_{½}$ = elimination half-life; V_{ss} = volume of distribution at steady-state

2.6.5.3.4. JTK303 AD 010 and JTK303-AD-012: Pharmacokinetics of EVG in Dogs After Oral or Intravenous Administration

Report Title	Study Type	Test Article	Report Number
Collection of Plasma from Dogs and Determination of Concentration of JTK-303 in Plasma	Single Dose Pharmacokinetics	EVG	JTK303-AD-010
Pharmacokinetic Analysis of the Plasma Parent Drug Concentration in Dogs After Oral or IV Administration of JTK-303			JTK303-AD-012

Species/Strain Number of Animals/ Group Sex	Administration Route	Dose Level (mg/kg)	Dose Volume (mL/kg)	Feeding Condition	t_{max} (h)	C_{max} (ng/mL)	$MRT_{0-\infty}$ (h)	$AUC_{0-\infty}$ (ng•h/ mL)	F (%)	Effect of Diet	Linearity
Dog/Beagle (NOSAN) 3 animals/group male	Oral (MC)	1	2	Post-prandial	0.67 ± 0.29	58 ± 24	5.1 ± 1.1	255 ± 40	26.7 ± 2.4	No significant difference in C_{max} and $AUC_{0-\infty}$	C_{max}: 1 to 10 mg/kg
		3			1.00 ± 0.87	136 ± 61	7.6 ± 3.8	843 ± 73	29.6 ± 1.7		
		3		Fasting	0.83 ± 0.29	312 ± 158	2.8 ± 0.7	923 ± 320	33.0 ± 13.7		$AUC_{0-\infty}$: 1 to 10 mg/kg
		10		Post-prandial	0.67 ± 0.29	529 ± 126	7.6 ± 5.3	2495 ± 682	26.0 ± 4.3		

Species/Strain Number of Animals/ Group Sex	Administration Route	Dose Level (mg/kg)	Dose Volume (mL/kg)	Feeding Condition	C_{5min} (ng/mL)	$t_{½\alpha}$ (h)	$MRT_{0-\infty}$ (h)	$t_{½\gamma}$ (h)	$AUC_{0-\infty}$ (ng•h/ mL)	CL (L/h/kg)	V_{ss} (L/kg)
Dog/Beagle (NOSAN) 3 animals/ group male	Intra-venous (PEG400)	1	0.2	Post-prandial	684 ± 214	0.5 ± 0.1	2.5 ± 0.2	5.0[a]	954 ± 130	1.0 ± 0.2	2.6 ± 0.4

AUC = area under the plasma concentration-time curve; C_{5min} = concentration at 5 minutes after administration; CL = total body clearance; MC = 0.5% (w/v) aqueous methylcellulose; PEG400 = 80% (v/v) aqueous polyethylene glycol 400; $t_{½}$ = elimination half-life; MRT = mean residence time; V_{ss} = volume of distribution at steady-state
a The mean of 2 individuals

2.6.5.3.5. JTK303-AD-006 and JTK303-AD-008: Pharmacokinetics of Plasma Radioactivity in Dogs After Oral or Intravenous Administration of [^{14}C]EVG

Report Title	Study Type	Test Article	Report Number
Pharmacokinetics in Dogs After Single Administration of [^{14}C]JTK-303	Single Dose Pharmacokinetics	[^{14}C]EVG	JTK303-AD-006
Calculation of Pharmacokinetic Parameters of Plasma Radioactivity Concentration in Dogs After Oral or Intravenous Administration of [^{14}C]JTK-303			JTK303-AD-008

Species/Strain Number of Animals/Group Sex	Administration Route	Dose Level (mg/kg)	Dose Volume (mL/kg)	Feeding Condition	C_{5min} (ng·eq./mL)	$t_{½\alpha}$ (h)	$t_{½\beta}$ (h)	$t_{½\gamma}$ (h)	$AUC_{0-\infty}$ (ng·eq.•h/mL)	CL (L/h/kg)	V_{ss} (L/kg)
Dog/Beagle (NOSAN) 3 animals/group male	IV	1 (PEG400)	0.2	Post-prandial	691 ± 149	0.5 ± 0.1	2.2 ± 0.1	34.4 ± 11.6	1504 ± 310	0.7 ± 0.2	11.3 ± 3.2

Species/Strain Number of Animals/Group Sex	Administration Route	Dose Level (mg/kg)	Dose Volume (mL/kg)	Feeding Condition	t_{max} (h)	C_{max} (ng·eq./mL)	$t_{½}$ (h)	$AUC_{0-\infty}$ (ng·eq.•h/mL)	F (%)
Dog/Beagle (NOSAN) 3 animals/group male	Oral	3 (MC)	2	Post-prandial	3.33 ± 4.04	152 ± 69	9.2 ± 2.3	1867 ± 683	41.4 ± 15.1

AUC = area under the plasma concentration-time curve; F = bioavailability; C_{5min} = plasma concentration at 5 minutes after administration; CL = total body clearance; C_{max} = maximum plasma concentration; EVG = elvitegravir; IV = intravenous; MC = 0.5% (w/v) aqueous methylcellulose; PEG400 = 80% (v/v) aqueous polyethylene glycol; $t_{½}$ = elimination half-life; t_{max} = time to reach the maximum plasma concentration; V_{ss} = volume of distribution at steady-state

2.6.5.3.6. JTK303-P2-102: Comparative Study of Oral Absorption Between EVG Tablets, 50 mg and EVG Tablets, 50 mg (SD)

Report Title	Study Type	Test Article	Report Number
Comparative Studies on Dissolution and Oral Absorption Between JTK-303 Tablets, 50 mg and JTK-303 Tablets, 50 mg (SD)	Formulation Comparison (Dissolution and Oral Absorption)	EVG	JTK303-P2-102

Species	**Dog**	**Dog**	**Dog**	**Dog**
Gender (M/F) / N of Animals	4M	4M	4M	4M
Feeding Condition	Fasted	Fasted	Fed	Fed
Vehicle/Formulation	Tablet	Tablet	Tablet	Tablet
Method of Administration	Oral	Oral	Oral	Oral
Dose (mg) (tablet type)	50 mg	50 mg (SD)	50 mg	50 mg (SD)
Analyte	EVG	EVG	EVG	EVG
Assay	LC/MS/MS	LC/MS/MS	LC/MS/MS	LC/MS/MS
PK Parameters				
t_{max} (h)	1.38 ± 0.75	1.25 ± 0.50	1.38 ± 0.75	1.25 ± 0.50
C_{max} (ng/mL)	162 ± 81	580 ± 0.05	247 ± 25	302 ± 52
AUC_{0-12} (ng • h/mL)	691 ± 321	1827 ± 702	862 ± 138	1121 ± 179
$t_{½}$ (h)[a]	2.1 ± 0.3	1.7 ± 0.1	2.1 ± 0.3	2.0 ± 0.4

AUC = area under the plasma concentration-time curve; C_{max} = maximum plasma concentration; EVG = elvitegravir; F = female; M = male; SD = solid dispersion; $t_{½}$ = elimination half-life; t_{max} = time to reach the maximum plasma concentration

Each value represents the mean ± standard deviation (n = 4).

a t_{max} to 12 hours

2.6.5.3.7. AD-216-2023: Caco-2 Permeability of COBI (In Vitro)

Report Title	Study Type	Test Article	Report Number
Bi-directional Permeability of GS-9350 and Ritonavir in Caco-2 Cell Monolayers	Absorption study (in vitro)	COBI	AD-216-2023

Bi-directional Permeability of COBI Through Caco-2 Cells

Direction	Target Conc. (μM)	Initial Conc. (μM)	Recovery (%)	P_{app} (10^{-6} cm/s)			Efflux Ratio
				Replicate 1	Replicate 2	Average	
Cell-Free	1	1.2	ND	9.45	--	9.45	
Forward		1.4	73.8	7.28	7.95	7.61	1.1
Reverse		1.3	55.0	5.26	11.8	8.51	

Caco-2 = human colonic adenocarcinoma cell line; COBI = cobicistat; Conc. = concentration; ND = not determined due to missing donor well concentration at 120 minutes; P_{app} = apparent permeability

2.6.5.3.8. PC-216-2013-PK: Pharmacokinetics of COBI in Mice After Single Oral Dose Administration

Report Title	Study Type	Test Article	Report Number
Determination of the Pharmacokinetics of GS-9350 Following a Single Oral Gavage Dose to Male and Female 001178-W (wild-type) Mice	Single-Dose Pharmacokinetics	COBI	PC-216-2013-PK

Mean Pharmacokinetic Parameters of COBI Following Single Oral Doses in Female and Male CByB6F1-Tg(HRAS)2Jic (001178-W) Mice

Species/Strain Number of Animals/Group Sex	Administration Route	Dosage (mg/kg)	Gender	Feeding Condition	AUC_{0-24} (ng•h/mL)	C_{max} (ng/mL)	t_{max} (h)	C_{24h} (ng/mL)
01178-W (wild), CByB6F1-Tg(HRAS)2Jic mice 24M and 24F/group	Oral (10% Propylene glycol in 40 mM acetate buffer, pH 4.0)	30	Female	Nonfasted	46,306	10,158	1.0	1.28
			Male		35,535	5940	2.0	1.67
		100	Female		128,930	16,205	1.0	1532
			Male		108,796	11,130	2.0	1418
		300	Female		NC	23,464	2.0	NC
			Male		NC	29,392	4.0	NC

AUC = area under the plasma concentration-time curve; C_{24h} = plasma concentration at 24 hours after administration; C_{max} = maximum plasma concentration; COBI = cobicistat; NC = not calculated due to insufficient data (animals euthanized at 4 hour time point); t_{max} = time to reach the maximum plasma concentration

2.6.5.3.9. AD-216-2020: Pharmacokinetics of COBI in Rats

Report Title	Study Type	Test Article	Report Number
Pharmacokinetics of GS-9350 in Sprague-Dawley Rats	Single-Dose Pharmacokinetics	COBI	AD-216-2020

Pharmacokinetic Parameters of COBI in Male and Female Sprague-Dawley Rats (mean ± SD, n = 3)

Species/Strain Number of Animals/Group Sex	Administration Route	Dose Level (mg/kg)	Dose Volume (mL/kg)	Feeding Condition	t_{max} (h)	C_{max} (nM)	$t_{½}$ (h)	$AUC_{0-\infty}$ (nM•h)	CL (L/h/kg)	V_{ss} (L/kg)	F (%)
Sprague-Dawley Rat 3 Male or 3 Female animals/group	IV Infusion (M)[a]	1	5	Fasted	0.48 ± 0.0	664 ± 31.4	0.40 ± 0.02	351 ± 12.6	3.59 ± 0.14	0.76 ± 0.14	—
	IV Infusion (F)[a]	1	5		0.48 ± 0.0	890 ± 74.3	0.35 ± 0.01	566 ± 50.1	2.37 ± 0.18	0.70 ± 0.09	—
	Oral (M)[b]	5	10		0.50 ± 0.0	764 ± 506	0.92 ± 0.22	594 ± 42.6	—	—	33 ± 3

AUC = area under the plasma concentration-time curve; CL = clearance; C_{max} = maximum plasma concentration; COBI = cobicistat; F = bioavailability; IV = intravenous; SD = standard deviation; t½ = elimination half-life; t_{max} = time to reach the maximum plasma concentration; V_{ss} = volume of distribution at steady state

a Intravenous dosing vehicle was 5% ethanol, 10% propylene glycol, and 85% water

b Oral dosing vehicle was 5% ethanol, 15% propylene glycol, 80% water (pH 3.5, HCl) for the male rat groups and 10% ethanol, 30% propylene glycol, and 60% water for the female rat groups

2.6.5.3.9. AD-216-2020: Pharmacokinetics of COBI in Rats (Continued)

Test Article: COBI

Pharmacokinetic Parameters of COBI Following Escalating Oral Doses of COBI in Male and Female Sprague-Dawley Rats (mean ± SD, n = 3)

Species/Strain Number of Animals/Group Sex	Administration Route	Dosage (mg/kg)	Dose Volume (mL/kg)	Gender	Feeding Condition	PK Parameter				
						AUC_{0-t} (nM•h)	C_{max} (nM)	t_{max} (h)	C_{last} (nM)	t_{last} (h)
Sprague-Dawley Rat 3 Male or 3 Female animals/group	Oral[a]	25	10	M	Fasted	13,233 ± 1942	4000 ± 684	1.08 ± 0.88	6.58 ± 2.02	8
		25	10	F		26,087 ± 6923	4506 ± 237	0.83 ± 1.01	1.24 ± 0.16	24
		100	10	M		65,185 ± 21,658	6895 ± 933	1.42 ± 1.01	14.0 ± 8.70	24
		110	10	F		170,525 ± 20,189	12,784 ± 956	6.67 ± 2.31	2708 ± 1510	24

AUC = area under the plasma concentration-time curve; C_{last} = concentration of last measurable sample; C_{max} = maximum plasma concentration; COBI = cobicistat; F = female; M = male; SD = standard deviation; t_{last} = the last time point at which a quantifiable drug concentration can be measured; t_{max} = time to reach the maximum plasma concentration

a Oral dosing vehicle was 5% ethanol, 15% propylene glycol, 80% water (pH 3.5, HCl) for the male rat groups and 10% ethanol, 30% propylene glycol, and 60% water for the female rat groups

2.6.5.3.10. AD-216-2021: Pharmacokinetics of COBI in Dogs

Report Title	Study Type	Test Article	Report Number
Pharmacokinetics of GS-9350 in Male Beagle Dogs	Single-Dose Pharmacokinetics	COBI	AD-216-2021

Pharmacokinetic Parameters of COBI in Male Beagle Dogs (mean ± SD, n = 3)

Species/Strain Number of Animals/Group Sex	Administration Route	Dose Level (mg/kg)	Dose Volume (mL/kg)	Feeding Condition	t_{max} (h)	C_{max} (nM)	$t_{½}$ (h)	$AUC_{0-\infty}$ (nM•h)	CL (L/h/kg)	V_{ss} (L/kg)	F (%)
Beagle Dog 3 animals/group	IV Infusion[a]	1	1	Fasted	0.48 ± 0.0	924 ± 267	1.02 ± 0.04	565 ± 155	2.18 ± 0.69	1.33 ± 0.69	—
	Oral[b,c]	5	2		1.00 ± 0.43	313 ± 186	1.12 ± 0.14	331 ± 130	—	—	11 ± 4

AUC = area under the plasma concentration-time curve; CL = clearance; C_{max} = maximum plasma concentration; COBI = cobicistat; F = bioavailability; IV = intravenous; SD = standard deviation; t½ = elimination half-life; t_{max} = time to reach the maximum plasma concentration; V_{ss} = volume of distribution at steady state

a Intravenous (via 30-minute infusion) dosing vehicle was 5% ethanol, 15% propylene glycol, and 80% water

b Oral dosing vehicle was 5% ethanol, 30% propylene glycol, 65% water

c Elvitegravir was coadministered with COBI in this group of animals

2.6.5.3.10. AD-216-2021: Pharmacokinetics of COBI in Dogs (Continued)

Test Article: COBI

Pharmacokinetic Parameters of COBI Following Escalating Oral Doses of COBI in Beagle Dogs (mean +/- SD, n = 3)

Species/Strain Number of Animals/Group Sex	Adminis-tration Route	Dosage (mg/kg)	Dose Volume (mL/kg)	Feeding Condition	PK Parameter				
					AUC_{0-t} (nM•h)	C_{max} (nM)	t_{max} (h)	C_{last} (nM)	t_{last} (h)
Beagle Dog 3 animals/group	Oral[a]	10	5	Fasted	355 ± 435	118 ± 57.6	1.50 ± 2.17	2.90 ± 2.73	9.33 ± 2.31
		30			34,538 ± 13,033	4373 ± 2307	2.33 ± 1.53	13.6 ± 14.3	24.0 ± 0.0
		100			102,223 ± 23,511	9640 ± 572	1.67 ± 2.02	872 ± 752	24.0 ± 0.0

AUC = area under the plasma concentration-time curve; C_{last} = concentration of last measurable sample; C_{max} = maximum plasma concentration; COBI = cobicistat; SD = standard deviation; t_{last} = the last time point at which a quantifiable drug concentration can be measured; t_{max} = time to reach the maximum plasma concentration

a Oral dosing vehicle (by volume) was 1.5% ethanol, 1.5% propylene glycol, 6% Labrasol, 6% Solutol, and 85% water

2.6.5.3.11. AD-216-2042: Comparative Study of Oral Absorption in Dogs Between Several COBI Tablet Formulations

Report Title	Study Type	Test Article	Report Number
Pharmacokinetics of GS-9350 after Oral Doses in Various Formulations in Beagle Dogs	Single-Dose Pharmacokinetics	COBI	AD-216-2042

Pharmacokinetic Parameters of COBI After an Oral Dose of COBI at 1 mg/kg in Pentagastrin Pretreated Dogs (mean ± SD)

Species/Strain Number of Animals/Group Sex	Adminis-tration Route	Dosage (mg/kg)	API % in Tablets	Dose Volume (mL/kg)	Number and Gender	Feeding Condition	PK Parameter		
							t_{max} (h)	C_{max} (nM)	$AUC_{0-\infty}$ (nM•h)
Beagle dog 3 to 6 male animals/ group	Oral Solution[a]	1	N/A	1	3M	Fasted	0.67 ± 0.29	89.2 ± 65.9	120 ± 60.9
	Oral Tablets[b]	1	33.3%	N/A	6M		0.83 ± 0.26	27.1 ± 11.7	40.3 ± 11.7
		1	8.3%	N/A	6M		1.25 ± 0.61	24.4 ± 14.6	47.0 ± 18.3
		1	3.3%	N/A	6M		1.00 ± 0.55	21.4 ± 10.2	39.7 ± 16.7

AUC = area under the plasma concentration-time curve; C_{max} = maximum plasma concentration; COBI = cobicistat; F = female; IV = intravenous; M = male; N/A = not applicable; SD = standard deviation; t_{max} = time to reach the maximum plasma concentration

a Dosing vehicle was 5% ethanol, 15% propylene glycol, and 80% water (HCl, pH 3.0)

b Tablet components were 38.3% colloidal silicon dioxide, 5% croscarmellose sodium, 2% hydroxypropyl cellulose, and 1% magnesium stearate; microcrystalline cellulose amount in the tablets ranged from 20.3% to 50.3% based on the loading of COBI in the tablets

2.6.5.3.12. AD-216-2022: Pharmacokinetics of COBI in Cynomolgus Monkeys

Report Title	Study Type	Test Article	Report Number
Pharmacokinetics of GS-9350 in Cynomolgus Monkeys	Single-Dose Pharmacokinetics	COBI	AD-216-2022

Pharmacokinetic Parameters of COBI in Male Cynomolgus Monkeys (mean ± SD, n = 3)

Species/Strain Number of Animals/Group Sex	Administration Route	Dose Level (mg/kg)	Dose Volume (mL/kg)	Feeding Condition	t_{max} (h)	C_{max} (nM)	$t_{½}$ (h)	$AUC_{0-\infty}$ (nM•h)	CL (L/h/kg)	V_{ss} (L/kg)	F (%)
Cynomolgus Monkey 3 animals/group Male	IV Infusion[a]	1	1	Fasted	0.48 ± 0.0	1222 ± 41.1	1.42 ± 0.07	977 ± 83.7	1.36 ± 0.14	1.31 ± 0.12	—
	Oral[b]	6	2.5		2.17 ± 1.76	161 ± 102	1.36 ± 0.21	445 ± 280	—	—	7.3 ± 4.6

AUC = area under the plasma concentration-time curve; CL = clearance; C_{max} = maximum plasma concentration; COBI = cobicistat; F = bioavailability; IV = intravenous; SD = standard deviation; t½ = elimination half-life; t_{max} = time to reach the maximum plasma concentration; V_{ss} = volume of distribution at steady state

a Intravenous (via 30-minute infusion) dosing vehicle was 5% ethanol, 10% propylene glycol, and 85% water (pH 3.0)

b Oral dosing vehicle was 5% ethanol, 10% propylene glycol, 85% water

2.6.5.3.13. AD-216-2061: Pharmacokinetics of EVG, COBI, FTC, and TFV after Oral Dosing in Various Formulations in Beagle Dogs

Report Title	Study Type	Test Article	Report Number
Pharmacokinetics of EVG, FTC, TDF, and COBI After Oral Dosing in Various Formulations in Beagle Dogs	Formulation Comparison (Combination tablet)	EVG, FTC, TDF, COBI	AD-216-2061

Plasma Pharmacokinetic Parameters (Mean ± SD, n = 12)	EVG 37.5 mg, TDF 75 mg, FTC 50 mg, and COBI 25 mg Coadministered				EVG 37.5 mg, TDF 75 mg, FTC 50 mg, and COBI 25 mg (Bilayer Tablet)				EVG 37.5 mg, TDF 75 mg, FTC 50 mg, and COBI 25 mg (Trilayer Tablet)			
	EVG	COBI	FTC	TFV	EVG	COBI	FTC	TFV	EVG	COBI	FTC	TFV
t_{max} (h)	2.5 ± 1.2	1.2 ± 0.9	1.5 ± 0.9	1.2 ± 1.0	2.7 ± 1.2	1.6 ± 0.5	1.5 ± 0.5	1.3 ± 0.6	2.8 ± 1.1	2.2 ± 2	2.3 ± 2	1.5 ± 0.9
C_{max} (ng/mL)	192 ± 76	113 ± 115	2859 ± 1132	815 ± 574	230 ± 104	126 ± 122	3618 ± 1087	974 ± 497	273 ± 87	154 ± 138	2804 ± 1022	979 ± 596
AUC_{0-t} (ng•h/mL)	1083 ± 427	225 ± 248	10,578 ± 3884	3266 ± 1891	1433 ± 721	265 ± 239	14,109 ± 5002	3608 ± 1199	1559 ± 641	292 ± 243	11,176 ± 2961	3459 ± 1609

COBI = cobicistat; EVG = elvitegravir; FTC = emtricitabine; TDF = tenofovir disoprixil fumarate; SD = standard deviation; AUC = area under the plasma concentration-time curve; t_{max} = time to reach the maximum plasma concentration

2.6.5.4. Pharmacokinetics: Absorption after Repeated Doses

2.6.5.4.1. JTK303-AD-022 and JTK303-AD-028: 7-Day Repeat-Dose Pharmacokinetic Study of [^{14}C]EVG in the Rat

Report Title	**Study Type**	**Test Article**	**Report Number**
Pharmacokinetics in Rats After Repeated Oral Administration of [^{14}C]JTK-303	Multiple Dose Pharmacokinetics	[^{14}C]EVG	JTK303-AD-022
Analysis of Pharmacokinetic Parameters of the Plasma Radioactivity Concentration in Rats Treated with Repeated Oral Administration of [^{14}C]JTK-303			JTK303-AD-028
Species	**Rat**		
Gender (M/F) / No. of Animals	3M per Group		
Feeding Condition	Not Fasted		
Vehicle / Formulation	Methylcellulose (0.5% w/v)/ Suspension		
Route/Frequency of Administration	Oral/Once Daily for 7 Days		
Dose (mg/kg)	3		
Sample	Plasma		
Analyte	Carbon-14		
Assay	Scintillation Counting		

2.6.5.4.1. JTK303-AD-022 and JTK303-AD-028: 7-Day Repeat-Dose Pharmacokinetic Study of [^{14}C]EVG in the Rat (Continued)

Test Article: [^{14}C]EVG

Time		Plasma Radioactivity Concentrations (Day 1 to Day 7)
Day	Hour Since Start	
1	0.25	565 ± 200
	24	9 ± 2
2	24.25	1155 ± 97
	48	13 ± 2
3	48.25	1004 ± 409
	72	18 ± 4
4	72.25	1058 ± 375
	96	19 ± 3
5	96.25	1269 ± 127
	120	21 ± 4
6	120.25	1003 ± 207
	144	21 ± 4
7	144.25	1107 ± 331
	168	24 ± 4

2.6.5.4.1. JTK303-AD-022 and JTK303-AD-028: 7-Day Repeat-Dose Pharmacokinetic Study of [^{14}C]EVG in the Rat (Continued)

Test Article: [^{14}C]EVG

PK Parameters[a]	Dose No. 1	Dose No. 7
t_{max} (h)	0.7 ± 0.3	0.5 ± 0.0
C_{max} (ng eq./mL)	996 ± 236	1411 ± 178
C_{max} Ratio[b]	—	1.45 ± 0.23
$t_{½\alpha}$ (h)	1.3 ± 0.1[c]	1.7 ± 0.2[d]
$t_{½\beta}$ (h)	5.2 ± 1.0[e]	20.6 ± 0.7[f]
$AUC_{0-\tau}$ (ng eq•h/mL)[g]	2828 ± 97	3284 ± 679
$AUC_{0-\tau}$ Ratio[b]	—	1.16 ± 0.24
$AUC_{0-\infty}$ (ng eq•h/mL)	2897 ± 98	—
$MRT_{0-\infty}$ (h)	4.6 ± 0.2	15.3 ± 1.6
CL/F (L/h/kg)	1.0 ± 0.1	0.7 ± 0.1
V_Z/F (L/kg)	7.8 ± 1.5	21.7 ± 3.3

a Data are expressed as the mean values ± standard deviation of 3 animals.

b Ratio of values obtained after the first and seventh administrations.

c $t_{½\alpha}$: t_{max} to 4 hours

d $t_{½\alpha}$: t_{max} to 8 hours

e $t_{½\beta}$: 6 to 24 hours

f $t_{½\beta}$: 8 to 48 hours

g τ: administration interval (τ = 24 hours)

2.6.5.4.2. COBI: Absorption after Repeated Doses

No pharmacokinetic studies of absorption of COBI after repeated doses have been conducted to date. Repeat dose studies were performed in support of safety evaluation and toxicokinetics are presented in Module 2.6.7.

2.6.5.5. Pharmacokinetics: Organ Distribution Studies

2.6.5.5.1. JTK303-AD-005: Distribution in Rats after Single Administration of [^{14}C]EVG

Report Title	Study Type	Test Article	Report Number (Study Number)
Pharmacokinetics in Rats after Single Administration of ^{14}C-JTK-303	Distribution	[^{14}C]EVG	JTK303-AD-005 (AE-3857-G)

Absorption

Species/Strain Number of Animals/Group Sex	Administration Route	Dose Level (mg/kg)	Dose Volume (mL/kg)	Feeding Condition	C_{5min} (ng eq./mL)
Rat/SD (Crj:CD(SD)IGS) 3 animals/group male	Intravenous	1 (PEG400)	1	Non-fasting	4824 ± 780
	Oral	3 (MC)	5		NA

C_{5min} = plasma concentration at 5 minutes after administration; EVG = elvitegravir; MC = 0.5% (w/v) aqueous methylcellulose; PEG400 = 80% (v/v) aqueous polyethylene glycol 400

2.6.5.5.1. JTK303-AD-005: Distribution in Rats after Single Administration of [^{14}C]EVG (Continued)

Test Article: [^{14}C]EVG

	Concentration - ng eq. of EVG/g or mL of tissue			
Tissue	**30 min**	**4 h**	**24 h**	**96 h**
Plasma	1181 ± 238 (1.00)	332 ± 5 (1.00)	9 ± 3 (1.00)	1 ± 0 (1.00)
Blood	703 ± 138 (0.60)	194 ± 6 (0.58)	5 ± 2 (0.56)	1 ± 0 (1.00)
Cerebrum	15 ± 6 (0.01)	4 ± 1 (0.01)	<1 (0.00)	N.D.
Cerebellum	21 ± 9 (0.02)	6 ± 1 (0.02)	<1 (0.00)	N.D.
Pituitary gland	360 ± 111 (0.30)	95 ± 22 (0.29)	N.D.	N.D.
Eyeball	35 ± 10 (0.03)	18 ± 1 (0.05)	1 ± 1 (0.11)	N.D.
Harderian gland	149 ± 48 (0.13)	92 ± 11 (0.28)	1 ± 1 (0.11)	<1 (0.00)
Thyroid gland	308 ± 91 (0.26)	80 ± 33 (0.24)	N.D.	N.D.
Trachea	211 ± 97 (0.18)	81 ± 11 (0.24)	3 ± 1 (0.33)	N.D.
Mandibular gland	393 ± 89 (0.33)	97 ± 17 (0.29)	2 ± 1 (0.22)	<1 (0.00)
Thymus	71 ± 15 (0.06)	40 ± 4 (0.12)	1 ± 0 (0.11)	<1 (0.00)

2.6.5.5.1. JTK303-AD-005: Distribution in Rats after Single Administration of [^{14}C]EVG (Continued)

Test Article: [^{14}C]EVG

	Concentration - ng eq. of EVG/g or mL of tissue			
Tissue	**30 min**	**4 h**	**24 h**	**96 h**
Heart	403 ± 100 (0.34)	108 ± 16 (0.33)	2 ± 1 (0.22)	< 1 (0.00)
Lung	330 ± 91 (0.28)	106 ± 12 (0.32)	2 ± 1 (0.22)	<1 (0.00)
Liver	1488 ± 89 (1.26)	374 ± 59 (1.13)	27 ± 3 (3.00)	8 ± 2 (8.00)
Kidney	593 ± 75 (0.50)	176 ± 5 (0.53)	6 ± 1 (0.67)	1 ± 1 (1.00)
Adrenal gland	746 ± 68 (0.63)	140 ± 26 (0.42)	2 ± 2 (0.22)	N.D.
Spleen	206 ± 29 (0.17)	49 ± 4 (0.15)	1 ± 1 (0.11)	<1 (0.00)
Pancreas	330 ± 82 (0.28)	92 ± 9 (0.28)	1 ± 1 (0.11)	<1 (0.00)
Fat	45 ± 12 (0.04)	23 ± 4 (0.07)	1 ± 1 (0.11)	N.D.
Brown fat	205 ± 14 (0.17)	82 ± 9 (0.25)	3 ± 1 (0.33)	<1 (0.00)
Skeletal muscle	117 ± 7 (0.10)	43 ± 4 (0.13)	1 ± 0 (0.11)	N.D.
Skin	97 ± 25 (0.08)	73 ± 4 (0.22)	3 ± 1 (0.33)	1 ± 0 (1.00)

2.6.5.5.1. JTK303-AD-005: Distribution in Rats after Single Administration of [^{14}C]EVG (Continued)

Test Article: [^{14}C]EVG

	Concentration - ng eq. of EVG/g or mL of tissue			
Tissue	**30 min**	**4 h**	**24 h**	**96 h**
Bone marrow	248 ± 35 (0.21)	56 ± 7 (0.17)	N.D.	N.D.
Aorta	248 ± 175 (0.21)	69 ± 8 (0.21)	2 ± 1 (0.22)	N.D.
Mesenteric lymph node	597 ± 126 (0.51)	138 ± 25 (0.42)	3 ± 1 (0.33)	1 ± 1 (1.00)
Testis	46 ± 13 (0.04)	64 ± 8 (0.19)	1 ± 1 (0.11)	<1 (0.00)
Epididymis	68 ± 15 (0.06)	70 ± 4 (0.21)	2 ± 0 (0.22)	< 1 (0.00)
Prostate gland	101 ± 14 (0.09)	47 ± 14 (0.14)	1 ± 0 (0.11)	N.D.
Seminal vesicle	70 ± 9 (0.06)	42 ± 4 (0.13)	1 ± 0 (0.11)	N.D.
Stomach	1589 ± 345 (1.35)	1227 ± 167 (3.70)	9 ± 9 (1.00)	< 1 (0.00)
Small intestine	2545 ± 792 (2.15)	2139 ± 383 (6.44)	12 ± 5 (1.33)	N.D.
Cecum	176 ± 31 (0.15)	419 ± 276 (1.26)	207 ± 144 (23.00)	<1 (0.00)

2.6.5.5.1. JTK303-AD-005: Distribution in Rats after Single Administration of [^{14}C]EVG (Continued)

Test Article: [^{14}C]EVG

	Concentration - ng eq. of EVG/g or mL of tissue			
Tissue	**30 min**	**4 h**	**24 h**	**96 h**
Large intestine	152 ± 24	207 ± 115	48 ± 21	<1
	(0.13)	(0.62)	(5.33)	(0.00)
Urinary bladder	128 ± 17	85 ± 8	2 ± 1	N.D.
	(0.11)	(0.26)	(0.22)	

Data are expressed as the mean values ± standard deviation of 3 animals.
Figures in parentheses are expressed as the ratio of concentration in tissue relative to plasma.
N.D.: Not detected

2.6.5.5.1. JTK303-AD-005: Distribution in Rats after Single Administration of [^{14}C]EVG (Continued)

Test Article: [^{14}C]EVG

Distribution

Species/Strain Number of Animals/Group Sex	Examination Item	Adminis-tration Route	Dose Level (mg/kg)	Dose Volume (mL/kg)	Feeding Condition	Sampling Time (h)	Results
Rat/SD (Crj:CD(SD)IGS) 1 animal/group male	Semi-quantitative whole-body autoradio-grams	Oral	3 (MC)	5	Non-fasting	0.25	Higher levels of radioactivity than those in the blood were found in the gastric contents, intestinal contents, stomach, liver, adrenal gland, and kidney.
						24	A high level of radioactivity was found in the intestinal contents, a low level of radioactivity was found in the intestine, and a trace level of radioactivity was found in the liver.
						96	Trace levels of radioactivity were found only in the liver and intestinal contents.
Rat/SD (Crj:CD(SD)IGS) 3 animals/group male	Concentration of radioactivity in tissues	Oral	3 (MC)	5	Non-fasting	0.5	The radioactivity concentrations in the small intestine, stomach, and liver were high, being 2.15, 1.35, and 1.26 times as compared with that in the plasma (1181 ng eq./mL), respectively. The radioactivity concentrations in the other tissues were lower than those in the plasma.
						4	The radioactivity concentrations in the small intestine, stomach, cecum, and liver were high, being 6.44, 3.70, 1.26, and 1.13 times as compared with that in the plasma (332 ng eq./mL), respectively. The radioactivity concentrations in the other tissues were not higher than those in the plasma.
						24	The radioactivity distributed to each tissue declined in parallel with that in the plasma.
						96	The percentage distribution of radioactivity was 0.01% of the radioactivity administered in the liver and skin; and 0.00% or below the detection limit in the other tissues at this time point.

MC = 0.5% (w/v) aqueous methylcellulose

2.6.5.5.2. 60N-0518: Tissue Distribution in Albino Rats After a Single Oral Dose of [^{14}C]EVG With or Without RTV

Report Title	Study Type	Test Article	Report Number
Quantitative Tissue Distribution of Drug-Related Material Using Whole-Body Autoradiography Following a Single Oral Dose of [^{14}C]GS-9137 With or Without Ritonavir to Male and Female Sprague Dawley Rats	Organ distribution study	[^{14}C]EVG	60N-0518

Species:	Crl:CD IGS, Sprague Dawley Rat	
Gender (M/F) / No. of Animals:	Group 1: 2M/2F	Group 2: 2M/2F
Feeding Condition:	Non-fasted	Non-fasted
Vehicle / Formulation:	1% (w/v) aqueous methylcellulose	EVG: 1% (w/v) aqueous methylcellulose RTV: Norvir® solution diluted with ethanol
Method of Administration:	Oral	Oral
Dose (mg/kg):	1 dose of [^{14}C]EVG 10 mg/kg (actual dose range: 10.39–10.98 mg/kg)	2 doses of RTV 20 mg/kg (12 h and 2 h prior to EVG) (actual dose range: 19.87–20.17 mg/kg); 1 dose of [^{14}C]EVG 10 mg/kg (actual dose range: 10.13–11.04 mg/kg)
Radionuclide:	Carbon-14	
Specific Activity:	27 μCi/mg (in dose)	
Sampling Time:	1 and 8 hours postdose	
Analyte/Assay:	[^{14}C]/Quantitative whole body autoradiography	

2.6.5.5.2. 60N-0518: Tissue Distribution in Albino Rats After a Single Oral Dose of [^{14}C]EVG With or Without RTV (Continued)

Test Article: [^{14}C]EVG

Tissue Type	Tissue	Concentration - µg eq./g tissue							
		[^{14}C]EVG 10 mg/kg				[^{14}C]EVG 10 mg/kg + RTV 20 mg/kg			
		Male 1 h	Female 1 h	Male 8 h	Female 8 h	Male 1 h	Female 1 h	Male 8 h	Female 8 h
Vascular/ Lymphatic	Blood (cardiac)	0.692	2.225	NI	NI	0.288	1.390	0.358	0.267
	Bone marrow	0.258	0.667	NI	NI	0.127	0.422	0.263	0.109
	Lymph node	0.116	0.441	NI	NI	BQL	0.216	BQL	0.191
	Spleen	0.121	0.418	0.106	0.108	0.154	0.374	0.154	BQL
	Thymus	0.168	0.382	NI	NI	BQL	0.242	0.155	BQL
Excretory/ Metabolic	Renal cortex	0.571	1.305	0.885	0.135	0.258	0.605	0.343	0.181
	Renal medulla	0.391	1.404	0.158	0.108	0.183	0.703	0.360	0.175
	Liver	1.857	2.422	0.333	0.285	0.426	1.331	0.776	0.422
	Urinary bladder	0.140	0.821	NI	NI	BQL	0.446	0.488	0.284
	Urinary bladder (contents)	0.747	0.861	NI	NI	0.266	0.267	0.380	BQL
CNS	Brain	BQL	BQL	BQL	BQL	BQL	BQL	BQL	BQL
	Spinal cord	BQL	BQL	BQL	BQL	BQL	BQL	BQL	BQL
Endocrine	Adrenal gland	0.640	1.698	BQL	0.138	0.295	0.994	0.523	0.273
	Pituitary gland	0.302	0.820	NI	NI	0.288	0.496	0.205	0.151
	Thyroid gland	0.260	0.777	NI	NI	0.152	0.465	0.335	BQL
Secretory	Harderian gland	0.193	0.694	NI	NI	BQL	0.362	0.264	0.152
	Pancreas	0.211	0.861	BQL	BQL	0.120	0.502	0.248	BQL
	Salivary gland	0.320	0.774	BQL	BQL	0.181	0.574	0.240	BQL
Adipose	Adipose (brown)	0.510	1.332	0.125	0.127	0.196	0.862	0.393	0.241
	Adipose (white)	BQL	0.326	BQL	NI	0.180	BQL	0.401	0.201
Dermal	Skin	0.155	0.458	0.126	BQL	BQL	0.253	0.265	0.255

2.6.5.5.2. 60N-0518: Tissue Distribution in Albino Rats After a Single Oral Dose of [^{14}C]EVG With or Without RTV (Continued)

Test Article: [^{14}C]EVG

Tissue Type	Tissue	Concentration - µg eq./g tissue							
		[^{14}C]EVG 10 mg/kg				[^{14}C] EVG 10 mg/kg + RTV 20 mg/kg			
		Male 1 h	Female 1 h	Male 8 h	Female 8 h	Male 1 h	Female 1 h	Male 8 h	Female 8 h
Reproductive	Epididymis	0.119	NA	NI	NA	BQL	NA	0.248	NA
	Prostate gland	0.133	NA	NI	NA	BQL	NA	0.134	NA
	Seminal vesicles	BQL	NA	0.138	NA	BQL	NA	BQL	NA
	Testis	BQL	NA	BQL	NA	BQL	NA	0.235	NA
	Mammary glands	NA	0.552	NA	NI	NA	0.305	NA	0.254
	Ovary	NA	0.900	NA	NI	NA	0.781	NA	0.340
	Uterus	NA	0.484	NA	NI	NA	0.561	NA	0.283
	Vagina	NA	0.458	NA	NI	NA	0.402	NA	0.379
Skeletal/ Muscular	Bone	BQL	BQL	NI	NI	BQL	BQL	BQL	BQL
	Heart	0.428	1.198	NI	NI	0.144	0.625	0.295	0.122
	Skeletal muscle	0.109	0.316	BQL	BQL	BQL	0.287	0.139	BQL
Respiratory Tract	Lung	0.397	1.494	0.129	0.289	0.248	1.026	0.401	0.200
	Nasal turbinates	3.083	0.538	NI	NI	BQL	12.743	0.115	BQL
Alimentary Canal	Cecum	0.216	1.392	4.214	15.492	0.176	0.846	5.717	9.093
	Cecum (contents)	BQL	BQL	347.002	375.769	BQL	BQL	164.155	342.518
	Large intestine	0.180	0.522	0.973	9.452	BQL	0.327	0.680	0.172
	Large intestine (contents)	BQL	BQL	203.144	1609.01[a]	BQL	BQL	617.214	831.008
	Stomach (gastric mucosa)	0.174	0.740	0.137	BQL	6.842	31.441	0.250	0.842
	Stomach (contents)	999.030	1330.232[a]	0.422	0.162	500.515	1000.260	14.084	58.901
	Small intestine	15.219	16.268	2.315	1.855	7.387	4.588	10.565	3.261
	Small intestine (contents)	976.895	970.503	23.259	10.713	198.764	51.343	74.918	39.240

2.6.5.5.2. 60N-0518: Tissue Distribution in Albino Rats After a Single Oral Dose of [^{14}C]EVG With or Without RTV (Continued)

Test Article: [^{14}C]EVG

Tissue Type	Tissue	Concentration - µg eq./g tissue							
		[^{14}C]EVG 10 mg/kg.				[^{14}C]EVG 10 mg/kg. + RTV 20 mg/kg.			
		Male 1 h	Female 1 h	Male 8 h	Female 8 h	Female 1 h	Male 8 h	Female 8 h	Male 1 h
Ocular	Eye uveal tract	0.333	0.360	NI	NI	BQL	0.338	BQL	0.252
	Eye lens	BQL	BQL	NI	NI	BQL	BQL	BQL	BQL

BQL = Below Quantifiable Limits, value is below the LLOQ; NI = Image Not Identified due to little or no radioactivity (treated as BQL); LLOQ = 0.0008426 µCi/g / 0.0080 µCi/µg = 0.105 µg equivalent / g tissue; ULOQ = 8.177 µCi/g / 0.0080 µCi/µg = 1022.125 µg equivalent / g tissue

a Above Upper Limit of Quantitation (ULOQ) and so extrapolated

2.6.5.5.3. JTK303-AD-022: Excretion in Rats After Repeated Oral Administration of [^{14}C]EVG

Report Title	Study Type	Test Article	Report Number (Study Number)
Pharmacokinetics in Rats after Repeated Oral Administration of [^{14}C]JTK-303	Distribution	EVG	JTK303-AD-022

Species	**Rat**			
Gender (M/F) / No. of Animals	3M per Group			
Feeding Condition	Not Fasted			
Vehicle/Formulation	Methylcellulose (0.5% w/v)/ Suspension			
Method of Administration	Oral/Once Daily for 7 Days			
Dose (mg/kg)	3			
Analyte	[^{14}C]EVG			
Assay	Radio-HPLC			
Tissue	**Radioactivity concentration (ng eq. of EVG/g or mL)**			
	Dose 1 – 24 h	**Dose 4 – 24 h**	**Dose 7 – 24 h**	**Dose 7 –168 h**
Plasma	11 ± 5 (1.00)	13 ± 4 (1.00) [1.2]	17 ± 4 (1.00) [1.5]	2 ± 0 (1.00)
Blood	7 ± 3 (0.64)	8 ± 2 (0.62) [1.1]	10 ± 5 (0.59) [1.4]	2 ± 0 (1.00)
Cerebrum	<1	<1	<1	N.D.

2.6.5.5.3. JTK303-AD-022: Excretion in Rats After Repeated Oral Administration of [^{14}C]EVG (Continued)

Test Article: [^{14}C]EVG

Tissue	Radioactivity concentration (ng eq. of EVG/g or mL)			
	Dose 1 – 24 h	**Dose 4 – 24 h**	**Dose 7 – 24 h**	**Dose 7 –168 h**
Cerebellum	N.D.	N.D.	N.D.	N.D.
Pituitary gland	N.D.	N.D.	N.D.	N.D.
Eyeball	N.D.	2 ± 1 (0.15)	1 ± 1 (0.06)	1 ± 1 (0.50)
Harderian gland	2 ± 1 (0.18)	1 ± 1 (0.08) [0.5]	2 ± 1 (0.12) [1.0]	<1
Thyroid gland	N.D.	N.D.	N.D.	N.D.
Trachea	N.D.	N.D.	N.D.	N.D.
Mandibular gland	2 ± 1 (0.18)	1 ± 1 (0.08) [0.5]	2 ± 1 (0.12) [1.0]	1 ± 1 (0.50)
Thymus	N.D.	1 ± 0 (0.08)	1 ± 1 (0.06)	<1
Heart	2 ± 1	2 ± 1	3 ± 1	<1
	(0.18)	(0.15) [1.0]	(0.18) [1.5]	

2.6.5.5.3. JTK303-AD-022: Excretion in Rats After Repeated Oral Administration of [^{14}C]EVG (Continued)

Test Article: [^{14}C]EVG

Tissue	Radioactivity concentration (ng eq. of EVG/g or mL)			
	Dose 1 – 24 h	**Dose 4 – 24 h**	**Dose 7 – 24 h**	**Dose 7 –168 h**
Lung	2 ± 1	3 ± 1	4 ± 2	1 ± 0
	(0.18)	(0.23) [1.5]	(0.24) [2.0]	(0.50)
Liver	22 ± 3	52 ± 10	73 ± 9	15 ± 2
	(2.00)	(4.00) [2.4]	(4.29) [3.3]	(7.50)
Kidney	6 ± 2	9 ± 1	13 ± 2	3 ± 1
	(0.55)	(0.69) [1.5]	(0.76) [2.2]	(1.50)
Adrenal gland	N.D.	4 ± 1	3 ± 3	N.D.
		(0.31)	(0.18)	
Spleen	1 ± 1	1 ± 1	2 ± 0	1 ± 0
	(0.09)	(0.08) [1.0]	(0.12) [2.0]	(0.50)
Pancreas	2 ± 1	1 ± 1	2 ± 1	<1
	(0.18)	(0.08) [0.5]	(0.12) [1.0]	
Fat	N.D.	3 ± 1	3 ± 1	1 ± 1
		(0.23)	(0.18)	(0.50)
Brown fat	3 ± 1	3 ± 1	4 ± 1	1 ± 1
	(0.27)	(0.23) [1.0]	(0.24) [1.3]	(0.50)

2.6.5.5.3. JTK303-AD-022: Excretion in Rats After Repeated Oral Administration of [^{14}C]EVG (Continued)

Test Article: [^{14}C]EVG

Tissue	Radioactivity concentration (ng eq. of EVG/g or mL)			
	Dose 1 – 24 h	**Dose 4 – 24 h**	**Dose 7 – 24 h**	**Dose 7 –168 h**
Skeletal muscle	1 ± 1 (0.09)	1 ± 0 (0.08) [1.0]	1 ± 1 (0.06) [1.0]	<1
Skin	3 ± 1 (0.27)	5 ± 1 (0.38) [1.7]	6 ± 1 (0.35) [2.0]	1 ± 0 (0.50)
Bone marrow	N.D.	N.D.	N.D.	N.D.
Aorta	N.D.	N.D.	2 ± 2 (0.12)	N.D.
Mesenteric lymph node	2 ± 2 (0.18)	3 ± 1 (0.23) [1.5]	5 ± 1 (0.29) [2.5]	3 ± 1 (1.50)
Testis	2 ± 1 (0.18)	2 ± 1 (0.15) [1.0]	2 ± 1 (0.12) [1.0]	<1
Epididymis	2 ± 2 (0.18)	3 ± 1 (0.23) [1.5]	3 ± 1 (0.18) [1.5]	1 ± 1 (0.50)
Prostate gland	1 ± 1 (0.09)	1 ± 1 (0.08) [1.0]	1 ± 1 (0.06) [1.0]	1 ± 0 (0.50)

2.6.5.5.3. JTK303-AD-022: Excretion in Rats After Repeated Oral Administration of [^{14}C]EVG (Continued)

Test Article: [^{14}C]EVG

Tissue	Radioactivity concentration (ng eq. of EVG/g or mL)			
	Dose 1 – 24 h	**Dose 4 – 24 h**	**Dose 7 – 24 h**	**Dose 7 –168 h**
Seminal vesicle	1 ± 1 (0.09)	1 ± 0 (0.08) [1.0]	1 ± 1 (0.06) [1.0]	<1
Stomach	25 ± 27 (2.27)	5 ± 2 (0.38) [0.2]	8 ± 6 (0.47) [0.3]	<1
Small intestine	13 ± 11 (1.18)	5 ± 5 (0.38) [0.4]	5 ± 4 (0.29) [0.4]	N.D.
Cecum	156 ± 194 (14.18)	28 ± 22 (2.15) [0.2]	41 ± 7 (2.41) [0.3]	<1
Large intestine	82 ± 89 (7.45)	26 ± 18 (2.00) [0.3]	42 ± 12 (2.47) [0.5]	1 ± 1 (0.50)
Urinary bladder	N.D.	3 ± 2 (0.23)	4 ± 1 (0.24)	N.D.

EVG = elvitegravir; N.D. = not detected

Data are expressed as the mean values ± standard deviation of 3 animals. The concentration <1 ng eq./g indicates the value between N.D. and 1 ng eq./g.

Figures in parentheses are expressed as the ratio of concentration in tissue relative to plasma. Figures in brackets are expressed as the ratio of concentration in tissue relative to that after a single dose.

2.6.5.5.4. JTK303-AD-006: Pharmacokinetics in Dogs after Single Administration of [^{14}C]EVG

Report Title	Study Type	Test Article	Report Number (Study Number)
Pharmacokinetics in Dogs after Single Administration of [^{14}C]-JTK-303	Distribution	[^{14}C]EVG	JTK303-AD-006 (AE-3858-G)

Absorption

Species/Strain Number of Animals/Group Sex	Administration Route	Dose Level (mg/kg)	Dose Volume (mL/kg)	Feeding Condition	C_{5min} (ng eq./mL)
Dog/Beagle (NOSAN) 3 animals/group male	IV	1 (PEG400)	0.2	Not fasted (Postprandial)	691 ± 149
	Oral	3 (MC)	2		NA

C_{5min} = plasma concentration at 5 minutes after administration; IV = intravenous; MC = 0.5% (w/v) aqueous methylcellulose; PEG400 = 80% (v/v) aqueous polyethylene glycol 400

2.6.5.5.4. JTK303-AD-006: Pharmacokinetics in Dogs after Single Administration of [^{14}C]EVG (Continued)

Test Article: [^{14}C]EVG

Tissue	Radioactivity Concentration at 168 Hours Postdose (ng eq. of EVG/g or mL)	
	Single Oral Administration of [^{14}C]EVG (dose: 3 mg /kg)	Single IV administration [^{14}C]EVG (dose: 1 mg /kg)
Plasma	2 ± 1 (1.00)	2 ± 1 (1.00)
Blood	1 ± 1 (0.50)	1 ± 1 (0.50)
Cerebrum	N.D.	N.D.
Cerebellum	N.D.	N.D.
Pituitary gland	N.D.	N.D.
Eyeball	<1 (0.00)	<1 (0.00)
Thyroid gland	1 ± 1 (0.50)	<1 (0.00)
Trachea	1 ± 1 (0.50)	<1 (0.00)
Mandibular gland	N.D.	1 ± 1 (0.50)
Thymus	<1 (0.00)	(0.00)
Heart	N.D.	<1 (0.00)
Lung	1 ± 0 (0.50)	1 ± 0 (0.50)
Liver	15 ± 6 (7.50)	8 ± 1 (4.00)
Kidney	2 ± 3 (1.00)	2 ± 1 (1.00)
Adrenal gland	N.D.	1 ± 1 (0.50)
Spleen	N.D.	<1 (0.00)
Pancreas	1 ± 1 (0.50)	1 ± 1 (0.50)

2.6.5.5.4. JTK303-AD-006: Pharmacokinetics in Dogs after Single Administration of [^{14}C]EVG (Continued)

Test Article: [^{14}C]EVG

Tissue	Radioactivity Concentration at 168 Hours Postdose (ng eq. of EVG/g or mL)	
	Single Oral Administration of [^{14}C]EVG (dose: 3 mg/kg)	Single IV administration [^{14}C]EVG (dose: 1 mg/kg)
Fat	N.D.	N.D.
Brown fat	1 ± 0 (0.50)	1 ± 0 (0.50)
Skeletal muscle	N.D.	N.D.
Skin	1 ± 0 (0.50)	1 ± 0 (0.50)
Bone marrow	1 ± 0 (0.50)	1 ± 0 (0.50)
Aorta	N.D.	N.D.
Mesenteric lymph node	1 ± 1 (0.50)	1 ± 0 (0.50)
Testis	N.D.	<1 (0.00)
Epididymis	N.D.	<1 (0.00)
Prostate gland	1 ± 1 (0.50)	<1 (0.00)
Stomach	1 ± 1 (0.50)	1 ± 0 (0.50)
Small intestine	1 ± 1 (0.50)	<1 (0.00)
Cecum	1 ± 1 (0.50)	<1 (0.00)
Large intestine	1 ± 1 (0.50)	1 ± 1 (0.50)
Urinary bladder	1 ± 0 (0.50)	<1 (0.00)
Gall bladder	3 ± 2 (1.50)	2 ± 1 (1.00)

EVG = elvitegravir; N.D. = not detected; MC = 0.5% (w/v) aqueous methylcellulose; PEG400 = 80% (v/v) aqueous polyethylene glycol 400

Data are expressed as the mean values ± standard deviation of 3 animals. Figures in parentheses are expressed as the ratio of concentration in tissue relative to plasma.

2.6.5.5.4. JTK303-AD-006: Pharmacokinetics in Dogs after Single Administration of [^{14}C]EVG (Continued)

Test Article: [^{14}C]EVG

Tissue	Percentage distribution (% of dose)	
	Single Oral Administration of [^{14}C]EVG (dose: 3 mg/kg)	**Single IV administration [^{14}C]EVG (dose: 1 mg/kg)**
Blood	0.00 ± 0.00	0.01 ± 0.01
Cerebrum	N.D.	N.D.
Cerebellum	N.D.	N.D.
Pituitary gland	N.D.	N.D.
Eyeball	0.00 ± 0.00	0.00 ± 0.00
Thyroid gland	0.00 ± 0.00	0.00 ± 0.00
Trachea	0.00 ± 0.00	0.00 ± 0.00
Mandibular gland	N.D.	0.00 ± 0.00
Thymus	0.00 ± 0.00	0.00 ± 0.00
Heart	N.D.	0.00 ± 0.00
Lung	0.00 ± 0.00	0.00 ± 0.00
Liver	0.01 ± 0.01	0.02 ± 0.00
Kidney	0.00 ± 0.00	0.00 ± 0.00
Adrenal gland	N.D.	0.00 ± 0.00
Spleen	N.D.	0.00 ± 0.00
Pancreas	0.00 ± 0.00	0.00 ± 0.00
Fat	N.D.	N.D.
Skeletal muscle	N.D.	N.D.
Skin	0.01 ± 0.01	0.02 ± 0.01
Testis	N.D.	0.00 ± 0.00
Epididymis	N.D.	0.00 ± 0.00

2.6.5.5.4. JTK303-AD-006: Pharmacokinetics in Dogs after Single Administration of [^{14}C]EVG (Continued)

Test Article: [^{14}C]EVG

Tissue	Percentage distribution (% of dose)	
	Single Oral Administration of [^{14}C]EVG (dose: 3 mg/kg)	**Single IV administration [^{14}C]EVG (dose: 1 mg/kg)**
Prostate gland	0.00 ± 0.00	0.00 ± 0.00
Stomach	0.00 ± 0.00	0.00 ± 0.00
Small intestine	0.00 ± 0.00	0.00 ± 0.00
Cecum	0.00 ± 0.00	0.00 ± 0.00
Large intestine	0.00 ± 0.00	0.00 ± 0.00
Urinary bladder	0.00 ± 0.00	0.00 ± 0.00
Gall bladder	0.00 ± 0.00	0.00 ± 0.00
Bile in gall bladder	0.00 ± 0.00	0.00 ± 0.01
Gastric contents	N.D.	N.D.
Small intestinal contents	N.D.	N.D.
Large intestinal contents	0.00 ± 0.01	0.00 ± 0.01

EVG = elvitegravir; N.D. = not detected; MC = 0.5% (w/v) aqueous methylcellulose; PEG400 = 80% (v/v) aqueous polyethylene glycol 400
Data are expressed as the mean values ± standard deviation of 3 animals. Blood, fat, skeletal muscle and skin weights were assumed to be 8.3%, 14.5%, 46%, and 17% of body weight, respectively.

2.6.5.5.4. JTK303-AD-006: Pharmacokinetics in Dogs after Single Administration of [^{14}C]EVG (Continued)

Test Article: [^{14}C]EVG

Species/Strain Number of Animals/Group Sex	Examination Item	Adminis-tration Route	Dose Level (mg/kg)	Dose Volume (mL/kg)	Feeding Condition	Sampling Time (h)	Results
Dog/Beagle (NOSAN) 3 animals/group male	Concentration of radioactivity in tissues	IV	1 (PEG400)	0.2	Not fasted (Post-prandial)	168	The percentage distribution of radioactivity was 0.02% of the radioactivity administered in the liver and skin, 0.01% in the blood, and 0.00% or below the detection limit in the other tissues at this time point.
		Oral	3 (MC)	2			The percentage distribution of radioactivity was 0.01% of the radioactivity administered in the liver and skin; and 0.00% or below the detection limit in the other tissues at this time point.

EVG = elvitegravir; IV = intravenous; MC = 0.5% (w/v) aqueous methylcellulose; PEG400 = 80% (v/v) aqueous polyethylene glycol 400

2.6.5.5.5. AD-216-2034: Distribution in Albino Rats After Single Administration of [^{14}C]COBI

Report Title	Study Type	Test Article	Report Number
Pharmacokinetics, Distribution, Metabolism, and Excretion of [^{14}C]GS-9350 Following Oral Administration to Rats	Distribution	[^{14}C]COBI	AD-216-2034
Species:	Sprague Dawley Rat (H1a:[SD]CVF)		
Gender (M/F) / No. of Animals:	Group 3: 6 male (one per time point)		
Feeding Condition:	Fasted		
Vehicle / Formulation:	5% (v/v) ethanol, 15% (v/v) propylene glycol adjusted to pH 3.60 with HCl		
Method of Administration:	Oral		
Dose (mg/kg):	1 dose of [^{14}C]COBI 10 mg/kg		
Radionuclide:	Carbon-14		
Specific Activity:	21.5 μCi/mg (in dose)		
Sampling Time:	0.25, 1, 4, 8, 12, and 24 hours postdose		
Analyte/Assay:	[^{14}C]/Quantitative whole body autoradiography		

2.6.5.5.5. AD-216-2034: Distribution in Albino Rats After Single Administration of [^{14}C]COBI (Continued)

Test Article: [^{14}C]COBI

	ng Equivalents [^{14}C]COBI/g					
	Animal Number (Sacrifice Time)					
	B07114	B07115	B07116	B07117	B07118	B07119
Tissue	(0.25 Hours)	(1 Hour)	(4 Hours)	(8 Hours)	(12 Hours)	(24 Hours)
Adipose (brown)	1320	2870	1330	1030	1480	1280
Adipose (white)	205	748	142	128	117	87.8
Adrenal gland	5090	28,800	4290	1390	1480	1740
Bile	353,000[a]	214,000	89,300	14,400	11,500	11,000
Blood	347	723	200	119	117	77.7
Bone	74.0	142	54.6	94.1	52.7	BLQ
Bone marrow	1020	3710	1170	1210	1260	650
Brain	BLQ	47.7	49.0	55.4	49.1	BLQ
Cecum	890	1210	1840	2540	1820	1030
Cecum contents	BLQ	58.5	398,000[a]	229,000	89,200	6660
Choroid plexus	1620	2580	824	1210	1350	1550
Diaphragm	870	2050	787	451	556	357
Epididymis	59.5	267	165	214	263	208
Esophageal contents	33,600	53.0	641	115	BLQ	BLQ
Esophagus	557	1230	613	487	300	278
Exorbital lacrimal gland	515	3530	2290	1960	1870	1410
Eye	87.0	144	85.0	54.5	98.3	62.0
Eye (lens)	BLQ	BLQ	BLQ	BLQ	BLQ	BLQ
Eye (uveal tract)	349	979	545	557	318	197
Harderian gland	367	2650	1670	2270	3410	1720
Heart	1070	2260	707	775	763	634

2.6.5.5.5. AD-216-2034: Distribution in Albino Rats After Single Administration of [^{14}C]COBI (Continued)

Test Article: [^{14}C]COBI

Tissue	ng Equivalents [^{14}C]COBI/g					
	Animal Number (Sacrifice Time)					
	B07114 (0.25 Hours)	B07115 (1 Hour)	B07116 (4 Hours)	B07117 (8 Hours)	B07118 (12 Hours)	B07119 (24 Hours)
Intra-orbital lacrimal gland	368	3650	2020	2150	1730	1370
Kidney	3630	6350	1810	1390	1550	1030
Large intestinal contents	NR	51.2	BLQ	487,000[a]	330,000	11,600
Large intestine	582	2350	1620	1380	2540	1900
Liver	49,800	33,900	16,500	6280	5570	2620
Lung	865	2230	579	508	540	486
Lymph nodes	279	2860	708	567	650	477
Muscle (skeletal)	424	1150	231	215	349	149
Nasal turbinates	111	395	186	277	324	220
Pancreas	1280	2960	1370	1090	1010	725
Pituitary gland	1550	6720	2820	1820	3500	1550
Preputial gland	461	1760	795	1080	NR	NR
Prostate	242	1100	751	443	720	342
Renal cortex	3550	6160	1920	1480	1660	1080
Renal medulla	3690	6900	1740	1190	1340	941
Salivary gland	1430	5190	1950	1540	1170	691
Seminal vesicles	BLQ	137	133	189	212	146
Skin	191	521	232	188	236	186
Small intestinal contents	318,000[a]	608,000[a]	803,000[a]	6410	3910	1910
Small intestine	1440	4110	2670	1920	961	623
Spinal cord	BLQ	BLQ	BLQ	52.6	BLQ	BLQ
Spleen	1990	6060	1470	1400	1630	785

2.6.5.5.5. AD-216-2034: Distribution in Albino Rats After Single Administration of [^{14}C]COBI (Continued)

Test Article: [^{14}C]COBI

Tissue	ng Equivalents [^{14}C]COBI/g					
	Animal Number (Sacrifice Time)					
	B07114 (0.25 Hours)	B07115 (1 Hour)	B07116 (4 Hours)	B07117 (8 Hours)	B07118 (12 Hours)	B07119 (24 Hours)
Stomach	1340	2550	1550	1820	1470	1230
Stomach contents	198,000	147,000	3610	183	BLQ	5840
Testis	BLQ	128	120	166	282	136
Thymus	247	1360	602	552	462	366
Thyroid	2520	6140	536	1270	1200	748
Urinary bladder	630	1830	1660	360	NR	NR
Urine	2300	5680	5990	319	NR	NR

BLQ = below limit of quantitation (<43.5 ng equivalents [^{14}C]COBI/g); COBI = cobicistat; NR = not represented (tissue not present in section)

a One or more samples were above the upper limit of quantitation (ULOQ, >424,000 ng equivalents [^{14}C]COBI/g)

2.6.5.5.6. AD-216-2060: Distribution in Pigmented Rats Following Single Oral Dose of [^{14}C]COBI

Report Title	Study Type	Test Article	Report Number
Whole-Body Autoradiography (WBA) of Rats Following Oral Administration of [^{14}C]GS-9350	Distribution	[^{14}C]COBI	AD-216-2060
Species:	Long Evans rats (HsdBlu:LE)		
Gender (M/F) / No. of Animals:	Group 1: 7 male (one per time point)		
Feeding Condition:	Fasted		
Vehicle / Formulation:	5% (v/v) ethanol, 15% (v/v) propylene glycol adjusted to pH 3.61 with HCl		
Method of Administration:	Oral		
Dose (mg/kg):	1 dose of [^{14}C]COBI 10 mg/kg		
Radionuclide:	Carbon-14		
Specific Activity:	250 μCi/kg (in dose)		
Sampling Time:	0.25, 1, 4, 12, 24, 48, and 72 hours postdose		
Analyte/Assay:	[^{14}C]/Quantitative whole body autoradiography		

2.6.5.5.6. AD-216-2060: Distribution in Pigmented Rats Following Single Oral Dose of [^{14}C]COBI (Continued)

Test Article: [^{14}C]COBI

Tissue	ng Equivalents [^{14}C]COBI/g						
	Animal Number (Sacrifice Time)						
	B10527 (0.25 Hours)	B10528 (1 Hour)	B10529 (4 Hours)	B10530 (12 Hours)	B10531 (24 Hours)	B10532 (48 Hours)	B10533 (72 Hours)
Adipose (brown)	1430	7610	1180	1080	1270	711	806
Adipose (white)	297	2380	BLQ	82.5	113	69.2	BLQ
Adrenal gland	8530	35,400	3280	1850	2600	812	1330
Bile	175,000	94,100	30,000	ND	8170	3860	5070
Blood	960	1700	192	132	127	BLQ	BLQ
Bone	51.8	255	128	65.6	52.7	BLQ	63.5
Bone marrow	1070	5000	902	817	735	263	251
Brain	BLQ	BLQ	53.4	BLQ	BLQ	BLQ	BLQ
Cecum	1070	3210	1150	2040	809	225	99.6
Cecum contents	BLQ	3430	281,000	259,000	3450	595	276
Diaphragm	1860	3940	604	672	540	250	245
Epididymis	109	674	254	207	216	74.8	91.6
Esophageal contents	148,000	483	55.1	60.2	BLQ	BLQ	BLQ
Esophagus	2770	3300	443	338	386	193	200
Exorbital lacrimal gland	942	6930	2750	1660	1300	357	698
Eye	63.7	587	480	709	678	324	566
Eye (lens)	BLQ	BLQ	BLQ	BLQ	BLQ	BLQ	BLQ
Eye (uveal tract)	1030	5820	4400	6620	6530	3760	4500
Harderian gland	374	3790	2870	2440	1670	482	476
Heart	2010	4440	815	643	669	183	242

2.6.5.5.6. AD-216-2060: Distribution in Pigmented Rats Following Single Oral Dose of [^{14}C]COBI (Continued)

Test Article: [^{14}C]COBI

Tissue	ng Equivalents [^{14}C]COBI/g						
	Animal Number (Sacrifice Time)						
	B10527 (0.25 Hours)	B10528 (1 Hour)	B10529 (4 Hours)	B10530 (12 Hours)	B10531 (24 Hours)	B10532 (48 Hours)	B10533 (72 Hours)
Intra-orbital lacrimal gland	623	5730	2650	1770	1170	391	582
Kidney	5290	11,500	1530	1260	1230	578	570
Large intestinal contents	BLQ	4520	9030	145,000	11,000	1730	405
Large intestine	594	3250	2060	947	709	460	203
Liver	77,400	48,000	12,700	6350	3850	2070	1560
Lung	2160	6090	642	523	522	222	205
Lymph nodes	496	3880	726	664	397	225	245
Muscle (skeletal)	465	2190	246	260	249	101	137
Nasal turbinates	154	836	147	559	159	BLQ	120
Pancreas	2150	5010	1510	1280	820	240	293
Pituitary gland	2600	14,200	3130	3520	4570	1120	1030
Preputial gland	407	3630	884	1010	1060	534	593
Prostate	279	2030	605	552	537	93.5	194
Renal cortex	5230	9490	1550	1320	1260	644	617
Renal medulla	5350	13,200	1530	1220	1180	550	531
Salivary gland	2410	7660	1410	895	564	208	190
Seminal vesicles	72.1	438	98.5	159	240	136	222
Skin (nonpigmented)	244	1280	233	238	224	73.2	88.8
Skin (pigmented)	292	1440	396	502	315	197	147
Small intestinal contents	205,000	310,000	316,000	2870	613	190	107

2.6.5.5.6. AD-216-2060: Distribution in Pigmented Rats Following Single Oral Dose of [^{14}C]COBI (Continued)

Test Article: [^{14}C]COBI

Tissue	ng Equivalents [^{14}C]COBI/g						
	Animal Number (Sacrifice Time)						
	B10527 (0.25 Hours)	B10528 (1 Hour)	B10529 (4 Hours)	B10530 (12 Hours)	B10531 (24 Hours)	B10532 (48 Hours)	B10533 (72 Hours)
Small intestine	1150	10,600	2440	1730	961	269	160
Spinal cord	BLQ	46.6	51.1	BLQ	BLQ	BLQ	BLQ
Spleen	2330	8220	1620	1060	726	323	311
Stomach	1220	3150	1070	1040	829	335	377
Stomach contents	291,000	74,300	1400	BLQ	BLQ	BLQ	BLQ
Testis	BLQ	174	125	122	122	55.5	68.7
Thymus	274	2340	524	305	297	167	189
Thyroid	3510	6350	1120	756	1110	254	398
Urinary bladder	2240	8350	10,200	281	477	279	187
Urine	2020	1870	4770	494	1240	88.6	108

BLQ = below the limit of quantitation (< 46.2 ng equivalents [^{14}C]COBI/g); ND = not detectable (sample shape not discernible from background or surrounding tissue)

Note: ng Equivalent/g values are reported to 3 significant figures with a maximum of 3 decimal places

2.6.5.6. Pharmacokinetics: Plasma Protein Binding

2.6.5.6.1. AD-183-2024: Ex Vivo Plasma Protein Binding of EVG in Mice

Report Title	Study Type	Test Article	Report Number
Ex Vivo Plasma Protein Binding Determination of EVG in CD-1 Mice Receiving Once Daily Oral Administration of EVG for 7 Days	Plasma protein binding study (ex vivo)	[^{14}C]EVG	AD-183-2024

Study System:	The plasma protein binding of EVG in mice receiving once daily oral administration of EVG (200 mg/kg or 2000 mg/kg) for 1 to 7 days, with or without ritonavir (RTV), was studied by equilibrium dialysis (with a 4-hour dialysis equilibrium time). From 265 CD-1 mouse plasma samples (from Study 60N-0630), samples from the same group were pooled to create 14 plasma samples (7 males and 7 females). Control mouse plasma was pooled from at least 3 males and 3 females. [^{14}C]EVG was spiked into each pooled plasma sample to obtain a [^{14}C]EVG concentration of 0.1 µg/mL in the initial experiment. Twelve of those plasma samples were repeated by increasing the [^{14}C]EVG concentration to 0.5µg/mL due to low radioactivity detected in postdialysis buffer samples. [^{14}C]EVG radioactiviy in plasma and buffer was determined by liquid scintillation counting.
Species:	CD-1 mouse
Spiked [^{14}C]EVG Concentration:	0.5 µg/mL

Pooled Plasma Sample			% Unbound
Group No.	Treatment	Gender	
1	EVG 200 mg/kg 1 Dose on Day 1	Male	0.39
		Female	0.33
2	EVG 2000 mg/kg 1 Dose on Day 1	Male	0.30
		Female	0.26

2.6.5.6.1. AD-183-2024: Ex Vivo Plasma Protein Binding of EVG in Mice (Continued)

Test Article: EVG

Pooled Plasma Sample			% Unbound
Group No.	Treatment	Gender	
3	EVG 200 mg/kg 1 Dose/Day on Days 1 to 7	Male	0.34
		Female	0.22
4	EVG 2000 mg/kg 1 Dose/Day on Days 1 to 7	Male	0.36
		Female	0.23
5	EVG 200 mg/kg + RTV 25 mg/kg 1 Dose/Day on Days 1 to 7	Male	0.39
		Female	0.28
6	EVG 2000 mg/kg + RTV 25 mg/kg 1 Dose/Day on Days 1 to 7	Male	0.41
		Female	0.32
Overall Mean % Unbound ± SD		0.32 ± 0.06	
Pooled Control Overall Mean % Unbound ± SD (n = 3)		0.28 ± 0.00	

2.6.5.6.2. JTK303-AD-014: Protein Binding of EVG In Vitro

Report Title	Study Type	Test Article	Report Number (Study Number)
Protein Binding of JTK-303 in Vitro	Distribution study	[^{14}C]EVG	JTK303-AD-014 (JK303PK031)

Species	Sample	Concentration (μg/mL)	Fraction Bound (%) Mean ± SD (n = 3)	Mean % Unbound
Rat	Plasma	0.1	99.89 ± 0.01	0.11
		1	99.93 ± 0.01	0.07
		10	99.93 ± 0.00	0.07
Dog	Plasma	0.1	99.23 ± 0.17	0.77
		1	99.22 ± 0.15	0.78
		10	99.19 ± 0.16	0.81
Monkey	Plasma	0.1	98.83 ± 0.11	1.17
		1	98.81 ± 0.09	1.19
		10	98.80 ± 0.09	1.20

2.6.5.6.2. JTK303-AD-014: Protein Binding of EVG In Vitro (Continued)

Test Article: EVG

Species	Sample	Concentration (μg/mL)	Fraction Bound (%)	Mean % Unbound
Human	Plasma	0.1	99.35 ± 0.05	0.65
		1	99.34 ± 0.07	0.66
		10	99.31 ± 0.04	0.69
	5% HSA	0.1	99.40 ± 0.02	0.60
		1	99.39 ± 0.01	0.61
		10	99.38 ± 0.01	0.62
	0.07% AAG	0.1	39.25 ± 1.04	60.75
		1	39.05 ± 0.93	60.95
		10	40.68 ± 1.99	59.32
	0.05% / 5% AAG/HSA	0.1	99.45 ± 0.01	0.55
		1	99.39 ± 0.01	0.61
		10	99.36 ± 0.03	0.64
	0.1% / 5% AAG/HSA	0.1	99.06 ± 0.63	0.94
		1	99.33[a]	0.67
		10	99.44 ± 0.01	0.56
	0.2% / 5% AAG/HSA	0.1	99.44 ± 0.02	0.56
		1	99.43 ± 0.01	0.57
		10	99.41 ± 0.01	0.59

Mean % Unbound = (100% - Mean Fraction Bound)

AAG = α1-acid glycoprotein; HSA = human serum albumin; SD = standard deviation

a The mean of 2 measurements

2.6.5.6.3. AD-216-2026 and AD-216-2076: Plasma protein binding of COBI

Report Title	Study Type	Test Article	Report Number
Plasma Protein Binding of GS-9350 in CD-1 Mice	Plasma protein binding	COBI	AD-216-2076
Plasma Protein Binding of GS-9350			AD-216-2026

Study System: Plasma from Mouse, Rat, Dog, Monkey, and Human

Target Entry, Test System, and Method: Equilibrium dialysis for 3 hours at 37°C against 0.133 M phosphate buffer, pH 7.4. Analysis by LC/MS/MS.

	Fraction Unbound (%)			
	Concentration			
Matrix	1 µM	10 µM	30 µM	Mean
Mouse Plasma	3.31 ± 0.14	4.78 ± 0.27	6.15 ± 0.48	4.75
Rat plasma	2.33 ± 0.06	5.34 ± 0.24	8.51 ± 0.48	5.40
Dog plasma	5.68 ±0.60	6.46 ± 0.60	6.33 ± 0.40	6.16
Cynomolgus monkey plasma	4.31 ± 0.50	6.17 ± 0.50	9.13 ± 0.30	6.54
Human plasma	6.33 ± 0.80	8.92 ± 0.9	7.54 ± 0.60	7.60

COBI = cobicistat

2.6.5.7. Pharmacokinetics: Study in Pregnant or Nursing Animals

2.6.5.7.1. TX-183-2006: Excretion of EVG in Milk

Report Title	Study Type	Test Article	Report Number (Study Number)
Oral (Gavage) Developmental and Perinatal/Postnatal Reproduction Toxicity Study of GS-9137 in Rats, Including a Postnatal Behavioral/Functional Evaluation and a 28-Day Juvenile Toxicity Evaluation	Distribution study	[^{14}C]EVG	TX-183-2006

Administration Route:	Oral
Dose level:	0, 300, 100, 2000 mg/kg/day
Animals:	Female Crl:CD(SD) rat, F0 at Day 14 of lactation (4/group)
Matrices:	Plasma, Milk
Analytes:	EVG, GS-9200, GS-9202
Assay:	LC-MS/MS

		Concentration (ng/mL) 30 min After Dosing (mean ± SD)			
		EVG Dose (mg/kg)			
Analyte	**Matrix**	**0**	**300**	**1000**	**2000**
EVG	Milk	< 100	1360 ± 514	2780 ± 755	4160 ± 1980
	Plasma	< 100	17500 ± 5600	34700 ± 8120	36000 ± 6380
GS-9200	Milk	< 100	< 100	< 100	< 100
	Plasma	< 100	3100 ± 998	5260 ± 1710	6640 ± 3390
GS-9202	Milk	< 100	< 100	< 100	< 100
	Plasma	< 100	< 100	< 100	30 ± 60

Plasma data: TX-183-2006 Appendix 6 Table 1 (EVG), Table 2 (GS-9200), Table 3 (GS-9202)

Milk data: TX-183-2006 Appendix 7 Table A11

2.6.5.7.2. COBI: Study in Pregnant or Nursing Animals

Studies of COBI in pregnant or nursing animals are presented in Module 2.6.7, Sections 2.6.7.11, 2.6.7.12, 2.6.7.13, and 2.6.7.14.

2.6.5.8. Pharmacokinetics: Other Distribution Study

2.6.5.8.1. JTK303-AD-013: Distribution of EVG to Blood Cells in Vitro

Report Title	Study Type	Test Article	Report Number (Study Number)
Distribution of JTK-303 into Blood Cells in Vitro	Distribution study	[^{14}C]EVG	JTK303-AD-013 (JK303PK030)

Species	[^{14}C]EVG Concentration (µg/mL)	Distribution into Blood Cells (%)	Whole Blood/Plasma Ratio[a]
Rat	0.1	2.2 ± 1.9	0.6
	1	3.0 ± 2.0	0.6
	10	3.2 ± 2.8	0.6
Dog	0.1	32.4 ± 1.9	0.8
	1	30.8 ± 3.0	0.8
	10	25.6 ± 3.4	0.7
Monkey	0.1	26.4 ± 4.9	0.8
	1	28.6 ± 3.4	0.8
	10	26.1 ± 8.0	0.8
Human	0.1	24.0 ± 5.4	0.7
	1	21.9 ± 6.4	0.7
	10	20.8 ± 2.0	0.6

EVG = elvitegravir

a Whole Blood/Plasma Ratio calculated as: (100 – Hematocrit %)/(100 – Distribution %)

2.6.5.9. Pharmacokinetics: Metabolism in Vivo

2.6.5.9.1. JTK303-AD-019: Metabolite Profiling of Samples from Rats after Administration of [^{14}C]EVG

Report Title	Study Type	Test Article	Report Number (Study Number)
Metabolite Profiling of Biological Samples from Rats after Administration of [^{14}C]-JTK-303	Metabolism study	[^{14}C]EVG	JTK303-AD-019 (JK303PK040)

Species/Strain Number of Animals/Group Sex	Administration Route (Dose level)	Sample	Time (h)	Concentration (plasma or liver; ng eq./mL or g)							
				Total	EVG	M1 GS-9202	M2	M3	M4 GS-9200	M7	Others
Rat/SD (Crj:CD(SD)IGS) 3 animals/group male	Oral (3 mg/kg)	Plasma	0.5	1181 (100.0)	993 (84.1)	N.D.	N.D.	N.D.	91 (7.7)	N.D.	96 (8.1)
			4	332 (100.0)	264 (79.8)	N.D.	N.D.	N.D.	35 (10.5)	5 (1.6)	27 (8.1)
			24	9 (100.0)	N.D.	N.D.	N.D.	N.D.	N.D.	N.D.	6 (69.7)
		Liver	0.5	1488 (100.0)	997 (67.0)	107 (7.2)	30 (2.0)		302 (20.3)	N.D.	52 (3.5)
			4	374 (100.0)	231 (61.9)	46 (12.3)	N.D.	N.D.	66 (17.8)	N.D.	30 (8.0)
			24	27 (100.0)	N.D.	N.D.	N.D.	N.D.	N.D.	N.D.	19 (72.0)

EVG = elvitegravir; N.D. = not detected
Note: The parent drug and its metabolites are pooled samples from 3 animals.
The values in parentheses are the ratio (%) to the radioactivity in the sample. Radioactivity: the mean value (n = 3).

2.6.5.9.1. JTK303-AD-019: Metabolite Profiling of Samples from Rats after Administration of [^{14}C]EVG (Continued)

Test Article: [^{14}C]EVG

Composition of Radioactivity in Rat Urine, Feces and Bile after Administration of [^{14}C]EVG

Species	Route of administration	Sample	Time	Percent of Dose Radioactivity (%)							
				Total	EVG	M1 GS-9202	M2	M3	M4 GS-9200	M7	Others
Rat	Oral	Urine	0-48 h	0.1 (100.0)	ND	ND	ND	ND	0.0 (41.7)	0.1 (58.3)	ND
		Feces	0-48 h	96.5 (100.0)	65.8 (68.2)	17.5 (18.1)	1.4 (1.5)	ND	ND	ND	11.7 (12.2)
Rat (biliary cannulated)	Oral	Bile	0-24 h	23.0 (100.0)	0.8 (3.7)	0.2 (0.9)	0.1 (0.6)		9.5 (41.4)	6.5 (28.2)	5.8 (25.4)
		β-Glucuronidase treated bile	0-24 h	23.0 (100.0)	9.6 (41.8)	7.5 (32.6)	0.5 (2.2)		0.4 (1.9)	0.2 (1.0)	4.7 (20.5)
Rat	IV	Urine	0-48 h	0.4 (100.0)	ND	ND	ND	ND	0.4 (100.0)	ND	ND
		Feces	0-48 h	97.5 (100.0)	38.9 (39.9)	34.9 (35.9)	3.6 (3.7)	ND	ND	ND	20.1 (20.6)

EVG = elvitegravir; IV = intravenous; N.D. = not detected

Note: The parent drug and its metabolites are pooled samples from 3 animals.

Dose: 3 mg/kg for oral administration and 1 mg/kg for IV administration.

The values in parentheses are the ratio (%) to the radioactivity in the sample. Radioactivity: the mean value (n = 3).

2.6.5.9.2. JTK303-AD-020: Metabolite Profiling of Samples from Dogs After Administration of [^{14}C]EVG

Report Title	Study Type	Test Article	Report Number (Study Number)
Metabolite Profiling of Biological Samples from Dogs after Administration of [^{14}C]-JTK-303	Metabolism study	[^{14}C]EVG	JTK303-AD-020 (JK303PK039)

Peak Area Ratio of EVG and Its Metabolites in the Soluble Fraction of Biological Samples from Dogs after Administration of [^{14}C]EVG

				[^{14}C] Peak Area Ratio (%)								
Species/Strain Number of Animals/ Group Sex	**Admini-stration Route (Dose level)**	**Sample**	**Time**	**EVG**	**M1 GS-9202**	**M2**	**M3**	**M4 GS-9200**	**M5**	**M6**	**M7**	**Other Peaks**
Dog/Beagle (NOSAN) 3 animals/group male	Oral (3 mg/kg)	Plasma	2 h	92.25	ND	ND	ND	ND	ND	7.75	ND	ND
			6 h	68.71	ND	ND	ND	31.29	ND	ND	ND	ND
		Urine	0–48 h	ND	ND	ND	ND	ND	32.26	25.99	41.75	ND
		Feces	0–48 h	79.87	13.17	3.45	ND	ND	3.51	ND	ND	ND
	IV (1 mg/kg)	Plasma	5 min	92.52	ND	1.68	ND	5.80	ND	ND	ND	ND
			30 min	90.73	2.00	ND	ND	6.14	ND	ND	ND	1.13
			6 h	100	ND	ND	ND	ND	ND	ND	ND	ND
		Urine	0–48 h	15.61	10.04	ND	ND	11.31	4.54	12.16	26.44	19.90
		Feces	0–48 h	71.47	18.68	5.66	ND	ND	2.37	ND	1.83	ND

2.6.5.9.2. JTK303-AD-020: Metabolite Profiling of Samples from Dogs After Administration of [^{14}C]EVG (Continued)

Test Article: [^{14}C]EVG

Composition of Radioactivity in Dog Urine and Feces after Administration of [^{14}C]EVG

Species/Strain Number of Animals/Group Sex	Administration Route (Dose level)	Sample	Time	Plasma concentration (ng eq./mL)							
				Total	EVG	M1 GS-9202	M2	M4 GS-9200	M6	M7	Others
Dog/Beagle (NOSAN) 3 animals/group male	Oral (3 mg/kg)	Plasma	2 h	122 (100.0)	108 (88.4)	ND	ND	ND	9 (7.4)	ND	5 (4.2)
			6 h	80 (100.0)	52 (65.4)	ND	ND	24 (29.8)	ND	ND	4 (4.8)
	IV (1 mg/kg)	Plasma	5 min	691 (100.0)	624 (90.2)	ND	11 (1.6)	39 (5.7)	ND	ND	17 (2.5)
			30 min	375 (100.0)	326 (86.8)	7 (1.9)	ND	22 (5.9)	ND	ND	20 (5.4)
			6 h	38 (100.0)	33 (86.6)	ND	ND	ND	ND	ND	5 (13.4)

2.6.5.9.2. JTK303-AD-020: Metabolite Profiling of Samples from Dogs After Administration of [^{14}C]EVG (Continued)

Test Article: [^{14}C]EVG

Composition of Radioactivity in Dog Urine and Feces after Administration of [^{14}C]EVG

Species/Strain Number of Animals/Group Sex	Administration Route (Dose level)	Sample	Time (h)	Excretion of Radioactivity (% of dose)								
				Total	EVG	M1 GS-9202	M2	M4 GS-9200	M5	M6	M7	Others
Dog/Beagle (NOSAN) 3 animals/group male	Oral (3 mg/kg)	Urine	0–48	0.5 (100.0)	ND	ND	ND	ND	0.2 (32.3)	0.1 (26.0)	0.2 (41.8)	ND
		Feces	0–48	95.0 (100.0)	70.9 (74.6)	11.7 (12.3)	3.1 (3.2)	ND	3.1 (3.3)	ND	ND	6.2 (6.6)
	IV (1 mg/kg)	Urine	0–48	1.0 (100.0)	0.2 (15.6)	0.1 (10.0)	ND	0.1 (11.3)	0.0 (4.5)	0.1 (12.2)	0.3 (26.4)	0.2 (19.9)
		Feces	0–48	98.0 (100.0)	62.2 (63.5)	16.3 (16.6)	4.9 (5.0)	ND	2.1 (2.1)	ND	1.6 (1.6)	11.0 (11.2)

EVG = elvitegravir; IV = intravenous; ND = not detected
The parent drug and its metabolites are pooled samples from 3 animals.
The values in parentheses are the ratio (%) to the radioactivity in the sample. Radioactivity is the mean value (n = 3).

2.6.5.9.3. AD-216-2073: Metabolism of [^{14}C]COBI Following Oral Administration to Mice

Report Title	Study Type	Test Article	Report Number (Study Number)
Pharmacokinetics, Metabolism, and Excretion of [^{14}C]GS-9350 Following Oral Administration to Mice	Metabolism study	[^{14}C]COBI	AD-216-2073

Species/Strain Number of Animals/Group Sex	Administration Route (Dose level)	Sample	Time (h)	Concentration in plasma; ng eq. [^{14}C]COBI /g						
				Total (LSC)[a]	Total	COBI	M55	M21	M31	M69
ICR mice [Hsd:ICR(CD-1)] 15 animals/Group 2 male	Oral (30 mg/kg)	Plasma	1	6670 ± 1690	6240 (96.3)	5900 (91.02)	ND	158 (2.44)	141 (2.18)	43.4 (0.67)
			2	4270 ± 2270	3870 (96.2)	3530 (87.78)	ND	154 (3.83)	146 (3.62)	39.8 (0.99)
			4	4310 ± 320	3810 (96.4)	3440 (87.06)	ND	165 (4.18)	146 (3.68)	56.5 (1.43)
			8	1890 ± 1210	1470 (94.1)	1340 (85.97)	22.0 (1.41)	54.4 (3.48)	35.6 (2.28)	14.5 (0.93)

COBI = cobicistat; LSC = liquid scintillation counting; ND = peak not detected or below the established limit of quantitation (1% of run)

a Total concentration of radioactivity determined by liquid scintillation counting (mean ± SD, n = 3)

Note: The values in parentheses are the percent of radioactivity injected (% of run).

2.6.5.9.3. AD-216-2073: Metabolism of [^{14}C]COBI Following Oral Administration to Mice (Continued)

Test Article: [^{14}C]COBI

Composition of Radioactivity in Pooled Mouse Urine After Oral Administration of [^{14}C]COBI (Group 1; n = 4)

Final Metabolite Designation	Collection Interval (0-24 hours)	
	Percent of Radioactivity Injected (% of Run)	Percent of Radioactive Dose
M55	6.19	0.11
M56	1.19	0.02
M57	1.52	0.03
M10	7.30	0.13
M14	3.88	0.07
M21 (GS-343006)	38.21	0.66
M26 (GS-341842)	1.68	0.03
M31 (GS-364751)	6.35	0.11
M32	1.66	0.03
COBI	3.02	0.05
Total	71.0	1.23

2.6.5.9.3. AD-216-2073: Metabolism of [^{14}C]COBI Following Oral Administration to Mice (Continued)

Test Article: [^{14}C]COBI

Composition of Radioactivity in Pooled Mouse Feces After Oral Administration of [^{14}C]COBI (n = 4)			
	Collection Interval (hours)		Total
	0-24	24-48	
Final Metabolite Designation	Percent of Radioactive Dose		
M57	ND	0.06	0.06
M10	0.93	0.19	1.12
M58	ND	0.06	0.06
M14	3.29	0.39	3.68
M59	0.57	0.06	0.63
M60	ND	0.06	0.06
M61	ND	0.06	0.06
M62	0.49	0.05	0.54
M21 (GS-342006)	11.9	1.48	13.4
M48	0.83	0.04	0.86
M49	0.73	0.14	0.87
M26 (GS-341842)	1.99	0.07	2.06
M50	1.04	0.04	1.09
M29	2.35	0.15	2.50
M63	0.68	0.05	0.74
M31 (GS-364751)	5.04	0.16	5.21
M64	0.38	0.06	0.45
M65	2.37	0.07	2.44
M66	0.51	0.13	0.64
M67	0.74	ND	0.74
M68	0.97	0.07	1.04
M69	3.98	0.17	4.15
M39	0.54	0.06	0.60
COBI	14.3	0.22	14.5

COBI = cobicistat; ND = peak not detected or below the established limit of quantitation (1% of run); NA = not applicable
Note regarding data from pooled fecal samples: If at least one interval had a reportable value above the limit of quantitation, then other intervals may include a value below the limit of quantitation.

2.6.5.9.4. AD-216-2082: Metabolite Profiling and Identification of Rat Plasma, Bile, Urine, and Feces Following Oral Administration of [^{14}C]COBI

Report Title	Study Type	Test Article	Report Number (Study Number)
Metabolite Profiling and Identification of Rat Plasma, Bile, Urine, and Feces Following Oral Administration of [^{14}C]GS-9350	Metabolism study	[^{14}C]COBI	AD-216-2082

Species/Strain Number of Animals/Group Sex	Administration Route (Dose level)	Sample	Time (h)	Concentration (plasma; ng eq. [^{14}C]COBI /g)						
				Total (LSC)[a]	Total	COBI	M1	M9	M21	M31
Sprague Dawley Rat (H1a:[SD]CVF) Pooled samples from 3 rats per time point	Oral (10 mg/kg)	Plasma	0.083	160 ± 89	125 (81.0)	111 (71.57)	ND	ND	9.78 (6.32)	4.74 (3.06)
			0.25	1170 ± 580	933 (85.7)	815 (74.83)	14.1 (1.29)	16.3 (1.50)	73.2 (6.72)	14.5 (1.33)
			1	2170 ± 210	1710 (85.8)	1490 (75.00)	54.4 (2.73)	ND	116 (5.81)	44.8 (2.25)
			2	844 ± 480	618 (92.3)	526 (78.51)	29.7 (4.43)	ND	35.2 (5.25)	27.3 (4.08)
			4	567 ± 194	288 (87.3)	201 (60.70)	37.7 (11.40)	ND	38.3 (11.58)	12.0 (3.62)

COBI = cobicistat; LSC = liquid scintillation counting; ND = peak not detected or below the established limit of quantitation (1% of run)

a Total concentration of radioactivity determined by liquid scintillation counting (mean ± SD, n = 3) from AD-216-2034

Note: The values in parentheses are the percent of radioactivity injected (% of run).

2.6.5.9.4. AD-216-2082: Metabolite Profiling and Identification of Rat Plasma, Bile, Urine, and Feces Following Oral Administration of [^{14}C]COBI (Continued)

Test Article: [^{14}C]COBI

Composition of Radioactivity in Pooled Rat Urine After Oral Administration of [^{14}C]COBI

Final Metabolite Designation	Percent of Radioactive Dose					
	Male Rats			Male Bile Duct-Cannulated Rats		
	Collection Interval (hours)			Collection Interval (hours)		
	0-12	12-24	Total	0-12	12-24	Total
M1	0.16	0.05	0.21	0.10	0.02	0.12
M2	ND	ND	0.00	ND	0.01	0.01
M3	ND	ND	0.00	ND	0.00	0.00
M4	0.04	0.00	0.04	ND	0.00	0.00
M5	0.02	0.01	0.03	ND	ND	0.00
M6	0.07	0.02	0.10	0.06	0.00	0.07
M7	0.03	ND	0.03	0.04	ND	0.04
M8	0.02	ND	0.02	ND	0.00	0.00
M10	0.03	ND	0.03	0.04	0.00	0.05
M11	0.05	0.01	0.05	0.17	0.01	0.18
M12	0.02	ND	0.02	0.04	ND	0.04
M14	0.02	ND	0.02	0.10	0.01	0.12
M17	ND	ND	0.00	0.04	ND	0.04
M21 (GS-342006)	0.40	0.03	0.43	1.10	0.09	1.19
M26 (GS-341842)	0.02	ND	0.02	0.06	ND	0.06
M28	0.02	ND	0.02	0.06	0.01	0.06
M31 (GS-364751)	0.21	ND	0.21	0.74	0.02	0.76
M34	0.03	ND	0.03	0.06	ND	0.06
M39	0.02	ND	0.02	0.06	0.00	0.06
COBI	0.05	ND	0.05	0.19	0.01	0.19
M41	ND	ND	0.00	ND	0.00	0.00

2.6.5.9.4. AD-216-2082: Metabolite Profiling and Identification of Rat Plasma, Bile, Urine, and Feces Following Oral Administration of [^{14}C]COBI (Continued)

Test Article: [^{14}C]COBI

Composition of Radioactivity in Pooled Rat Bile Samples After Oral Administration of [^{14}C]COBI

Final Metabolite Designation	Percent of Radioactive Dose									
	Collection Interval (hours)									Total
	0-2	2-4	4-6	6-8	8-12	12-24	24-48	48-72	72-96	
M10	0.39	ND	0.33	ND	0.08	0.22	0.03	ND	ND	1.05
M11	ND	ND	ND	ND	ND	0.11	0.04	ND	ND	0.15
M14	0.65	0.85	0.71	0.33	0.38	0.34	0.11	0.07	ND	3.44
M16	ND	ND	ND	ND	0.12	ND	ND	ND	0.02	0.14
M19	ND	ND	ND	0.22	0.35	ND	ND	ND	ND	0.57
M21 (GS-342006)	0.59	0.95	0.57	0.34	0.54	0.51	ND	ND	ND	3.50
M22	0.41	ND	0.68	ND	ND	ND	ND	ND	ND	1.09
M23	0.33	0.63	ND	ND	ND	ND	ND	ND	ND	0.96
M24	0.43	ND	ND	ND	ND	0.07	ND	ND	ND	0.50
M25	0.44	ND	ND	ND	ND	0.13	0.13	0.06	ND	0.76
M26 (GS-341842)	0.66	0.85	0.48	0.16	ND	ND	0.13	ND	0.07	2.35
M27	0.56	ND	0.39	0.14	ND	ND	ND	0.05	ND	1.14
M28	0.65	1.23	0.90	0.19	ND	ND	ND	ND	ND	2.97
M29	ND	ND	0.36	ND	0.17	ND	0.03	0.02	ND	0.58
M31 (GS-364751)	0.80	0.72	ND	0.20	ND	0.14	0.06	ND	ND	1.92
M32	0.38	0.61	0.30	0.11	ND	ND	ND	ND	ND	1.40
M33	0.61	0.71	0.50	0.13	ND	ND	ND	ND	ND	1.95
M34	0.74	0.85	0.53	ND	ND	ND	ND	ND	ND	2.12
M39	0.63	0.76	0.53	0.22	0.12	0.08	ND	ND	ND	2.34
M42	ND	0.42	ND	ND	ND	ND	ND	ND	ND	0.42

2.6.5.9.4. AD-216-2082: Metabolite Profiling and Identification of Rat Plasma, Bile, Urine, and Feces Following Oral Administration of [^{14}C]COBI (Continued)

Test Article: [^{14}C]COBI

Composition of Radioactivity in Pooled Rat Feces After Oral Administration of [^{14}C]COBI

	Percent of Radioactive Dose							
	Male Rats					Male Bile Duct-Cannulated Rats		
	Collection Interval (hours)					Collection Interval (hours)		
Final Metabolite Designation	0-24	24-48	48-72	72-96	Total	0-12	12-24	Total
M9	ND	ND	0.01	0.00	0.01	ND	ND	0.00
M10	1.00	0.16	0.02	0.00	1.17	ND	ND	0.00
M12	ND	0.10	0.01	0.00	0.11	ND	ND	0.00
M13	ND	ND	0.01	0.00	0.01	ND	ND	0.00
M14	1.84	0.36	0.04	0.01	2.25	0.18	0.03	0.22
M15	ND	ND	ND	0.00	0.00	ND	ND	0.00
M16	ND	ND	ND	0.00	0.00	ND	ND	0.00
M17	ND	ND	0.01	0.00	0.01	ND	ND	0.00
M18	ND	ND	ND	0.00	0.00	ND	ND	0.00
M19	ND	0.11	0.01	0.00	0.13	ND	ND	0.00
M20	1.16	0.28	0.03	0.01	1.48	ND	0.02	0.02
M21 (GS-342006)	9.69	1.48	0.15	0.04	11.4	3.03	0.40	3.44
M23	ND	ND	0.01	0.00	0.01	ND	ND	0.00
M25	1.92	0.22	0.02	0.00	2.16	ND	0.02	0.02
M26 (GS-341842)	2.53	0.28	0.02	ND	2.83	ND	0.02	0.02
M28	2.95	0.34	0.02	ND	3.31	0.26	0.03	0.29
M29	2.14	0.19	0.02	0.00	2.35	0.19	0.03	0.22
M30	ND	0.09	ND	ND	0.09	ND	ND	0.00
M31 (GS-364751)	6.60	0.57	0.04	0.00	7.22	1.11	0.12	1.24
M33	0.67	0.20	0.01	0.00	0.88	ND	0.02	0.02
M34	1.11	0.11	0.01	0.00	1.23	ND	ND	0.00
M35	0.69	ND	0.01	ND	0.70	ND	ND	0.00
M36	0.76	0.11	ND	ND	0.88	ND	0.03	0.03
M37	ND	0.09	ND	ND	0.09	ND	ND	0.00

2.6.5.9.4. AD-216-2082: Metabolite Profiling and Identification of Rat Plasma, Bile, Urine, and Feces Following Oral Administration of [^{14}C]COBI (Continued)

Test Article: [^{14}C]COBI

Composition of Radioactivity in Pooled Rat Feces After Oral Administration of [^{14}C]COBI

Final Metabolite Designation	Percent of Radioactive Dose							
	Male Rats					Male Bile Duct-Cannulated Rats		
	Collection Interval (hours)				Total	Collection Interval (hours)		Total
	0-24	24-48	48-72	72-96		0-12	12-24	
M38	0.68	ND	0.01	ND	0.69	ND	ND	0.00
M39	3.24	0.44	0.03	0.00	3.72	0.65	0.06	0.71
M40	0.68	0.12	ND	ND	0.80	0.18	ND	0.18
COBI	5.33	0.32	0.01	ND	5.67	7.14	0.55	7.69
M41	1.49	ND	ND	ND	1.49	ND	ND	0.00
M43	ND	0.12	ND	ND	0.12	ND	0.12	ND
M44	ND	ND	ND	0.00	0.00	0.00	0.00	ND

COBI = cobicistat; NA = not applicable; ND = peak not detected or below the established limit of quantitation (1% of run for plasma, urine, and fecal samples; 2% of run for bile samples)

2.6.5.9.5. AD-216-2101: Profiling and Identification of Metabolites in Plasma, Urine, Bile, and Feces Samples from Dogs after Oral Administration of [^{14}C]COBI

Report Title	Study Type	Test Article	Report Number (Study Number)
Profiling and Identification of Metabolites in Selected Plasma, Urine, Bile, and Feces Samples from Intact and Bile Duct Cannulated Dogs after Oral Administration of [^{14}C]GS-9350	Metabolism study	[^{14}C]COBI	AD-216-2101

Species/Strain Number of Animals/Group Sex	Administration Route (Dose level)	Sample	Time (h)	Concentration (plasma; ng eq. [^{14}C]COBI /g)						
				Total (LSC)[a]	Total	COBI	M21 (GS-342006)	M22	M31 (GS-364751)	M37
Beagle Dog Pooled samples from 3M/group	Oral (5 mg/kg)	Plasma	0.5	519 ± 472	595 (93.4)	419 (65.76)	64.0 (10.04)	ND	47.9 (7.52)	64.0 (10.04)
			1	821 ± 447	544 (94.4)	423 (73.33)	59.0 (10.24)	ND	25.7 (4.46)	36.8 (6.39)
			2	796 ± 191	652 (91.2)	473 (66.17)	53.8 (7.53)	12.6 (1.76)	41.2 (5.77)	70.9 (9.92)
			4	456 ± 151	301 (89.2)	226 (66.99)	19.6 (5.82)	ND	23.6 (7.00)	31.6 (9.38)

COBI = cobicistat; LSC = liquid scintillation counting; ND = peak not detected or below the established limit of quantitation (1% of run)

a Total concentration of radioactivity determined by liquid scintillation counting (mean ± SD, n = 3) from AD-216-2067

Note: The values in parentheses are the percent of radioactivity injected (% of run).

2.6.5.9.5. AD-216-2101: Profiling and Identification of Metabolites in Plasma, Urine, Bile, and Feces Samples from Dogs after Oral Administration of [^{14}C]COBI (Continued)

Test Article: [^{14}C]COBI

Composition of Radioactivity in Pooled Dog Urine After Oral Administration of [^{14}C]COBI

Final Metabolite Designation	Percent of Radioactive Dose					
	Male Dogs			Male Bile Duct-Cannulated Dogs		
	Collection Interval (hours)			Collection Interval (hours)		
	0-24	24-48	Total	0-24	24-48	Total
M56	0.11	0.06	0.17	0.09	0.03	0.12
M4	ND	ND	ND	ND	0.01	0.01
M5	ND	0.00	0.00	0.06	0.01	0.07
M6	0.02	0.00	0.02	0.03	0.01	0.04
M7	0.04	0.01	0.05	0.02	0.01	0.03
M10	0.08	0.01	0.09	0.08	0.00	0.08
M57	ND	ND	ND	ND	0.01	0.01
M58	ND	0.00	0.00	ND	0.01	0.01
M14	0.03	0.01	0.04	0.05	0.01	0.06
M21 (GS-342006)	0.15	0.03	0.18	0.23	0.03	0.25
M26 (GS-341842)	0.02	ND	0.02	0.03	0.00	0.03
M31 (GS-364751)	0.35	0.01	0.37	0.35	0.02	0.36
M30	0.03	ND	0.03	0.04	0.00	0.04
M39	0.04	0.01	0.05	0.01	ND	0.01
COBI	0.03	0.01	0.04	0.05	ND	0.05

Note: For plasma and urine samples, if at least one analyzed time point has a value above the limit of quantitation, values below the limit of quantitation may be reported for other time points.

a Represents an individual sample (Animal No. 1001)

b Represents an individual sample (Animal No. 1001; 12-24-hour sample

2.6.5.9.5. AD-216-2101: Profiling and Identification of Metabolites in Plasma, Urine, Bile, and Feces Samples from Dogs after Oral Administration of [^{14}C]COBI (Continued)

Test Article: [^{14}C]COBI

Composition of Radioactivity in Dog Pooled Bile Samples After Oral Administration of [^{14}C]COBI

Final Metabolite Designation	Percent of Radioactive Dose				
	Collection Interval (hours)				Total
	0-4	4-12	12-24	24-48	
M10	1.09	0.26	ND	ND	1.35
M14	1.95	0.84	ND	ND	2.79
M79	0.84	ND	ND	ND	0.84
M21 (GS-342006)	4.75	0.38	0.14	ND	5.27
M19	ND	1.48	ND	ND	1.48
M48	1.32	0.86	ND	0.03	2.21
M22	1.16	0.35	ND	0.13	1.63
M26 (GS-341842)	1.69	0.45	0.14	0.04	2.31
M25	0.84	ND	0.17	ND	1.01
M50	1.33	0.38	0.08	ND	1.79
M27	ND	0.65	0.18	ND	0.84
M80	2.12	0.68	0.11	0.56	3.47
M29	1.41	0.96	0.11	0.12	2.60
M31 (GS-364751)	3.64	ND	0.07	0.03	3.74
M63	1.16	ND	ND	0.04	1.20
M30	1.22	2.24	ND	ND	3.46
M65	1.34	0.48	0.27	0.16	2.25
M81	ND	0.66	0.21	0.08	0.94
M82	0.96	0.32	0.10	0.07	1.45
M39	2.93	1.13	0.28	0.04	4.38
COBI	1.01	0.44	0.09	0.12	1.65

2.6.5.9.5. AD-216-2101: Profiling and Identification of Metabolites in Plasma, Urine, Bile, and Feces Samples from Dogs after Oral Administration of [^{14}C]COBI (Continued)

Test Article: [^{14}C]COBI

Composition of Radioactivity in Dog Pooled Bile Samples After Oral Administration of [^{14}C]COBI

Final Metabolite Designation	Percent of Radioactive Dose				
	Collection Interval (hours)				Total
	0-4	4-12	12-24	24-48	
M40	ND	ND	0.12	ND	0.12
M41	ND	ND	0.10	ND	0.10
M42	ND	ND	0.13	ND	0.13
M83	ND	ND	ND	0.05	0.05
M84	ND	ND	ND	0.04	0.04
M43	ND	ND	0.12	0.03	0.15

2.6.5.9.5. AD-216-2101: Profiling and Identification of Metabolites in Plasma, Urine, Bile, and Feces Samples from Dogs after Oral Administration of [^{14}C]COBI (Continued)

Test Article: [^{14}C]COBI

Composition of Radioactivity in Dog Feces After Oral Administration of [^{14}C]COBI

Final Metabolite Designation	Percent of Radioactive Dose							
	Male Dogs				Male Bile Duct-Cannulated Dogs			
	Collection Interval (hours)				Collection Interval (hours)			
	0-24[b]	24-48	48-72	Total	0-24	24-48	48-72	Total
M10	0.53	1.04	0.05	1.62	0.01	0.18	0.19	0.38
M14	0.71	2.07	0.08	2.86	ND	ND	0.17	0.17
M21 (GS-342006)	4.10	7.86	0.46	12.4	0.08	1.01	0.76	1.85
M48	0.37	2.06	0.04	2.47	ND	ND	ND	ND
M49	0.60	1.33	0.03	1.96	ND	ND	0.20	0.20
M26 (GS-341842)	0.75	1.46	0.04	2.25	0.03	0.31	0.19	0.53
M25	0.27	0.79	0.02	1.08	ND	ND	ND	ND
M50	0.37	1.60	0.02	2.00	ND	ND	0.05	0.05
M29	1.25	3.38	0.10	4.72	0.01	0.14	0.19	0.34
M31 (GS-364751)	2.58	6.09	0.09	8.76	0.17	1.84	0.60	2.61
M63	0.61	1.42	0.05	2.08	ND	ND	ND	ND
M30	0.27	0.65	ND	0.92	ND	ND	0.08	0.08
M65	1.00	3.16	0.05	4.22	0.01	ND	0.06	0.07
M81	ND	ND	ND	ND	ND	ND	0.05	0.05
M76	0.30	0.79	0.02	1.12	ND	ND	ND	ND
M39	2.87	5.64	0.12	8.63	0.03	0.39	0.22	0.64
COBI	5.13	1.96	0.05	7.15	0.73	8.20	0.61	9.54

COBI = cobicistat; NA = not applicable; ND = peak not detected or below the established limit of quantitation (1% of run and 10 cpm peak height for plasma, urine, and fecal samples; 2% of run and 10 cpm peak height for bile samples)

2.6.5.10. Pharmacokinetics: Metabolism in Vitro

2.6.5.10.1. AD-183-2019: Determination of In Vitro Metabolic Stability of EVG in Mouse Liver Microsomes

Report Title	Study Type	Test Article	Report Number (Study Number)
Determination of In Vitro Metabolic Stability of [^{14}C]-GS-9137 in Mouse Liver Microsomes	Metabolism study	[^{14}C]EVG	AD-183-2019 (60N-0629)

Study Methods: The stability of [^{14}C]EVG (2 µM) with male or female CD-1 mouse hepatic microsomal fractions was investigated. Commercially obtained mouse hepatic microsomal fractions were from male CD-1 mice treated with corn oil or with prototypic inducers (β-naphthoflavone, dexamethasone, or clofibric acid). Microsomal fractions from female mice were from untreated animals. Incubations were performed with NADPH in the absence and presence of UDPGA. Positive control substrates for oxidation (7-ethoxycoumarin) and conjugation (7-hydroxycoumarin) were tested in parallel.

Sex	Pre-treatment	EVG Remaining at 30 min (%)	
		NADPH	NADPH+UDPGA
Male	Corn oil	53.40	49.31
	Dexamethasone	11.84	7.29
	β-Naphthoflavone	45.88	46.35
	Clofibric acid	59.28	46.60
Female	Untreated	69.93	61.79

2.6.5.10.2. JTK303-AD-015: Hepatic Microsomal Oxidative Metabolism of [^{14}C]EVG

Report Title	Study Type	Test Article	Report Number (Study Number)
In Vitro Metabolism of [^{14}C]-JTK-303 (Oxidative Reaction in Liver Microsomes)	Metabolism study	[^{14}C]EVG	JTK303-AD-015 (JK303PK037)

Reaction conditions: 1.0 µg/mL [^{14}C]EVG, 1.0 mg/mL protein, incubation at 37°C for 10 minutes, 1.3 mM $NADP^+$, 3.3 mM magnesium chloride, 3.3 mM Glucose-6-Phosphate, 0.4 unit/mL Glucose-6-Phosphate Dehydrogenase, 100 mM potassium phosphate buffer (pH 7.4)

Species[a]	Rate of Metabolism of EVG and Formation Rate of Metabolites (pmol/min/mg protein)				
	EVG	M1 GS-9202	M8	M5	Others
Rat	130.8 (40.0)	99.2 (45.1)	2.6 (1.2)	N.D.	29.0 (13.7)
Dog	15.4 (92.1)	16.2 (7.4)	ND	1.1 (0.5)	ND
Monkey	193.8 (10.3)	155.0 (71.4)	10.0 (4.6)	8.4 (3.8)	20.3 (10.0)
Human	129.4 (40.9)	113.3 (51.5)	2.6 (1.2)	9.9 (4.5)	3.7 (2.0)

EVG (JTK-303) = elvitegravir; ND = not detected
Each value is shown as the mean of 2 measurements.
Values in parentheses are the percentage of radioactivity in the sample.
a Liver microsomes were pooled samples from 30 male and 20 female humans, from 10 male dogs, from 200 male rats, and from 8 male monkeys.

2.6.5.10.3. JTK303-AD-016: Hepatic Microsomal Glucuronidation of [^{14}C]EVG

Report Title	Study Type	Test Article	Report Number (Study Number)
In Vitro Metabolism of [^{14}C]-JTK-303 (Glucuronide Conjugation in Liver Microsomes)	Metabolism study	[^{14}C]EVG	JTK303-AD-016 (JK303PK038)

Reaction conditions: 1.0 µg/mL [^{14}C]EVG, incubation at 37°C for 60 minutes, 1 mg protein/mL, 50 mM Tris-HCl buffer, 10 mM magnesium chloride, 5 mM UDP-Glucuronic Acid, 5 mM D-Saccharic acid 1,4-Lactone, and 25 µg/mL alamethicin

Species	Rate of Metabolism of EVG and Formation Rate of Metabolites (pmol/min/mg protein)		
	EVG	M3	M4 (GS-9200)
Rat[a]	17.9 (51.1)	0.8 (2.1)	17.2 (46.8)
Dog[b]	3.7 (90.0)	0.3 (0.7)	3.4 (9.3)
Monkey[c]	7.1 (79.9)	ND	7.4 (20.1)
Human[d]	0.9 (96.8)	ND	1.2 (3.2)

EVG = elvitegravir; ND = not detected

The rate of metabolism, rate of formation of metabolites and the formation ratio in parentheses are the mean of 2 measurements.

a Pooled from 200 male rats

b Pooled from 10 male dogs

c Pooled from 8 male monkeys

d Pooled from 30 men and 20 women, 50 humans in total

2.6.5.10.4. JTK303-AD-017: Metabolism of EVG by Recombinant Human CYP Enzymes

Report Title	Study Type	Test Article	Report Number (Study Number)
Metabolism of JTK-303 by Recombinant Human CYP Isoforms	Metabolism study	[^{14}C]EVG	JTK303-AD-017 (JK303PK036)

Reaction condition: Incubated for 30 minutes in 100 mM potassium phosphate buffer (pH 7.4) (CYP1A1, CYP1A2, CYP2B6, CYP2C8, CYP2C19, CYP2D6, CYP2E1, CYP3A4, and CYP3A5) or 100 mM Tris-HCl buffer (pH 7.5) (CYP2A6 and CYP2C9) containing 10 µg/mL (22 µM) of [^{14}C]EVG, 50 pmol/mg protein/mL of P450, 3.3 mM $MgCl_2$, 1.3 mM $NADP^+$, 3.3 mM D-glucose-6-phosphate, and 0.4 unit/mL glucose-6-phosphate dehydrogenase.

CYP	Rate of Metabolism of EVG and Formation Rate of Metabolites (pmol/min/pmol P450)					
	EVG	M1 (GS-9202)	M2	M8	M5	Others
1A1	0.9 (92.2)	< 0.1 (0.3)	0.9 (6.1)	N.D.	N.D.	< 0.1 (1.4)
1A2	< 0.1 (97.9)	N.D.	< 0.1 (0.5)	N.D.	N.D.	< 0.1 (1.6)
2A6	< 0.1 (98.2)	N.D.	< 0.1 (0.4)	N.D.	N.D.	< 0.1 (1.4)
2B6	< 0.1 (98.3)	N.D.	< 0.1 (0.2)	N.D.	N.D.	< 0.1 (1.5)
2C8	< 0.1 (98.1)	N.D.	< 0.1 (0.4)	N.D.	N.D.	< 0.1 (1.5)
2C9	< 0.1 (98.0)	N.D.	< 0.1 (0.5)	N.D.	N.D.	< 0.1 (1.5)
2C19	< 0.1 (98.1)	N.D.	< 0.1 (0.4)	N.D.	N.D.	< 0.1 (1.5)

2.6.5.10.4. JTK303-AD-017: Metabolism of EVG by Recombinant Human CYP Enzymes (Continued)

Test Article: [^{14}C]EVG

CYP	Rate of Metabolism of EVG and Formation Rate of Metabolites (pmol/min/pmol P450)					
	EVG	**M1 (GS-9202)**	**M2**	**M8**	**M5**	**Others**
2D6	< 0.1 (98.2)	ND	< 0.1 (0.4)	ND	ND	< 0.1 (1.4)
2E1	< 0.1 (98.3)	ND	< 0.1 (0.3)	ND	ND	NC (1.4)
3A4[a]	9.4 (34.8)	7.5 (50.3)	0.1 (0.5)	0.5 (3.1)	0.1 (0.9)	1.3 (10.4)
3A5	0.4 (95.6)	0.4 (2.5)	< 0.1 (0.4)	ND	ND	< 0.1 (1.5)
Human MS	(28.9)	(51.0)	(0.9)	(4.6)	(6.5)	(8.0)

CYP = cytochrome P450; EVG =elvitegravir; MS = hepatic microsomal fraction, ND = not detected, NC = not calculated
Note: Each value is the mean of 2 measurements for recombinant human CYP enzymes, and 1 measurement for human microsomes. Values in parentheses are the percentage of radioactivity in the sample.
a Values for CYP3A4 are re-assay values.

2.6.5.10.5. JTK303-AD-024: Determination of Km and Vmax for EVG Metabolism Using Human Liver Microsomes

Report Title	Study Type	Test Article	Report Number (Study Number)
In Vitro Study of JTK-303 (II) Determination of Km and Vmax Using Human Liver Microsomes	Metabolism study	[^{14}C]EVG	JTK303-AD-024 (AE-3981-G)

Study Methods: The Km and Vmax were determined from [^{14}C]EVG metabolic activity and M1 formation activity using human liver microsomes. [^{14}C]EVG (final concentrations of test article: 2, 4, 10, 20, 40, 60, and 120 µM) was incubated for 10 min with human liver microsomes (final concentration: 1 mg protein/mL), and the incubation mixture was pretreated and analyzed by HPLC-RAD. The Km and Vmax were determined by fitting the individual data to the Michaelis-Menten equation from the relationship between the metabolic activity (V), calculated from the amount of EVG degraded and the amount of M1 formed, and the initial concentration ($[S]_0$) of EVG.

	Km (µM)	Vmax (pmol/min/mg protein)
EVG degradation	21.46	1265
M1 (GS-9202) formation	20.36	1083

EVG = elvitegravir; Km = Michaelis-Menten affinity constant; Vmax = Theoretical maximum rate of metabolism

2.6.5.10.6. AD-183-2034: UDP-Glucuronosyl Transferase Phenotyping of EVG

Report Title	Study Type	Test Article	Report Number (Study Number)
UDP-Glucuronosyl Transferase Phenotyping of Elvitegravir	Metabolism study	EVG	AD-183-2034

Study Methods: EVG (20 µM) was incubated with insect cell microsomal fractions (2 mg/mL) containing twelve individual recombinant baculovirus-expressed human UGTs. The rates of formation of the acyl glucuronide metabolite, GS-9200 (M4), were then determined by LC tandem MS. Positive control UGT substrates (3 µM raloxifene, 3 µM trifluoperazine, 10 µM 7-hydroxycoumarin, 10 µM 4-hydroxyestradiol, or 10 µM scopoletin) were tested in parallel and metabolism was quantified as the in vitro half-life for loss of substrate.

Enzyme	Positive Control	Positive control t½ (min)	GS-9200 (M4) formation (pmol/mg protein/min)
None (control insect cell microsomes)	(None)		< 0.1
UGT1A1	Raloxifene	31.5	3.75
UGT1A3	Raloxifene	89.1	16.6
UGT1A4	Trifluoperazine	176	< 0.1
UGT1A6	7-Hydroxycoumarin	< 10	< 0.1
UGT1A7	7-Hydroxycoumarin	18.0	< 0.1
UGT1A8	7-Hydroxycoumarin	193	< 0.1
UGT1A9	7-Hydroxycoumarin	< 10	0.2
UGT1A10	Raloxifene	122	< 0.1
UGT2B4	4-Hydroxyestradiol	51.1	< 0.1
UGT2B7	4-Hydroxyestradiol	< 10	< 0.1
UGT2B15	Scopoletin	< 10	0.12
UGT2B17	4-Hydroxyestradiol	58.3	< 0.1

2.6.5.10.7. AD-216-2024 and AD-216-2074: Rate of Metabolism of COBI In Vitro

Report Title	Study Type	Test Article	Report Number (Study Number)
Identification of Major Metabolites of GS-9350 in CD-1 Mouse Microsomes In Vitro	Metabolism study	COBI	AD-216-2074
In Vitro Metabolism of GS-9350 in Hepatocytes and Hepatic Subcellular Fractions from Rat, Dog, Monkey, and Human			AD-216-2024

Type of Study: Determination of rates of metabolism of COBI by hepatic microsomal fraction

Method: Cobicistat (3 µM) was incubated with pooled hepatic microsomal fractions from CD-1 mice, Sprague-Dawley rats, beagle dogs, cynomolgus monkeys, and humans, with NADPH cofactor. Rates of metabolism (in vitro half-life values) were determined, and hepatic clearance and hepatic extraction were predicted using the well-stirred liver model. Analysis was by LC/MS/MS.

In Vitro Rate of Metabolism of COBI at 3 µM in Hepatic Microsomes (Mean Values, N=2–6)

Species	Half-Life (min)	Predicted Hepatic Clearance (L/h/kg)	Predicted Hepatic Extraction (%)
Mouse	137.0	0.99	19.1
Rat	82.1	1.50	35.6
Dog	43.7	0.88	48.8
Monkey	8.9	1.35	84.7
Human	154.9	0.37	28.3

COBI = cobicistat; LC/MS/MS = high performance liquid chromatography coupled to tandem mass spectrometry

2.6.5.10.8. AD-216-2025: Cytochrome P450 Phenotyping for COBI

Report Title	Study Type	Test Article	Report Number (Study Number)
Cytochrome P450 Phenotyping for GS-9350	Metabolism study	COBI	AD-216-2025

Study System: Rates of metabolism of COBI catalyzed by cDNA expressed major human cytochrome P450 enzyme preparations coexpressed with human NADPH CYP450 reductase (min^{-1} $pmol^{-1}$)

Compound	CYP1A2	CYP2C9	CYP2C19	CYP2D6	CYP3A4
COBI (% of Positive Control)	0.00 (0.0%)	0.00 (0.0%)	0.00 (0.0%)	0.105 (22.5%)	0.003 (4.5%)
Ethoxycoumarin	0.407	--	--	--	--
Diclofenac	--	0.467	--	--	--
Diazepam	--	--	0.035[a]	--	--
Dextromethorphan	--	--	--	0.467	--
Testosterone	--	--	--	--	0.066

cDNA = complementary deoxyribonucleic acid; COBI = cobicistat; CYP = cytochrome P450 enzyme(s)

a Diazepam is a selective substrate for CYP2C19, but is metabolized relatively slowly

2.6.5.11. Pharmacokinetics: Possible Metabolic Pathways

2.6.5.11.1. AD-183-2020: Metabolite Profiling of EVG in Mouse Liver Microsomes

Report Title	Study Type	Test Article	Report Number (Study Number)
Metabolite Profiling and Identification of [^{14}C]GS-9137/GS-9137 in Mouse Liver Microsomes	Metabolism study	[^{14}C]EVG	AD-183-2020 (60N-0627)

Study Methods: The in vitro biotransformation of [^{14}C]EVG was conducted in pooled male and female mouse liver microsomes. [^{14}C]EVG was incubated with mouse liver microsomes at 50 µM in duplicate for 60 minutes. HPLC/tandem MS coupled with an in-line radiochemical detector was used for metabolite profiling and identification.

Relative Abundance of EVG and its Metabolites after Incubation with Mouse Liver Microsomes at 50 µM for 60 Minutes (% of Radioactivity)

		EVG or Metabolite				
		M7a	M7b	M3 or M4	M1c	EVG
Male	200 mg/kg EVG	12.34	7.88	11.29	D	68.49
	2000 mg/kg EVG	13.12	12.56	12.46	D	61.86
	200 mg/kg EVG plus 25 mg/kg RTV	ND	ND	18.83	ND	81.17
	2000 mg/kg EVG plus 25 mg/kg RTV	ND	ND	11.79	ND	88.21
	Control	9.81	7.71	10.73	D	71.74
	Corn oil treated	10.49	8.53	11.17	8.87	60.93
	BNF treated	15.43	8.71	11.30	9.62	54.93
	DEX treated	15.77	13.13	7.37	3.36	60.37
	CLOF treated	14.17	13.29	9.81	D	62.73
Female	200 mg/kg EVG	17.06	9.70	7.70	6.52	59.02
	2000 mg/kg EVG	12.00	6.28	6.84	D	74.88
	200 mg/kg EVG plus 25 mg/kg RTV	ND	ND	3.56	ND	96.44
	2000 mg/kg EVG plus 25 mg/kg RTV	ND	ND	11.69	ND	88.31
	Control	6.98	5.10	6.71	D	81.21
	Untreated	9.38	4.76	7.51	D	78.36

BNF = β-Naphthoflavone; CLOF = Clofibrate; D = Detected by MS, but not by radioactivity; DEX = Dexamethasone, EVG = Elvitegravir; ND = Not detected by either MS or radioactivity; RTV = ritonavir.

2.6.5.11.2. JTK303-AD-021: Identification and Characterization of Metabolites of [^{14}C]EVG In Vivo and In Vitro Samples

Report Title	Study Type	Test Article	Report Number (Study Number)
Identification and Characterization of Metabolites of [^{14}C]-JTK-303 In Vivo and In Vitro Samples	Metabolism study	[^{14}C]EVG	JTK303-AD-021 (JK303PK042)

Test System:

Samples:

In vivo: Dog; feces and urine
Rat; bile

In vitro: metabolite using human, dog, rat or monkey liver microsomes

Method:

Radio-LC/MS/MS

2.6.5.11.2. JTK303-AD-021: Identification and Characterization of Metabolites of [^{14}C]EVG In Vivo and In Vitro Samples (Continued)

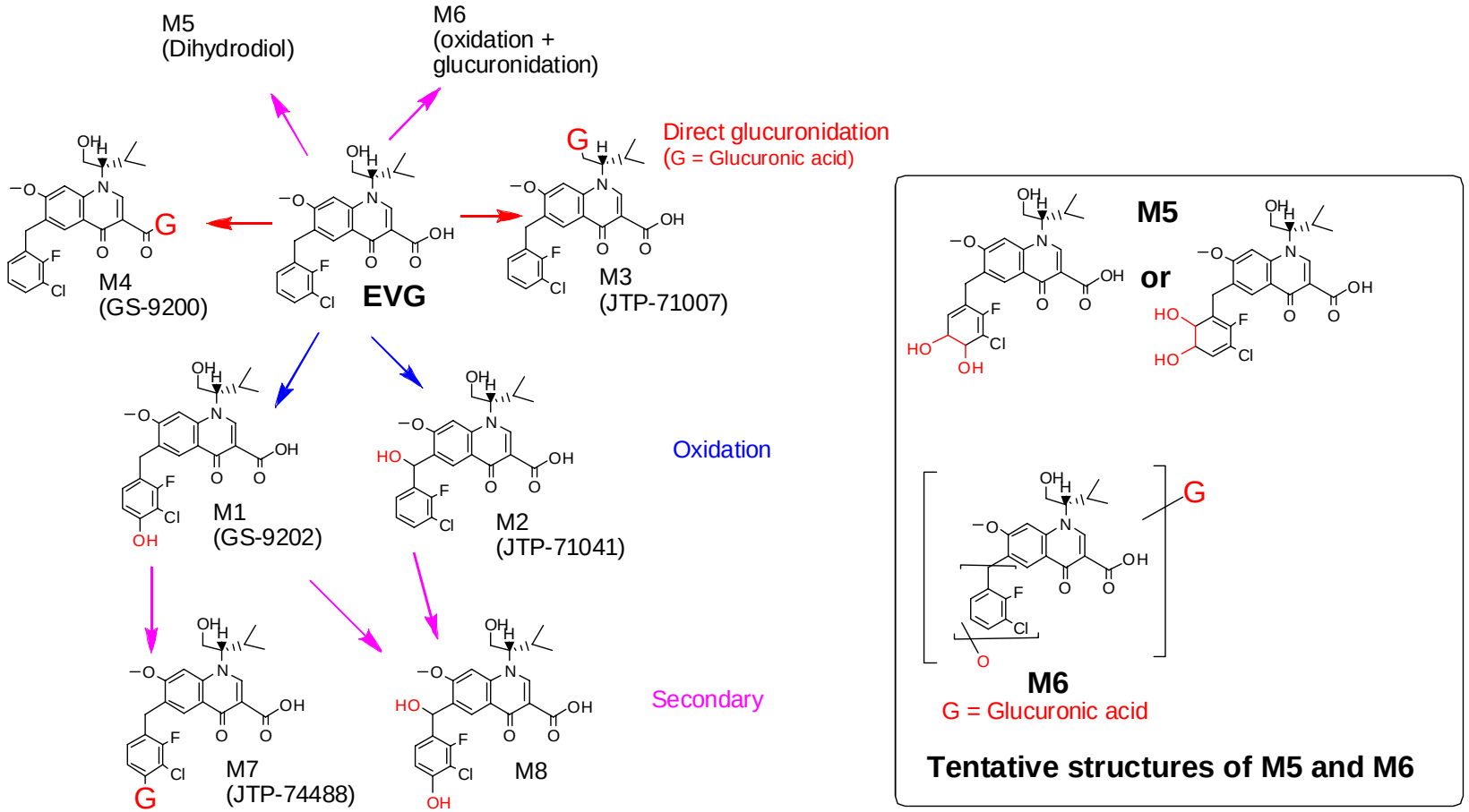

2.6.5.11.3. 60N-0508: Elvitegravir Metabolite Profiling in Rabbits In Vitro

Report Title	Study Type	Test Article	Report Number (Study Number)
Metabolite Profiling and Identification of [^{14}C]EVG/EVG in Pooled Female New Zealand Rabbit Liver Microsomes	Metabolism study	[^{14}C]EVG	60N-0508

Study Methods: The in vitro biotransformation of [^{14}C]EVG was conducted in pooled female New Zealand rabbit liver microsomes. [^{14}C]EVG at 10 and 50 µM was incubated with female rabbit liver microsomes in a 37ºC incubator for 30 and 60 minutes. The microsomal concentration was 2 mg/mL, and the total incubation volume was 1 mL. Incubation with positive controls, 7-ethoxycoumarin (2 µM) and 7-hydroxycoumarin (20 µM), were performed concurrently with the test article to assess phase I and phase II metabolic activities. At the designated time, 2 volumes of acetonitrile for test article samples or positive controls were added to the incubation mixture to stop the metabolic reaction. HPLC/tandem MS coupled with in-line radiochemical detector was used for metabolite profiling and identification. Metabolites of EVG were separated using reverse phase chromatography, and detected by radiochemical detector and mass spectrometer simultaneously. Tandem MS of the molecular ions was performed, and the structures of the metabolites were proposed by interpretation of their mass spectra.

EVG and Metabolites	Percentage of Peak Area on Radiochromatogram
EVG	41.0
M1 (GS-9202)	13.3
M1a	Not Available
M1b	1.3
M5	16.3
M5a	2.1
HM1	2.2
M3 or M4	1.0
M6	11.7
M7	2.5

EVG = elvitegravir

2.6.5.11.4. Common Primary and Secondary Routes of COBI Metabolism in Mouse, Rat, Dog, and Human In Vivo and In Vitro

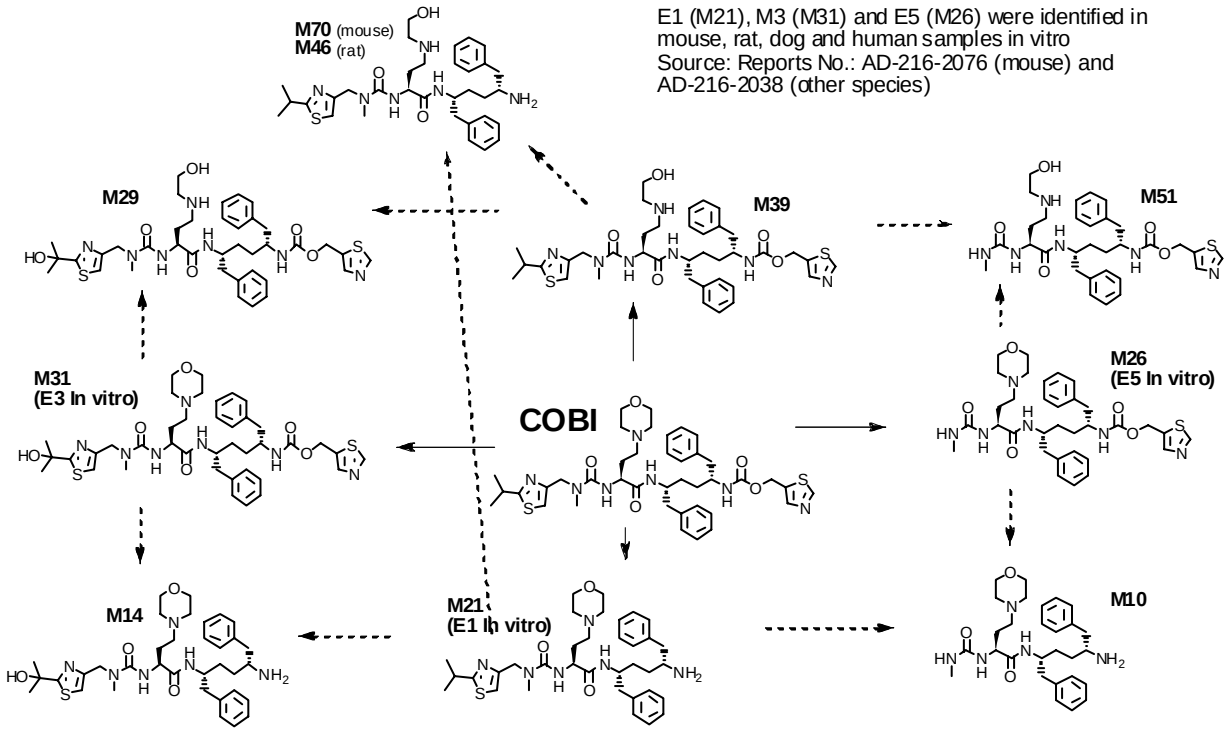

COBI and all metabolites were detected in samples from mouse, rat, dog, and human, except M29 (not in human), M51 (rat only) and M70/M46 (mouse and rat only).
Dashed arrows indicate combinations of primary metabolic pathways, not proven routes of metabolism.
Source: Reports AD-216-2038, AD-216-2076 (in vitro), AD-216-2073 (mouse), AD-216-2082 (rat), AD-216-2101 (dog), and GS-US-216-0111 (human)

2.6.5.11.5. Routes of COBI Metabolism Involving 2-Isopropyl-5 Thiazole Oxidation and 4-Thiazole Oxidation

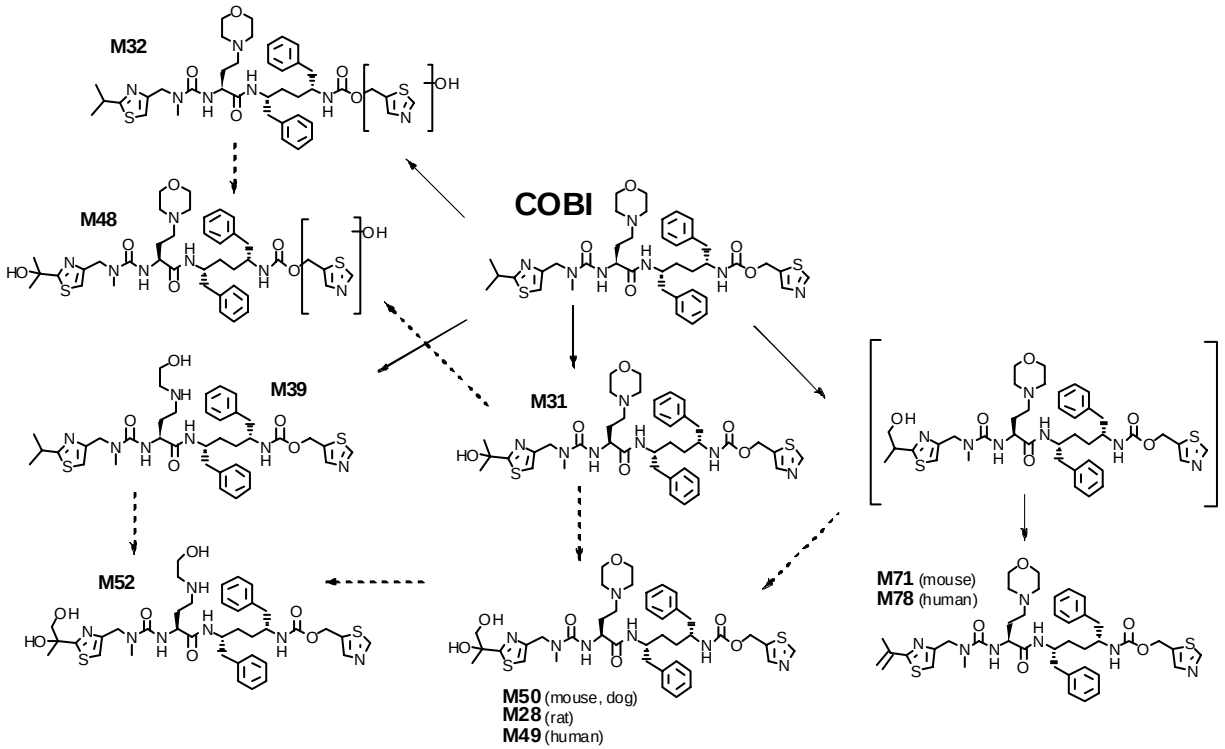

Bracketed metabolite was not detected, but its formation is implied by the presence of secondary metabolites.

COBI, M31, M39 and the dihydroxy-isopropyl metabolite (M50/M28/M49) were detected in all 4 species (mouse, rat, dog, and human).

The dehydro isopropyl metabolite (M71/M78) was detected in mouse and human. M32 was not detected in dog. M48 and M52 were only detected in rat.

Dashed arrows indicate combinations of primary metabolic pathways, not proven routes of metabolism.

Source: Reports AD-216-2073 (mouse), AD-216-2082 (rat), AD-216-2101 (dog), and GS-US-216-0111 (human)

2.6.5.11.6. Other Metabolic Routes of COBI

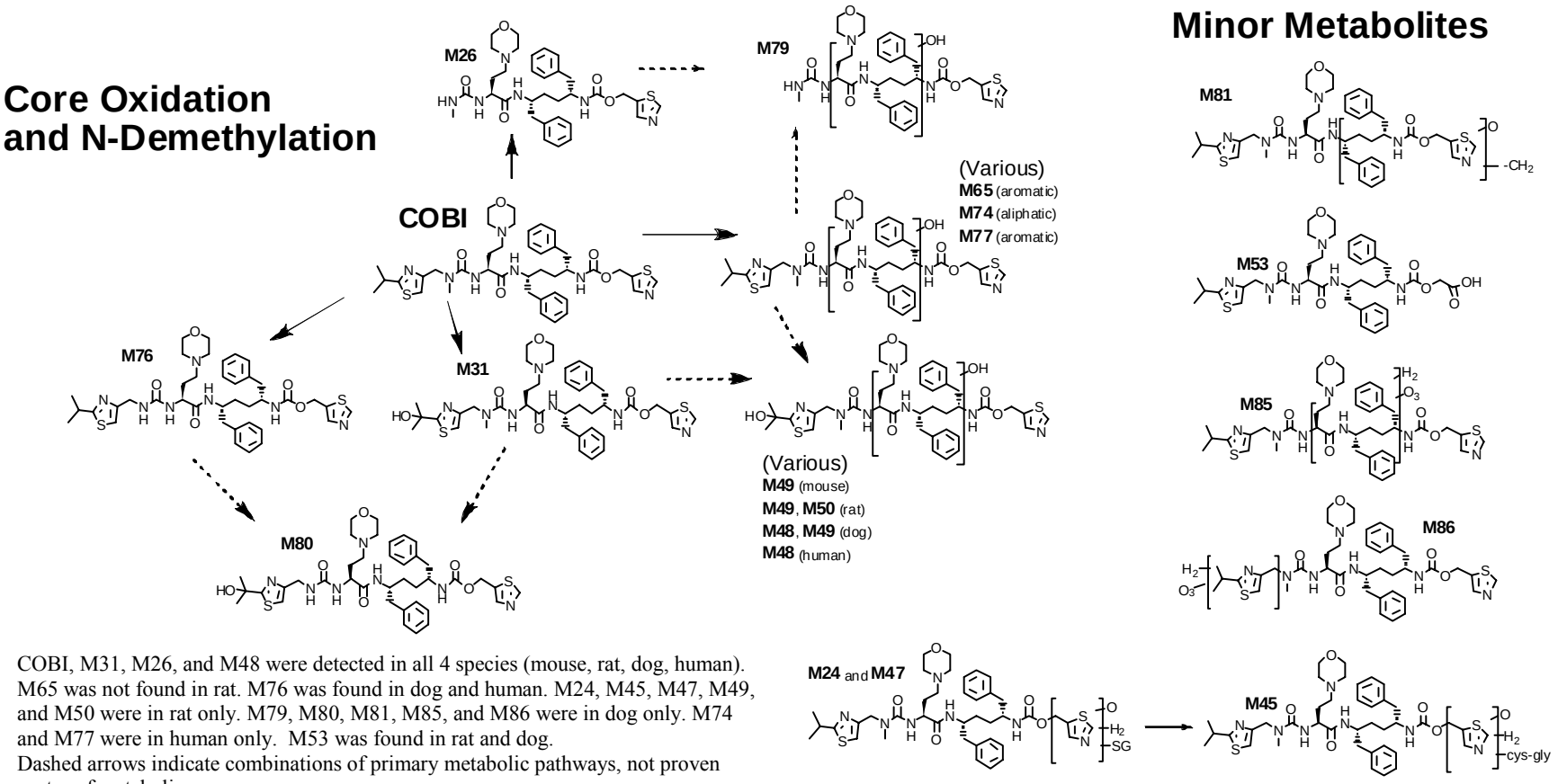

COBI, M31, M26, and M48 were detected in all 4 species (mouse, rat, dog, human). M65 was not found in rat. M76 was found in dog and human. M24, M45, M47, M49, and M50 were in rat only. M79, M80, M81, M85, and M86 were in dog only. M74 and M77 were in human only. M53 was found in rat and dog.
Dashed arrows indicate combinations of primary metabolic pathways, not proven routes of metabolism.
Source: Reports AD-216-2073 (mouse), AD-216-2082 (rat), AD-216-2101 (dog), and GS-US-216-0111 (human)

2.6.5.12. Pharmacokinetics: Induction/Inhibition of Drug Metabolizing Enzymes

2.6.5.12.1. JTK303-AD-027: Inhibition of Human Cytochrome P450 Enzymes by EVG

Report Title	Study Type	Test Article	Report Number (Study Number)
In Vitro Metabolism Study of JTK-303 (I) Enzyme Inhibition Study Using Human Liver Microsomes – Determination of IC_{50}	Metabolism study	[^{14}C]EVG	JTK303-AD-027

Study Methods: The inhibitory effect of JTK-303 on human P450 enzymes (CYP1A2, CYP2A6, CYP2C9, CYP2C19, CYP2D6, CYP2E1, and CYP3A4) was investigated using human liver microsomes at EVG concentrations of 0, 0.1, 0.3, 1, 3, 10, and 30 µg/mL (0, 0.2, 0.7, 2.2, 6.7, 22.3, and 67.0 µM).

Enzyme	Activity	EVG	Control Inhibitor[a]
		Calculated IC_{50} (µg/mL)	Activity remaining (%)
CYP1A2	Ethoxyresorufin O-deethylase	> 30	5.6%
CYP2A6	Coumarin 7-hydroxylase	> 30	< 10.2%
CYP2C9	Tolbutamide 4-hydroxylase	> 30	42.5%
CYP2C19	(S) Mephenytoin 4'-hydroxylase	> 30	29.6%
CYP2D6	Bufuralol 1'-hydroxylase	> 30	< 17.5%
CYP2E1	Chlorzoxazone 6-hydroxylase	> 30	48.3%
CYP3A	Midazolam 1'-hydroxylase	> 30	< 9.6%
	Testosterone 6β-hydroxylase	28.32	5.6%

a Control inhibitors: CYP1A2, α Naphthoflavone (1 µM); CYP2A6, Methoxsalen (5 µM); CYP2C9, Sulfaphenazole (3 µM); CYP2C19, Tranylcypromine (20 µM); CYP2D6, Quinidine (4 µM); CYP2E1 Diethyldithiocarbamate (100 µM); CYP3A, Ketoconazole (1 µM).

2.6.5.12.2. JTK303-AD-023: Enzyme Induction Study of EVG in Primary Cultured Human Hepatocytes

Report Title	Study Type	Test Article	Report Number (Study Number)
Enzyme Induction Study of JTK-303 in Fresh Primary Cultured Human Hepatocytes	Metabolism study	EVG	JTK303-AD-023 (GE-0113-G)

Study Methods: The induction potential of EVG on hepatic drug-metabolizing enzymes was investigated by assay of enzyme activities (CYP1A2, CYP2C9, CYP2C19, and CYP3A) in fresh primary cultured human hepatocytes (2 individuals) after exposure to EVG at 0.1, 1, and 10 μg/mL (0.2, 2.2, and 22.3 μM) for 3 days.

Test Compound		Effect of EVG on CYP1A2 (Phenacetin O-deethylation)		Effect of EVG on CYP2C9 (Tolbutamide 4-hydroxylation)	
		Enzyme Activity[a] (pmol/h/mg protein)	IR[b]	Enzyme Activity[a] (pmol/h/mg protein)	IR[b]
0.1% DMSO (Solvent Control)	Lot 66	174	1.00 (3)	294	1.00 (32)
	Lot 68	21.9	1.00 (2)	93.7	1.00 (23)
0.1 μg/mL (0.2 μM) EVG	Lot 66	205	1.18 (4)	281	0.956 (30)
	Lot 68	23.7	1.08 (2)	86.4	0.922 (21)
1 μg/mL (2.2 μM) EVG	Lot 66	216	1.24 (4)	350	1.19 (38)
	Lot 68	34.7	1.58 (3)	154	1.64 (38)
10 μg/mL (22.3 μM) EVG	Lot 66	110	0.632 (2)	437	1.49 (47)
	Lot 68	25.3	1.16 (2)	255	2.72 (63)
Positive Control[c]	Lot 66	5320	30.6 (100)	924	3.14 (100)
	Lot 68	1060	48.4 (100)	402	4.29 (100)

2.6.5.12.2. JTK303-AD-023: Enzyme Induction Study of EVG in Primary Cultured Human Hepatocytes (Continued)

Test Article: EVG

Test Compound		Effect of EVG on CYP2C19 (S Mephenytoin 4'-hydroxylation)		Effect of EVG on CYP3A (Midazolam 1'-hydroxylation)	
		Enzyme Activity[a] (pmol/h/mg protein)	IR[b]	Enzyme Activity[a] (pmol/h/mg protein)	IR[b]
0.1% DMSO (Solvent Control)	Lot 66	< 4.54	--	96.1	1.00 (3)
	Lot 68	< 6.39	--	107	1.00 (4)
0.1 μg/mL (0.2 μM) EVG	Lot 66	< 4.51	--	167	1.74 (5)
	Lot 68	< 6.73	--	158	1.48 (6)
1 μg/mL (2.2 μM) EVG	Lot 66	< 4.60	--	616	6.41 (19)
	Lot 68	< 6.49	--	676	6.32 (25)
10 μg/mL (22.3 μM) EVG	Lot 66	< 4.77	--	1840	19.1 (56)
	Lot 68	< 6.40	--	1130	10.6 (41)
Positive Control[c]	Lot 66	< 4.86	--	3280	34.1 (100)
	Lot 68	9.62	-- (100)	2750	25.7 (100)

DMSO = dimethylsulfoxide; EVG = elvitegravir; IR = induction ratio (relative to 0.1% DMSO)

a Mean values was calculated from values of 2 wells.

b The values in parentheses express activity as percent of positive control (not corrected for vehicle control).

c Positive controls: 20 μM β-naphthoflavone (CYP1A2), 20 μM rifampicin (CYP2C9, CYP2C19), 10 μM rifampicin (CYP3A)

2.6.5.12.3. AD-183-2021: Determination of Activities of NADPH-Cytochrome P450 Reductase and Cytochrome P450 Enzymes in Hepatic Microsomal Fractions from Mice Treated with EVG

Report Title	Study Type	Test Article	Report Number (Study Number)
Determination of Activities of NADPH-Cytochrome P450 Reductase and Cytochrome P450 Isozymes in Mouse Liver Microsomes from Commercial Source and from Mouse Treated with GS-9137	Metabolism study	EVG	AD-183-2021

Study Methods: The induction potential of EVG for CYP1A1/2, CYP2B9/10, CYP3A11/13, and CYP4A was evaluated ex vivo using liver samples collected as part of a multiple-dose PK study in CD-1 mice dosed with EVG (200 and 2000 mg/kg/day) orally, with and without RTV, for 7 days. Mouse livers were pooled from 12 male and 12 female mice for each treatment group (200 mg/kg/day of EVG, 2000 mg/kg/day of EVG, 200 mg/kg/day of EVG + 25 mg/kg/day of RTV, and 2000 mg/kg/day of EVG + 25 mg/kg/day of RTV). The vehicle control livers were pooled from 8 males and 8 females. Microsomes were prepared from mouse livers using differential ultracentrifugation and were incubated with enzyme-selective probe substrates. The marker metabolites of the probe substrate were acetaminophen for CYP1A1/2, 16β-hydroxytestosterone for CYP2B9/10, 6β hydroxytestosterone for CYP3A11/13, and 12-hydroxylauric acid for CYP4A. The extent of induction was evaluated by comparing CYP activities in different EVG dosing groups to the vehicle control group. Incubations with commercially available induced mouse liver microsomes, as references, were performed concurrently with the microsomes prepared from EVG treated study samples.

	Fold Over Vehicle Control							
	CYP1A1/2 Activity		CYP2B9/10 Activity		CYP3A11/13 Activity		CYP4A Activity	
Treatment	Male	Female	Male	Female	Male	Female	Male	Female
EVG 200 mg/kg	1.81	2.09	0.90	ND	0.78	3.50	0.96	2.00
EVG 2000 mg/kg	1.57	3.50	1.06	ND	1.18	8.18	0.93	2.13
EVG 200 mg/kg + RTV 25 mg/kg	1.59	2.13	1.15	ND	0.05	0.30	1.00	1.61
EVG 2000 mg/kg + RTV 25 mg/kg	1.35	2.76	1.00	ND	0.07	0.42	0.85	1.32
Positive Control[a]	1.75	--	1.92	--	6.47	--	7.43	--

EVG = Elvitegravir; ND = not detected; RTV = ritonavir

Corn oil was used as the vehicle control for the positive control.

a Positive controls, male mice were treated as follows: β-naphthoflavone for CYP1A1/2; dexamethasone for CYP2B9/10 and CYP3A11/13; and clofibric acid for CYP4A.

2.6.5.12.4. AD-216-2028: Human CYP3A Mechanism-Based Inhibition Potential of COBI In Vitro

Report Title	Study Type	Test Article	Report Number (Study Number)
Inhibition of Human CYP3A Activity by GS-9350 In Vitro	Metabolism study	COBI	AD-216-2028

Type of Study: Mechanistic and kinetic study of human CYP3A mechanism-based inhibition potential of COBI

Method: The preincubation time and cofactor dependence of the CYP3A inhibitory potency were determined. Values refer to the fractional decrease in CYP3A activity due to preincubation with NADPH, compared to preincubation in the absence of cofactor. Mifepristone, a known mechanism-based inhibitor of human CYP3A enzymes, and mibefradil, another compound showing both direct and mechanism-based inhibition of human CYP3A enzymes, were run as positive controls. To confirm and quantify the potency of COBI as a mechanism-based inhibitor, the kinetics for the inactivation of human CYP3A enzymes were determined using midazolam 1'-hydroxylase as a selective activity and a 2-step incubation protocol (10 × dilution between steps). Ritonavir was tested as a comparator.

Compound	Cofactor- and Preincubation-Dependent Inhibition of CYP3A Activities by COBI, RTV, and Positive Control Compounds					
	Cofactor-Dependent Inhibition (%, Mean ±SD, n=2)					
	Midazolam 1'Hydroxylase Activity			Testosterone 6β-Hydroxylase Activity		
COBI	69.6	±	0.15	82.1	±	0.23
RTV	55.9	±	13.5	74.8	±	5.22
Mibefradil	67.3	±	4.87	80.3	±	1.12
Mifepristone	83.9	±	1.56	71.2	±	3.69

COBI = cobicistat; CYP = cytochrome P450 enzyme(s); RTV = ritonavir

2.6.5.12.4. AD-216-2028: Human CYP3A Mechanism-Based Inhibition Potential of COBI In Vitro (Continued)

Test Article: COBI

Kinetics for Inactivation[a] of Human Hepatic Microsomal CYP3A Activity by COBI and RTV

Parameter	Inhibitor	
	COBI	RTV
K_I (μM)	1.07	0.26
K_{inact} (min^{-1})	0.47	0.23

COBI = cobicistat; CYP = cytochrome P450 enzyme(s); RTV = ritonavir
a Inactivation kinetics were determined using midazolam 1'hydroxylase as the probe activity.

2.6.5.12.5. AD-216-2040: Inhibition of CYP3A Activity in Rat, Dog, and Monkey by COBI In Vitro

Report Title	Study Type	Test Article	Report Number (Study Number)
Inhibition of CYP3A Activity in Rat, Dog and Monkey by GS-9350 In Vitro	Metabolism study	COBI	AD-216-2040

Method: The potential for COBI to inhibit the catalytic activity of CYP3A enzymes of rat, dog, and cynomolgus monkey was assessed in vitro and compared to RTV. The inhibitory effects of COBI and RTV on hepatic microsomal midazolam 1'-hydroxylase activity were measured, and IC_{50} values were determined. Inactivation kinetics were determined, where possible, using a 2-stage incubation protocol with a 10-fold dilution step.

Inactivation Kinetics for COBI and RTV for Hepatic Microsomal CYP3A Activity in Rat, Dog and Monkey				Effect of COBI and RTV on Hepatic Microsomal CYP3A Activity in Rat, Dog and Monkey	
				Calculated IC_{50} (µM)	
Species	Parameter	COBI	RTV	COBI	RTV
Sprague Dawley Rat	K_I (µM)	0.32	0.24	0.17	0.06
	k_{inact} (min^{-1})	0.045	0.028		
Beagle Dog	K_I (µM)	ND	ND	0.12	0.04
	k_{inact} (min^{-1})	ND	ND		
Cynomolgus Monkey	K_I (µM)	ND	ND	0.43	0.12
	k_{inact} (min^{-1})	ND	ND		

COBI = cobicistat; CYP = cytochrome P450 enzyme(s); IC_{50} = concentration at which 50% maximum inhibition is achieved; K_I = affinity constant for enzyme inactivation; K_{inac} = theoretical maximum enzyme inactivation rate; RTV = ritonavir

ND = Cannot be determined (curve fit does not converge)

2.6.5.12.6. AD-216-2029 and AD-216-2070: Cytochrome P450 Inhibition Potential of COBI

Report Title	Study Type	Test Article	Report Number (Study Number)
In Vitro Assessment of Human Liver Cytochrome P450 Inhibition Potential of GS-9350	Metabolism study	COBI	AD-216-2029
In Vitro Assessment of Human Liver CYP2B6 and CYP2C8 Inhibition Potential of GS-9350			AD-216-2070

Method: With human hepatic microsomal fraction as the catalyst the rates of enzyme-specific metabolite formation for each cytochrome P450 enzyme were determined in the presence or absence of increasing concentrations of the test compound (0.05, 0.25, 0.5, 2.5, 5, and 25 μM). Substrates concentrations were equal to, or less than, their respective Km values and reactions were linear with respect to protein and time. IC_{50} values were determined for COBI and positive control inhibitors.

Enzyme	Activity	Calculated IC_{50} Value (μM)		
		Control Inhibitor[a]	COBI	RTV
CYP1A2	Ethoxyresorufin O-deethylase	0.03	> 25	> 25
CYP2B6	Bupropion 4-hydroxylase	2.80	2.8	2.9
CYP2C8	Paclitaxel 6α-hydroxylase	0.06	30.1	5.5
CYP2C9	Tolbutamide 4-hydroxylase	1.58	> 25	3.9
CYP2C19	(S) Mephenytoin 4'-hydroxylase	10.8	> 25	> 25
CYP2D6	Dextromethorphan O-demethylase	0.04	9.17	3.4
CYP3A	Midazolam 1'-hydroxylase	0.07	0.154	0.10
	Testosterone 6β-hydroxylase	0.09	0.151	0.11

COBI = cobicistat; CYP = cytochrome P450 enzyme(s); IC_{50} = concentration at which 50% maximum inhibition is achieved; RTV = ritonavir

a Positive Control Inhibitors: CYP1A2, α-Naphthoflavone (0–100 μM); CYP2B6, Triethylenethiophosphoramide (0–30 μM); CYP2C8 Montelukast (0–30 μM); CYP2C9, Sulfaphenazole (0–10 μM); CYP2C19, Tranylcypromine (0–100 μM); CYP2D6, Quinidine (0–10 μM); CYP3A, Ketoconazole (0–10 μM)

2.6.5.12.7. AD-216-2041: Drug Interaction Properties of Human Metabolites of COBI

Report Title	Study Type	Test Article	Report Number (Study Number)
Drug Interaction Properties of Putative Human Metabolites of GS-9350	Metabolism study	COBI, GS-342006, GS-364751, GS-341842	AD-216-2041

Method: The effects of 3 human metabolites of COBI on the activities of 5 major human drug metabolizing cytochromes P450 were assessed and compared to COBI. In addition PXR and AhR activation by COBI, putative metabolites, and positive controls was assessed. The metabolites of COBI were identified during incubations with both human hepatocytes and human hepatic microsomal fractions and were later identified in vivo.

Enzyme	Activity	Calculated IC_{50} Value (μM)			
		COBI[a]	GS-342006 (E1 or M21)	GS-364751 (E3 or M31)	GS-341842 (E5 or M26)
CYP1A2	Ethoxyresorufin O-deethylase	> 25	> 25	> 25	> 25
CYP2C9	Tolbutamide 4-hydroxylase	> 25	> 25	> 25	> 25
CYP2C19	(S) Mephenytoin 4'-hydroxylase	> 25	> 25	2.95	> 25
CYP2D6	Dextromethorphan O-demethylase	9.17	> 5	0.21	> 5
CYP3A	Midazolam 1'-hydroxylase	0.154	2.41	0.179	0.23
	Testosterone 6β-hydroxylase	0.151	> 5	0.287	0.71
	Terfenadine oxidase	0.25	> 25	1.85	> 25

COBI = cobicistat; CYP = cytochrome P450 enzyme(s); IC_{50} = concentration at which 50% maximum inhibition is achieved

a Data for COBI are provided for comparison (Studies AD-216-2028 and AD-216-2029).

2.6.5.12.7. AD-216-2041: Drug Interaction Properties of Human Metabolites of COBI (Continued)

Test Article: COBI

PXR Activation							
	Fold Induction Over 0.1% DMSO Control						
Concentration (µM)	**COBI[a]**	**GS-342006 (E1 or M21)**	**GS-364751 (E3 or M31)**	**GS-341842 (E5 or M26)**	**Rifampicin**	**Mifepristone**	**Androstanol**
1	1.57	0.85	0.84	1.38	—	—	—
3	1.61	1.50	0.92	1.17	—	—	—
10	2.24	1.62	1.24	1.42	12.49[a]	7.10[a]	3.67[a]
AhR Activation							
1	1.12	0.86	0.93	0.81	**Omeprazole[b]**		
3	1.28	0.83	0.84	0.75	—		
10	1.60	0.83	0.76	0.68	—		
25	—	—	—	—	5.94		
50	—	—	—	—	13.83		
100	—	—	—	—	32.74		
200	—	—	—	—	52.45		

AhR = aryl hydrocarbon receptor; COBI = cobicistat; PXR = pregnane X receptor

a Data for COBI are provided for comparison (Study AD-216-2027)

b Average of values from GIL-20[redacted]-107 and GIL-20[redacted]-108

2.6.5.12.8. AD-216-2075: In Vitro Assessment of Human UGT1A1 Inhibition Potential of COBI

Report Title	Study Type	Test Article	Report Number (Study Number)
In Vitro Assessment of Human UGT1A1 Inhibition Potential of GS-9350	Metabolism study	COBI	AD-216-2075

Method: The potential for COBI to inhibit the catalytic activity of human UGT1A1 was assessed. The rates of formation of β-estradiol-3-glucuronide from estradiol substrate by hepatic microsomal fractions were determined in the presence and absence of test compound, and, where possible, IC_{50} values were determined. Ritonavir and ATV were used as comparators.

Enzyme	Activity	Calculated IC_{50} (μM)[a]		
		ATV	RTV	COBI
UGT1A1	β-estradiol-3-glucuronidation	0.83	4.73	16.3

ATV = atazanavir; COBI = cobicistat; RTV = ritonavir; UGT = uridine diphosphate glucuronosyl transferase
a Mean, n = 3

2.6.5.12.9. AD-216-2027: Induction of Metabolizing Enzymes by COBI In Vitro

Report Title	Study Type	Test Article	Report Number (Study Number)
Induction of Metabolizing Enzymes by GS-9350 In Vitro	Metabolism study	COBI	AD-216-2027

Method: Assessments of induction were done using hepatoma-derived cell lines. DRE12.6 cells are transformed with an expression vector for human AhR and the Dioxin Response Element (DRE) of the human CYP1A2 gene linked to a luciferase reporter. DPX2 express human PXR and have the promoter for CYP3A4 linked to the luciferase reporter. Following 24 hours of exposure to the test articles, the luciferase substrate was added and the luminescence was read in a luminometer. The average luminescent units for the three replicates were divided by the average for the DMSO solvent control to determine the fold-induction. Positive control inducers were tested in parallel.

Concentration (μM)	Fold Induction of Human AhR Over 0.1% DMSO Control (DRE12.6 cells)			
	COBI	RTV	β-Naphthoflavone	Omeprazole
0.1 μM	—	—	2.17	
1 μM	1.12	0.80	5.91	
3 μM	1.28	0.69	—	
5 μM	—	—	17.72	
10 μM	1.60	0.80	27.31	
25 μM	—	—	—	8.16
50 μM	—	—	—	13.46
100 μM	—	—	—	27.34
200 μM	—	—	—	67.33

AhR = aryl hydrocarbon receptor; COBI = cobicistat; CYP = cytochrome P450 enzyme; RTV = ritonavir

2.6.5.12.9. AD-216-2027: Induction of Metabolizing Enzymes by COBI In Vitro (Continued)

Test Article: COBI

Concentration	Fold Induction of Human PXR Over 0.1% DMSO Control (DPX2 cells)				
	COBI	**RTV**	**Rifampicin**	**Mifepristone**	**Androstanol**
0.3 μM	—	—	3.15	—	—
1 μM	1.57	3.64	6.09	—	—
3 μM	1.61	7.62	9.90	—	—
10 μM	2.24	10.14	14.30	8.58	3.38

COBI = cobicistat; PXR = pregnane X receptor (NR1I2); RTV = ritonavir

2.6.5.12.10. AD-216-2071: In Vitro Assessment of the Induction Potential of COBI in Primary Cultures of Human Hepatocytes

Report Title	Study Type	Test Article	Report Number (Study Number)
In Vitro Assessment of the Induction Potential of GS-9350 in Primary Cultures of Human Hepatocytes	Metabolism study	COBI	AD-216-2071

Method: Cobicistat (1, 3, 10, and 30 μM) and known CYP inducers, 3-methylcholanthrene (3-MC), phenobarbital (PB), and rifampicin (RIF) were incubated in cultures of human hepatocytes from 3 separate donors for 3 consecutive days. Microsomes were isolated and CYP1A2, CYP2B6, and CYP3A levels were determined using enzyme-selective activities. Messenger RNA (mRNA) content for each of these CYP enzymes, UGT1A1 (UDP-glucuronosyltransferase), and MDR1 (multi-drug resistance protein) was also analyzed using TaqMan-based quantitative real-time polymerase chain reaction (qRT-PCR). Western immunoblotting was performed to detect the immunoreactive CYP3A protein.

Enzyme	CYP 1A2			CYP2B6			CYP3A		
Activity	Phenacetin O-deethylase			Bupropion 4-hydroxylase			Testosterone 6β-hydroxylase		
Donor	Hu790	Hu793	Hu8053	Hu790	Hu793	Hu8053	Hu790	Hu793	Hu8053
Summary of Enzyme Activity (Percent Adjusted Positive Control) after Treatment with COBI or Positive Control Inducers									
3-MC (2 μM)	100	100	100	4.8	0.10	4.7	0.01	–4.2	4.9
Phenobarbital (1000 μM)	3.3	6.1	–2.7	100	100	100	70.6	65.4	72.9
Rifampicin (10 μM)	2.5	3.7	–3.5	80.2	54.1	38.5	100	100	100
COBI (1 μM)	0.54	–0.38	–5.8	8.4	1.2	5.2	–1.4	–6.7	–0.23
COBI (3 μM)	0.26	–0.31	–5.1	3.5	–1.7	9.0	–1.7	–6.5	0.16
COBI (10 μM)	1.7	1.3	–1.5	3.7	4.4	12.8	–1.6	–6.0	0.04
COBI (30 μM)	0.61	4.2	–1.4	20.5	2.5	3.8	8.2	–6.5	–1.2

2.6.5.12.10. AD-216-2071: In Vitro Assessment of the Induction Potential of COBI in Primary Cultures of Human Hepatocytes (Continued)

Test Article: COBI

Treatment	CYP 1A2			CYP2B6			CYP3A			UGT1A1			MDR1		
Donor	Hu-790	Hu-793	Hu-8053	Hu-790	Hu-793	Hu-8053	Hu-790	Hu-793	Hu-8053	Hu-790	Hu-793	Hu-8053	Hu-790	Hu-793	Hu-8053
Summary of Enzyme Activity (Fold Induction over DMSO Vehicle Control) after Treatment with COBI or Positive Control Inducers															
3-MC (2 µM)	102.6	42.5	15.5	1.2	1.0	1.8	1.0	0.6	2.2	—	—	—	—	—	—
Phenobarbital (1000 µM)	4.3	3.5	0.6	5.5	9.0	17.4	16.0	7.3	19.1	—	—	—	—	—	—
Rifampicin (10 µM)	3.5	2.5	0.5	4.6	5.3	7.3	22.2	10.6	25.9	—	—	—	—	—	—
COBI (1 µM)	1.5	0.8	0.2	1.4	1.1	1.8	0.7	0.4	0.9	—	—	—	—	—	—
COBI (3 µM)	1.3	0.9	0.3	1.2	0.9	2.5	0.6	0.4	1.0	—	—	—	—	—	—
COBI (10 µM)	2.7	1.5	0.8	1.2	1.4	3.1	0.7	0.4	1.0	—	—	—	—	—	—
COBI (30 µM)	1.6	2.7	0.8	1.9	1.2	1.6	2.7	0.4	0.7	—	—	—	—	—	—

2.6.5.12.10. AD-216-2071: In Vitro Assessment of the Induction Potential of COBI in Primary Cultures of Human Hepatocytes (Continued)

Test Article: COBI

Treatment	CYP 1A2			CYP2B6			CYP3A4			UGT1A1			MDR1		
Donor	Hu-790	Hu-793	Hu-8053	Hu-790	Hu-793	Hu-8053	Hu-790	Hu-793	Hu-8053	Hu-790	Hu-793	Hu-8053	Hu-790	Hu-793	Hu-8053
Summary of mRNA Content (Percent Adjusted Positive Control) after Treatment with COBI or Positive Control Inducers															
3-MC (2 µM)	100	100	100	3.1	–0.53	0.65	–0.97	–1.3	–2.8	140	81.2	83.6	–25.5	–33.1	–31.2
Phenobarbital (1000 µM)	0.14	0.34	0.15	100	100	100	61.0	79.6	47.8	124	127	107	89.8	98.9	106
Rifampicin (10 µM)	0.07	0.01	0.16	32.1	40.9	78.1	100	100	100	100	100	100	100	100	100
COBI (1 µM)	0.08	0.05	–0.01	0.65	–0.67	6.2	7.0	14.4	10.0	3.4	7.6	8.4	–3.6	–35.8	–11.4
COBI (3 µM)	0.15	–0.14	0.07	0.65	–0.02	13.2	17.6	25.2	32.0	3.4	10.6	17.6	–4.5	–21.5	8.0
COBI (10 µM)	0.53	0.04	0.65	0.29	–0.12	8.9	22.9	27.9	31.3	0.37	10.2	18.4	14.8	–6.9	2.3
COBI (30 µM)	1.4	3.0	1.7	–1.2	–1.2	–6.4	2.7	19.0	4.0	–4.4	6.2	–1.7	28.2	8.4	49.4
Summary of mRNA Content (Relative-Fold Induction) after Treatment with COBI or Positive Control Inducers															
3-MC (2 µM)	400	406	565	3.10	0.825	1.07	0.270	0.528	0.227	12.0	9.63	3.94	0.693	0.573	0.687
Phenobarbital (1000 µM)	1.55	2.46	1.78	65.3	46.4	12.1	45.2	31.9	12.2	10.8	14.5	4.78	1.96	2.30	2.00
Rifampicin (10 µM)	1.26	1.15	1.85	21.7	19.6	9.64	73.5	39.7	24.6	8.85	11.6	4.53	2.07	2.31	1.94
COBI (1 µM)	1.30	1.28	0.864	1.55	0.763	1.69	6.08	6.58	3.26	1.22	1.85	1.25	0.933	0.538	0.875
COBI (3 µM)	1.58	0.522	1.33	1.54	1.06	2.46	13.8	10.8	8.48	1.22	2.16	1.58	0.923	0.724	1.06
COBI (10 µM)	3.10	1.27	4.60	1.32	1.01	1.99	17.6	11.8	8.32	0.980	2.12	1.61	1.14	0.914	1.01
COBI (30 µM)	6.62	13.3	10.4	0.377	0.501	0.293	2.91	8.36	1.85	0.603	1.70	0.890	1.28	1.11	1.45

2.6.5.12.10. AD-216-2071: In Vitro Assessment of the Induction Potential of COBI in Primary Cultures of Human Hepatocytes (Continued)

Test Article: COBI

Summary of Changes in Enzyme Activity After Treatment of Primary Human Hepatocytes with COBI or Positive Controls (Mean ± SD, N = 3)

Treatment	Conc. (µM)	CYP1A2		CYP2B6		CYP3A	
		Phenacetin O-deethylase		Bupropion 4-hydroxylase		Testosterone 6β-hydroxylase	
		Fold change[a]	%Max[b]	Fold change[a]	%Max[b]	Fold change[a]	%Max[b]
3-Methylcholanthrene	2	53.5 ± 44.6[c]	100%	1.3 ± 0.4	3.2%	1.3 ± 0.8	0.2%
Phenobarbital	1000	2.8 ± 1.9	2.2%	10.6 ± 6.1[c]	100%	14.1 ± 6.1	69.6%
Rifampicin	10	2.2 ± 1.5	0.9%	5.7 ± 1.4	57.6%	19.6 ± 8[c]	100%
COBI	1	0.8 ± 0.7	-1.9%	1.4 ± 0.4	4.9%	0.7 ± 0.3	-2.8%
	3	0.8 ± 0.5	-1.7%	1.5 ± 0.9	3.6%	0.7 ± 0.3	-2.7%
	10	1.7 ± 1	0.5%	1.9 ± 1	7.0%	0.7 ± 0.3	-2.5%
	30	1.7 ± 1	1.1%	1.6 ± 0.4	8.9%	1.3 ± 1.3	0.2%

COBI = cobicistat; CYP = cytochrome P450 enzyme

a Fold increase in enzyme activity compared to cells treated with 0.1% (v/v) DMSO vehicle control

b Change in enzyme activity as a fraction of that achieved by the positive control = (Fold Change of Treatment – 1) / (Fold Change of Positive Control – 1) x 100%

c Positive control for this activity

2.6.5.12.10. AD-216-2071: In Vitro Assessment of the Induction Potential of COBI in Primary Cultures of Human Hepatocytes (Continued)

Test Article: COBI

Summary of Changes in mRNA Content After Treatment of Primary Human Hepatocytes with COBI or Positive Controls (Mean ± SD, N = 3)

Treatment	Conc. (µM)	CYP1A2		CYP2B6		CYP3A4		UGT1A1		MDR1	
		Fold change[a]	%Max[b]	Fold change[a]	%Max[b]	Fold change[a]	%Max[b]	Fold change[a]	%Max[b]	Fold change[a]	%Max[b]
3-Methylcholanthrene	2	457 ± 93.6[c]	100%	1.7 ± 1.2	1.1%	0.3 ± 0.2	-1.7%	8.5 ± 4.1	101.6%	0.7 ± 0.1	-29.9%
Phenobarbital	1000	1.9 ± 0.5	0.2%	41.3 ± 27[c]	100%	29.8 ± 16.6	62.8%	10 ± 4.9	119.3%	2.1 ± 0.2	98.2%
Rifampicin	10	1.4 ± 0.4	0.1%	17 ± 6.4	50.4%	45.9 ± 25[c]	100%	8.3 ± 3.6[c]	100%	2.1 ± 0.2[c]	100%
COBI	1	1.1 ± 0.2	0%	1.3 ± 0.5	2.1%	5.3 ± 1.8	10.5%	1.4 ± 0.4	6.5%	0.8 ± 0.2	-16.9%
	3	1.1 ± 0.6	0%	1.7 ± 0.7	4.6%	11 ± 2.7	24.9%	1.7 ± 0.5	10.5%	0.9 ± 0.2	-6.0%
	10	3.0 ± 1.7	0.4%	1.4 ± 0.5	3.0%	12.6 ± 4.7	27.4%	1.6 ± 0.6	9.7%	1.0 ± 0.1	3.4%
	30	10.1 ± 3.3	2.0%	0.4 ± 0.1	-2.9%	4.4 ± 3.5	8.6%	1.1 ± 0.6	0%	1.3 ± 0.2	28.7%

COBI = cobicistat; CYP = cytochrome P450 enzyme; MDR1 = P-glycoprotein (multidrug resistance protein 1); UGT = uridine diphosphate glucuronosyl transferase

a Fold increase in mRNA expression compared to cells treated with 0.1% (v/v) DMSO vehicle control

b Change in mRNA expression as a fraction of that achieved by the positive control = (Fold Change of Treatment – 1) / (Fold Change of Positive Control – 1) x 100%

c Positive control for this activity

2.6.5.12.10. AD-216-2071: In Vitro Assessment of the Induction Potential of COBI in Primary Cultures of Human Hepatocytes (Continued)

Test Article: COBI

CYP3A Western Immunoblotting of Primary Human Hepatocytes after Treatment with COBI or Positive Control Inducers

	1	2	3	4	5	6	7	8	9	10
Donor Hu790										
Donor Hu793										
Donor Hu8053										

Treatments

1. Dimethylsulfoxide vehicle (0.1%)
2. 3-Methylcholanthrene (2 µM)
3 Phenobarbital (1000 µM)
4. Rifampicin (10 µM)
5. COBI (1 µM)
6. COBI (3 µM)
7. COBI (10 µM)
8. COBI (30 µM)
9. CYP3A4 standard
10. Electrophoresis standards

2.6.5.12.11. AD-216-2039: Induction of Rat Metabolizing Enzymes By COBI In Vitro

Report Title	Study Type	Test Article	Report Number (Study Number)
Induction of Metabolizing Enzymes of Rat by GS-9350 In Vitro	Metabolism study	COBI	AD-216-2039

Method: The potential for induction of rat drug-metabolizing enzymes and transporters through the activation of the pregnane X receptor (PXR) by COBI was assessed in vitro, and the results were compared to those of ritonavir and positive control compounds (dexamethasone and miconazole). Assessments of induction were performed using a rat DAO hepatoma-derived cell line (rPXR) expressing rat PXR and with the CYP3A promoter linked to luciferase as a reporter. Positive control inducers were tested in parallel.

Rat PXR Activation by COBI, RTV, and Positive Controls

Concentration	Fold Induction Over DMSO Control			
	COBI	RTV	Dexamethasone	Miconazole
1 µM	1.25	1.36	—	—
3 µM	1.5	1.62	—	—
5 µM	—	—	6.54	—
10 µM	5.87	4.94	8.75	5.68
30 µM	5.14	6.53	—	—
100 µM	0.88	1.17	—	—

COBI = cobicistat; CYP = cytochrome P450 enzyme; PXR = pregnane X receptor (NR1I2); RTV = ritonavir

2.6.5.13. Pharmacokinetics: Excretion

2.6.5.13.1. JTK303-AD-005: Excretion in Rats after Single Administration of [^{14}C]EVG

Report Title	Study Type	Test Article	Report Number (Study Number)
Pharmacokinetics in Rats after Single Administration of ^{14}C-JTK-303	Excretion	[^{14}C]EVG	JTK303-AD-005 (AE-3857-G)

Species/Strain Number of Animals/ Group Sex	Adminis-tration Route	EVG Dose	Feeding Condition	Time (h)	Cumulative Excretion of Radioactivity (% of dose)			
					Urine	Feces	Cage Washing	Total
Rat/SD (Crj:CD(SD)IGS) 3 animals/group male	Oral	3 mg/5 mL/kg, vehicle; MC	Non-fasting	0-24	0.1 ± 0.1	79.6 ± 14.2	0.0 ± 0.0	79.7 ± 14.2
				0-48	0.1 ± 0.1	96.5 ± 2.0	0.0 ± 0.0	96.7 ± 1.9
				0-72	0.2 ± 0.1	97.5 ± 0.9	0.0 ± 0.0	97.7 ± 0.9
				0-96	0.2 ± 0.1	97.6 ± 0.9	0.0 ± 0.0	97.7 ± 0.8
Rat/SD (Crj:CD(SD)IGS) 3 animals/group male	IV	1 mg/1 mL/kg, vehicle; PEG400	Non-fasting	0-24	0.4 ± 0.1	80.5 ± 14.1	0.0 ± 0.0	80.9 ± 14.1
				0-48	0.4 ± 0.1	97.5 ± 0.2	0.0 ± 0.0	97.9 ± 0.2
				0-72	0.4 ± 0.1	98.2 ± 0.7	0.0 ± 0.0	98.6 ± 0.7
				0-96	0.4 ± 0.1	98.2 ± 0.8	0.0 ± 0.0	98.6 ± 0.7

EVG = elvitegravir; IV = intravenous; MC = 0.5% (w/v) aqueous methylcellulose; PEG400 = 80% (w/v) aqueous polyethylene glycol 400; NA = not applicable

Data are expressed as the mean values ± standard deviation of 3 animals.

2.6.5.13.2. JTK303-AD-022: Excretion in Rats after Repeated Oral Administration of [^{14}C]EVG

Report Title	Study Type	Test Article	Report Number (Study Number)
Pharmacokinetics in Rats after Repeated Oral Administration of [^{14}C]JTK-303	Excretion	[^{14}C]EVG	JTK303-AD-022 (AE-3896-G)

Species/Strain Number of Animals/ Group Sex	Administration Route	EVG Dose	Feeding Condition	Dose # / Time after dose (h)	Cumulative Excretion of Radioactivity (% of dose)			
					Urine	Feces	Cage Washing	Total
Rat/SD (Crj:CD(SD)IGS) 3 animals/group male	Oral	3 mg/5 mL/kg daily for 7 days, vehicle; MC	Non-fasting	1 / 24	0.1 ± 0.1	88.2 ± 4.1	<0.1	88.3 ± 4.2
				2 / 24	0.1 ± 0.1	93.3 ± 0.8	<0.1	93.4 ± 0.8
				3 / 24	0.1 ± 0.1	94.9 ± 0.5	<0.1	95.0 ± 0.5
				4 / 24	0.1 ± 0.0	93.3 ± 0.7	<0.1	93.4 ± 0.7
				5 / 24	0.1 ± 0.0	93.9 ± 0.5	<0.1	94.0 ± 0.4
				6 / 24	0.1 ± 0.0	94.1 ± 0.2	<0.1	94.1 ± 0.2
				7 / 24	0.1 ± 0.0	94.5 ± 0.1	<0.1	94.6 ± 0.1
				7 / 48	0.1 ± 0.0	95.3 ± 0.2	<0.1	95.4 ± 0.1
				7 / 72	0.1 ± 0.0	95.3 ± 0.1	<0.1	95.4 ± 0.1
				7 / 96	0.1 ± 0.0	95.3 ± 0.1	<0.1	95.4 ± 0.1
				7 / 120	0.1 ± 0.0	95.3 ± 0.1	<0.1	95.4 ± 0.1
				7 / 144	0.1 ± 0.0	95.3 ± 0.1	<0.1	95.4 ± 0.1
				7 / 168	0.1 ± 0.0	95.3 ± 0.1	<0.1	95.4 ± 0.1

EVG = elvitegravir; MC = 0.5% (w/v) aqueous methylcellulose

Data are expressed as the mean values ± standard deviation of 3 animals.

2.6.5.13.3. JTK303-AD-006: Excretion in Dogs after Single Administration of [^{14}C]EVG

Report Title	Study Type	Test Article	Report Number (Study Number)
Pharmacokinetics in Dogs after Single Administration of [^{14}C]-JTK-303	Excretion	[^{14}C]EVG	JTK303-AD-006 (AE-3858-G)

Species/Strain Number of Animals/ Group Sex	Administration Route	EVG Dose	Feeding Condition	Time (h)	Cumulative Excretion of Radioactivity (% of dose)			
					Urine	Feces	Cage Washing	Total
Dog/Beagle (NOSAN) 3 animals/group male	Oral	3 mg/ 2 mL/kg, vehicle; MC	Non-fasting	0-4	0.1 ± 0.1	—	—	—
				0-8	0.2 ± 0.1	—	—	—
				0-12	0.2 ± 0.1	—	—	—
				0-24	0.4 ± 0.1	79.9 ± 4.6	0.0 ± 0.1	80.4 ± 4.7
				0-48	0.5 ± 0.1	95.0 ± 0.9	0.0 ± 0.1	95.5 ± 0.9
				0-72	0.5 ± 0.1	96.8 ± 1.7	0.0 ± 0.1	97.4 ± 1.7
				0-96	0.5 ± 0.1	97.2 ± 1.9	0.1 ± 0.1	97.7 ± 1.9
				0-120	0.5 ± 0.1	97.3 ± 2.0	0.1 ± 0.1	97.9 ± 2.1
				0-144	0.5 ± 0.1	97.3 ± 2.0	0.1 ± 0.1	97.9 ± 2.1
				0-168	0.5 ± 0.1	97.4 ± 2.0	0.1 ± 0.1	98.0 ± 2.1

2.6.5.13.3. JTK303-AD-006: Excretion in Dogs after Single Administration of [^{14}C]EVG (Continued)

Test Article: [^{14}C]EVG

Species/Strain Number of Animals/ Group Sex	Administration Route	EVG Dose	Feeding Condition	Time (h)	Cumulative Excretion of Radioactivity (% of dose)			
					Urine	Feces	Cage Washing	Total
Dog/Beagle (NOSAN) 3 animals/group male	IV	1 mg/ 0.2 mL/kg, vehicle; PEG400	Non-fasting	0-4	0.6 ± 0.4	—	—	—
				0-8	0.8 ± 0.5	—	—	—
				0-12	0.9 ± 0.5	—	—	—
				0-24	0.9 ± 0.5	89.6 ± 5.4	0.1 ± 0.1	90.7 ± 5.8
				0-48	1.0 ± 0.5	98.0 ± 0.6	0.2 ± 0.0	99.2 ± 0.2
				0-72	1.0 ± 0.5	98.5 ± 0.7	0.2 ± 0.0	99.7 ± 0.3
				0-96	1.0 ± 0.5	98.7 ± 0.7	0.2 ± 0.0	99.8 ± 0.4
				0-120	1.0 ± 0.5	98.7 ± 0.7	0.2 ± 0.0	99.9 ± 0.4
				0-144	1.0 ± 0.5	98.8 ± 0.7	0.2 ± 0.0	100.0 ± 0.4
				0-168	1.0 ± 0.5	98.8 ± 0.8	0.2 ± 0.0	100.0 ± 0.5

EVG = elvitegravir; IV = intravenous; MC = 0.5% (w/v) aqueous methylcellulose; PEG400 = 80% (w/v) aqueous polyethylene glycol 400

Data are expressed as the mean values ± standard deviation of 3 animals.

2.6.5.13.4. AD-216-2073: Excretion of [^{14}C]COBI Following Single Oral Dose Administration to Mice

Report Title	Study Type	Test Article	Report Number
Pharmacokinetics, Metabolism, and Excretion of [^{14}C]GS-9350 Following Oral Administration to Mice	Excretion	[^{14}C]COBI	AD-216-2073

Species/Strain Number of Animals/ Group Sex	Administration Route	Dose	Feeding Condition	% of Radioactive Dose				
				Time (h)	Urine	Time (h)	Feces	Cage Rinse
ICR mice [Hsd:ICR(CD-1)] 2 pairs of animals/ Group 1 male	Oral	[^{14}C]COBI 30 mg/kg	Nonfasting	0-6	1.00	0-24	79.1	0.06
				6-12	0.49			
				12-24	0.30			
				24-48	0.10	24-48	5.37	0.02
				48-72	0.05	48-72	0.94	0.01
				72-96	0.03	72-96	0.19	0.01
				96-120	0.02	96-120	0.12	0.01
				120-144	0.01	120-144	0.07	0.00
				144-168	0.01	144-168	0.05	—

COBI = cobicistat

Additional Information: Recovery of radioactivity from cage wash, cage wipe, and residual carcass totaled 0.7% of total dose.

2.6.5.13.5. AD-216-2034: Excretion of [^{14}C]COBI Following Single Oral Dose Administration in the Rat

Report Title	Study Type	Test Article	Report Number
Pharmacokinetics, Distribution, Metabolism, and Excretion of [^{14}C]GS-9350 Following Oral Administration to Rats	Excretion	[^{14}C]COBI	AD-216-2034

Species/Strain Number of Animals/ Group Sex	Adminis-tration Route	Dose	Feeding Condition	% of Radioactive Dose							
				Time (h)	Urine		Time (h)	Feces		Cage Rinse	
					Mean	SD		Mean	SD	Mean	SD
Sprague Dawley Rat (H1a:[SD]CVF) Group 1: 3 male rats (bile duct-intact)	Oral	[^{14}C]COBI 10 mg/kg	Fasted until 4 h post-dose	0-12	1.57	0.22	0-24	77.8	15.2	0.05	0.02
				12-24	0.20	0.05					
				24-48	0.11	0.03	24-48	11.7	13.2	0.01	0.01
				48-72	0.06	0.01	48-72	0.94	0.70	0.01	0.01
				72-96	0.04	0.01	72-96	0.27	0.06	0.01	0.01
				96-120	0.03	0.01	96-120	0.33	0.11	0.00	0.01
				120-144	0.02	0.01	120-144	0.17	0.04	0.00	0.01
				144-168	0.02	0.00	144-168	0.11	0.02	—	—

COBI = cobicistat; SD = standard deviation

Additional Information: Further recovery of radioactivity from cage wash and cage wipe totaled 0.03% of total dose.

2.6.5.13.6. AD-216-2067: Excretion of [^{14}C]COBI After Oral Administration in the Dog

Report Title	Study Type	Test Article	Report Number
Mass Balance of Radioactivity after Oral Administration of [^{14}C]GS-9350 to Naive Male Beagle Dogs	Excretion	[^{14}C]COBI	AD-216-2067

Species/ Strain Number of Animals/ Group Sex	Adminis -tration Route	Dose (mg/kg)	Feeding Condition	Collection Period (h)	Cumulative Recovery of Total Radioactivity (% Dose) by Excretion Route (Mean ± SD, n = 3)					
					Urine		Feces		Cage Debris	
					Mean	SD	Mean	SD	Mean	SD
Beagle Dog 3M/group (bile duct-intact)	Oral	5	Fasted	0-12	1.37	0.56	0.04	0.08	0.07	0.04
				0-24	1.60	0.56	33.54	30.77	1.78	2.20
				0-48	1.81	0.59	76.84	4.27	2.05	2.27
				0-72	1.89	0.59	78.95	4.27	2.30	2.54
				0-96	1.96	0.59	79.56	4.14	2.46	2.75
				0-120	1.99	0.59	79.95	4.11	2.51	2.84
				0-144	2.04	0.58	80.30	4.17	2.56	2.93
				0-168	2.06	0.58	80.53	4.13	3.5[a]	—

COBI = cobicistat; SD = standard deviation

Note: Cage residue samples contained 3.52% of the radioactive dose.

a Includes hair, cage wash and cage wipe at 168 h post-dose

2.6.5.13.7. AD-216-2095: Assessment of the Potential for COBI and RTV to be Substrates of the Human OCT2 Uptake Transporter

Report Title	Study Type	Test Article	Report Number
Assessment of the Potential for GS-9350 and Ritonavir to be Substrates of the Human OCT2 Uptake Transporter	Excretion study (in vitro)	COBI	AD-216-2095

Method: The potential for COBI to be a substrate of the human organic cation uptake transporter OCT2 (SLC22A2) was assessed using a CHO cell line that stably expresses this protein. Time- and concentration-dependent accumulation of radioactivity was compared to that in wild type CHO cells and the effects of the OCT2 inhibitor, verapamil (100 µM), were tested. RTV and the OCT2 substrate, metformin, were tested as substrates in parallel.

Compound	Conc. (µM)	Time (min)	Verapamil (100 µM)	Accumulation (pmol/mg protein)		Ratio (OCT2/wt)
				CHO-OCT2	CHO-K (wt)	
[^{14}C]COBI	2	2	Without verapamil	401.9 ± 18.8	280.2 ± 1.7	1.43
			With verapamil	375.8 ± 17.8	235.4 ± 3.5	1.60
			Δ	6.5%	16.0%	—
		20	—	725.9 ± 22.9	508 ± 106.5	1.43
	20	2	—	3241.2 ± 184.2	2258.1 ± 330.9	1.44
		20	—	5872.5 ± 487.4	4614.6 ± 945.2	1.27
[^{3}H]RTV	10	2	Without verapamil	1872.8 ± 106.8	1119.7 ± 74.2	1.68
			With verapamil	1373.7 ± 155.1	798.1 ± 89.0	1.72
			Δ	26.6%	28.7%	—
		20	—	1834.8 ± 190.4	903.3 ± 352.3	2.03
	100	2	—	7682.8 ± 337	5684.0 ± 485.0	1.35
		20	—	11,454.7 ± 1380.7	6347.8 ± 1686.0	1.80
[^{14}C]Metformin	2	2	Without verapamil	215.2 ± 17.0	6.0 ± 1.3	35.9
			With verapamil	5.6 ± 1.1	6.6 ± 1.1	0.9
			Δ	97.4%	–10.0%	—

CHO = Chinese hamster ovary cell; COBI = cobicistat; OCT2 = organic cation transporter 2; RTV = ritonavir

2.6.5.14. Pharmacokinetics: Excretion into Bile

2.6.5.14.1. JTK303-AD-005: Excretion into Bile in Rats after Single Administration of [^{14}C]EVG

Report Title	Study Type	Test Article	Report Number (Study Number)
Pharmacokinetics in Rats after Single Administration of ^{14}C-JTK-303	Excretion	[^{14}C]EVG	JTK303-AD-005 (AE-3857-G)

Species/Strain Number of Animals/ Group Sex	Adminis-tration Route	EVG Dose	Feeding Condition	Time (h)	Cumulative Excretion of Radioactivity (% of oral dose or % radioactivity injected)				
					Bile	Urine	Feces	GI Contents	Carcass
Rat/SD (Crj:CD(SD)IGS) 3 animals/group male	Oral	EVG 3 mg/5 mL/kg, vehicle; MC	Non-fasting	0-0.5	0.1 ± 0.1	—	—	—	—
				0-1	0.9 ± 0.3	—	—	—	—
				0-2	3.2 ± 0.6	—	—	—	—
				0-4	7.4 ± 1.5	—	—	—	—
				0-8	13.5 ± 4.2	—	—	—	—
				0-24	23.0 ± 2.9	0.1 ± 0.0	42.4 ± 2.4	—	—
				0-48	25.0 ± 3.7	0.1 ± 0.0	69.2 ± 6.1	3.3 ± 0.9	0.0 ± 0.1
Rat/SD (Crj:CD(SD)IGS) 3 animals/group male	Intraduodenal Injection of Bile Sample[a]	12.51 μg eq. of EVG in bile/body	Non-fasting	0-2	1.6±0.5	—	—	—	—
				0-4	3.2±1.2	—	—	—	—
				0-8	4.4 ± 1.8	—	—	—	—
				0-24	5.7 ± 1.7	0.1 ± 0.0	65.0 ± 22.5	—	—
				0-48	5.9 ± 1.6	0.1 ± 0.0	91.5 ± 2.5	0.9 ± 0.8	0.0 ± 0.0

EVG = elvitegravir; IV = intravenous; MC = 0.5% (w/v) aqueous methylcellulose

Data are expressed as the mean values ± standard deviation of 3 animals.

a Obtained from non-fasting male rats (0–24 h) after single oral administration of [^{14}C]EVG (dose: 3 mg/5 mL/kg, vehicle; MC).

2.6.5.14.2. AD-216-2034: Excretion of [^{14}C]COBI Following Single Oral Dose Administration in the Rat

Report Title	Study Type	Test Article	Report Number
Pharmacokinetics, Distribution, Metabolism, and Excretion of [^{14}C]GS-9350 Following Oral Administration to Rats	Distribution	[^{14}C]COBI	AD-216-2034

Species/Strain Number of Animals/ Group Sex	Administration Route	Dose	Feeding Condition	Time (h)	% of Radioactive Dose in Urine Mean	% of Radioactive Dose in Urine SD	Time (h)	% of Radioactive Dose in Bile Mean	% of Radioactive Dose in Bile SD	Time (h)	% of Radioactive Dose in Feces Mean	% of Radioactive Dose in Feces SD	% of Radioactive Dose in Cage Rinse Mean	% of Radioactive Dose in Cage Rinse SD
Sprague Dawley Rat (H1a:[SD]CVF) Group 4: 3 bile duct-cannulated male rats	Oral	[^{14}C]COBI 10 mg/kg	Fasted until 4 h post-dose	0-12	3.56	0.91	0-2	17.6	4.8	0-24	17.2	3.9	0.08	0.05
							2-4	19.9	4.8					
							4-6	14.7	1.3					
							6-8	5.27	2.87					
							8-12	4.22	1.97					
				12-24	0.24	0.12	12-24	3.47	0.37					
				24-48	0.16	0.06	24-48	1.52	0.19	24-48	2.06	1.19	0.01	0.01
				48-72	0.09	0.03	48-72	0.90	0.05	48-72	0.25	0.16	0.01	0.01
				72-96	0.05	0.02	72-96	0.62	0.06	72-96	0.08	0.06	0.01	0.01
				96-120	0.04	0.01	96-120	0.43	0.05	96-120	0.04	0.01	0.01	0.01
				120-144	0.03	0.00	120-144	0.31	0.03	120-144	0.02	0.01	0.00	0.01
				144-168	0.02	0.01	144-168	0.22	0.03	144-168	0.01	0.01	0.13	0.07

COBI = cobicistat; SD = standard deviation

Additional Information: Recovery of radioactivity from cage washes and cage wipes totaled 0.01% of total dose.

2.6.5.14.3. AD-216-2068: Mass Balance of Radioactivity after Oral Administration of [^{14}C]COBI to Naive Male Bile Duct-Cannulated Beagle Dogs

Report Title	Study Type	Test Article	Report Number
Mass Balance of Radioactivity after Oral Administration of [^{14}C]GS-9350 to Naive Male Bile Duct-Cannulated Beagle Dogs	Excretion	[^{14}C]COBI	AD-216-2068

Species/ Strain Number of Animals/ Group Sex	Adminis-tration Route	Dose (mg/kg)	Feeding Condition	Collection Period (h)	Cumulative Recovery of Total Radioactivity (% Dose) by Excretion Route (Mean ± SD, n = 2[a])			
					Bile	Urine	Feces	Mean Total
Beagle Dog 2M/group[a] (Bile duct cannulated)	Oral	5	Fasted	0–2	22.3 ± 0.01	—	—	22.3
				0–4	39.3 ± 0.33	—	—	39.3
				0–6	48.7 ± 1.51	—	—	48.7
				0–8	53.5 ± 2.97	—	—	53.5
				0–12	57.1 ± 3.25	1.07 ± 0.34	0.24 ± 0.33	58.5
				0–24	61.6 ± 3.38	1.40 ± 0.12	1.26 ± 1.12	64.3
				0–48	63.9 ± 3.70	1.56 ± 0.01	16.1 ± 1.43	81.7
				0–72	63.9 ± 3.70	1.72 ± 0.02	21.3 ± 3.41	87.1
				0–96	63.9 ± 3.70	1.78 ± 0.04	22.4 ± 3.07	88.3
				0–120	63.9 ± 3.70	1.82 ± 0.04	23.4 ± 2.78	89.4
				0–144	63.9 ± 3.70	1.85 ± 0.04	23.9 ± 2.68	89.9
				0–168	63.9 ± 3.70	1.88 ± 0.04	24.3 ± 2.73	90.3

COBI = cobicistat; SD = standard deviation Note: Cage residue samples contained 3.52% of the radioactive dose.

a One dog of original three excluded as an outlier (90.19% of dosed radioactivity recovered in urine 0 – 12 h postdose)

2.6.5.15. Pharmacokinetics: Drug-Drug Interactions

2.6.5.15.1. JTK303-AD-018: Effects of CYP Inhibitors on the Metabolism of EVG in Human Liver Microsomes

Report Title	Study Type	Test Article	Report Number (Study Number)
Effects of CYP Inhibitors on the Metabolism of JTK-303 in Human Liver Microsomes	Drug-drug interaction study	[^{14}C]EVG	JTK303-AD-018 (JK303PK044)

Reaction conditions: Incubated for 10 minutes at 37°C in the 100 mM potassium phosphate buffer (pH 7.4) containing 1.0 µg/mL (2.2 µM) of [^{14}C]EVG, 1.0 mg protein/mL of liver microsomes, 3.3 mM $MgCl_2$, 1.3 mM $NADP^+$, 3.3 mM glucose-6-phosphate, and 0.4 unit/mL glucose-6-phosphate dehydrogenase. Human liver microsomes were a pooled sample from 50 human subjects (30 males and 20 females).

Inhibitor (Target Enzyme)	Concentration (µM)	Rate of Metabolism of EVG and Rate of Formation of Metabolites (pmol/min/mg protein)				
		EVG	M1	M8	M5	Other Metabolites
Control	0	144.6	123.7	3.0	12.3	5.6
Sulfaphenazole (CYP2C9)	2	133.0 (8.0)	115.2 (6.9)	4.2 (NC)	11.8 (4.1)	1.9 (66.1)
	20	123.5 (14.6)	111.3 (10.0)	0.9 (70.0)	11.3 (8.1)	0.1 (98.2)
Quinidine (CYP2D6)	0.2	137.2 (5.1)	119.1 (3.7)	3.2 (NC)	11.1 (9.8)	3.8 (32.1)
	2	138.6 (4.1)	123.2 (0.4)	2.5 (16.7)	11.7 (4.9)	1.2 (78.6)
Ketoconazole (CYP3A)	0.2	43.7 (69.8)	39.6 (68.0)	NC (100.0)	3.8 (69.1)	0.5 (91.1)
	2	3.6 (97.5)	4.0 (96.8)	NC (100.0)	NC (100.0)	NC (100.0)

EVG = elvitegravir; N.C. = not calculated
Values in parentheses are the percentage of inhibition. Values are represented as the mean of 2 measurements.

2.6.5.15.2. JTK303-AD-025: In Vitro Interaction Study of Coadministered Drugs with EVG Metabolism

Report Title	Study Type	Test Article	Report Number (Study Number)
Interaction Study of JTK-303 with Coadministered Drugs	Drug-drug interaction study	[^{14}C]EVG	JTK303-AD-025

Study Method: The effect of potential comedications on the in vitro metabolism of [^{14}C]EVG by human liver microsomal fraction was investigated. Mixtures were incubated at 37°C for 10 minutes to determine % of control and the degree of inhibition of metabolic activity for EVG by human liver microsomes. The final concentration of [^{14}C]EVG was 2 μM, and the concentration of protein was 1 mg protein/mL. The amounts of EVG and metabolite M1 (% of peak on radiochromatogram) were determined and the rate of metabolism of EVG was calculated. The % of control and degree of inhibition were calculated. When the degree of inhibition at each concentration of coadministered drug was 50% or more, the IC_{50} value was calculated.

Potential Coadministered Drug	IC_{50} (μM)
APV	1.1
EFV	> 50
IDV	0.51
Ketoconazole	0.099
LPV	3.1
NFV	1.1
NVP	> 50
RTV	0.079
SQV	4.5
ZDV	> 100

APV = amprenavir; EFV = efavirenz; IDV = indinavir sulfate; LPV = lopinavir; NFV = nelfinavir; NVP = nevirapine; RTV = ritonavir; SQV = saquinavir; ZDV = zidovudine

2.6.5.15.3. AD-183-2028: In Vitro Assessment of Inhibition of Human EVG Glucuronidation by Ketoconazole and ATV

Report Title	Study Type	Test Article	Report Number (Study Number)
In Vitro Assessment of Inhibition of Human Elvitegravir Glucuronidation by Ketoconazole	Drug-drug interaction study	EVG	AD-183-2028

Study Method: The rates of formation of EVG-acyl glucuronide (GS-9200) from EVG substrate (10 μM) by human hepatic microsomal fractions were determined in the presence and absence of ketoconazole (concentrations ranging to 100 μM) and IC_{50} values were determined. Atazanavir (ATV), an inhibitor of human UGT1A1 activity was used as a comparator.

Activity	Calculated IC_{50} (μM)	
	Ketoconazole	ATV
EVG acyl glucuronidation	9.6	0.4

EVG = elvitegravir; ATV = atazanavir

2.6.5.15.4. JTK303-AD-026: Involvement of MDR1 in Membrane Permeation of EVG and Inhibitory Effect of EVG on Digoxin Transport

Report Title	Study Type	Test Article	Report Number (Study Number)
Involvement of MDR1 in Membrane Permeation of JTK-303 and Inhibitory Effect of JTK-303 on Digoxin Transport	Drug-drug interaction study	EVG	JTK303-AD-026

Study Method: This study investigated transcellular transport activities of [^{14}C]EVG across MDR1-expressing cells (porcine kidney epithelial LLC-PK1 cells transfected with vectors containing human MDR1 cDNA) and control cells (LLC-PK1 cells transfected with vector only) to determine whether or not EVG is a substrate of MDR1. In addition, the inhibitory effect of EVG on the transcellular transport activities of a typical substrate of MDR1, digoxin, across MDR1 expressing cells and control cells was investigated. Cells were incubated at 37°C with test article or reference compound in HBSS on either the apical or basal side. After incubation for 1, 2, and 4 hours, 50 µL of HBSS was collected from the opposite compartment. Radioactivity was measured using a liquid scintillation counter. From the radioactivity, the transcellular transported amounts of the test article were determined. Transcellular transport activity was determined from the observed concentrations of the test article and model substrate before incubation and from cellular protein amount.

Effect of EVG on digoxin transport across control and MDR1-expressing cell monolayers

Inhibitor	Concentration (µM)	Control Cells			MDR1-expressing cells		
		Flux (µL/mg protein/h)			Flux (µL/mg protein/h)		
		Apical to Basal	Basal to Apical	Flux Ratio	Apical to Basal	Basal to Apical	Flux Ratio
None	0	20.6 ± 2.9	44.8 ± 6.7	2.2	18.5 ± 5.8	183.6 ± 10.6	9.9
EVG	0.3	53.4 ± 3.5	73.5 ± 8.6	1.4	19.6 ± 7.1	204.6 ± 19.2	10.4
	1	47.7 ± 4.4	75.7 ± 4.7	1.6	27.0 ± 4.6	213.8 ± 21.1	7.9
	3	28.1 ± 2.8	46.6 ± 3.2	1.7	19.2 ± 1.7	205.9 ± 13.5	10.7
	10	29.1 ± 1.8	33.9 ± 3.3	1.2	18.0 ± 1.0	176.1 ± 9.3	9.8
	30	24.6 ± 2.8	29.9 ± 2.3	1.2	27.5 ± 6.8	164.6 ± 11.4	6.0
Verapamil	10	24.9 ± 1.1	25.4 ± 2.9	1.0	34.6 ± 14.6	110.0 ± 6.8	3.2
[^{14}C]Mannitol	1	16.9 ± 1.2	12.8 ± 1.4	0.8	29.1 ± 0.4	24.7 ± 3.3	0.8

EVG = elvitegravir

2.6.5.15.5. AD-183-2030: In Vitro Assessment of EVG Inhibition of Human OATP1B1 and OATP1B3

Report Title	Study Type	Test Article	Report Number (Study Number)
In Vitro Assessment of Elvitegravir Inhibition of Human OATP1B1 and OATP1B3	Drug-drug interaction study	EVG	AD-183-2030

Study Methods: The potential of EVG to inhibit the uptake of the fluorescent probe substrate, Fluo 3, was measured in OATP1B1 and -1B3 transfected CHO cells. Cells were washed twice with 37ºC assay buffer followed by a 0.5 hour pre-incubation with assay buffer. Test compounds were diluted in assay buffer containing 2 µM Fluo 3 and pre-incubated with cells for 1 hour. Following removal of assay buffer containing Fluo 3 and test compound, cells were washed 3 times with 200 µl of ice cold assay buffer and then lyzed at room temperature for 15 minutes in a lysis buffer containing 0.05 % SDS in a 1 mM $CaCl_2$ solution. Wells were analyzed for Fluo 3 fluorescence at an excitation of 485 nm and emission of 530 nm.

Inhibition of OATP1B1-Dependent and OATP1B3-Dependent uptake of Fluo 3 by EVG

Test Article	Inhibition assay	IC_{50} (µM)	Inhibition potential[a] (%)
EVG	OATP1B1	> 2	~ 40
	OATPB1B3	0.44 ± 0.22	~ 80

EVG = elvitegravir; OATP = organic anion transporting polypeptide; IC_{50} = the test article concentration needed to inhibit the maximal transporter specific transport by 50 %
Note: IC_{50} values from 2 to 3 individual experiments done in duplicate
a Percent of inhibition at the highest investigated concentration

2.6.5.15.6. AD-216-2072: Inhibition of P-glycoprotein-dependent Bidirectional Transport of Digoxin Through Caco-2 Cell Monolayers by COBI

Report Title	Study Type	Test Article	Report Number
Inhibition of P-glycoprotein-Dependent Bi-Directional Transport of Digoxin Through Monolayers of Caco-2 Cells by GS-9350	Drug-drug interaction study	COBI	AD-216-2072

Method: The potential for intestinal P-glycoprotein (MDR1) inhibition by COBI was assessed by measuring its effects on bidirectional transport of digoxin (a known MDR1 substrate) through Caco-2 monolayers. The known MDR1 inhibitors cyclosporin A and RTV were used for comparison.

Inhibitor	Inhibitor Conc. (µM)	Direction	Initial Digoxin Conc. (µM)	Digoxin P_{app} (10^{-6} cm/s)			Efflux Ratio
				Replicate 1	Replicate 2	Average	
None		Cell-Free	11.6	38.5	—	38.5	7.72
		Forward	13.6	1.07	1.53	1.30	
		Reverse	8.00	8.96	11.1	10.0	
Cyclosporin A	10	Cell-Free	9.30	47.0	—	47.0	1.68
		Forward	10.3	1.83	2.68	2.25	
		Reverse	10.0	3.56	4.00	3.78	
RTV	20	Cell-Free	8.50	45.6	—	45.6	1.84
		Forward	10.4	2.77	3.56	3.17	
		Reverse	8.60	5.57	6.05	5.81	
COBI	90	Cell-Free	10.8	51.1	—	51.1	1.69
		Forward	11.9	2.74	1.74	2.24	
		Reverse	11.6	5.33	2.26	3.80	

COBI = cobicistat; RTV = ritonavir

2.6.5.15.7. AD-216-2104: Inhibition of Breast Cancer Resistance Protein-Dependent Bidirectional Transport of Prazosin through Monolayers of Caco-2 Cells by COBI

Report Title	Study Type	Test Article	Report Number
Inhibition of Breast Cancer Resistance Protein-Dependent Bidirectional Transport of Prazosin through Monolayers of Caco-2 Cells by Cobicistat	Drug-drug interaction study	COBI	AD-216-2104

Method: The potential for intestinal breast cancer resistance protein (BCRP) inhibition by COBI was assessed by measuring its effects on the bidirectional transport of prazosin, a known BCRP substrate, through Caco-2 monolayers. The known BCRP inhibitor, fumitremorgin C, was used for comparison. Ritonavir was also tested for its effect on prazosin.

Inhibitor	Inhibitor Conc. (µM)	Direction	Prazosin P_{app} (10^{-6} cm/s)					Efflux Ratio
			Replicate 1	Replicate 2	Replicate 3	Replicate 4	Average	
None	0	Cell-Free	49.84	—	24.04	—	36.94	5.1
		Forward	1.59	2.05	2.8	3.56	2.50	
		Reverse	9.12	13.91	12.92	15.08	12.78	
Fumitremorgin C	2	Cell-Free	58.80	—	34.70	—	46.75	2.6
		Forward	3.51	3.95	4.97	5.33	4.44	
		Reverse	11.55	12.45	11.18	11.14	11.58	
RTV	20	Cell-Free	51.30	—	28.44	—	39.87	2.8
		Forward	3.22	3.49	4.17	4.98	4.00	
		Reverse	9.98	12.62	9.93	12.49	11.26	
COBI	90	Cell-Free	41.75	—	34.90	—	38.33	2.4
		Forward	3.36	3.57	5.78	6.24	4.74	
		Reverse	11.34	12.50	9.68	11.29	11.20	

BCRP = breast cancer resistance protein; COBI = cobicistat; RTV = ritonavir

2.6.5.15.8. AD-216-2103: Bidirectional Permeability of COBI Through Monolayers of P-glycoprotein and BCRP Overexpressing Cells

Report Title	Study Type	Test Article	Report Number
Bidirectional Permeability of Cobicistat Through Monolayers of P-glycoprotein and BCRP Overexpressing Cells	Excretion study (in vitro)	COBI	AD-216-2103

Method: The potential for COBI to act as a substrate for Pgp (MDR1) and BCRP was tested in monolayers of either wild type, MDR1 transfected or BCRP transfected Madin-Darby canine kidney (MDCK II) cells (MDCK II-WT, MDCK II-MDR1 and MDCK II-BCRP, respectively). The effects of transporter-selective inhibitors were also assessed.

Cell Type	Direction	Initial Conc. (µM)	Recovery (%)	P_{app} (x 10^{-6} cm/s)			Efflux Ratio
				R1	R2	Average	
Wild Type and MDR1 Transfected MDCK II Cells							
MDCK II-WT	Cell-Free	9.85	110.12	28.88	—	28.88	3.7
	Forward	10.18	81.81	3.26	3.27	3.26	
	Reverse	10.06	97.65	10.51	13.88	12.19	
MDCK II-MDR1	Cell-Free	10.19	103.94	33.68	—	33.68	60.9
	Forward	10.34	85.84	0.32	0.32	0.32	
	Reverse	9.72	102.22	17.56	21.20	19.38	
MDCK II-MDR1 (10 µM Cyclosporin A)	Cell-Free	11.2	102.90	26.84	—	26.84	3.8
	Forward	11.2	91.24	3.40	3.66	3.53	
	Reverse	10.1	94.85	12.41	14.00	13.21	

2.6.5.15.8. AD-216-2103: Bidirectional Permeability of COBI Through Monolayers of P-glycoprotein and BCRP Overexpressing Cells (Continued)

Test Article: COBI

Cell Type	Direction	Initial Conc. (µM)	Recovery (%)	P_{app} (x 10^{-6} cm/s)			Efflux Ratio
				R1	R2	Average	
Wild Type and BCRP Transfected MDCK II Cells							
MDCK II-WT	Cell-Free	9.49	100.66	30.35	—	30.35	7.0
	Forward	9.35	78.66	1.71	2.27	1.99	
	Reverse	8.60	102.55	13.43	14.62	14.03	
MDCK II-BCRP	Cell-Free	9.15	96.97	26.81	—	26.81	13.4
	Forward	9.29	79.49	1.54	1.50	1.52	
	Reverse	8.43	110.12	19.15	21.50	20.33	
MDCK II-BCRP (10 µM Ko134)	Cell-Free	8.90	102.29	31.72	—	31.72	3.2
	Forward	9.12	76.97	3.54	4.04	3.79	
	Reverse	9.14	87.59	11.22	12.67	11.94	

2.6.5.15.9. AD-216-2030: Interaction of COBI with Human MRP1, MRP2, and MDR1

Report Title	Study Type	Test Article	Report Number
Interaction of GS-9350 and Ritonavir with MRP1, MRP2, and Pgp	Drug-drug interaction study	COBI	AD-216-2030

Method: Cobicistat and RTV were incubated with Madin Darby canine kidney cells (MDCK II) transfected with ABCB1 (encodes Pgp/MDR1), ABCC1 (encodes MRP1), and ABCC2 (encodes MRP2). All incubations were carried out in cell culture medium (without FBS supplement) containing 10 µM calcein AM. Following removal of medium containing calcein AM and COBI, cells were lyzed at room temperature for 45 minutes in a buffer containing 20 mM Tris-HCl pH 9.0 and 0.4% Triton X-100. Each well was analyzed for calcein fluorescence.

	Percent Inhibition (%)		
COBI Concentration (µM)	**MRP1**	**MRP2**	**MDR1**
1.41	0	5.7	1.50
2.81	1.6	11.6	2.10
5.63	2.6	11.5	0.70
11.3	26.8	13.7	6.20
22.5	36.3	19.7	14.9
45.0	48.7	28.8	57.1
90.0	65.7	55.1	88.8
RTV Concentration (µM)			
0.31	1.6	0.4	3.50
0.63	11.1	2.4	4.90
1.25	11.3	1.5	5.90
2.50	20.2	3.3	3.70
5.00	29.4	2.9	12.0
10.0	23.2	2.4	28.8
20.0	52.9	5.5	69.3

COBI = cobicistat; MRP = multi-drug resistance-associated protein; MDR1 = P-glycoprotein (Pgp, ABCB1); RTV = ritonavir

2.6.5.15.10. AD-216-2099: In Vitro Assessment of COBI and RTV Inhibition of Human Breast Cancer Resistance Protein

Report Title	Study Type	Test Article	Report Number
In Vitro Assessment of Cobicistat and Ritonavir Inhibition of Human Breast Cancer Resistance Protein	Drug-drug interaction study	COBI, RTV	AD-216-2099

Method: The inhibition of the ATP-Binding Cassette (ABC) efflux transporter Breast Cancer Resistance Protein (BCRP, ABCG2 gene product) by COBI and RTV was assessed in vitro using the Madin Darby Canine Kidney (MDCK II) cell line transfected with BCRP. Hoechst 33342 (10 μM) was the substrate, and fumitremorgin C (2 μM) was the positive control inhibitor. Fumitremorgin C treatment eliminated detectable transport activity.

Test compound	IC_{50} (μM)	Maximal inhibition (%)
COBI	59 ± 28	~ 73
RTV	> 20[a]	~ 25

COBI = cobicistat; RTV = ritonavir

a Maximum concentration of RTV tested was 20 μM

2.6.5.15.11. AD-216-2100: In Vitro Assessment of COBI and RTV Inhibition of Human OATP1B1 and OATP1B3

Report Title	Study Type	Test Article	Report Number
In Vitro Assessment of Cobicistat and Ritonavir Inhibition of Human OATP1B1 and OATP1B3	Drug-drug interaction study	COBI	AD-216-2100

Method: The inhibition of the Solute Carrier influx transporters organic anion transporting polypeptides 1B1 and 1B3 (OATP1B1 and OATP1B3) by COBI and RTV was assessed in vitro using Chinese hamster ovary cells transfected with the individual human transporters. Fluo3 (2 µM) was the substrate and rifampicin (50 µM) was the positive control inhibitor and reduced transport by ≥ 99%. Transport in transfected cells was ~10-fold (OATP1B1) or ~20-fold higher than in wild-type CHO cells.

Test Articles	Transporters	IC_{50} (µM)	Maximal inhibition (%)
COBI	OATP1B1	3.50 ± 0.72	~ 98.5
	OATP1B3	1.88 ± 0.76	~ 99.5
RTV	OATP1B1	2.05 ± 1.33	~ 98.7
	OATP1B3	1.83 ± 1.13	~ 99.1

COBI = cobicistat; OATP = organic anion transporting polypeptide; RTV = ritonavir

2.6.5.15.12. AD-216-2093: In Vitro Interaction Studies of COBI with Human OCT2 Uptake Transporter

Report Title	Study Type	Test Article	Report Number
In vitro Interaction Studies of GS-9350 with human OCT2 Uptake Transporter	Drug-drug interaction study	COBI	AD-216-2093

Method: The inhibitory effect of COBI on recombinant expressed human organic cation transporter 2 (OCT2 or SLC22A2) was assessed using metformin (2 μM) as the substrate and an incubation period of 10 minutes. This study used Chinese hamster ovary cells expressing human OCT2. Ritonavir, an agent used for clinical pharmacokinetic enhancement of other drugs, was also tested. Cimetidine and trimethoprim, which have been shown to interact with human OCT2, were used for comparison. The positive control, verapamil (100 μM) inhibited transport by ≥ 91.5%.

Compound	IC_{50} (μM)	Inhibitory Efficacy (%)[a]
COBI	8.24	88
RTV	22.6	85
Cimetidine	44.5	70
Trimethoprim	29.4	90

COBI = cobicistat; IC_{50} = concentration at which 50% maximum inhibition is achieved; OCT2 = organic cation transporter 2; RTV = ritonavir

a Maximum concentrations tested were 100 μM (COBI and RTV) or 300 μM (cimetidine and trimethoprim).

2.6.5.15.13. AD-216-2094: In Vitro Interaction Studies of COBI with Human MATE1 and MATE2-K Efflux Transporters

Report Title	Study Type	Test Article	Report Number
In vitro Interaction Studies of GS-9350 with human MATE1 and MATE2-K Efflux Transporters	Drug-drug interaction study	COBI	AD-216-2094

Method: The potential for COBI to inhibit the human multidrug and toxin extrusion (MATE) transporters MATE1 (SLC47A1 gene product) and MATE2 K (SLC47A2 gene isoform 2 product).was assessed using tetraethylammonium (TEA, 5 µM) as the substrate and an incubation time of 10 minutes. These studies employed the human embryonic kidney cell line, HEK293, transfected with expression vectors for human MATE1, human MATE2-K or empty vector. Cimetidine and trimethoprim were included as positive controls. Ritonavir was also included as a test article. Transport of TEA in MATE1-transfected cells was 27–52-fold higher than in vector control cells. Transport of TEA in MATE2-K-transfected cells was 9–18-fold higher than in vector control cells.

Compound	MATE1 IC_{50} (µM)	MATE2-K IC_{50} (µM)[a]
COBI	1.87	33.5
RTV	1.34	100
Cimetidine	1.64	43.4
Trimethoprim	6.35	1.38

COBI = cobicistat; MATE1 = multidrug and toxin extrusion protein 1 (SLC47A1); MATE2-K = multidrug and toxin extrusion protein 2-K (SLC47A2); RTV = ritonavir

a Maximum concentrations tested were 100 µM (COBI and RTV) or 300 µM (cimetidine and trimethoprim).

2.6.5.15.14. AD-216-2098: In Vitro Interaction Studies of COBI and RTV With Human OCTN1 Transporter

Report Title	Study Type	Test Article	Report Number
In Vitro Interaction Studies of Cobicistat and Ritonavir with Human OCTN1 Transporter	Drug-drug interaction study	COBI	AD-216-2098

Method: The potential for COBI and RTV to inhibit the human organic cation transporter OCTN1 (SLC22A4) was assessed in vitro using Drosophila Schneider S_2 cells transfected with OCTN1. [^{14}C]Tetraethylammonium (5 µM) was the substrate and verapamil (100 µM) was the positive control inhibitor. Transport of the substrate was determined after 5 minutes, and was 7.6–9.0-fold higher than in untransfected S_2 cells. Verapamil inhibited substrate transport by 85.8%–90.2%.

Compound	IC_{50} (µM)	Maximal inhibition [a] (%)
COBI	2.49	~ 94
RTV	2.08	~ 91

COBI = cobicistat; IC_{50} = concentration at which 50% maximum inhibition is achieved; OCTN1 = organic cation transporter N1; RTV = ritonavir

a Maximum concentrations tested were 100 µM

2.6.5.15.15. AD-216-2105: In Vitro Interaction Studies of COBI and RTV With Human OAT1 and OAT3 Transporters

Report Title	Study Type	Test Article	Report Number
In vitro Inhibition Studies of Cobicistat and Ritonavir with Human OAT1, OAT3 and MRP4 Transporters	Drug-drug interaction study	COBI	AD-216-2105

Method: The potential for COBI and RTV to inhibit the human organic anion transporters, OAT1 (SLC22A6) and OAT3 (SLC22A8) was assessed in vitro using transfected Chinese Hamster Ovary (CHO) cells (for OAT1) or transfected Human Embryonic Kidney HEK293 cells (for OAT3). Substrates were 0.5 µM [^{3}H]para-aminohippuric acid for OAT1 (3 min incubation) and 0.2 µM [^{3}H]estrone-3-sulfate for OAT3 (5 min incubation). Positive control inhibitors were 200 µM benzbromarone for OAT1 and 200 µM probenecid for OAT3, and inhibited transport by ≥ 98.9% and ≥ 96.4%, respectively.

Transporter	Compound	IC_{50} (µM)	Maximal inhibition [a] (%)
OAT1	COBI	> 100	140% activation
	RTV	> 20	ND
OAT3	COBI	> 100	ND
	RTV	8.46	~ 62

COBI = cobicistat; IC_{50} = concentration at which 50% maximum inhibition is achieved; OAT = organic anion transporter; RTV = ritonavir; ND = Not Determined

a Maximum concentrations tested were 100 µM

2.6.5.15.16. AD-216-2105: In Vitro Interaction Studies of COBI and RTV With Human MRP4 Transporter

Report Title	Study Type	Test Article	Report Number
In vitro Inhibition Studies of Cobicistat and Ritonavir with Human OAT1, OAT3 and MRP4 Transporters	Drug-drug interaction study	COBI	AD-216-2105

Method: The potential for COBI and RTV to inhibit the multidrug resistance-associated protein MRP4 (ABCC4) was assessed in vitro using vesicles prepared from porcine kidney LLC-PK1 cells transfected with human MRP4. [^{3}H]5-Dehydroepiandrosterone sulfate (DHEAS, 0.02 µM) was the substrate and MK571 (150 µM) was the positive control inhibitor. ATP-Dependent transport of the substrate was determined after 8 minutes and was inhibited 80% by the positive control.

Compound	IC_{50} (µM)	Maximal inhibition [a] (%)
COBI	20.7	~ 92
RTV	> 20	~ 15

COBI = cobicistat; IC_{50} = concentration at which 50% maximum inhibition is achieved; MRP = multi-drug resistance-associated protein; RTV = ritonavir

a Maximum concentrations tested were 100 µM (COBI) and 20 µM (RTV).

2.6.5.16. Pharmacokinetics: Other

There are no additional studies to report under this heading.